Gene & Protein in Disease

ACCSCIENCE PUBLISHING

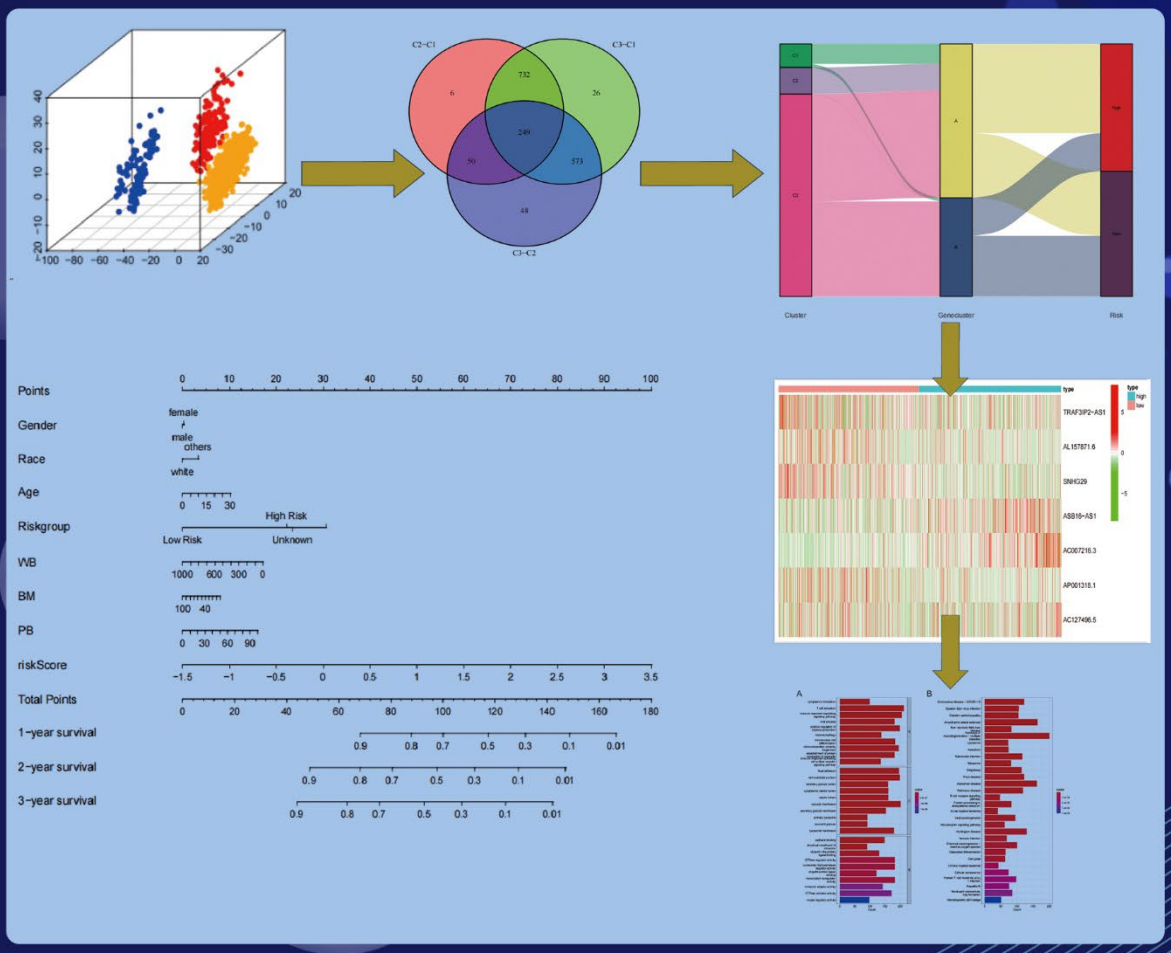

A novel signature identified by pyroptosis-related lncRNAs clusters predicts prognosis and tumor immune microenvironment for pediatric acute myeloid leukemia

ISSN: 2811-003X (Online)
Volume 2 · Issue 1
March 2023

Online ISSN: 2811-003X

Gene & Protein in Disease

Gene & Protein in Disease is an international journal for molecular and translational medicine. The journal primarily focuses on publishing investigations on the molecular bases and experimental therapeutics of human diseases.

Scan to access website:

Scan to submit papers:

About the Publisher

AccScience Publishing is a publishing company based in Singapore. We publish a range of high-quality, open-access, peer-reviewed journals and books from a broad spectrum of disciplines.

Contact Us

Managing Editor
gpd.office@accscience.sg

AccScience Publishing
8 Burn Road, #15-03 Trivex, Singapore 369977.

Volume 2 • Issue 1 • March 2023
ISSN 2811-003X (online)

GENE & PROTEIN IN DISEASE

ACCSCIENCE PUBLISHING

Access Science Without Barriers

GENE & PROTEIN IN DISEASE

ISSN: 2811-003X (online)

Editorial and Production Credits

Publisher: AccScience Publishing
Managing Editor: Juliana Meng
Production Editor: Ian Wong
Journal Development Editor: Felicia Wang
Special Issue Commissioning Editor: Felicia Wang
Article Layout and Typeset: Sinjore Technologies (India)
Cover Design: ProPub (China)

For all advertising queries, contact gpd.office@accscience.sg.

Supplementary file

Supplementary files of articles can be obtained at https://accscience.com/journal/GPD/2/1.

About the Cover

A graphic illustration of double-stranded DNA

Disclaimer

AccScience Publishing is not liable to the statements, perspectives, and opinions contained in the publications. The appearance of advertisements in the journal shall not be construed as a warranty, endorsement, or approval of the products or services advertised and/or the safety thereof. AccScience Publishing disclaims responsibility for any injury to persons or property resulting from any ideas or products referred to in the publications or advertisements. AccScience Publishing remains neutral with regard to jurisdictional claims in published maps and institutional affiliations.

Gene & Protein in Disease

Editorial Board

ACCSCIENCE PUBLISHING

Volume 2 | Issue 1 | March 2023 |

Gene & Protein in Disease

https://accscience.com/journal/GPD

CONTENTS

REVIEW ARTICLES

1 **Application of artificial intelligence in drug repositioning**
Qingkai Hu, Xianfang Wang, Yifeng Liu, Yu Sang, Dongfang Zhang

2 **Hydrogen sulfide donors and inhibitors in cancer research: A state-of-the-art review**
Nazeer Hussain Khan, Ebenezeri Erasto Ngowi, Yan Li, Saadullah Khattak, Yingshuai Zhao, Muhammad Shahid, Ujala Zafar, Irum Waheed, Fatima Khan, Razia Virk, Istaqlal Hussain, Jiebin Cao, Hongxia Liu, Zhihui Liu, Dong-Dong Wu, Xin-Ying Ji

PERSPECTIVE ARTICLE

3 **A hypothesis on the equilibrium between dopamine toxicity and detoxification: The roles of NQO2 and UDP-glucuronosyltransferases**
Jean A. Boutin, Gilles Ferry, Karine Reybier

ORIGINAL RESEARCH ARTICLES

4 **A novel signature identified by pyroptosis-related lncRNAs clusters predicts prognosis and tumor immune microenvironment for pediatric acute myeloid leukemia**
Jie Lu, Xinyu Chang, Guowei Zheng, Xiting Cao, Zhenwei Wang, Hao Zhu, Shuaijie Gao, Yuanlin Xi

5 **Alkylation repair homolog 3-regulated esophageal squamous cell carcinoma associated long non-coding RNA 1 is required for maintaining the stemness of esophageal cancer**
Yuanbo Cui, Yanan Lou, Pengju Lv, Wei Cao

6 **A pan-cancer analysis of high mobility group box 1 and its role in human tumorigenesis**
Wenqing Long, Jiaqi Li, Hao Shi, Lijun Zhang, Liqun Yang, Zhuoyan Jiang, Lei Xia, Lin Wang, Hongnu Yu

7 **Underexpression of SCN7A is associated with poor prognosis in lung adenocarcinoma**
Hehui Lv, Hongyuan Song, Zhouping Qin, Rongchun Xing, Yulian Chen

CASE REPORT

8 **Autoimmune thyroid disease in narcolepsy: A case report**
Chaofan Geng, Zhenzhen Yang, Hongju Zhang,

ACCSCIENCE PUBLISHING

Gene & Protein in Disease

REVIEW ARTICLE

Application of artificial intelligence in drug repositioning

Qingkai Hu[1]*, Xianfang Wang[2]*, Yifeng Liu[2], Yu Sang[1], and Dongfang Zhang[1]

[1]College of Computer Science and Technology, Henan Institute of Technology, Xinxiang, Henan, 453000, China

[2]College of Management, Henan Institute of Technology, Xinxiang, Henan, 453000, China

Abstract

The use of artificial intelligence technologies in biology, pharmacy, and medicine has brought about a dramatic change in these industries. Drug repositioning is a method of drug development in the process of applying existing therapeutic agents to new diseases. This paper first outlines the use of artificial intelligence technology in the field of drug repositioning, then reviews a variety of application methods of artificial intelligence in the realm of drug repositioning, and finally summarizes the advantages and disadvantages of these methods, and proposes the difficulties faced by artificial intelligence in drug repositioning in the future and the corresponding suggestions to achieve the goal of helping researchers to develop more effective methods of drug repositioning.

Keywords: Drug repositioning; Drug targets; Deep learning; Artificial intelligence; Drug target interaction

***Corresponding authors:**
Qingkai Hu
(hiekay@163.com)
Xianfang Wang
(2wangfang@163.com)

Citation: Hu Q, Wang X, Liu Y, *et al*., 2023, Application of artificial intelligence in drug repositioning. *Gene Protein Dis*, 2(1):201. https://doi.org/10.36922/gpd.v1i3.201

Received: September 21, 2022
Accepted: October 21, 2022
Published Online: November 7, 2022

1. Introduction

More and more artificial intelligence technologies have been applied in the medical field in recent years. Artificial intelligence technology was first applied in pharmaceutical research and development in the field of health care, and has been widely used and developed in many areas such as drug mining, drug dispensing, health management, assisted diagnosis and treatment, and even the rational use of clinical drugs. With the exponential growth of modern technology, artificial intelligence technology has also quietly entered the ranks of drug repositioning.

Drug repositioning (also known as drug reconfiguration or drug repurposing) is the process of taking an existing drug and treating it for a new disease[1]. Drug repositioning can save R&D time and development costs compared to conventional drug development methods. A major benefit of drug repositioning is that it is safe for humans in clinical models and has a low failure rate because only the effectiveness of the drug is tested against a specific disease[2]. In addition, repositioned drugs save the early cost and time required to bring medicines to market, thereby accelerating the transition from basic research efforts to clinical treatments. Nosengo *et al.* concluded that it currently takes 13 – 15 years to bring new drugs to market, costs between $2 and $3 billion, and is increasing in cost[3]. However, the average cost of repositioning a drug is only $300 million and takes about 6.5 years to enter the market.

The recent drug development case of COVID-19[4] is a typical case of faster and further exploration of drug repositioning. Traditional new drug development requires a lot of investment, takes a long time, and is risky. With the help of artificial intelligence technology, virtual high-throughput screening of candidate compounds can be performed, thus enhancing the efficiency of drug development. The techniques related to artificial intelligence are applied in different aspects of drug repositioning to solve many key problems[5]. For example, active compound screening, molecule generation, drug target discovery, and protein structure and protein-ligand interaction prediction are widely used.

In this paper, we introduce the research progress of drug repositioning in recent years, focusing on three categories: Network-based methods, feature-based methods, and matrix-based methods, as shown in Figure 1.

2. Net-based approach

For modeling biological and biomedical entities, and their relationships and interactions, networks are the best way to go. Networks can provide models of how drugs and indications, as well as drug targets, work to determine therapeutic drug potential. When representing biological data by networks, usually genes, molecules, proteins, and other biological entities can be represented by nodes; and their relationships such as mode of action, similarity, association, and interaction are represented by edges[6]. For specific attribution information, it is generally represented by the weighted values of edges and node; examples include gene-gene interaction networks, networks of drug-target interactions, and networks of interactions between various other biological entities. For learning graphical data with nonlinear relationships, the graphical neural network in neural networks can be used; the network can also be used to represent biological entity data. Moreover, a network-based chemical similarity correlation analysis method can be used to discover side effects of new drugs as well as to reposition the already marketed drugs.

Many network-based drug repositioning methods have been proposed by researchers in recent years, as shown in Table 1.

A network-based inference method was invented by Cheng *et al.*[7]. To derive new targets for already marketed drugs, this method only needs to use the drug-target dichotomous network topological similarity. Guney *et al.*'s team used the metric of disease-drug similarity to calculate the magnitude of the interaction between a disease and a drug target[8]. The method is highly systematic and comprehensive by introducing chemical similarity for correlation and by considering the necessary biological information. Wang *et al.* team invented a heterogeneous network modeling framework that computes by capturing various interrelationships between targets, drugs, and diseases with each other to predict the effectiveness of new drug use[9].

On the basis of similarity-based heterogeneous networks, deep learning techniques can be used to represent proteins

Table 1. Net-based approach

Methods	Features	References
NBI	Using only drug-target dichotomous network topological similarities to infer new targets for known drugs	[7]
Drug-disease proximity	A drug-disease similarity metric was introduced	[8]
TL_HGBI	Using Disease Information to Predict New Drug Targets	[9]
NRWRH	Enables large-scale prediction of potential drug-target interactions	[10]
DTI-CNN	Drug-target interactions based on feature representation learning and deep neural networks	[12]

NBI: Network-based inference, TL_HGBI: Triple-layer heterogeneous graph-based inference, NRWRH: Network-based random walk with restart on the heterogeneous network, DTI-CNN: Drug target interaction prediction.

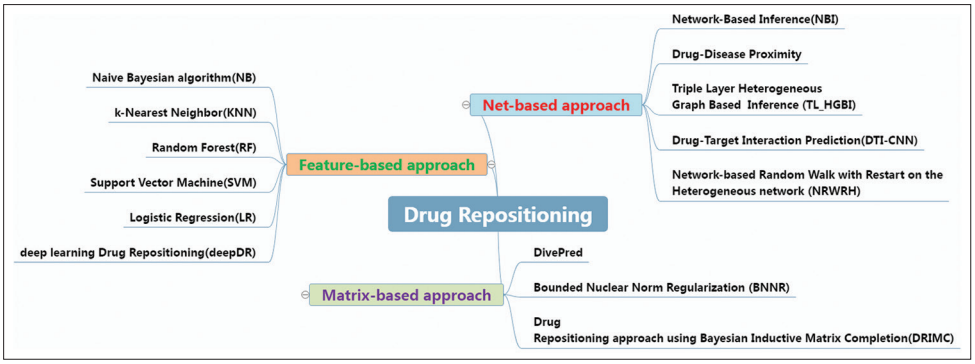

Figure 1. Artificial intelligence technology applied in various aspects of drug repositioning.

and drugs in heterogeneous networks more easily and efficiently. Chen *et al.* invented a heterogeneous network supporting different relationships, which include drugs and proteins linked by known drug-target interaction, chemical similarity between drugs, and sequence similarity between proteins to mine potential drug-disease associations[10]. In 2018, Olayan RS used a nonlinear fusion approach to fuse drug-protein features from different similarity networks and pathway-based features in these networks together[11]. Peng *et al.* completed random wandering with restarts using a similarity-based heterogeneous network model, and based on that, a denoising autoencoder was used to implement a convolutional neural network predictive classifier and learn the basic features[12]. Ji *et al.* used a heterogeneous network combining a large amount of functional information and a large amount of information about the structure of the network nodes to perfectly solve the problem of excessive feature generation by the nodes in the heterogeneous network to calculate the final feature vector[13]. Lu *et al.* investigated a drug-target interaction prediction method based on multisource data fusion and network structure perturbation[14]. He *et al.* invented and disclosed a computational drug relocation method based on memory networks and attention[15]. Wang *et al.* investigated a hybrid graph network and ion channel-based drug repositioning technique for COVID-19[16]. They designed a hybrid graph network model for predicting the affinity of COVID-19 ion channel targets to drugs. Based on the simplified specification of drug molecular input line input (SMILES) code, the atomic features were first extracted to construct the point set, and the atomic bonds were used to construct the edge set; then, RDKit was used to generate undirected graphs with atomic features, and drug feature information was extracted using the graph attention layer. A convolutional neural network was used to extract protein features from five ion channel target proteins screened from the SARS-CoV-2 whole-genome sequence of the NCBI database. The extracted drug features were then connected with the target feature information using graph convolutional network (GCN) and attention mechanism. The drug-target affinity is outputted after two layers of fully connected operation, and finally the drug-target affinity model is obtained. One of the hybrid graphs network-based drug-target affinity prediction model framework is shown in Figure 2.

3. Feature-based approach

The feature extraction method uses a new feature space of lower dimensionality to map the original feature projection, while the new features are usually a combination of the original features, with the aim of finding more meaningful information. The common feature extraction techniques are principal component analysis and singular value decomposition[17]. The purpose of the selection method is to select small portions of features from the complete set of input features based on some design criteria to be used as input to the model. In the process of predicting drug sensitivity, a priori biological knowledge is usually incorporated into the feature fraction.

At present, drug repositioning approaches are not only limited to relying on biomedical data of drug similarity alone but also innovative machine learning methods have also been applied. The combination of machine learning algorithms with drug-target interaction network information provides new ideas for drug development. The main methods include the use of plain Bayes, k-nearest neighbors (KNN)[18], random forest[19], and support vector machines (SVMs)[20], and more recently for binary classification, superclass classification, and value prediction, as shown in Table 2.

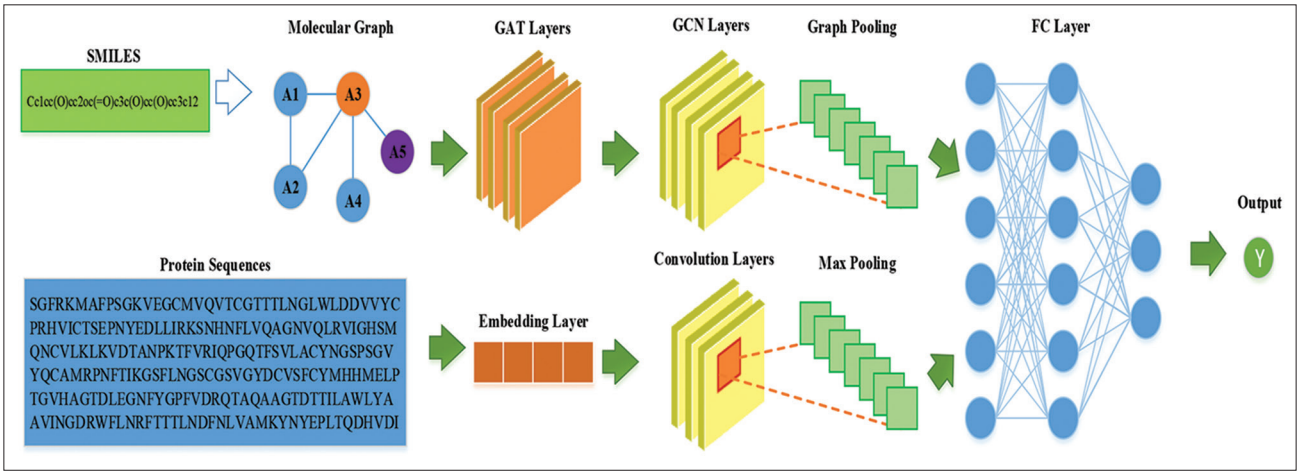

Figure 2. Framework of hybrid graph network-based drug-target affinity prediction model.

Table 2. Feature-based approach

Methods	Features	References
KNN	No need to estimate parameters and train drug target data	[18]
SVM	Requires a relatively small number of drug target samples	[20]
DT	Can handle both continuous and discrete drug target data	[22]
LR	The weights of the target features can see how different features affect the final results	[24]

KNN: K-nearest neighbor, SVM: Support vector machine, DT: Decision tree, LR: Logistic regression.

In 2006, Guengerich used machine learning algorithms to reveal the role of P450 enzymes arising in drug metabolism and toxicity[21]. In 2011, Dr. Feixiong Cheng proposed a method to predict P450 enzymes using traditional classifiers such as KNN, DT, and SVM[22]. A large number of new algorithms to predict human cytochrome P450 enzymes were published immediately afterward. Napolitano *et al.* applied non-linear SVMs to the classification of drug efficacy[23]. Gottlieb *et al.* used logistic regression algorithm for drug repositioning[24]. Gönen used Bayesian algorithm in machine learning for drug-target protein prediction to find new drug-target protein association relationships. First, drug and side effect information, drug chemical structure information, and disease and gene-related information were integrated, and then, the training data were obtained by feature selection and feature extraction. Then, suitable machine learning algorithms were selected to train them, and finally, the trained algorithm models are used to obtain drug repositioning results[25].

Nowadays, the technology of drug repositioning is influenced by deep learning, of which feature learning is the main embodiment of deep learning technology. Deep learning builds computational models by simulating the human brain, which can not only extract features automatically but also obtain effective feature information at different levels. Based on these advantages, deep learning has also been applied in drug repositioning. Deep learning technique is a concept closely related to artificial neural network.

To predict the pharmacological characteristics of a drug, Aliper *et al.* fully used connected deep neural networks to make predictions. The drug characteristics were also used to calculate the therapeutic potential as well as new drug indications. They constructed a deep neural network model using gene expression signature data and pathway data. This model has a high accuracy in prediction for drug indication classification and has better performance than support vector machine model. Therefore, this deep neural network model was used for drug repurposing. In addition, they proposed that a deep neural network confusion matrix can be used for drug repositioning[26]. Segler *et al.*'s[27] method based on deep learning combined with Monte Carlo algorithm is simple and efficient and has been affirmed by professionals. Hughes *et al.* developed the first model capable of fast screening of compounds using deep learning models[28]. Turk *et al.* extracted matched molecules from the ChEMBL database as a dataset for deep learning models[29]. Zhang *et al.* proposed an extraction strategy based on multisource features to construct a protein-ligand interaction prediction model using an integrated learning approach, which outperformed the single classifier prediction model in terms of sensitivity and Youden index and could effectively solve the data imbalance problem[30]. Chen *et al.* proposed a multisimilarity fusion-based drug relocation recommendation algorithm to address the shortcomings of traditional drug relocation recommendation algorithms. First, disease similarity was calculated based on drug-disease data sources. Then, three similarities were calculated based on drug-chemical structure, drug-target protein, and drug side effect data sources and were fused into drug similarity. Finally, the predicted values of drug-disease correspondence were calculated using two similarities and fused into the final predicted values by the prediction fusion method[31]. Zhang *et al.* obtained knowledge associations from PubMed, DrugBank, CTD, and other databases, constructed semantic knowledge graphs by knowledge fusion, attribute definition, and used drug repositioning as empirical evidence to reason about new uses of drugs in tumor therapy by two methods: Path search and link prediction[32]. Zeng *et al.* investigated a deep learning drug repositioning (deepDR) based on a network deep learning approach using multimodal deep self-encoder and variational self-encoder models to discover drug-disease associations, which is shown in the steps in Figure 3. They combined many drug association data phases into one dataset (drug-disease association, drug-target association, drug-drug association, and drug side effects) and then used this dataset to train a multimodal deep autoencoder and then define advanced drug features[33]. Next, to identify new indications based on features that can be identified, they used a variational autoencoder to encode and decode combinations of advanced drug features and disease-drug associations in clinical reports. These studies have been tested on datasets with common disease-drug associations and have shown better results than previous machine learning models.

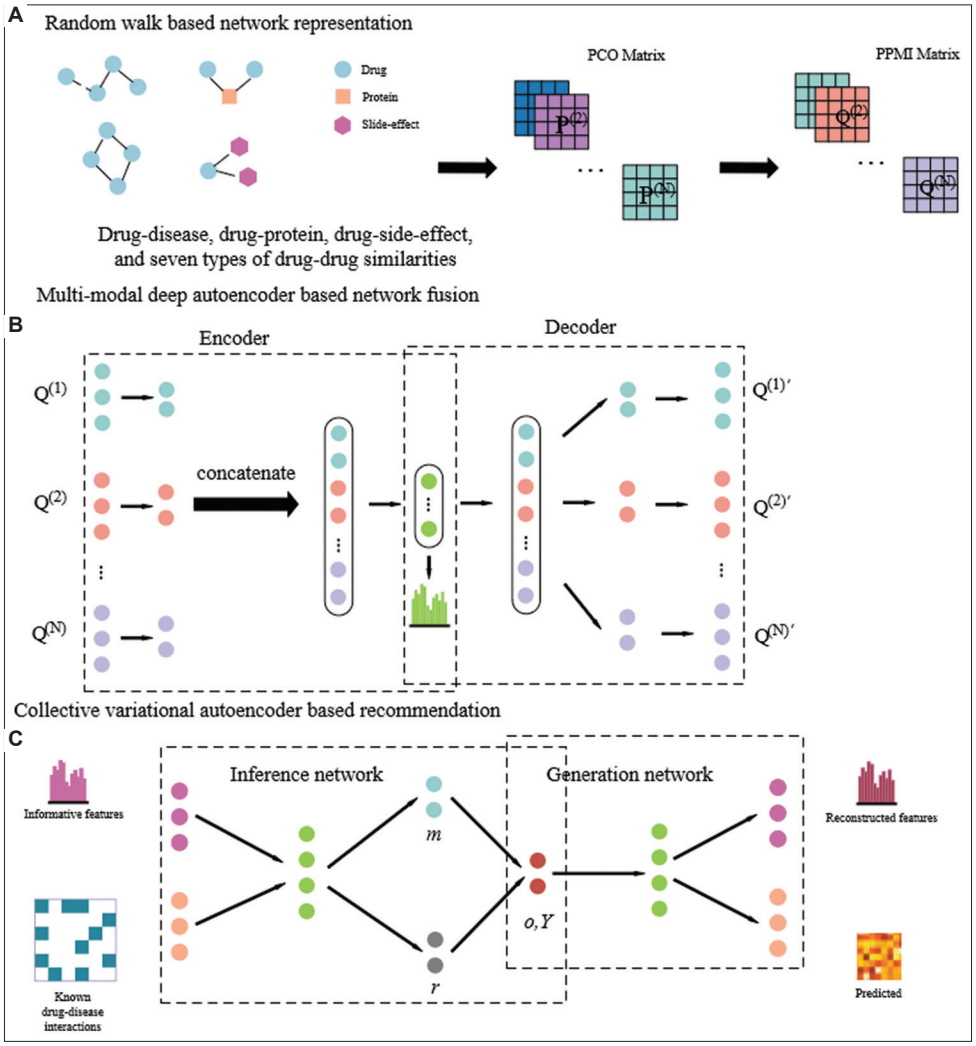

Figure 3. deepDR method steps. (A) deepDR generates random walk-based network representations from multiple drug-related complex heterogeneous networks. (B) deepDR uses multimodal deep autoencoder (MDA) to take the entire punctual mutual information (PPMI) matrix in each network into compact low-dimensional features shared by all networks and then obtains the low-dimensional features in the intermediate layer of MDA. (C) deepDR uses a collective variant autoencoder (cVAE) for prediction of disease-drug relationships.

4. Matrix-based approach

Both network-based drug relocation methods and feature-based drug relocation methods perform well, but both methods require feature extraction as well as the selection of appropriate negative samples. To remedy this deficiency, more efficient methods, matrix decomposition, and matrix complementation methods have emerged. In recent years, researchers have proposed various methods to predict drug-target interaction, among which, Bayesian-based matrix decomposition methods are widely used for drug-target interaction matrices. Matrix decomposition can map higher dimensional data to the product of two lower dimensional matrices, which can solve the problem of data sparsity, and the specific implementation and solution of matrix decomposition are concise and easy to

Table 3. Matrix-based approach

Methods	Features	References
DivePred	Projection of high-dimensional drug features into a low-dimensional feature space to generate a dense feature representation of the drug	[34]
BNNR	Balancing the approximation error and the rank property by introducing a regularization term	[35]
DRIMC	Integrates drug and disease multisource data and models the probability of correlation through inductive matrix completion (IMC)	[36]
MLMC	Introduction of matrix completion as a preprocessing of sparse correlation matrix	[38]

BNNR: Bounded nuclear norm regularization, DRIMC: Repositioning approach using Bayesian inductive completion, MLMC: Multiview learning with matrix completion.

understand. Matrix completion is the decomposition of an incomplete matrix to obtain two or more submatrices, which are multiplied together to obtain a new matrix that approximates the original missing matrix, and then, the values in the new matrix are used to fill the missing values in the missing matrix. Many matrix-based drug repositioning methods have been proposed by researchers in recent years, as shown in Table 3.

Xuan *et al.* proposed a prediction method for disease-drug associations, and this method uses a non-negative matrix decomposition (DivePred) technique. To indicate the characteristics of drugs from various perspectives, DivePred incorporates the similarities of various drugs[34]. A low-rank matrix complementation method was proposed by Yang *et al.* This method can use the regularization term to reduce the similarity noise, while the resultant values

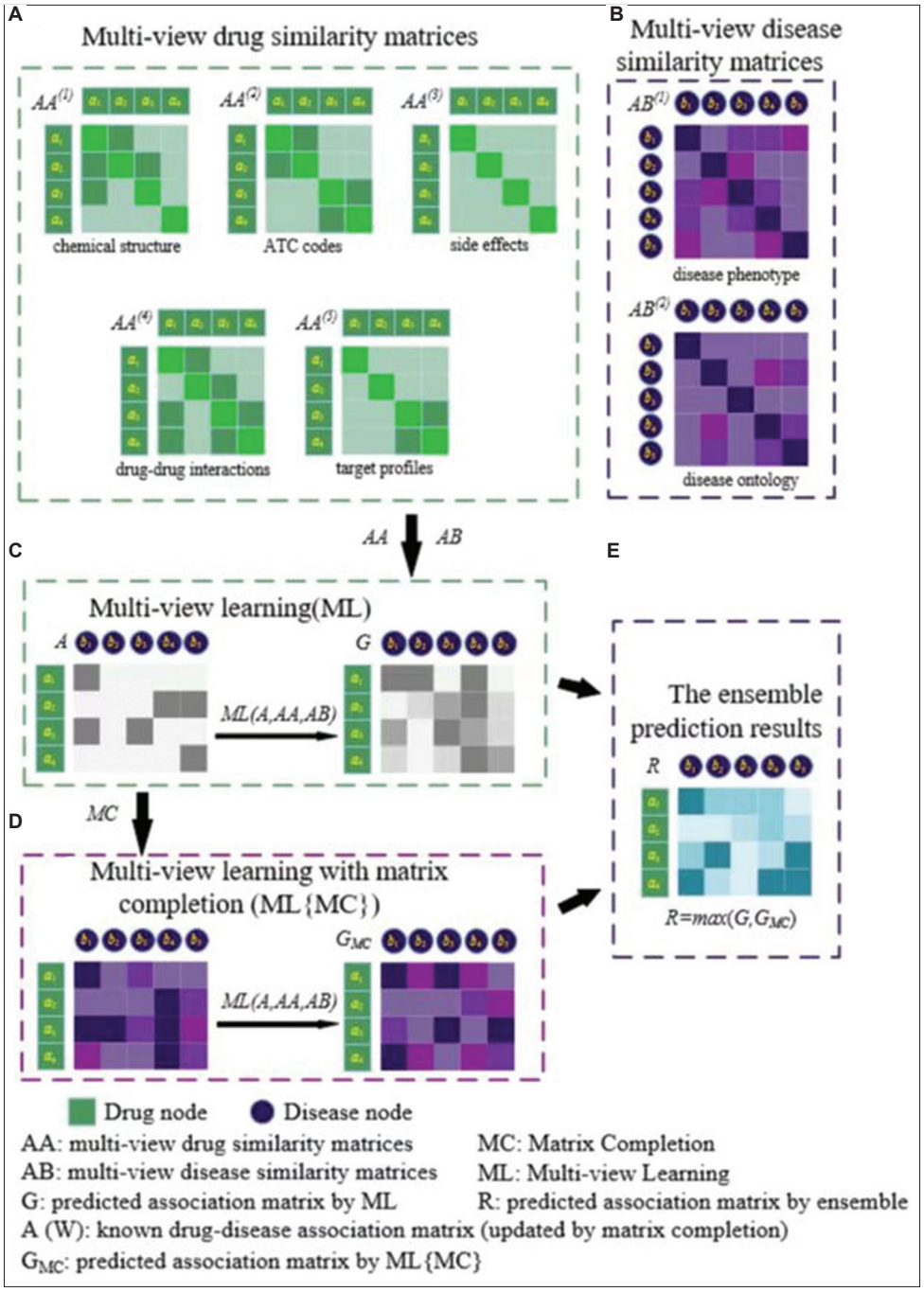

Figure 4. (A-E) Overall workflow of multiview learning with matrix completion.

can be obtained within their own specified range[35]. A new method called DRIMC was proposed by Zhang *et al.* The DRIMC method integrates data from multiple sources such as drugs and diseases, while using inductive matrices to complete the modeling of relevant probabilities[36]. Peng *et al.* proposed a drug-target relationship prediction method based on deep forest and positive and unlabeled (PU) learning, which constructs a similarity matrix between drugs and a similarity matrix between targets based on drug structure information and target sequence information, respectively[37]. Yi *et al.* developed a multiple attempt learning based on matrix completion for drug repositioning method multiview learning with matrix completion (MLMC)[38]. They used multiple view learning so as to predict new indications, while using matrix completion for the associated sparse matrices for preprocessing so that features between multiple similarity matrices can be computed. First, to calculate the best similarity matrix, they used multiview learning to predict multiple disease similarity matrices and multiple drug similarity matrices. Second, to make the multiview learning predictions more accurate, the values of the related matrices were populated using matrix complementation methods. Finally, the above two steps were merged into one strategy in MLMC. The execution flow of MLMC is shown in Figure 4.

4. Conclusion

This paper presents the research progress of artificial intelligence-based drug repositioning, focusing on network-based approach, feature-based approach, and matrix-based approach.

Each method of AI-based drug repositioning has its advantages and disadvantages. Network-based approaches are simple and reliable and are able to explore disease-drug target network relationships, but they cannot predict the targets of new drugs and are very limited. However, network-based approaches have great potential for deciphering the underlying mechanisms of complex diseases, the mode of action of drugs, and for repositioning disease-specific drugs. With feature-based approaches, drug development takes relatively long because the data requirements are relatively high and require specialized expertise to design the label. In particular, the development of robust model for feature-based computational drug repositioning is a very complex process. One of the biggest difficulties is to put theoretical computational approach into practice, because mapping between the theoretical approach and the behavior of biological organisms is more complex. As for matrix-based methods, because they do not rely on feature extraction and negative sample selection, they do not require setting labels and have a relatively short development time. However, inaccuracy, extreme data, and missing data can occur among samples, there is a deviation between the calculated and actual results of the matrix approach.

Hence, it is recommended that researchers combine different strategies and methods to achieve higher rates of success. The effective combination of different methodological strategies and available data will also lead to great advances in the field of drug repositioning. As artificial intelligence technology develops, more and more effective ways will emerge to help understand disease mechanisms and develop appropriate treatments. More algorithms being used in the drug development process in the future, combined with the foundation of traditional biological experiments, will be the basis for newly developed drugs with greater relevance and adaptability to the human body.

Acknowledgments

None.

Funding

This work is supported by the National Natural Science Foundation of China (Grant no. 62072157, 61802116) and the Natural Science Foundation of Henan Province (Grant no. 202300410102).

Conflict of interest

The authors declare that they have no competing interests.

Author contributions

Conceptualization: Qingkai Hu and Xianfang Wang
Visualization: Yifeng Liu, Yu Sang, and Dongfang Zhang
Writing – original draft: Qingkai Hu and Xianfang Wang
Writing – review & editing: Qingkai Hu and Xianfang Wang

Ethics approval and consent to participate

Not applicable.

Consent for publication

Not applicable.

Availability of data

Not applicable.

References

1. Peng C, Hu Y, Chen L, *et al.*, 2020, A review of drug repositioning algorithms based on machine learning and big data mining. *Adv Pharm*, 44(1): 6.

2. Zhang W, Gu F, Fu YK, *et al.*, 2021, Research progress of drug repositioning in new drug development. *Anim Husbandry*

Vet Med, 53(12): 123–127.

3. Nelson BS, Kremer DM, Lyssiotis CA, 2018, New tricks for an old drug. *Nat Chem Biol*, 14: 990–991.
4. Li FT, Liu MX, Wang XB, *et al*., 2022, Progress of COVID-19 drug repositioning study. *China Pharm Biotechnol*, 17(4): 8.
5. Huang F, Yang HF, Zhu X, 2021, Advances in the application of artificial intelligence in new drug discovery. *Adv Pharm*, 2021(7): 502–511.
6. Jarada TN, Rokne JG, Alhajj R, 2020, A review of computational drug repositioning: strategies, approaches, opportunities, challenges, and directions. *J Cheminform*, 12(1): 46.

   https://doi.org/10.1186/s13321-020-00450-7
7. Cheng, Fei X, Liu, *et al*., 2012, Prediction of drug-target interactions and drug repositioning via network-based inference. *PLoS Comput Biol*, 8(5): e1002503.

   https://doi.org/10.1371/journal.pcbi.1002503
8. Guney E, Menche J, Vidal M, *et al*., 2016, Network-based *in silico* drug efficacy screening. *Nat Commun*, 7(1): 10331.

   https://doi.org/10.1038/ncomms10331
9. Wang W, Yang S, Zhang X, *et al*., 2014, Drug repositioning by integrating target information through a heterogeneous network model. *Bioinformatics*, 30(20): 2923–2930.

   https://doi.org/10.1093/bioinformatics/btu403
10. Chen, X, Liu, Yan GY, 2012, Drug-target interaction prediction by random walk on the heterogeneous network. *Mol Biosyst*, 8(7): 1970–1978.
11. Olayan RS, Haitham A, Bajic VB, 2018, DDR: Efficient computational method to predict drug–target interactions using graph mining and machine learning approaches. *Bioinformatics*, 34(7): 1164–1173.

    https://doi.org/10.1093/bioinformatics/btx731
12. Peng J, Li J, Shang X, 2020, A learning-based method for drug-target interaction prediction based on feature representation learning and deep neural network. *BMC Bioinformatics*, 21(Suppl 13): 394.
13. Ji B, You ZH, Jiang HJ, *et al*., 2020, Prediction of drug-target interactions from multi-molecular network based on LINE network representation method. *J Transl Med*, 18(1): 347.

    https://doi.org/10.1186/s12967-020-02490-x
14. Lu XG, Liu F, Li JX, *et al*., 2021, A drug target prediction method based on multi-source data fusion and network structure perturbation CN112420126A. China: Hunan Province.
15. He JY, Yang XX, Gong Z, 2021. A computational drug repositioning method based on memory network and attention CN112331275A. China: Jiangsu Province.
16. Wang X, Li Q, Liu Y, *et al*., 2022, Drug repositioning of COVID-19 based on mixed graph network and ion channel. *Math Biosci Eng*, 19(4): 3269–3284.
17. Wall ME, Rechtsteiner A, Rocha LM, 2002, Singular Value Decomposition and Principal Component Analysis. Springer, Germany.
18. Shen M, Xiao Y, Golbraikh A, *et al*., 2003, Development and validation of k-nearest-neighbor QSPR models of metabolic stability of drug candidates. *J Med Chem*, 46(3): 3013–3020.

    https://doi.org/10.1021/jm020491t
19. Susnow RG, Dixon SL, 2003, Use of robust classification techniques for the prediction of human cytochrome P450 2D6 inhibition. *J Chem Inform Comput Sci*, 43(4): 1308–1315.
20. Christianini N, Shawe-Taylor J, 2002, Support Vector Machines and other Kernel-based Learning Methods. Cambridge University Press, United Kingdom.
21. Guengerich FP, 2006, Cytochrome P450s and other enzymes in drug metabolism and toxicity. *AAPS J*, 8(1): E101–E111.
22. Cheng F, Yu Y, Shen J, *et al*., 2011, Classification of cytochrome P450 inhibitors and noninhibitors using combined classifiers. *J Chem Inform Model*, 51: 996–1011.

    https://doi.org/10.1021/ci200028n
23. Napolitano F, Zhao Y, Moreira VM, *et al*., 2013, Drug repositioning: A machine-learning approach through data integration. *J Cheminform*, 5(1): 30.
24. Gottlieb A, Stein GY, Ruppin E, *et al*., PREDICT: A method for inferring novel drug indications with application to personalized medicine. *Mol Syst Biol*, 7(1): 496.

    https://doi.org/10.1038/msb.2011.26
25. Gönen M, 2012, Predicting drug-target interactions from chemical and genomic kernels using Bayesian matrix factorization. *Bioinformatics*, 28(18): 2304–2310.

    https://doi.org/10.1093/bioinformatics/bts360
26. Aliper A, Plis S, Artemov A, *et al*., 2016, Deep learning applications for predicting pharmacological properties of drugs and drug repurposing using transcriptomic data. *Mol Pharm*, 13(7): 2524–2530.

    https://doi.org/10.1021/acs.molpharmaceut.6b00248
27. Segler MH, Preuss M, Waller MP, 2018, Planning chemical syntheses with deep neural networks and symbolic AI. *Nature*, 555(7698): 604–610.

    https://doi.org/10.1038/nature25978
28. Hughes TB, Swamidass SJ, 2017, Deep learning to predict the formation of quinone species in drug metabolism. *Chem Res Toxicol*, 30(2): 642–656.
29. Turk S, Merget B, Rippmann F, *et al*., Coupling matched molecular pairs with machine learning for virtual compound optimization. *J Chem Inform Model*, 57(12): 3079–3085.

https://doi.org/10.1021/acs.jcim.7b00298

30. Zhang L, 2017, Research on Protein Class and Protein-Ligand Interaction Prediction Based on Machine Learning. Shandong University, China.

31. Chen P, Bao TJ, Yu SH, 2021, Drug relocation recommendation algorithm based on multi-similarity fusion. *Comput Technol Dev*, 31(1): 168-174.

32. Zhang H, An XY, Liu CH, 2022, Drug knowledge discovery based on multi-source semantic knowledge graphs: Empirical evidence with drug repositioning. *Data Anal Knowl Discov*, 6(7): 87–98.

33. Zeng X, Zhu S, Liu X, *et al*., 2019, deepDR: A network-based deep learning approach to *in silico* drug repositioning. *Bioinformatics*, 35(24): 5191–5198.

https://doi.org/10.1093/bioinformatics/btz418

34. Xuan P, Song Y, Zhang T, *et al*., 2019, Prediction of potential drug-disease associations through deep integration of diversity and projections of various drug features. *Int J Mol Sci*,1 20(17): 4102.

35. Yang M, Luo H, Li Y, *et al*., 2019, Drug repositioning based on bounded nuclear norm regularization. *Bioinformatics*, 35(14): i455–i463.

https://doi.org/10.1093/bioinformatics/btz331

36. Zhang W, Xu H, Li X, *et al*., 2020, DRIMC: An improved drug repositioning approach using Bayesian inductive matrix completion. *Bioinformatics*, 36(9): 2839–2847.

https://doi.org/10.1093/bioinformatics/btaa062

37. Peng LH, Tian XF, Zhou LQ, *et al*., 2021, A drug-target relationship prediction method based on deep forest and PU learning, CN112652355A. China: Hunan Province.

38. Yan Y, Yang M, Zhao H, *et al*., 2022, Drug repositioning based on multi-view learning with matrix completion. *Brief Bioinform*, 23(3): bbac054.

https://doi.org/10.1093/bib/bbac054

ACCSCIENCE PUBLISHING

Gene & Protein in Disease

REVIEW ARTICLE

Hydrogen sulfide donors and inhibitors in cancer research: A state-of-the-art review

Nazeer Hussain Khan[1†], Ebenezeri Erasto Ngowi[2†], Yan Li[3], Saadullah Khattak[1], Yingshuai Zhao[4], Muhammad Shahid[5], Ujala Zafar[6], Irum Waheed[7], Fatima Khan[8], Razia Virk[9], Istaqlal Hussain[10], Jiebin Cao[11], Hongxia Liu[12], Zhihui Liu[4]*, Dong-Dong Wu[12]*, and Xin-Ying Ji[1]*

[1]Henan International Joint Laboratory for Nuclear Protein Regulation, School of Basic Medical Sciences, Henan University, Kaifeng, Henan 475004, China
[2]Department of Biological Sciences, Faculty of Science, Dar es Salaam University College of Education, Dar es Salaam 2329, Tanzania
[3]Winship Cancer Institute of Emory University, 1365 Clifton Rd NE, Atlanta, GA 30322, USA
[4]Department of General Practice, Henan Provincial People's Hospital, People's Hospital of Zhengzhou University, Zhengzhou, Henan, 450003, China
[5]Department of Biological Sciences and Biotechnology, Faculty of Science and Technology, Universiti Kebangsaan Malaysia, Bangi, Selangor 43600, Malaysia
[6]Department of Materials science and engineering, Soft Matter Hybrid Laboratory Sungkyunkwan University Natural Sciences Campus, Sungkyunkwan South Korea
[7]Deprtment of Biological sciences, University of Agriculture Faisalabad, Faisalabad Pakistan
[8]Department of Chemistry, University of Sargodha, Sargodha Pakistan
[9]Department of Bio-Sciences, University of Wah, Rawalpindi Pakistan
[10]Department of Biological sciences, Government College University Faisalabad, Faisalabad Pakistan
[11]Center for Disease Control and Prevention, Erqi District, Zhengzhou, Henan 450001, China
[12]School of Stomatology, Henan University, Kaifeng, Henan 475004, China

[†]These authors contributed equally to this work.

***Corresponding authors:**
Zhihui Liu
(lzhh@163.com)
Dong-Dong Wu
(ddwubiomed2010@163.com)
Xin-Ying Ji
(10190096@vip.henu.edu.cn)

Citation: Khan NH, Ngowi EE, Li Y, *et al*., 2023, Hydrogen sulfide donors and inhibitors in cancer research: A state-of-the-art review. *Gene Protein Dis*, 2(1):164. https://doi.org/10.36922/gpd.v2i1.164

Received: July 30, 2022
Accepted: November 2, 2022
Published Online: December 15, 2022

Abstract

Hydrogen sulfide (H_2S), a gaseous biomolecule, is considered a key player in the regulation of various essential cellular events. Normal physiology is determined by the level of endogenous H_2S. Any alterations (upregulation and downregulation) to the level of endogenous H_2S may lead to illness, including the onset of tumorigenesis. Over the past two decades, extensive research on the role of H_2S in cancer development has affirmed the potential pharmacological means to suppress cancer progression by either inhibiting H_2S synthesis in cells or exposing exogenously supplied H_2S donors to treat different cancers. Some H_2S donors and inhibitors release H_2S or affect its synthesis. As a result, they have progressed through the development process into widespread clinical use and become increasingly important. The present study draws a detailed discussion on the types of H_2S donors and inhibitors and their role in cancer research. We believe that this state-of-the-art review will empower the synthesis of H_2S-based chemopreventive drugs and promote the need for further in-depth exploration of the associations between H_2S and cancer treatments in clinical settings.

Keywords: Cancer; Diagnosis; H_2S donors; H_2S inhibitors; Hydrogen sulfide; Treatment

1. Introduction

Hydrogen sulfide (H_2S) is a colorless, flammable gas with water-soluble properties and a rotten-egg odor. H_2S has historically been considered toxic and occupationally/

environmentally harmful[1]. In mammals, H_2S can be endogenously generated through the catalysis of L-cysteine and homocysteine by cystathionine γ-lyase (CSE) and cystathionine β-synthase (CBS), which are the two members of pyridoxal-5bers of pyri(PLP)-dependent enzymes that are predominantly found in the cytosol form[2]. Besides, 3-mercaptopyruvate sulfurtransferase (3-MPST), which is a non-PLP-dependent enzyme, acts in unison with cysteine aminotransferase (CAT) and in the presence of α-ketoglutarate to produce H_2S from L-cysteine. Both enzymes are colocalized in the cytosol and mitochondria[3]. Moreover, it has been indicated that D-amino acid oxidase can catalyze D-cysteine to form Achiral ketoacid and 3-mercaptopyruvate, which is further processed by 3-MPST into H_2S in both the brain and kidneys (Figure 1)[4]. The produced H_2S is then instantly released or converted into acid-labile sulfur or bound sulfane sulfur and stored in mammalian cells[5]. The catabolism of H_2S can occur through mitochondrial oxidation to sulfate and thiosulfate, excretion from the kidney or lung, sulfhemoglobin-mediated scavenging, and thiol methyltransferase and rhodanese-mediated methylation to generate methanethiol and dimethylsulfide[6].

Due to its unique chemistry, molecular reactivity mechanisms, ability to modify proteins, and active participation in many redox reactions with metal, H_2S has emerged as an essential signaling molecule in cancer biology. A huge volume of research has indicated the key roles of H_2S in a wide range of physiological activities related to cell cycle and tumorigenesis. H_2S is involved in angiogenesis, tumor growth, cellular and mitochondrial biogenesis, migration and invasion, tumor blood flow, metastases, epithelial-mesenchymal transition (EMT), DNA repair, protein sulfhydration, and chemotherapy resistance[7-10].

Since the last decades of research trend in translating H_2S to therapeutic forms, extensive efforts have been made by exploring natural H_2S-based molecules and designing synthetic ones (donors and inhibitors) to exploit the role of H_2S in cancer development. H_2S donors and inhibitors have gained importance and are being extensively explored to determine their clinical application in research, especially cancer. The research community is constantly struggling to design H_2S-based pharmacological drugs using these molecules and expecting significant breakthroughs in H_2S research in cancer. Considering the clinical importance of these naturally existing and those pharmacologically synthesized H_2S-based chemicals and research trends, it is worth summarizing the relevant literature that focuses on their use in translational research. The present study provides a detailed discussion of the types of H_2S donors and inhibitors and their role in cancer research. We anticipate that this state-of-the-art review will empower the synthesis of H_2S-based chemopreventive drugs and promote the need for further in-depth exploration of the associations between H_2S and cancer treatments in clinical settings.

2. Targeting exogenous H_2S for cancer treatment

2.1. Natural world

2.1.1. Allicin

Diallyl thiosulfinate, also known as allicin, is a biologically active compound found in garlic. Having antitumor and antimicrobial properties, this compound induces antitumor activities by regulating cellular processes, such as apoptosis, inflammation, oxidative stress, autophagy, and angiogenesis[11]. The mechanisms targeted in mediating its effects include post-translational modifications of the protein cell cycle, mitochondria apoptotic pathways, redox-sensitive signaling cascades, catalytic actions of telomerase enzyme, and activities of intercellular glutathione (GSH) and nucleic acid modifications[12]. The effects of allicin vary with different cancers and cell types[13]. It has been shown that the treatment of colon cancer cells (HCT-116) with allicin can effectively inhibit cell proliferation by promoting pro-apoptotic events characterized by the upregulation of Bax and cytochrome (Cyt)-c expressions, the downregulation of Bcl-2 and Bcl-xL, and subsequently, the activation of nuclear factor erythroid-2-related factor 2 (Nrf2) and deactivation of signal transducer and activator of transcription 3 (STAT-3) pathways[14]. The administration of allicin induces autophagic cell death in liver and thyroid cancer through the stimulation of p53 and the inactivation of protein kinase B (AKT)/mammalian target of rapamycin (mTOR) pathway, respectively[15].

In ovarian cancer, glioblastoma, gastric cancer, cervical cancer, and cholangiocarcinoma, the anti-carcinogenic effects of allicin have been found to be associated with the activation of c-Jun N-terminal kinase (JNK) mitogen-activated protein kinase (MAPK)/extracellular signal-regulated kinase (ERK) and p38 MAPK/Nrf2 pathways as well as the inhibition of STAT-3 cascades[16]. Furthermore, the loss of mitochondria potential, the activation of caspases, and the overexpression of p21, NOX4, and Bak have been reported in a breast cancer cellular model following the treatment with allicin[17]. A recent study has also revealed that allicin can effectively suppress the migration and invasion of gastric cancer cells by elevating miR-383-5p and inhibiting the receptor protein-tyrosine kinase ERBB4[18]. In addition, allicin effectively reverses the oncogenic properties of ornithine decarboxylase in neuroblastoma[19].

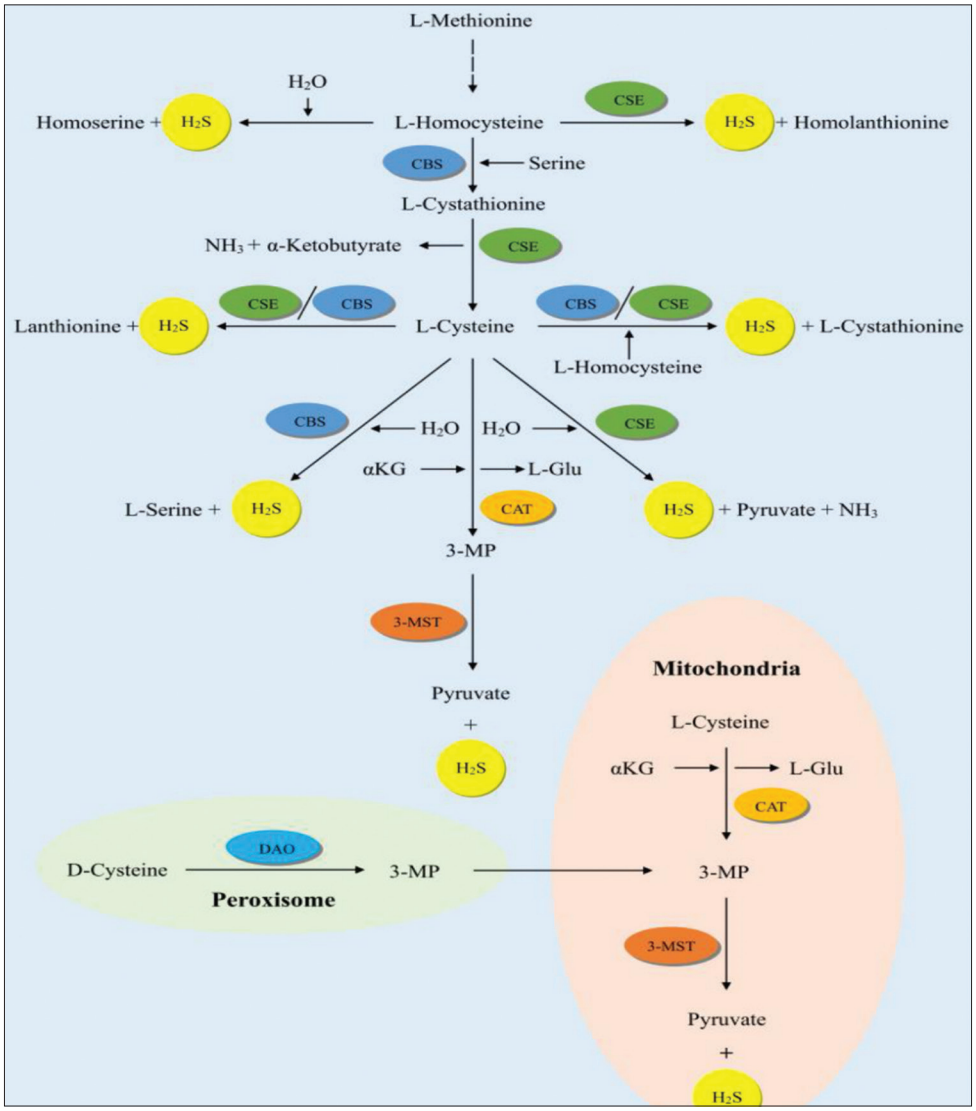

Figure 1. A schematic illustration of the biosynthesis of endogenous H_2S in mammals. H_2S: Hydrogen sulfide, H_2O: Water, CBS: Cystathionine β-synthase, CSE: Cystathionine γ-lyase, NH_3: ammonia, L-Glu: L-glutamate, αKG: α-ketoglutarate, 3-MST: 3-mercaptopyruvate sulfurtransferase, CAT: Cysteine aminotransferase, 3-MP: 3-mercaptopyruvate, DAO: D-amino acid oxidase.

Besides that, numerous studies have revealed the potential of allicin in enhancing the sensitivity effects of other anticancer therapeutics when used synergistically. For example, a combination of artesunate and allicin induces osteosarcoma cell death through caspase-dependent apoptotic pathways[20]. Similarly, the side effects of the anticancer drug cisplatin, especially in damaging stria vascularis, could be successfully reduced by synergizing the drug with allicin as shown in a mice model[21]. It has also been indicated that the sensitivity of temozolomide, a chemotherapy drug, can be significantly enhanced by allicin in glioblastoma through the upregulation of miR-486-3p[22]. The compound has also been reported to improve the sensitivity of 5-fluorouracil in different types of cancer, including hepatocellular, lung, and colorectal cancer (CRC)[23,24]. In addition, the cardiotoxicity of the anticancer drug doxorubicin in rats can be reduced by allicin through the attenuation of apoptotic, oxidative stress, and inflammatory responses[25].

In multiple myeloma, the use of allicin with dexamethasone increases the sensitivity of side population cells to the latter by upregulating the expression of miR-127-3p and inhibiting phosphatidylinositol 3-kinase (PI3K)/AKT/mTOR pathway[26]. Allicin can also increase the sensitivity of cisplatin-resistant lung cancer cells by suppressing hypoxia-inducing factors 1α and 2α in hypoxic cells. Apart from chemotherapy, allicin can enhance the

radiosensitivity of cancer cells by suppressing the nuclear factor-kappa B (NF-κB) signaling pathway in CRC[27] and through the promotion of intracellular DNA damage that is related to the downregulation of interleukin (IL)-6 and interferon-β as well as the increase in p53 expressions in glioblastoma[28]. Despite the promising anticancer effects of allicin, a recent study has shown that allicin can trigger hemolysis, eryptosis, and oxidative stress in erythrocytes through calcium overload and the activation of MAPK and casein kinase-1α[29]. The combined treatment of allicin with eryptosis inhibitors could be helpful in reducing the effect.

In recent years, nanoparticles have been established as effective and efficient carriers for delivering numerous drugs. In the case of allicin, its cytotoxicity in HepG2 cells has been demonstrated to be enhanced with the encapsulation of gelatin nanoparticles coated with glycyrrhetinic acid[30]. Moreover, the loading of allicin with cyclodextrin-based nanoparticles also enhances its delivery and the resulting corresponding pro-apoptotic effect on cancer cells[31]. Overall, allicin has shown promising anticancer activity. In addition, it is cost-efficient and can be used in combination with other drugs to increase sensitivity and alleviate side effects.

2.1.2. Ajoene

The anticancer properties of ajoene have been widely recognized and attentively investigated. Ajoene (4,5,9-trithiadodeca-1,6,11-triene-9-oxide) is a sulfur-containing organic compound formed after the rearrangement of allicin. Ajoene occurs in two forms: Z- and E-isomers. By characterization, the former is more bioactive, while the latter is relatively more stable. Recently, the compound has been shown to be synthesized in the laboratory through a new technique involving four key steps: (1) propargylation; (2) radical addition of thioacetate; (3) deprotection; and (4) disulfide formation/allylation. Ajoene has antimicrobial, antithrombosis, anti-inflammatory, and anticancer properties[32]. In cancer, the compound targets several activities, such as migration, apoptosis, oxidative stress, and protein folding[33]. A previous study has suggested that ajoene can induce anticancer effects in leukemia cells (HL-60) by triggering G2/M arrest, attenuating proteasome-mediated trypsin- and chymotrypsin-like activities as well as inhibiting ERK-1/2 signaling cascade[34]. Moreover, the ajoene has been shown to promote apoptosis in leukemic cells but not in peripheral mononuclear blood cells of healthy individuals by elevating the oxidative status and activating the NF-κB pathway[25]. Similarly, in lung adenocarcinoma, the treatment with 25 μM of ajoene significantly reduced the cell viability of cancerous cells A549, NCI-H1373, and NCI-H1395, but not non-carcinogenic bronchus cells BEAS-2B, partially through reactive oxygen species (ROS)-induced apoptosis and the activation of JNK/p38 cascade[25].

In a human study of basal cell carcinoma, the patients were topically treated with ajoene. The study showed that ajoene can effectively suppress tumor growth through the activation of mitochondria-dependent apoptosis and the subsequent reduction of antiapoptotic Bcl-2 expression[35]. Besides, apoptotic regulators such as p53, p63, and p73 have also been demonstrated to be activated by the compound in cellular models[36]. Furthermore, Z-ajoene could selectively inhibit cancer stem cells from glioblastoma multiform by attenuating phosphorylated (p)-SMAD4, p-AKT, and FOXO3A expressions[37]. In MDA-MB-231 and HeLa cancer cells, ajoene has shown to reduce migration and invasion activities through s-thiolation of cysteine-328 of the vimentin, thereby disrupting it and subsequently inhibiting metastatic activities[38].

An analog of ajoene, bis[(para-methoxy) benzyl], has more substantial anticancer effects. It acts by activating unfolded protein response mechanisms through CHOP/growth arrest- and DNA damage-inducible protein 153 (GADD153) in esophageal carcinoma[39]. In the treatment of colon cancer cells, Z-ajoene effectively inhibits tumor growth by decreasing the expression of β-catenin and increasing CK-1α-mediated β-catenin phosphorylation and prevents skeletal muscle atrophy induced by colon cancer by suppressing muscle-specific E3 ligases and NF-κB[40]. Therefore, ajoene can specifically and selectively target cancer cells as well as promote apoptosis and antimetastatic activities.

2.1.3. Diallyl sulfide (DAS)

DAS is a significant component of garlic with protective properties against various physiological disorders. The regulation of cellular markers associated with apoptosis, redox status, necrosis, angiogenesis, and cytotoxicity (cytochrome P450 2E1), as well as the interaction with membrane lipids are among the mechanisms targeted by the compound[41]. In cancer, DAS has been previously shown to delay the onset of cancer in chemically induced skin tumors in mice[42]. The corresponding effects of DAS are associated with the inhibition of key cellular pathways, such as p53, p21/Ras, PI3K/AKT, and p38 MAPK cascades, with JNK1 and ERK1/2 remaining unaffected[43]. *In vitro* evidence has revealed that DAS can effectively protect normal human breast cells MCF-10A from a carcinogenic chemical compound, diethylstilbestrol, which can cause DNA damage and lipid peroxidation[44].

In prostate cancer, DAS has been shown to improve oxidative status by suppressing a testosterone-mediated decrease in antioxidants[45]. It has also been reported that

DAS can potentially induce antiproliferative properties in thyroid carcinoma by activating the mitochondria apoptotic pathway as displayed by the elevation of Bax, caspase-3, -9, and cytochrome c (cyt c) expressions, as well as the suppression of Bcl-2 expression[46]. DAS can also prevent the progression of colon cancer by containing the gene expression and activities of arylamine N-acetyltransferase and downregulating ERK1/2 pathway[47]. In a leukemia model, DAS restored the elevated levels of P-glycoprotein (P-gp), a multidrug protein[48]. The treatment of cervical cancer cells with DAS has been reported to promote cell cycle arrest and apoptosis by increasing ROS, calcium ions (Ca^{2+}), and the number of cells accumulated in the gap 0 (G0)/G1 phase[49]. The treatment increases the expressions of p21, p27, p53, Bad, Bid, Bax, apoptosis-inducing factor (AIF), caspases, and cyt c but decreases the expressions of Bcl-xl, Bcl-2, cyclin-dependent kinase 2 (CDK2), CDK6, checkpoint kinase (CHK)2, and human papillomavirus (HPV) oncogenes E6 and E7[50].

Furthermore, treating neuroblastoma cells SH-SY5Y with DAS has been shown to suppress pro-proliferative activities and trigger apoptosis by increasing caspases activation and Ca^{2+} levels while suppressing NF-κB pathway[51]. In a mice lung cancer model, DAS significantly reduced tumor growth and increased antioxidant levels and apoptotic activities by suppressing the expression of fatty acid synthase[52]. In a recent study, the combination of paclitaxel and DAS has been demonstrated to improve skill texture and downregulate antiapoptotic protein Bcl-2 in a mice skin cancer model[53].

Alternatively, in esophageal carcinoma, a previous study has revealed that DAS is only effective when administered after its exposure to carcinogen, which suggests that the compound is more effective as a treatment rather than for prevention purposes[54,55]. Overall, DAS has considerable potential as a therapeutic option for cancer. However, further studies are required to shed light on the possible ways of improving its efficiency and reducing the side effects.

2.1.4. Diallyl disulfide (DADS)

DADS is an organosulfur compound from garlic with strong anticancer properties. It is formed from allicin. DADS has demonstrated its effects in different types of cancers through the regulation of apoptosis, oxidative stress, and cell cycle, along with several cellular pathways associated with cancer survival and progression[56]. For example, in colon cancer cells HT-29 and Caco-2, treatment with DADS has shown to induce anticancer effects by activating histone 3, inhibiting histone deacetylase (HDAC), and increasing p21 expression[57]. In HCT-116, DADS has been shown to trigger G2/M arrest by activating cyclin B1 and promoting apoptosis through ROS-mediated activation of p53 pathway, thereby promoting cell death[58]. In another colon cancer cell line SW480, treatment with DADS has shown to inhibit migration and invasion by downregulating glycogen synthase kinase (GSK)3β/NF-κB and LIM kinase-1 (LIMK-1)/dextrin/cofilin cascades, resulting in the suppression of vimentin, Ki-67, and CD-34 expressions and the elevation of E-cadherin[59]. Other signaling markers targeted with DADS treatment in colon cancer cells include the elevation of Ca^{2+} levels, phosphorylation of ERK, activation of STAT-1, and inhibition of Rac1/PAK1/LIMK1/cofilin pathways[60].

In leukemia, DADS induces cell death through the inhibition of Rac1/ROCK1/LIMK1/cofilin and ERK pathways as well as the activation of p38MAPK, Rac2/JNK, and caspase-dependent apoptotic pathways[61]. Its anticancer effects in leukemia cells are evident through the downregulation of vascular endothelial growth factor (VEGF) and calreticulin. It inactivates epidermal growth factor receptor (EGFR) and mTOR pathways that mediate the induction of G2/M and G0/G1 arrest through the downregulation of PARK-7, cofilin 1, and Rho GDP dissociation inhibitor 2[62].

In a mice prostate cancer model, testosterone and N-methyl N-nitroso urea-induced cancer and its associated features such as dysplasia, hyperplasia, and prostatic intraepithelial neoplasia were significantly reduced with DADS treatment[63]. In addition, it has also been reported that DADS treatment can promote apoptosis through G2/M arrest due to decreased CDK1 expression and the activation and inhibition of JNK and PI3K/AKT pathways, respectively. Furthermore, DADS also initiates histone hyperacetylation, increasing DNA damage, raising the expression of pro-apoptotic cell markers, and decreasing migration and invasion-associated proteins[64]. In hepatocellular carcinoma (HCC), DADS has been reported to reduce cell proliferation and migration by promoting apoptosis by regulating associated markers and G2/M arrest. Moreover, it also been reported to induce antiapoptotic activities and reduce toxicity by inhibiting CYP2E1[65]. Albeit, the pro-apoptotic effects of DADS can be increased in HCC by cotreating with other compounds, such as p38 or p42/44 MAPK inhibitors[66].

DADS enhances programmed cell death in breast cancer by promoting G0 arrest, altering Bcl-2 family proteins, inhibiting HDAC through histone-4 hyperacetylation, suppressing ERK, and activating SAPK/JNK and p38MAPK pathways[67]. The inhibition of ERK by DADS in breast cancer is initiated through the upregulation of miR-34a expression, leading to the inhibition of upstream cascades,

SRC and Ras[68]. Similarly, other studies have shown that DADS treatment can reduce breast cancer progression and metastases by elevating the expressions of tristetraprolin[68]. Furthermore, the investigation of normal breast cancer cells MCF-10A has indicated that DADS pre-treatment can protect against benzo(a)pyrene-induced cancer and the compound can help to avert environmentally induced cancer initiation[69]. It has also been demonstrated that DADS treatment can effectively inhibit pro-cancer activities in triple-negative breast cancer (TNBC) cells by suppressing antiapoptotic proteins and β-catenin activation[70]. In addition, nanoemulsions of DADS with α-linolenic acid can trigger G0/G1 arrest and regulate the ERK pathway in MCF-7 cells[71]. Moreover, the modification of DADS loaded in solid-lipid nanoparticles with receptor for advanced glycation end products antibody improves the efficiency of DADS by facilitating target-specific delivery and reducing off-target effects in TNBC[72].

DADS exerts its anticancer effects in lung cancer by regulating the expression of apoptotic proteins, increasing ROS levels, and Ca^{2+} elevation, inducing G2/M arrest, and activating p53, p42/44MAPK, and JNK pathways[73]. Cisplatin-resistant lung cancer cells A549/DPP can be sensitized to DADS by cotreating with small interfering (si)RNA *BCL-2*[74]. In a recent study, DADS has been shown to prevent cancer growth and EMT in A549 cells by suppressing E-cadherin and cytokeratin-18 as well as elevating N-cadherin and vimentin through inactivating Wingless and Int-1 (Wnt)/β-catenin pathway[75].

Moreover, the treatment of esophageal carcinoma models with DADS has been reported to cause cell death through the suppression of NAT and CYP2E1 expressions, the activation of mitochondria-apoptosis and p53/p21 pathways, and the inhibition of Raf/mitogen-activated protein kinase kinase (MEK)/ERK pathway[76].

In a recent study, DADS has also been shown to prevent the metastasis of type 2 esophageal-gastric junction adenocarcinoma cells by decreasing the expression of matrix metalloproteinases (MMPs) and increasing the expression of MMP tissue inhibitors partly through the inactivation of NF-κB and PI3K/AKT pathways[55]. Furthermore, DADS inhibits the cell cycle. DADS promotes ROS production, causes DNA damage, upregulates miR-34a, miR-22, and miR-200b expressions, as well as inhibits PI3K/AKT and Wnt/β-catenin cascades[77]. However, a possible resistance to DADS by gastric cancer cells has been found to be associated with the increase in GSH peroxidase or GSH levels, resulting in the alteration of ROS status. This suggests that the compound may not be fully efficient in treating this type of cancer[78]. Studies on skin cancer have demonstrated that DADS can prevent the progression of cancer by regulating cell cycle, apoptosis, and oxidative stress events by promoting the activation of p53- and p21-mediated Nrf2[42]. In brain tumors, treatment with DADS can effectively reduce p38 MAPK, NF-κB, and H-RAS expressions, increase peroxisome proliferator-activated receptor-gamma coactivator-1α and Ca^{2+} levels, trigger G2/M arrest, and activate JNK/c-Jun pathways and mitochondria-dependent apoptosis, which ultimately result in tumor suppression[79].

Furthermore, in the treatment of cervical cancer with DADS, the compound inhibits cell proliferation by targeting TAp73/ΔNp73 status and activating p53/p21 signaling pathways[80]. DADS induces its anticancer effects in bladder cancer by inhibiting N-acetyl transferase (NAT) activities as well as promoting ROS production and G2/M arrest[81]. Besides, the inhibitory effects of DADS have been reported in other types of cancers, including the suppression of EMT through MAPK/ERK inactivation in oral cancer, G2/M arrest in pancreatic cancer, G1/S arrest associated with MAPK phosphorylation in nasopharyngeal carcinoma, the upregulation of miR-34 and p21 expressions and inactivation of PI3K/AKT/mTOR in osteosarcoma[82], as well as C-MYC, specificity protein 1 (SP1), and MAD1-mediated attenuation of human telomerase reverse transcriptase (hTERT) in lymphoma. Overall, the role of DADS in cancer has been extensively studied, and numerous pathways have been implicated in the process. However, the research on the side effects of the drug and its elimination mechanisms is still lacking, thereby requiring further investigations.

2.1.5. Diallyl trisulfide (DATS)

Similar to DAS and DADS, DATS is an organic compound produced by garlic. It has immense therapeutic significance in different types of cancers. Dose combination also affects various cellular processes, including cell cycle, apoptosis, proliferation, EMT, and oxidative stress. Numerous *in vitro* and *in vivo* studies of different types of cancers have been conducted to investigate the drug's potential for therapeutic purposes. In prostate cancer models, DATS treatment has been shown to promote a decrease in the expression of X-linked inhibitor of apoptosis protein (XIAP), an increase in pro-apoptotic protein Bak, JNK1-mediated activation of ITCH ubiquitin ligase signaling axis, JNK1/2 and ERK1/2 activation; AKT, NF-κB, and p-STAT-3 inhibition; as well as G2/M arrest due to CHK1 activation and increase in p53 and p-Cdc25C expressions[82,83].

In breast cancer, DATS treatment suppresses the expressions of Bcl-2, Bcl-xL, MMP-2, estrogen receptor (ER)-α, lactate dehydrogenase-A (LDHA), Forkhead box Q1 (FOXQ1), hypoxia-inducible factor (HIF)-α, and

thioredoxin, increases ROS generation and Bak expression, stimulates activator protein (AP)-1 and apoptosis signal-regulating kinase (ASK)1-JNK-Bim signaling axis, and deactivates transforming growth factor (TGF)-β1, Wnt/β-catenin, NF-κB, ERK/MAPK, AKT, and Notch pathways[84]. In mice models, the combination of DATS and doxorubicin has been reported to induce multi-signaling targeted apoptosis, inhibit Notch and NF-κB pathways, and activate the p53 apoptotic axis[85]. Similarly, treatment with DATS in bladder cancer markedly suppresses EMT. DATS also elevates apoptotic activities in a caspase-dependent manner through the inhibition of PI3K/AKT and the activation of JNK pathway[86].

Recent studies have reported an increase in apoptosis and a decrease in EMT in bladder carcinoma cells following DATS treatment. G2/M arrest, NF-κ2 inactivation, ATM-mediated CHK2/Cdc25C/Cdc2 stimulation, and ERK1/2, JNK, and p38 phosphorylation were observed[87]. In gastric cancer, DATS treatment exerts pro-apoptotic properties by inducing mitotic arrest through ROS-dependent activation of AMP-activated protein kinase (AMPK) pathway, regulating apoptotic markers[88], and reducing ROS, sulfiredoxin, and malondialdehyde (MDA) levels. DATS also sensitizes gastric cancer cells to docetaxel and cisplatin by elevating the levels of metallothionein 2A, which leads to NF-κB pathway inhibition, and inhibiting Nrf2/AKT as well as activating p38MAPK/JNK signaling cascades, respectively[89].

Besides that, in the treatment of osteosarcoma with DATS, the compound also suppresses tumor growth by targeting G0/G1 through decreasing cyclin D1 and upregulating p21 and p27 by ROS-mediated PI3K/AKT inhibition[90]. DATS also suppresses P-gp and glucose-regulated protein 78, switches microRNA levels, downregulates NF-κB and Notch 1 pathways, as well as upregulates the expression of Ca^{2+}-binding protein calreticulin[91]. A recent study has also reported the downregulation of vimentin and Bcl-2 as well as the upregulation of Bax, Bak, and E-cadherin due to PI3K/AKT/GSK3β inhibition following the treatment of osteosarcoma cells with DATS[92].

Otherwise, in the treatment of lung cancer with DATS, the compound promotes DNA damage and apoptosis through the elevation of caspase-3, -8, -9, Bax, and Bak; the attenuation of Bcl-xl and Bcl-2 proteins; as well as the induction of JNK, p53, and p38 pathways[93]. DATS can also potentiate its protective effect in lung cancer by suppressing Wnt/β-catenin[94]. Furthermore, its modification with extracellular microparticle carriers enhances anti-inflammatory and ROS activities by suppressing S100 calcium-binding protein A8/A9, serum amyloid A, fibronectin, IL-6, and toll-like receptor-4. In thyroid carcinoma, it has been found that the induction of apoptosis is associated with the activation of ERK, JNK, and MAPK pathways, G2/M arrest through ATM and H2AX phosphorylation, and a positive feedback loop due to a rise in H_2S and CSE levels, resulting in NF-κB hyperactivation[95]. It has been shown that treating colon cancer cells with DATS can significantly promote cell death and reduce migration activities by inhibiting focal adhesion kinase (FAK), Src, and Ras, facilitating G1/S arrest by oxidating β-tubulin, ROS production, and mitochondria-mediated apoptosis[96].

The elevation of Ca^{2+} levels, the generation of ROS, the downregulation of antiapoptotic proteins, integrins, and FAK, and the activation of caspases and p53 pathway have been observed in skin cancer cells following DATS treatment[97]. Likewise, DATS improves the anticancer effects of cisplatin in ovarian cancer cells (SKOV-3)[98]. In leukemia, DATS treatment suppresses cancer progression by triggering G0/G1 arrest and caspase activation, the disruption of mitochondria potential due to high ROS levels[99], and the dimerization of heat shock protein (HSP)-27. In brain cancer, DATS reduces migration and proliferation activities by suppressing Wnt/β-catenin, mTOR, EGFR, C-MYC, active Bcl-2, and HDAC activity, and increasing histone acetylation and p21/p53 levels[100].

In pancreatic cancer, lymphoma, and nasopharyngeal carcinoma, DATS induces apoptosis through p53 elevation, TRAF-6 degradation and NF-κa inactivation, as well as caspase-8 and MAPK pathway activation, respectively[101]. Collectively, the above data confirms the potential of DATS in cancer treatment by targeting numerous vital signaling pathways associated with proliferation and migration activities. However, the research on the possible side effects and mode of action of this drug is still lacking regardless of the possibility. Figure 2 explains the signaling pathways involved in the apoptosis induction effect of DATS exposure.

2.1.6. Sulforaphane (SFN)

SFN is a sulfur-rich isothiocyanate (ITC) member commonly found in cruciferous vegetables, such as broccoli and cabbages. The compound is known to have anticancer properties. In a study, SFN has been reported to have a potent inhibitory effect in bladder cancer cells, which is associated with the suppression of growth promoters such as survivin, EGFR, and human epidermal growth factor receptor 2 (HER2)[102]. Treating bladder cancer cells with SFN also upregulates insulin-like growth factor (IGF)-binding protein-3, caspase-3, cyt c, and cell cycle inhibitor p27, resulting in G0/G1 arrest, as well as induces ROS-dependent mitotic arrest, Nrf-2 activation, HDAC inhibition[103], NF-κB

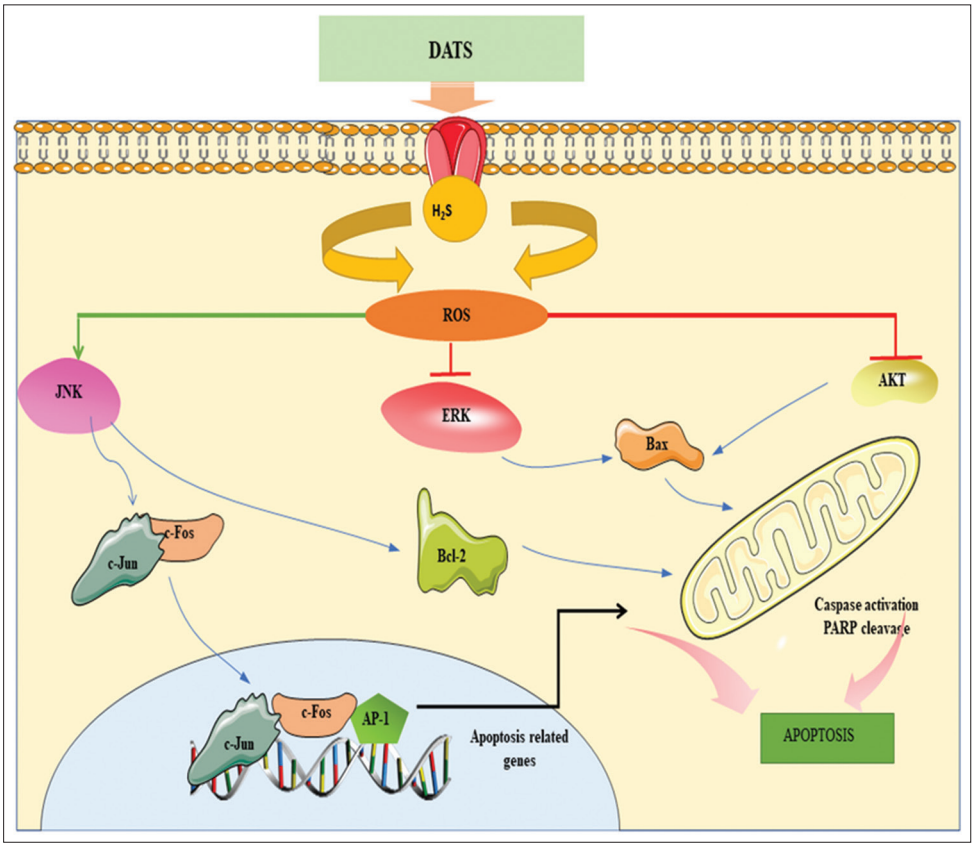

Figure 2. A schematic diagram of the signaling pathways involved in the apoptosis-induction effect of DATS exposure. DATS: Diallyl trisulfide, ROS: Reactive oxygen species, JNK: c-Jun N-terminal kinase, AP-1: Activator protein-1, ERK: Extracellular signal-regulated kinases, Bcl-2: B-cell lymphoma-2, Bax: Bcl-2-associated X protein, AKT/PKB: Protein kinase B, PARP: Poly-ADP-ribose polymerase.

deactivation, and cyclooxygenase (COX)-2 suppression through the elevation of p38 expression and activities. In addition, by downregulating COX-2 and upregulating miR-200c, SFN suppresses several EMT markers, including MMP-2, -9, Snail, and zinc-finger E-box-binding homeobox 1[104]. In recent studies, SFN has been shown to prevent the progression of bladder cancer by regulating the composition of gut bacteria and protecting the gut barrier, increasing the expression of FAT atypical cadherin[105], as well as downregulating HIF-1α expression and activities, thereby reducing glycolysis. The chemoresistance against everolimus, an mTOR inhibitor, and the upregulation of integrins α6, αV, and β1 in bladder cancer can be prevented by cotreatment with SFN[106]. In colon cancer, SFN promotes apoptotic activities by arresting cells at G1 and inhibiting ERK1/2 and AKT kinases, activating caspase-3 and chromatin condensation, upregulating p27 through S-phase kinase-associated protein inhibition, phosphorylating stress-activated protein kinase and suppressing C-MYC, overexpressing p21 and inducing G2/M arrest, activating MAPK pathways, suppressing HIF-1α and VEGF expressions, as well as increasing ROS generation[107]. Moreover, further studies have indicated that SFN treatment can also suppress the proliferation and metastasis of colon cancer by promoting Nrf2 expression through demethylation of its promoter, upregulating NmrA-like redox sensor 2, pseudogene and pseudogene activating ROS/p38 axis, and downregulating COX-2/microsomal prostaglandin E synthase-1 cascades as well as HDAC, hTERT, and miR-21 expressions. SFN also induces the downregulation of pro-inflammatory markers in colon cancer cells[108,109].

In breast cancer, SFN has been reported to prevent cell progression through the upregulation of early growth response 1 and thioredoxin reductase 1 expression and redox status, a reduction in the phosphorylation of AKT and S6K1 kinases, and a suppression in the expression of SERTA domain containing 1, cyclin D2, and HDAC 3, resulting in G1/S arrest[110]. In addition, the treatment of TNBC stem cells with SFN promotes cell death by inhibiting the expressions of Nanog, aldehyde dehydrogenase 1A1, Wnt3, Notch 4, and Crypto/Alk4 protein complex formation[111]. Moreover, in the treatment of gastric cancer with SFN, the compound inhibits the progression of cancer by mediating the induction

of G2/M arrest through the activation of mitochondria apoptotic pathway, p21 upregulation, and histone H3 phosphorylation, accompanied by the activation of ROS-AMPK pathway[112]. In addition, SFN causes cell death by inducing cell cycle arrest at the S phase through p21/53 upregulation and reducing the expressions of suppressor of variegation, enhancer of zeste, trithorax (SET) and myeloid-Nervy-DEAF1 domain-containing 3, myosin regulatory light chain 9, as well as cysteine-rich angiogenic inducer[113]. SFN also promotes the maturation of miR-29a-3p, reduces COL3A1 and COL5A1, inhibits the Wnt/β-catenin pathway phosphorylation of MAPK, deactivates EGFR and p-ERK1/2, and inhibits the Sonic hedgehog pathway[114].

In prostate cancer, SFN treatment facilitates apoptosis by increasing mitochondria ROS, apoptotic protease-activating factor-1, and Bax expression, and reduces the expression of phosphoglucomutase 3, the activation of caspases, the upregulation of Nrf2, the demethylation of cyclin D2, the suppression of androgen receptors, and the inhibition of STAT-3, HDAC6 deacetylase, ERK1/2, hTERT, and C-MYC[115,116]. In a recent study, treatment with N-acetyl-L-cysteine has been reported to inhibit fatty acid metabolism by acetyl-CoA carboxylase and fatty acid synthase suppression, which, in turn, inhibits prostate cancer inhibition[117]. SFN also induces the acetylation of histone H3 and H4, which leads to cell cycle arrest[118]. SFN has also been demonstrated to exert an inhibitory effect on ovarian cancer cell proliferation by attenuating retinoblastoma protein phosphorylation and E2F-1 expression[119]. Besides, SFN also triggers G1/G2/M arrest and inhibits the PI3K/AKT pathway[120]. In recent studies, SFN has been shown to increase the sensitivity of ovarian cancer cells to cisplatin by inhibiting NF-κB, HER2, and C-MYC as well as upregulating p53, p27, Bax, and miR-30a-3p, thus facilitating DNA damage[121]. In neuroblastoma, SFN promotes anticancer activities through caspase-dependent apoptosis, which is mediated by MEK/ERK activation[122]. Furthermore, in HCC, SFN reduces the expressions of Bcl-2, HIF-1α, and 6-phosphofructo-2-kinase/fructose-2,6-biphosphatase-4, increases the expression of caspase-3 and Bax, as well as activates Nrf2, p38, and ERK pathways to mediate cancer cell death[123]. SFN also activates Nrf2/antioxidant response element/heme oxygenase-1, inhibits STAT3/HIF-1α/VEGF, and ROS dependently inactivates TGF-β pathway and hTERT expression in HCC cells. SFN treatment significantly increases the demethylation of histone H4 on arginine 3 (H4R3me2s) in epidermal squamous cell carcinoma through the alleviation of protein arginine methyltransferase-5 and methylome protein 50 expressions[124].

In lung cancer, SFN upregulates the expressions of p21, p73, p53 upregulated modulator of apoptosis, Bax, cyclin D1, cyclin K, and caspases and downregulates the expressions of EGFR, cyclin B1, and Bcl-2[125]. SFN also suppresses miR-616-5p expression through histone modification, deactivates the GSK3β/β-catenin pathway to inhibit EMT and reduce stem cell-like properties in lung cancer cells, sensitizes lung cancer cells to treatments by upregulating miR-214, and inhibits IL-6/ΔNp63α/Notch pathways[126]. In nasopharyngeal carcinoma, SFN suppresses malignancy by preventing the reactivation of the Epstein–Barr virus lytic cycle, increases the expression of Wnt inhibitory factor 1, inhibits DNA methyltransferase 1, and inhibits the activation of STAT-3 through the upregulation of miRNA-124-3p[127]. Besides, in salivary gland adenoid cystic carcinoma, SFN treatment induces anticancer activities by mediating G2/M arrest, accompanied by the decrease in cyclin B1 and CDK1, the increase in caspases and Bax, and ultimately the inhibition of NF-κ pathway[128]. Overall, the effect of SFN on cancer suppression has been explicitly elaborated in different types of cancers, with the critical cellular markers and processes affected being identified. With the new focus on the drug clearance mechanism and potential side effects, vital information that might be useful in clinical application can be obtained.

2.1.7. 4-methylthiobutyl isothiocyanate (erucin)

Another common ITC compound is erucin. The protective power of this compound in cells is essentially attributed to its H_2S moiety. In addition to other mechanisms, erucin acts by regulating apoptosis and inflammatory processes[129]. In colon cancer, HCC, bladder cancer, prostate cancer, and lung cancer, treatment with erucin suppresses tumor growth and metastasis by promoting AKT and ERK phosphorylation and DNA damage, as well as blocking cell cycle at G2/M phase and p21/53 overexpression, respectively[130]. Erucin induces cell death in KRAS-mutated pancreatic cancer cell line AsPC-1 by suppressing ERK phosphorylation, which is a crucial mechanism to counteract KRAS-associated carcinogenic features associated with MAPK hyperphosphorylation[131]. Besides, treatment with erucin can effectively suppress carcinogenic activities by suppressing telomerase activities in ovarian cancer[132]. In breast cancer, erucin improves microtubule stability, induces cell cycle arrest, mitochondria translocation of cofilin and dynamin-related protein, mitochondria fission, and the downregulation of HER2 and S6 ribosomal protein phosphorylation[133]. Overall, erucin treatment exhibits anticancer activities in different cell types through a variety of mechanisms that are altered in cancer.

2.1.8. Allyl isothiocyanate (AIC)

AIC, a natural anti-inflammatory and anticancer compound, has been shown to have significant anticancer

effects. In breast cancer, AIC induces cell death by activating both mitochondria-dependent and -independent pathways[134]. G2/M arrest, ERK activation, and NF-κB inhibition have also been observed in breast cancer cells following AIC treatment[135]. However, in a recent study, AIC could not potentiate any significant apoptosis and its treatment yielded in the upregulation of antiapoptotic marker Bcl-2 and *MTOR* gene[136]. The reason behind this discrepancy is yet to be determined. Besides, in cervical cancer, oral cancer, lung cancer, and glioma, treatment with AIC significantly attenuates Bcl-2/Bax status, activates caspases, and promotes S/G2/M arrest, thus potentiating its anticancer effect[137]. In bladder cancer, AIC promotes pro-apoptotic activities by facilitating the activation of JNK, the phosphorylation of Bcl-2, and cell cycle arrest[138]. In a recent study, treatment with AIC nanoparticles in bladder cancer cells has demonstrated that AIC nanoparticles inhibit cell proliferation more potently compared to AIC by targeting pro-inflammatory markers, such as IL-6, tumor necrosis factor (TNF)-α, and inducible nitric oxide synthase (iNOS)[138,139]. Treatment with AIC also suppresses EMT events in HCC cells[139]. Moreover, in CRC, the antimetastatic effects of AIC have been reported to be associated with mitotic arrest, Ca^{2+} release, growth arrest and DNA damage inducible protein 153 (GADD153) activation, and the suppression of MMP expression and MAPK pathway[140]. Overall, AIC has shown potential in cancer treatment, although further studies are needed to understand the mechanisms involved and its clearance mechanism.

2.1.9. Benzyl isothiocyanate (BITC)

BITC is another natural H_2S donor and ITC derivative, which is strongly linked with cytoprotection and anti-carcinogenesis. The anticancer effect of BITC has been well-documented in several papers. In bladder cancer, BITC has been shown to reduce the incidence of cancer in mice that are treated with the carcinogenic compound N-butyl-N-(4-hydroxybutyl) nitrosamine and in cellular models through the upregulation of miR-99a-5p through ERK/c-Jun/AP-1 activation, which, in turn, downregulates the expressions of IGF1R, mTOR, and fibroblast growth factor receptor 3 cascades and reduces cell survival[141]. BITC treatment also promotes ROS production, G1 arrest, and protective autophagy through mTOR inhibition[142]. In breast cancer, treatment with BITC can effectively suppress pro-survival activities by targeting p53/liver kinase B1 (LKB1) and p73/LKB1 cascades and overexpressing transcription factor Krüppel-like factor 4 (KLF4)[143]. In addition, BITC can prevent osteoclast differentiation in breast cancer cells by inhibiting runt-related transcription factor 2 and receptor activator of NF-κF ligand[144]. The reduction of XIAP, FOXQ1, STAT-3, AKT, TGF-β, and TNF-α expressions and the elevation of ROS, caspases, FOXO1, and JNK/p38 MAPK activation have been observed in breast cancer cells following BITC treatment[145]. In lung cancer, BITC has been shown to suppress the resistance of cells to gefitinib and promote autophagy, apoptosis, and ROS generation[146]. It has also been suggested that BITC treatment can induce oral cancer cell death by mediating G2/M arrest and DNA damage by elevating pro-apoptotic markers and decreasing antiapoptotic ones[147]. In head-and-neck squamous cell carcinoma, BITC can suppress EMT markers such as vimentin and activate pro-apoptotic markers such as caspase-3 and poly-ADP ribose polymerase (PARP), thus resulting in anticancer activities[148].

Moreover, in HCC, BITC treatment has been reported to have anti-survival effects due to the reduction of MMPs and MAPK pathways[149]. In pancreatic cancer, BITC treatment can suppress the expressions of antiapoptotic proteins such as XIAP, p-PI3K, p-AKT, p-mTOR, p-FOXO1, p-FOXO3a, p-STAT-3, and NF-κB as well as activate MAPK pathways, resulting in increased cellular apoptosis and decreased angiogenesis[150,151]. Besides, BITC has antiproliferative effects when used to treat gastric cancer. These effects are associated with the inhibition of ERK1/2, Ras, iNOS, and COX-2 as well as the activation of death receptors[152]. The above evidence validates the potential of BITC in cancer treatment; however, further investigations are needed to understand the mechanisms of action for this donor and how H_2S moiety participates in ROS generation.

2.1.10. Phenylethyl isothiocyanate (PEITC)

PEITC is a slow-releasing H_2S donor and a member of ITCs. The donor works by regulating the cell cycle and oxidative stress, ultimately causing apoptosis. In oral cancer, PEITC has been reported to suppress the expressions of pro-migration markers, such as MMP-2 and -9, and increase the expressions of tissue inhibitor matrix metalloproteinase (TIMP)-1 and TIMP-2 by inhibiting several pathways, including MAPK, NF-κB, and EGFR signaling cascades[153]. PEITC also induces cell death by activating mitochondria-apoptotic pathways, death receptors, p21/53, and cell cycle arrest[154]. In glioblastoma, PEITC promotes apoptosis, cell cycle arrest, and anti-EMT activities through the activation of intrinsic and extrinsic pathways, along with the downregulation of MMPs, CDC20, cyclin B1, MCL-1, and XIAP expressions[155]. Similarly, PEITC treatment has also been shown to inhibit death receptors and activate TGFβ/Smad2 signaling pathways in cervical cancer[156]. In the treatment of gastric cancer with PEITC, the latter inhibits the expressions of MMPs, FAK, Ras, growth factor receptor-bound protein 2, COX-2, and VEGF

as well as disrupts microtubules to promote apoptosis and anti-migratory events[157]. In colon cancer, PEITC inhibits NF-κB, AKT, ERK, and JNK to mediate anticancer properties[158]. The treatment of ovarian cancer cells with PEITC has revealed that the latter exhibits pro-apoptotic activities through the activation of caspases, p38, and JNK, and the inactivation of AKT/ERK1/2 and CRM1-mTOR/STAT3 pathways[159].

In lung cancer, PEITC treatment promotes G2/M arrest, elevates cleaved caspase-3, PARP, GADD153, endonuclease G, and Bax, and inactivates the Janus kinase 2 (JAK2)/STAT3 pathway, thus facilitating cell death and reducing migration activities[160]. In melanoma, PEITC induces cell death through the activation of mitochondria apoptosis and the elevation of ROS level[161]. Moreover, PEITC administration suppresses Bcl-2 and Bcl-xL, elevates Bak, inhibits Notch 1 and 2 cascades in pancreatic cancer, and inhibits Wnt/β-catenin in CRC[162]. In prostate cancer, PEITC treatment decreases the expressions of CDK1, cyclin B1, CDC25C, α/β-tubulin, surviving, and XIAP, and increases the expressions of miR-194, caspases, p53, and WEE1 to mediate anticancer activities[148]. Furthermore, PEITC induces cell apoptosis in breast cancer cells through the elevation of p53, the suppression of ER-α36, metadherin, HER2, EGFR, and STAT-3 expressions, and the reactivation of cadherin[148,163]. The above data suggests that PEITC has potential in cancer treatment; however, little is known concerning the drug's mode of action and clearance mechanism.

2.1.11. N-acetyl cysteine (NAC)

NAC is a H_2S donor and a precursor for L-cysteine and reduced GSH. It is a cytoprotective compound with potent antioxidant properties[164]. NAC-derived cysteine releases H_2S in the mitochondria, elevating 3-MPST and sulfide quinone oxidoreductase (SQR), which are the potential upstream regulators of sulfane sulfur species[165]. In a recent study, NAC has been shown to serve as a substrate for 3-MPST and SQR in colon cancer cells. However, the event did not significantly alter their viability and rate of proliferation[166]. In contrast, NAC-mediated elevation of 3-MPST activities and intracellular H_2S level exhibits antiproliferative properties in neuroblastoma cells (SH-SY5Y)[167]. Besides, NAC can reverse the anti-tumor effect of xanthatin, including G2/M arrest and ROS-mediated autophagy and apoptosis, in colon cancer cells[168]. In gastric cancer, NAC promotes SJ-89 cell cycle arrest, apoptosis, and DNA damage[169]. Further evidence has shown that NAC treatment can suppress the metastasis and glycolysis of gastric cancer cells, resulting from autophagy inhibition-mediated ROS, through the deactivation of NF-κB and HIF-1α[170]. Cotreatment with NAC, however, may restore pro-cancer properties following treatment with anticancer drugs that initially work by raising ROS levels, such as piperlongumine.

Meanwhile, the combination of NAC with bromelain shows more potency in inhibiting the growth of gastrointestinal cancer by facilitating caspase-dependent apoptosis and autophagy[171]. Moreover, a clinical trial has revealed that the administration of NAC can reduce oxaliplatin-induced neuropathy in CRC and gastric cancer patients[172]. In lung cancer, individual treatment with NAC has pro-cancer effects that are associated with reduced ROS, p53 activity, and DNA damage; however, when administered in combination with other therapeutics, it shows solid anticancer activities[173]. NAC enhances glioblastoma cell death in an antioxidant-independent manner by facilitating lysosomal degradation of Notch 2 cascade, thus resulting in the attenuation of the pathway[174]. In gastric cancer cells, NAC can effectively attenuate ROS-induced apoptosis, triggered by anticancer drugs like curcumin[175].

In human breast cancer MDA-MB-435 cells, treatment with NAC induces cell death and vascular collapse by promoting apoptosis and the production of antiangiogenic mediator angiostatin, as well as shifting estrogen metabolism by inhibiting the formation of DNA adducts[176]. In addition, NAC suppresses cancer proliferation by attenuating Ki67 expression and the glycolysis marker stromal monocarboxylate transporter 4[177]. However, there have been conflicting studies, wherein NAC treatment, combined with other potential anticancer drugs, can either enhance or suppress the drug's cytotoxicity[178]. The mode of action of the treatment plays a key role in determining the synergistic effect of NAC. In a recent clinical trial, oral administration of NAC in breast cancer patients effectively reduced paclitaxel-induced peripheral neuropathy and improved the quality of life in these patients[179]. Moreover, NAC treatment also exhibits anticancer effects in bladder cancer linked with the activation of caspases, cell cycle arrest, and suppression of metastasis through MMP-2 downregulation[180]. In bladder cancer, the co-treatment of cis-dichlorodiammineplatinum and GSH with NAC significantly reduces ROS generation from the initial treatment, suggesting the restoration of carcinogenesis[181].

In prostate cancer, NAC treatment suppresses cancer metastasis through ROS regulation, CYR61 upregulation, NF-κB inhibition, and the partial activation of AKT and ERK1/2[182]. In addition, the pro-inflammatory effects of cisplatin and etoposide (VP-16) may be suppressed by NAC[183]. Besides, in ovarian cancer, the cotreatment of doxorubicin with NAC enhances its anticancer effect, which is associated with ATM/p53 pathway activation and mTOR

inhibition[184]. Furthermore, NAC treatment can inhibit radiotherapy-induced premature ovarian failure through the suppression of nicotinamide adenine dinucleotide phosphate oxidase 4 (NOX4)/MAPK/p53 pathway and the promotion of VEGF, thus conserving ovarian function[185]. In addition, NAC can reduce oxidative injury by increasing GSH peroxidase activity and decreasing the expression of nicotinamide adenine dinucleotide phosphate oxidase subunits (p22 and NOX4). It has also been demonstrated that NAC treatment can effectively attenuate cell invasiveness and proliferation in pancreatic cancer by regulating the cell cycle[186]. The combination of NAC with anticancer drugs, such as bromelain and curcumin, results in potent anticancer activities that are associated with attenuating migration markers such as MMP-2 and -9 as well as suppressing ROS-induced activation of ERK/NF-κB[187].

In HCC, treatment with NAC can restore intracellular GSH levels and IL-2-induced cytotoxicity of mononucleated cells[188]. NAC reduces liver damage and the incidence of post-embolization syndrome following transarterial chemoembolization in HCC patients[189]. In lung cancer, NAC adducts are significantly lowered, and its administration reduces the oxidative stress and senescence caused by the inactivation of transcription factor JunD, in addition to lung emphysema; however, it concurrently promotes the progression of cancer[190]. Briefly, these data suggest that NAC has inhibitory properties on different types of cancers. Its combination with other drugs may further enhance/attenuate the effect, depending on the drug's mode of action. Besides, the cotreatment of NAC with for drugs that initially work by facilitating ROS generation may not be a good option due to the antioxidant properties of nicotinamide adenine dinucleotide (NAD).

2.2. Native compound

2.2.1. Sodium hydrosulfide (NaHS)

NaHS is a fast-releasing H_2S compound and one of the most common donors in H_2S-related research. Being a fast-releasing donor, it produces enormous amounts of H_2S in a remarkably short period of time followed by a subsequent decline in production. Depending on the dose administered and the type of cancer and cell, the drug is known to induce dual effects; thus, there are numerous conflicting reports. The compound also regulates cellular processes, resulting in the modulation of tumor growth and sensitivity to drugs[191]. In a glioblastoma model, treatment with NaHS facilitated tumor growth in the animal model by upregulating HIF-α expression and in C6 cells by activating the p38MAPK/ERK1/2/COX-2 signaling axis[192]. However, another study has suggested that the treatment with NaHS promotes apoptotic activities through the activation of p38 and p53 cascades in C6 cells[193]. Similarly, in colon cancer, NaHS treatment promotes cancer progression and metastasis by upregulating the expressions of SIRT-1, p-AKT, and p-ERK as well as downregulating p21[194]. In a recent study, NaHS reduced cell proliferation in CRC, but it did not induce apoptosis by upregulating Ca^{2+} levels through the activation of transient receptor potential cation channel subfamily V member 1; the effect was only observed in metastatic cells but not in normal cells[195].

In multiple myeloma and oral squamous cell carcinoma, NaHS exhibits pro-cancer effects by promoting the phosphorylation of AKT and ERK1/2 cascades[196]. Moreover, it promotes cancer metastasis through the activation of HSP-90 and JAK2/STAT-3 in esophageal carcinoma EC109 cells; NF-κB, STAT-3/COX-2, and HIF-α/adenosine triphosphate-sensitive potassium channel activation in HCC; and the upregulation of MMP-2/-9 in bladder cancer EJ cells[197]. Alternatively, in lung cancer, treatment with NaHS alleviates carcinogenic activities, including EMT, through TGF-β1/Smad2/Smad3 suppression and the activation of caspase-3, p21, and p53 cascades[198,199].

NaHS also inhibits the proliferation of melanoma cells by blocking PI3K/AKT/mTOR activation and breast cancer cells by inducing G0/G1 arrest and p-p38 MAPK inhibition. In neuroblastoma, treatment with NaHS suppresses adenylyl cyclase and γ-secretase, reduces intracellular cyclic adenosine monophosphate levels and dynamin-like protein expression, and increases ERK phosphorylation[199,200]. These data imply that H_2S has a role in cancer progression; however, the potential of NaHS for cancer treatment is relatively insignificant.

2.2.2. Sodium sulfide (Na_2S)

Na_2S is another fast-releasing H_2S-donating compound that is associated with cancer therapeutics. In CRC patients, Na_2S treatment in human mesenteric arteries results in the relaxation of vessels by targeting potassium ion (K^+) channels[201]. The compound has been reported to selectively kill glioblastoma T98G and U87 cells, while showing no effect in cerebral microvascular endothelial cells (D3), through a mechanism that involves the elevation of ROS levels and the suppression of mitochondria activities, resulting in DNA damage and subsequent cell death[202]. In addition, Na_2S treatment also sensitizes glioblastoma cells to radiotherapy[203]. In an earlier study, the anticancer effect caused by the inhibition of CBS in ovarian cancer was found to be reversible with low doses of Na_2S[204]. Despite the fact that there are only a number of studies on Na_2S, evidence has indicated that Na_2S has protective and

robust anticancer effects. However, its inability to imitate the physiological production of H_2S affects its applicability.

2.2.3. Other metal sulfides

Apart from Na_2S, sulfides of other metals, such as calcium and copper, also have anticancer properties, as witnessed in experimental settings. Although there are no existing studies on individual drug administration containing the aforementioned metal sulfides in cancer; their nanoparticle formulations have been well-documented. Calcium sulfate (CaS) nanoparticles are known to trigger cell cycle arrest and induce apoptosis in lung cancer cells, but no significant effect has been reported in normal cells[205]. Similarly, copper sulfate (CuS) nanoparticles have been reported to possess the ability to target tumor cells and penetrate their nucleus by modifying surface peptides RGD and TAT[206]. In a study, the cotreatment of CuS nanoparticles with 980 nm near-infrared laser irradiation causes cell death by increasing the temperature of the nucleus and destroying the genetic materials. In cervical cancer cells, CuS nanoparticles have been shown to induce a concentration-dependent photothermal destruction with low cytotoxicity[207]. The evidence suggests that metal sulfides are useful as H_2S donors and have a role in cancer suppression; however, further research is needed to illuminate the mechanisms involved and side effects.

2.3. *De novo* design

2.3.1. Morpholin-4-ium 4 methoxyphenyl(morpholino) phosphinodithioate (GYY4137)

GYY4137 is the most common synthetic slow-releasing H_2S donor in research. It is soluble in water and exhibits a strong anticancer effect in both cellular and animal models. In various cellular models of cancer, including prostate, cervical, lung, breast, and ovarian cancer, treatment with GYY4137 can effectively promote pro-apoptotic activities by increasing lactate production, reducing intracellular pH levels, and facilitating G2/M arrest[208]. In CRC, treatment with GYY4137 promotes cell cycle arrest, apoptosis, and necrosis[209]. In addition, drug causes intracellular acidification in both ovarian and CRC cancer, due to uncoupling of sodium-calcium exchanger 1 and sodium-hydrogen exchanger1 channels[210]. Treating colon cancer cells HCT116 with GYY4137 also increase LDHA activity and induce concentration-dependent cell death by inactivating cGMP/VASP, AKT, and p44/42 MAPK (ERK1/2) pathways[187]. Moreover, in HCC, GYY4137 upregulates caspases and blocks STAT-3 activation, thereby inducing G1/S arrest and cell death[211]. In a recent study, GYY4137 has also been shown to protect neuroblastoma cells against lipopolysaccharide-induced elevation of inflammatory activities[212]. The above data suggest that GYY2137 could serve as a potential anticancer drug. However, further research is needed to investigate the mechanism of action, cellular marker, and signaling pathways involved.

2.3.2. 5-(4-hydroxyphenyl)-3H-1,2-dithiole-3-thione (ADT-OH)

ADT-OH is an artificial H_2S donor with significant chemoprotective effects against cancer cells. It is an extraction from amphiphilic block copolymers containing an ester bond linking ADT-OH using isoleucine and glycine linkers[213]. In a recent study, treating melanoma cells with ADT-OH have been shown to inhibit the progression of cancer by downregulating XIAP and Bcl-2 as well as stabilizing Fas-associated protein with death domain and IκB-α, resulting in NF-κB inactivation[214]. Furthermore, connecting ADT-OH with hyaluronic acid forms another novel H_2S donor (HA-ADT), which can produce more H_2S and induce more anticancer effects in breast cancer than commonly used donors, such as NaHS and GYY4137[215]. This effect is associated with the deactivation of PI3K/AKT/mTOR and RAS/RAF/MEK/ERK pathways. The above evidence supports the use of H_2S in the treatment of cancer and suggests that newly synthetic donors with high efficiency could be the key.

2.3.3. S-propargyl-cysteine (SPRC)

SPRC, also known as ZYZ-802, is a structural analog of S-acetyl cysteine and a crucial substrate for CSE, thus making it an endogenous H_2S donor. Like other H_2S donors, SPRC regulates cellular activities, including inflammation, apoptosis, and oxidative stress. In a mice model of gastric cancer implants, treatment with SPRC significantly reduced tumor weight and volume by promoting pro-apoptotic activities in cancer tissues through the elevation of Bax expression, cell cycle arrest at G1/S phase, and the activation of p53 pathway[216]. The anticancer effects of SPRC can be reversed with peginterferon alfa-2a (PAG) treatment. Likewise, in pancreatic cancer, treatment with SPRC causes the inhibition of cell viability and proliferation by triggering G2/M arrest and apoptosis through the upregulation of p53 and a reduction in JNK degradation through phosphorylation[217]. From the information above, SPRC has shown potential in cancer treatment; however, a dearth of research has limited its applicability in clinical settings.

2.3.4. (10-oxo-10-(4-(3-thioxo-3H-1,2-dithiol-5yl) phenoxy) decyl) triphenylphosphonium bromide (AP39)

AP39 is a compound that targets mitochondria through triphenylphosphonium moiety and releases H_2S inside the

organelle. According to preliminary studies, H_2S induces cytoprotective effects by promoting oxidative stress, apoptosis, and inflammation[217]. Treatment with AP39 has been shown to increase the population of early and late apoptotic cells among colon cancer cells[218]. In addition, it also protects against doxorubicin-induced cardiotoxicity, which is associated with mitochondrial toxicity and a decrease in H_2S level[219]. Despite the lack of vital information on the mechanisms and pathways targeted by this donor in different types of cancers, the available data suggest a potential anticancer effect and protective effect when combined with other drugs.

2.3.5. Ammonium tetrathiomolybdate (ATTM)

ATTM is a slow-releasing inorganic H_2S donor with cytoprotective capability. The chemical formula of ATTM is $(NH_4)_2MoS_4$. ATTM has been shown to exert antioxidant effects at lower concentrations in HaCaT cells[220]. Treating pancreatic cancer cell lines with ATTM dose and time dependently reduces intracellular high affinity copper uptake protein 1, VEGF, and cyclin D1 expressions, thus mediating anticancer activities[221]. In head-and-neck squamous cell carcinoma, ATTM has been reported to suppress resistance to cisplatin by attenuating the progression of cancer by downregulating the expression of ATPase copper transporting beta (ATP7B)[222]. Similarly, in breast cancer, treatment with ATTM reduces the expression of ATP7A, a copper ATPase transporter that is involved in the intercellular movement and sequestering of cisplatin, thereby potentiating cisplatin's nuclear bioavailability, which, in turn, promotes DNA damage, cell cycle arrest, and apoptosis[223]. The safety, tolerance, and anticancer effects of recurrent breast cancer in patients have been witnessed in a clinical study involving the drug[224]. Moreover, treating lung cancer cells with ATTM significantly increase the expression of H_2S-producing enzymes CBS and 3-MPST and promote cancer progression at low concentrations, with an opposite effect at higher concentrations[225]. At lower concentrations, ATTM triggers YTHDF1-dependent PRPF6 m^6A methylation through the upregulation of methyltransferase-like protein 3 and the downregulation of fat mass and obesity associated-protein (FTO). Overall, these data suggest that ATTM shows potential in cancer treatment; however, the information available on the mechanism of action involved is insufficient.

2.3.6. H_2S-releasing nonsteroidal anti-inflammatory drugs (H_2S-NSAIDs)

H_2S-NSAIDs are H_2S-moiety-containing anti-inflammatory drugs with potent anticancer properties. One of the most common H_2S-NSAIDs is ATB-346, a naproxen derivative [2-(6-methoxynapthalen-2-yl)-propionic acid 4-thiocarbamoyl phenyl ester]. In addition to producing H_2S, it inhibits COX-2 activity. The previous studies have shown that treatment with ATB-346 can significantly reduce colonic pre-cancerous lesions in mice, prostaglandin, and whole-blood thromboxane synthesis without causing gastrointestinal injury[226]. The anticancer effects of ATB-346 are associated with the inhibition of C-MYC and β-catenin expressions. Similarly, treating melanoma cells with ATB-346 inhibit pro-survival activities by suppressing NF-κB and AKT pathways[227]. This suggests that the donor ATB-346 has anticancer activities and can be used to treat different types of cancers.

2.4. Hydrogen sulfide-nitric oxide (H_2S-NO) donors

2.4.1. NOSH-aspirin (NBS-1120)

Both NO and H_2S are powerful neuromodulators, and their role in cancer is widely recognized. The two gaseous neuromodulators regulate one another. For the donor to logically contain the moiety for both gasotransmitters, it induces a more substantial regulatory effect. According to a previous study, NBS-1120 exhibits chemoprotective properties in the gastrointestinal tract, which are inextricably linked to its antioxidant and anti-inflammatory effects, thus making it superior to aspirin[228]. Moreover, treating colon cancer cells with NOSH-aspirin significantly facilitate apoptosis, G0/G1 arrest, ROS generation, and NF-κB deactivation[229]. Mechanistically, NOSH-aspirin mediates both S-sulfhydration and S-nitrosylation of p65 NF-κB, along with the denitrosylation and desulfhydration of caspase-3, thereby inhibiting the activation of caspase-3 and NF-κB[230]. According to another study, the compound preferentially inhibits COX-1 over COX-2, and its effect varies with different isomers, with the inhibitory effect in colon cancer ranking as follows: *o*-NOSH-aspirin > *m*-NOSH-sspirin > *p*-NOSH-aspirin[231]. In a mice colon cancer model, the combination of NOSH-aspirin with 5-fluorouracil induced a stronger effect compared to individual treatments and showed no side effects or weight loss in mice[232,233]. In breast cancer, the drug treatment results in tumor suppression through the reduction of proliferating cell nuclear antigen, an increase in cyt c, and ROS generation[234]. Similarly, a recent study has revealed that the treatment with NOSH-aspirin exerts anticancer effects in a mice model of pancreatic cancer by increasing ROS generation, caspase-3 activity, and mutated p53 expression, while suppressing NF-κB and FoxM1 expressions[235]. Overall, the above data suggest that NOSH-aspirin can be used to treat cancer, with minimal side effects and by primarily targeting the cell cycle, COX-1/2, and ROS.

2.4.2. NOSH-sulindac (AVT-18A)

Another H_2S and NO donor is NOSH-sulindac. This compound has been shown to induce apoptosis in cancer cells at a relatively lower concentration than normal cells. The treatment of NOSH-sulindac resulted in over 150 times cell growth inhibition in human breast cancer cells MCF-7, pancreatic cancer cells BxPC-3, and colon cancer cells HT-29 as compared to its treatment in normal lung cells IMR-90, pancreatic epithelial cells ACBRI 515, and normal breast cells HMEpC[236]. Its effect is associated with the suppression of pro-inflammatory TNF-α, oxidative marker MDA, the induction of G2/M arrest, and apoptosis[237]. The effect of this donor on colon cells has been reported to be independent of the cell's ability to produce prostaglandin[238]. As of now, no mechanism has been found to be associated with the inhibitory effect of NOSH-sulindac; hence, the potential of this donor has yet to be determined.

With all the given findings, it is widely recognized that the treatment with H_2S donors (exposure of H_2S) can inhibit the proliferation of cancer cells, induce apoptosis, and promote cell cycle arrest, thus resulting in cancer cell death (Figure 3). However, there is still room for investigation concerning H_2S donors induction, the initiation of cancer cell death signaling, and their causes. Figure 4 is a schematic presentation of exogenous H_2S-based natural and synthesized chemical compounds used in cancer research.

3. Targeting endogenous H_2S for cancer treatment

3.1. CSE inhibitor

CSE is a major contributor to H_2S production in numerous cells. Targeting this marker directly affects cell viability and progression. For example, CSE has been reported to be highly upregulated in breast cancer patients, in which the event positively corresponds to breast cancer metastasis by elevating angiogenic factor VEGF and activating various signaling pathways, such as PI3K/AKT, Ras/Raf/MEK/ERK, and STAT-3[239]. By knocking down CSE in breast cancer cells, MDA-MB-231 significantly suppresses both migration and proliferation activities[240]. Treatment with CSE drug inhibitors, such as I157172 and I194496, potently suppresses CSE activities with pro-cancer events through the promotion of sirtuin 1 and the inhibition of STAT-3, VEGF/FAK/paxillin, PI3K/AKT, and Ras/Raf/MEK/ERK pathways[241]. Similarly, CSE has a pro-cancer effect in gastric cancer; its inhibition prevents cell growth and metastasis through promoting apoptosis and improving anticancer drug sensitivity[242]. SP1-dependent activation of PI3K/AKT pathway in HCC cells has shown that it acts through CSE to enhance tumorigenesis[243,244]. Simultaneously, the inhibition of CSE suppresses EMT markers and EGFR though ERK1/2 inactivation, thus resulting in cancer suppression[245]. Knocking down CSE also increases radiosensitivity and reduces radiation-mediated promotion of EMT by blocking the p38 MAPK pathway[246]. However, a recent study has revealed that the inhibition of CSE in mice negatively regulates the immunosuppressive enzyme indoleamine 2,3-dioxygenase 1, creating an immune-tolerant tumor microenvironment. This event can be reduced by overexpressing CSE or increasing H_2S levels[247]. This negative correlation can also be confirmed in clinical samples. These conflicting results show a need for further studies on cancer and the role of CSE. In colon cancer, the activation of Wnt/β-catenin pathway is associated with the upregulation of CSE expression.

In a study, the proliferation of SW480 cells was significantly reduced by CSE-knockdown, suggesting the enzyme's potential role in colon cancer metastasis[248]. CSE-mediated production of H_2S has been reported to promote the progression of prostate cancer through the activation of Cav3.2 and IL-1β/NF-Kb cascades, whereas CSE inhibition results in anticancer effects in PC-3 cells[249]. Overall, the above data suggest that CSE inhibitors have the potential to be anticancer drugs in certain types of cancers; however, less is still known about their mechanism of action, clinical applicability, and possible side effects.

3.2. CBS inhibitor

CBS is also a key player in cancer activities. Therefore, understanding its inhibition effect on cancer is of paramount importance. It has been previously reported that CBS is highly upregulated in gastric cancer tissues compared to non-cancerous ones. Its inhibition with amino-oxyacetic acid (AOAA) enhances the anticancer effects of 3,3'-diindolylmethane by activating the p38/p53 axis[250]. Similarly, in another study, tissue samples of breast cancer patients exhibited high levels of CBS compared to normal tissues. Further examination had revealed that silencing CBS causes a significant reduction in cell growth and progression of breast cancer cells[251]. The inhibition of CBS also attenuates the antioxidant pathway Nrf2 and sensitizes the cells to doxorubicin[252].

Besides that, CBS modulates cancer cells by regulating nicotinamide phosphoribosyltransferase and ATP activities[253]. In HCC patients, low *CBS* mRNA expression correlates with higher disease progression stages and shorter overall survival[254]. However, the increased expression of CBS as a result of hypoxia-induced radioresistance can be attenuated following treatment with a CBS inhibitor and AOAA in HepG2 cells[255]. CBS has been found to be

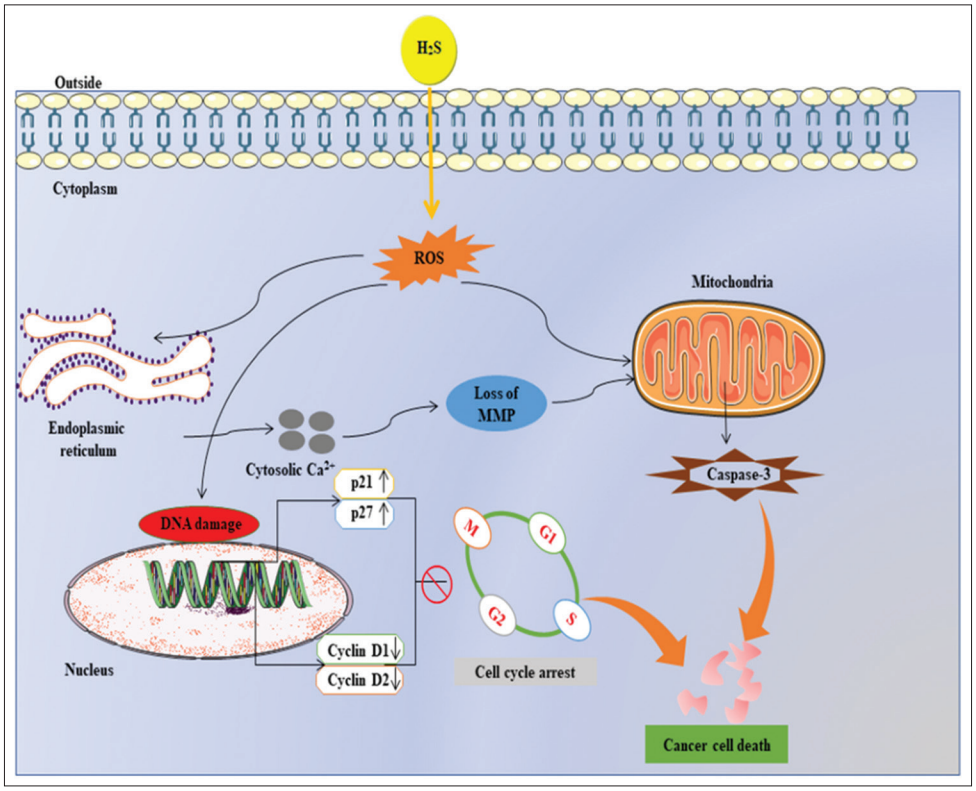

Figure 3. Proposed mechanism of H_2S effect on cell cycle arrest in cancer cells. H_2S increases ROS levels and disrupts Ca^{2+} homeostasis, leading to high intracellular Ca^{2+} with increased expression of p21 and p27, which can result in cell cycle arrest. H_2S: Hydrogen sulfide, ROS: Reactive oxygen species, MMP: Matrix metalloproteinase, G1: Pre-synthetic phase, S: Synthetic phase, G2: Post-synthetic phase, M: Mitotic phase.

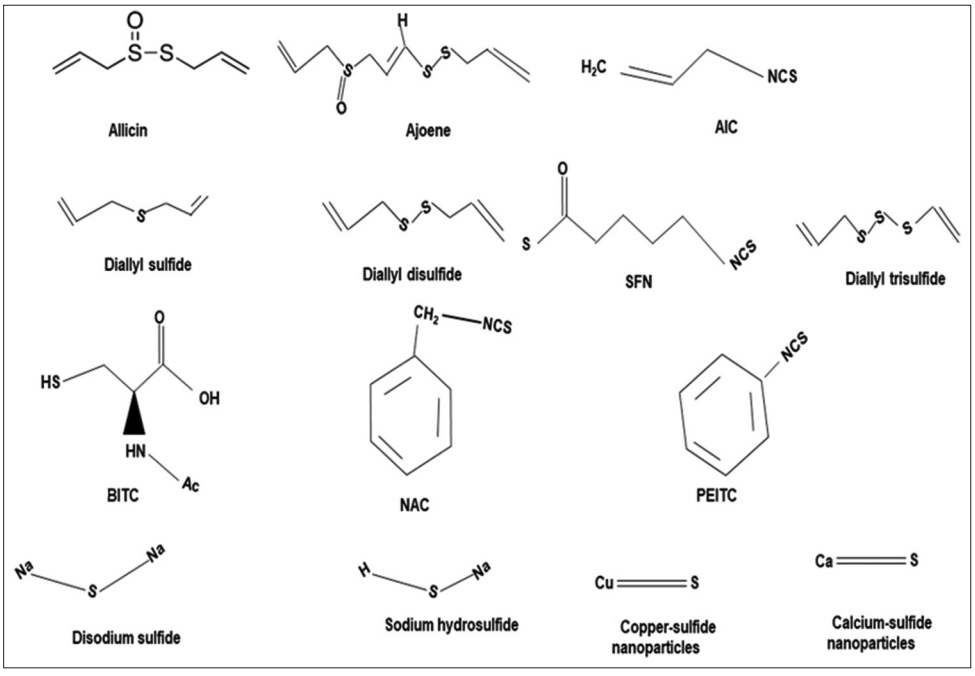

Figure 4. A schematic presentation of exogenous H_2S-based natural and synthesized chemical compounds used in cancer research: (a-i) natural world; (j-n) native compound; (o-w) *de novo* design.

upregulated in hepatoma cells SMMC-7721 and HepG2 but downregulated in BEL-7404 compared to normal cells HL-7702 and QSG-7701[237]. In addition, the silencing of CBS through siRNA or pharmacological inhibitors, AOAA and quinolone-indolone conjugate, effectively induced an anticancer effect in SMMC-7721 by promoting oxidative stress and activating caspase-3.

Besides, treatment with another inhibitor of CBS, CH004, has also been shown to cause cell death in HCC by promoting ferroptosis[256]. High CBS level has been found to be associated with drug resistance in HepG2 cells, and its inhibition increases their sensitivity to doxorubicin and sunitinib; however, in BEL-7404, the elevation of CBS levels enhances the sensitivity to the drugs[257]. This confirms that the effect of CBS in HCC is cell dependent. CBS expression has also been reported to be significantly increased and associated with poor prognosis in renal cancer and cholangiocarcinoma[258], suggesting that the enzyme is involved in cancer activities. However, evidence on its inhibition is still lacking. In ovarian cancer, *CBS* gene silencing reduces migration, angiogenesis, and lipid contents[241]. The inhibition of CBS also activates the JNK pathway and suppresses mitofusin, resulting in mitochondrial morphogenesis reprogramming and the sensitization of cells to erastin[259]. In a recent study, a nanoformulation comprising selenium-containing chrysin has been shown to induce its anticancer effects in ovarian cancer cells by reducing CBS expression, thereby causing oxidative stress[260]. In colon cancer, CBS overexpression is associated with cancer development and treatment with AOAA, and *CBS* gene silencing can significantly reverse pro-cancer activities[261]. AOAA also sensitizes colon cancer cells to oxaliplatin by impairing the antioxidant system and promoting ROS generation. Treatment with AOAA has also been indicated to induce the upregulation of E-cadherin and zonula occludens-1 as well as the suppression of fibronectin, thereby inhibiting the migration and invasion activities of colon cancer cells and promoting mesenchymal-epithelial transition[262]. Other CBS inhibitors that induce apoptosis in colon cancer cells include 2,3,4-trihydroxybenzylhydrazine and sikokianin C[263]. Moreover, treatment with AOAA in multiple myeloma reduces cell cycle progression by triggering G0/G1 arrest and promotes apoptosis through Bcl-2 inhibition and caspase-3 activation[264]. CBS knockdown in glioma cells is to have a fatal outcome, as it results in the progression and metastasis of cancer. These data suggest that CBS plays a role in cancer activities in different types of cells, with its effects varying accordingly; its anticancer effect is selective only to certain types of cancers or cells.

3.3. 3-mercaptopyruvate sulfurtransferase inhibitor

3-MPST in commonly found in cells. It regulates various cellular activities, including bioenergetics, angiogenesis, and the mitochondria electron transport system[265]. In an animal model of colon cancer, treatment with the 3-MPST inhibitor 2-[(4-hydroxy-6-methyl pyrimidin-2-yl)sulfanyl]-1-(naphthalen-1-yl)ethan-1-one (HMPSNE) suppresses H_2S production, CT26 cells proliferation, migration, and oxidative phosphorylation-associated cellular bioenergetics[266]. HMPSNE treatment also suppresses migration- and invasion-promoting markers in colon cancer cells by suppressing Wnt-β-catenin pathway[267]. In human breast cancer cells MCF-7, treatment with another inhibitor, S-Allyl-L-cysteine, has been shown to reduce cell viability by attenuating 3-MPST expression and, subsequently, H_2S level[268]. On the contrary, in neuroblastoma cells, the elevation of 3-MPST activities has shown anticancer properties[167]. The above evidence suggests an involvement of 3-MPST in cancer progression; however, its precise mechanism of action, the pathways involved, and its inhibition effect in different types of cancers are yet to be identified.

4. Translation of H_2S research into therapeutic format

The findings from the aforementioned research on H_2S donors and inhibitors show considerable potential for the development of H_2S-based chemopreventive cancer therapies in the near future. The research community expects substantial outcomes from the preclinical trials on H_2S-based chemopreventive drugs. However, to shape the future of H_2S research in oncology practice, it is highly significant to investigate the biochemistry and pharmacology of H_2S donors and inhibitors as well as characterize their dose-dependent responses to cancer cells. A huge gap remains in understanding how H_2S-producing enzymes respond to the exposure of inhibitors and donors in cancer cells and how they reinforce to generate signals of apoptosis and proliferation in the cancer microenvironment. To reach a large audience across multiple disciplines and promote the innovation of H_2S biomedicine, identifying potential therapeutic H_2S scavengers and donors are as important as assessing their biomedical applications.

5. Conclusion

H_2S is widely recognized for its enormous diagnostic and therapeutic advantages in various diseases, including cancer. Besides its involvement in other pathophysiological illnesses, H_2S plays a significant role in regulating various cellular activities, such as angiogenesis,

cellular bioenergetics, proliferation, apoptosis, EMT, and autophagy, all of which are involved in cancer. The current understanding of H_2S research reveals that both the upregulation and downregulation of H_2S might have anticancer effects, depending on the type of cancer. With the recent advancements in science and technology, researchers have testified that the ability of applied H_2S donor or inhibitor drugs to induce their corresponding effects on H_2S production varies, resulting in pro-cancer or anticancer properties of varying magnitude ranging from none or little to a strong influence depending on the drug type and targeted cells. Besides the individual impact, combining H_2S drugs with other anticancer drugs have been reported to induce significant anticancer effects and sensitize cells to treatments.

Furthermore, by alternating H_2S levels, numerous cellular markers that are associated with cell growth and progression have been reported to be affected, resulting in cancer inhibition or aggravation. Despite the huge potential of these H_2S-based natural, native, and designed chemicals in cancer treatment, little is known about the mechanism of action of these drugs. To shape the future of H_2S research in oncology practice, conclusive investigations are required to assess the drug concentration for treatment and the specificity of both H_2S donors and inhibitors before their use as candidate drugs for cancer treatment in clinical settings.

Acknowledgments

The authors thank the expert reviewers for taking time to review the manuscript and provide valuable suggestions to improve the manuscript. Hussain acknowledges and pays countless thanks to MTB for his presence and support in his PhD journey.

Funding

This work was supported by the National Natural Science Foundation of China (Grant Nos. 31902287 and 81670088).

Conflict of interest

All the authors declare no conflicts of interest.

Author contributions

Conceptualization: Nazeer Hussain Khan, Ebenezeri Erasto Ngowi, Dong-Dong Wu

Visualization: Jiebin Cao, Hongxia Liu

Supervised: Zhihui Liu, Xin-Ying Ji

Writing – original draft: Nazeer Hussain Khan, Ebenezeri Erasto Ngowi, Dong-Dong Wu, Yan Li, SaadUllah Khattak, Yingshuai Zhao, Muhammad Shahid, Ujala Zafar

Writing – review & editing: IIrum Waheed, Fatima Khan, Razia Virk, Istaqlal Hussain

Ethics approval and consent to participate

Not applicable.

Consent for publication

Not applicable.

Availability of data

Not applicable.

References

1. Mishanina TV, Libiad M, Banerjee R, 2015, Biogenesis of reactive sulfur species for signaling by hydrogen sulfide oxidation pathways. *Nat Chem Biol*, 11(7): 457–464.

   https://doi.org/10.1038/nchembio.1834

2. Cao X, Ding L, Xie ZZ, *et al*., 2019, A review of hydrogen sulfide synthesis, metabolism, and measurement: is modulation of hydrogen sulfide a novel therapeutic for cancer? *Antioxid Redox Signal*, 31(1): 1–38.

   https://doi.org/10.1089/ars.2017.7058

3. Augsburger F, Szabo C, 2020, Potential role of the 3-mercaptopyruvate sulfurtransferase (3-MST)—hydrogen sulfide (H2S) pathway in cancer cells. *Pharmacol Res*, 154: 104083.

   https://doi.org/10.1016/j.phrs.2018.11.034

4. Shi Y, Hussain Z, Zhao Y, 2022, Promising application of D-amino acids toward clinical therapy. *Int J Mol Sci*, 23(18): 10794.

   https://doi.org/10.3390/ijms231810794

5. Myszkowska J, Derevenkov I, Makarov SV, *et al*., 2021, Biosynthesis, quantification and genetic diseases of the smallest signaling thiol metabolite: Hydrogen sulfide. *Antioxidants (Basel)*, 10(7): 1065.

   https://doi.org/10.3390/antiox10071065

6. Kohl JB, Mellis AT, Schwarz G, 2019, Homeostatic impact of sulfite and hydrogen sulfide on cysteine catabolism. *Br J Pharmacol*, 176(4): 554–570.

   https://doi.org/10.1111/bph.14464

7. Khattak S, Rauf MA, Khan NH, *et al*., 2022, Hydrogen sulfide biology and its role in cancer. *Molecules*, 27(11): 3389.

   https://doi.org/10.3390/molecules27113389

8. Sun HJ, Wu ZY, Nie XW, *et al*., 2021, Implications of hydrogen sulfide in liver pathophysiology: Mechanistic insights and therapeutic potential. *J Adv Res*, 27: 127–135.

   https://doi.org/10.1016/j.jare.2020.05.010

9. Kumar M, Sandhir R, 2018, Hydrogen sulfide in physiological

and pathological mechanisms in brain. *CNS Neurol Disord Drug Targets*, 17(9): 654–670.

https://doi.org/10.2174/1871527317666180605072018

10. Mir JM, Maurya RC, 2018, Physiological and pathophysiological implications of hydrogen sulfide: A persuasion to change the fate of the dangerous molecule. *J Chin Adv Mater Soc*, 6(4): 434–458.

https://doi.org/10.1080/22243682.2018.1493951

11. Padilla-Camberos E, Zaitseva G, Padilla C, *et al*., 2010, Antitumoral activity of allicin in murine lymphoma L5178Y. *Asian Pac J Cancer Prev*, 11(5): 1241–1244.

12. Salehi B, Zucca P, Orhan IE, *et al*., 2019, Allicin and health: A comprehensive review. *Trends Food Sci Technol*, 86: 502–516.

https://doi.org/10.1016/j.tifs.2019.03.003

13. Haghi A, Azimi H, Rahimi R, 2017, A comprehensive review on pharmacotherapeutics of three phytochemicals, curcumin, quercetin, and allicin, in the treatment of gastric cancer. *J Gastroint Cancer*, 48(4): 314–320.

https://doi.org/10.1007/s12029-017-9997-7

14. Wang Z, Liu Z, Cao Z, *et al*., 2012, Allicin induces apoptosis in EL-4 cells *in vitro* by activation of expression of caspase-3 and-12 and up-regulation of the ratio of Bax/Bcl-2. *Nat Prod Res*, 26(11): 1033–1037.

https://doi.org/10.1080/14786419.2010.550894

15. Xiang Y, Zhao J, Zhao M, *et al*., 2018, Allicin activates autophagic cell death to alleviate the malignant development of thyroid cancer. *Exp Ther Med*, 15(4): 3537–3543.

https://doi.org/10.3892/etm.2018.5828

16. Zhang W, Ha M, Gong Y, *et al*., 2010, Allicin induces apoptosis in gastric cancer cells through activation of both extrinsic and intrinsic pathways. *Oncol Rep*, 24(6): 1585–1592.

https://doi.org/10.3892/or_00001021

17. McGrowder DA, Miller FG, Nwokocha CR, *et al*., 2020, Medicinal herbs used in traditional management of breast cancer: Mechanisms of action. *Medicines (Basel)*, 7(8): 47.

https://doi.org/10.3390/medicines7080047

18. Lv Q, Xia Q, Li J, *et al*., 2020, Allicin suppresses growth and metastasis of gastric carcinoma: The key role of microRNA-383-5p-mediated inhibition of ERBB4 signaling. *Biosci Biotechnol Biochem*, 84(10): 1997–2004.

https://doi.org/10.1080/09168451.2020.1780903

19. Schultz CR, Gruhlke MCH, Slusarenko AJ, *et al*., 2020, Allicin, a potent new ornithine decarboxylase inhibitor in neuroblastoma cells. *J Nat Prod*, 83(8): 2518–2527.

https://doi.org/10.1021/acs.jnatprod.0c00613

20. Jiang W, Huang Y, Wang JP, *et al*., 2013, The synergistic anticancer effect of artesunate combined with allicin in osteosarcoma cell line *in vitro* and *in vivo*. *Asian Pac J Cancer Prev*, 14(8): 4615–4619.

https://doi.org/10.7314/apjcp.2013.14.8.4615

21. Cai J, Wu X, Li X, *et al*., 2019, Allicin protects against cisplatin-induced stria vascularis damage: Possible relation to inhibition of Caspase-3 and PARP-1-AIF-mediated apoptotic pathways. *ORL J Otorhinolaryngol Relat Spec*, 81(4): 202–214.

22. Wu H, Li X, Zhang T, *et al*., 2020, Overexpression miR-486-3p promoted by allicin enhances temozolomide sensitivity in glioblastoma via targeting MGMT. *Neuromolecular Med*, 22(3): 359–369.

https://doi.org/10.1007/s12017-020-08592-5

23. Zou X, Liang J, Sun J, *et al*., 2016, Allicin sensitizes hepatocellular cancer cells to anti-tumor activity of 5-fluorouracil through ROS-mediated mitochondrial pathway. *J Pharmacol Sci*, 131(4): 233–240.

https://doi.org/10.1016/j.jphs.2016.04.017

24. Țigu AB, Toma VA, Moț AC, *et al*., 2020, The synergistic antitumor effect of 5-fluorouracil combined with allicin against lung and colorectal carcinoma cells. *Molecules*, 25(8): 1947.

https://doi.org/10.3390/molecules25081947

25. Terrasson J, Xu B, Li M, *et al*., 2007, Activities of Z-ajoene against tumour and viral spreading *in vitro*. *Fundam Clin Pharmacol*, 21(3): 281–289.

https://doi.org/10.1111/j.1472-8206.2007.00470.x

26. He W, Fu Y, Zheng Y, *et al*., 2021, Diallyl thiosulfinate enhanced the anti-cancer activity of dexamethasone in the side population cells of multiple myeloma by promoting miR-127-3p and deactivating the PI3K/AKT signaling pathway. *BMC Cancer*, 21(1): 1–10.

27. Pandey N, Tyagi G, Kaur P, *et al*., 2020, Allicin overcomes hypoxia mediated cisplatin resistance in lung cancer cells through ROS mediated cell death pathway and by suppressing hypoxia inducible factors. *Cell Physiol Biochem*, 54(4): 748–766.

https://doi.org/10.33594/000000253

28. Yang Z, Du J, Zhu J, *et al*., 2020, Allicin inhibits proliferation by decreasing IL-6 and IFN-β in HCMV-infected glioma cells. *Cancer Manag Res*, 12: 7305–7317.

https://doi.org/10.2147/CMAR.S259677

29. Sultan SA, Khawaji MH, Alsughayyir J, *et al*., 2020, Antileukemic activity of sulfoxide nutraceutical allicin against THP-1 cells is associated with premature phosphatidylserine exposure in human erythrocytes. *Saudi J Biol Sci*, 27(12): 3376–3384.

https://doi.org/10.1016/j.sjbs.2020.09.005

30. Ossama M, Hathout RM, Attia DA, *et al*., 2019, Enhanced allicin cytotoxicity on HEPG-2 cells using glycyrrhetinic acid surface-decorated gelatin nanoparticles. *ACS Omega*, 4(6): 11293–11300.

https://doi.org/10.1021/acsomega.9b01580

31. Chen X, Li H, Xu W, *et al*., 2020, Self-assembling cyclodextrin-based nanoparticles enhance the cellular delivery of hydrophobic allicin. *J Agric Food Chem*, 68(40): 11144–11150.

https://doi.org/10.1021/acs.jafc.0c01900

32. Klinck, J, 2022, Investigations into the Cytotoxic Mechanism of Action for the Garlic Compound Ajoene and its Derivatives in Breast Cancer Cells.

33. Kaschula CH, Hunter R, Cotton J, *et al*., 2016, The garlic compound ajoene targets protein folding in the endoplasmic reticulum of cancer cells. *Mol Carcinog*, 55(8): 1213–1228.

https://doi.org/10.1002/mc.22364

34. Fang ZJ, Huang WX, Huang MH, *et al*., 2002, Gene expression profiling of human promyelocytic leukemia HL-60 cell treated by ajoene. *Chin J Cancer Res*, 14(1): 11–17.

35. Kash N, Silapunt S, 2021, A review of emerging and non-US FDA-approved topical agents for the treatment of basal cell carcinoma. *Future Oncol*, 17(23): 3111–3132.

https://doi.org/10.2217/fon-2020-1147

36. Nagini S, 2008, Cancer chemoprevention by garlic and its organosulfur compounds-panacea or promise? *Anticancer Agents Med Chem*, 8(3): 313–321.

https://doi.org/10.2174/187152008783961879

37. Jung Y, Park H, Zhao HY, *et al*., 2014, Systemic approaches identify a garlic-derived chemical, Z-ajoene, as a glioblastoma multiforme cancer stem cell-specific targeting agent. *Mol Cells*, 37(7): 547–553.

https://doi.org/10.14348/molcells.2014.0158

38. Kaschula CH, Tuveri R, Ngarande E, *et al*., 2019, The garlic compound ajoene covalently binds vimentin, disrupts the vimentin network and exerts anti-metastatic activity in cancer cells. *BMC Cancer*, 19(1): 248.

https://doi.org/10.1186/s12885-019-5388-8

39. Siyo V, Schäfer G, Hunter R, *et al*., 2017, The cytotoxicity of the ajoene analogue BisPMB in WHCO1 oesophageal cancer cells is mediated by CHOP/GADD153. *Molecules*, 22(6): 892.

https://doi.org/10.3390/molecules22060892

40. Lee H, Heo JW, Kim AR, *et al*., 2019, Z-ajoene from crushed garlic alleviates cancer-induced skeletal muscle atrophy. *Nutrients*, 11(11): 2724.

https://doi.org/10.3390/nu11112724

41. Huang YS, Xie N, Su Q, *et al*., 2011, Diallyl disulfide inhibits the proliferation of HT-29 human colon cancer cells by inducing differentially expressed genes. *Mol Med Rep*, 4(3): 553–559.

https://doi.org/10.3892/mmr.2011.453

42. Shan Y, Wei Z, Tao L, *et al*., 2016, Prophylaxis of diallyl disulfide on skin carcinogenic model via p21-dependent Nrf2 stabilization. *Sci Rep*, 6(1): 35676.

https://doi.org/10.1038/srep35676

43. Khan A, Shukla Y, Kalra N, *et al*. 2007, Potential of diallyl sulfide bearing pH-sensitive liposomes in chemoprevention against DMBA-induced skin papilloma. *Mol Med*. 13(7-8): 443–451.

https://doi.org/10.2119/2006–00111.Khan

44. McCaskill ML, Rogan E, Thomas RD, 2014, Diallyl sulfide inhibits diethylstilbestrol induced DNA damage in human breast epithelial cells (MCF-10A). *Steroids*, 92: 96–100.

https://doi.org/100.10.1016/j.steroids.2014.09.005

45. Prasad S, Kalra N, Shukla Y, 2006, Modulatory effects of diallyl sulfide against testosterone-induced oxidative stress in Swiss albino mice. *Asian J Androl*, 8(6): p. 719-723.

https://doi.org/10.1111/j.1745-7262.2006.00201.x

46. Hwang JS, *et al*., 2017, DATS sensitizes glioma cells to TRAIL-mediated apoptosis by up-regulation of death receptor 5 via ROS. *Food Chem Toxicol*, 106(Pt A): 514–521.

https://doi.org/10.1016/j.fct.2017.05.056

47. Suman S, Shukla Y, 2016, Diallyl sulfide and its role in chronic diseases prevention. *Adv Exp Med Biol*, 929: 127–144.

https://doi.org/10.1007/978-3-319-41342-6_6

48. Arora A, Seth K, Shukla Y, 2004, Reversal of P-glycoprotein-mediated multidrug resistance by diallyl sulfide in K562 leukemic cells and in mouse liver. *Carcinogenesis*, 25(6): 941–949.

https://doi.org/10.1093/carcin/bgh060

49. Wu PP, Chung HW, Liu KC, *et al*., 2011, Diallyl sulfide induces cell cycle arrest and apoptosis in HeLa human cervical cancer cells through the p53, caspase-and mitochondria-dependent pathways. *Int J Oncol*, 38(6): 1605–1613.

https://doi.org/10.3892/ijo.2011.973

50. Ansari IA, Ahmad A, Imran MA, *et al*., 2021, Organosulphur compounds induce apoptosis and cell cycle arrest in cervical cancer cells via downregulation of HPV E6 and E7 oncogenes. *Anticancer Agents Med Chem*, 21(3): 393–405.

https://doi.org/10.2174/1871520620999200818154456

51. Aquilano K, Filomeni G, Baldelli S, *et al*., 2007, Neuronal nitric oxide synthase protects neuroblastoma cells from oxidative stress mediated by garlic derivatives. *J Neurochem*, 101(5): 1327–1337.

https://doi.org/10.1111/j.1471-4159.2006.04431.x

52. Khan A, Alhumaydhi FA, Alwashmi ASS, *et al*., 2020, Diallyl sulfide-mediated modulation of the fatty acid synthase (FASN) leads to cancer cell death in BaP-induced lung carcinogenesis in Swiss mice. *J Inflamm Res*, 13: 1075–1087.

https://doi.org/10.2147/JIR.S284279

53. Muninathan N, 2021, Amelioration of combination of paclitaxel and di allyl sulfide on the alterations of Bcl2, P53 and apoptosis changes against 7, 12 di methyl benz (A) anthracene induced skin cancer in experimental animals. *Indian J Clin Biochem*, 36(2): 143–150.

https://doi.org/10.1007/s12291-019-0817-7

54. Wargovich MJ, Imada O, Stephens LC, 1992, Initiation and post-initiation chemopreventive effects of diallyl sulfide in esophageal carcinogenesis. *Cancer Lett*, 64(1): 39–42.

https://doi.org/10.1016/0304-3835(92)90019-r

55. Yin X, Feng C, Han L, *et al*., 2018, Diallyl disulfide inhibits the metastasis of type II esophageal-gastric junction adenocarcinoma cells via NF-κB and PI3K/AKT signaling pathways *in vitro*. *Oncol Rep*, 39(2): 784–794.

https://doi.org/10.3892/or.2017.6113

56. Yi L, Su Q, 2013, Molecular mechanisms for the anti-cancer effects of diallyl disulfide. *Food Chem Toxicol*, 57: 362–370.

https://doi.org/10.1016/j.fct.2013.04.001

57. Druesne N, Pagniez A, Mayeur C, *et al*., 2004, Repetitive treatments of colon HT-29 cells with diallyl disulfide induce a prolonged hyperacetylation of histone H3 K14. *Ann N Y Acad Sci*, 1030(1): 612–621.

https://doi.org/10.1196/annals.1329.071

58. Yang JS, Chen GW, Hsia TC, *et al*., 2009, Diallyl disulfide induces apoptosis in human colon cancer cell line (COLO 205) through the induction of reactive oxygen species, endoplasmic reticulum stress, caspases casade and mitochondrial-dependent pathways. *Food Chem Toxicol*, 47(1): 171–179.

59. Su J, Zhou Y, Pan Z, *et al*., 2017, Downregulation of LIMK1–ADF/cofilin by DADS inhibits the migration and invasion of colon cancer. *Scientific Reports*, 7(1): 1–12.

60. Yi L, Ji XX, Lin M, *et al*., 2010, Diallyl disulfide induces apoptosis in human leukemia HL-60 cells through activation of JNK mediated by reactive oxygen. *Pharmazie*, 65(9): 693–698.

61. Ling H, He J, Tan H, *et al*., 2017, Identification of potential targets for differentiation in human leukemia cells induced by diallyl disulfide. *Int J Oncol*, 50(2): 697–707.

https://doi.org/10.3892/ijo.2017.3839

62. Liu R, Yang YN, Yi L, *et al*., 2018, Diallyl disulfide effect on the invasion and migration ability of HL-60 cells with a high expression of DJ-1 in the nucleus through the suppression of the Src signaling pathway. *Oncol Lett*, 15(5): 6377–6385.

https://doi.org/10.3892/ol.2018.8139

63. Arunkumar A, Vijayababu MR, Venkataraman P, *et al*., 2006, Chemoprevention of rat prostate carcinogenesis by diallyl disulfide, an organosulfur compound of garlic. *Biol Pharm Bull*, 29(2): 375–379.

https://doi.org/10.1248/bpb.29.375

64. Arunkumar R, Sharmila G, Elumalai P, *et al*., 2012, Effect of diallyl disulfide on insulin-like growth factor signaling molecules involved in cell survival and proliferation of human prostate cancer cells *in vitro* and *in silico* approach through docking analysis. *Phytomedicine*, 19(10): 912–923.

https://doi.org/10.1016/j.phymed.2012.04.009

65. Wang HC, Yang JH, Hsieh SC, *et al*., 2010, Allyl sulfides inhibit cell growth of skin cancer cells through induction of DNA damage mediated G2/M arrest and apoptosis. *J Agric Food Chem*, 58(11): 7096–7103.

https://doi.org/10.1021/jf100613x

66. Lei XY, Yao SQ, Zu XY, *et al*., 2008, Apoptosis induced by diallyl disulfide in human breast cancer cell line MCF-7 1. *Acta Pharmacol Sin*, 29(10): 1233–1239.

https://doi.org/10.1111/j.1745-7254.2008.00851.x

67. Xiao X, Chen B, Liu X, *et al*., 2014, Diallyl disulfide suppresses SRC/Ras/ERK signaling-mediated proliferation and metastasis in human breast cancer by up-regulating miR-34a. *PLoS One*, 9(11): e112720.

https://doi.org/10.1371/journal.pone.0112720

68. Xiong T, Liu XW, Huang XL, *et al*., 2018, Tristetraprolin: A novel target of diallyl disulfide that inhibits the progression of breast cancer. *Oncol Lett*, 15(5): 7817–7827.

https://doi.org/10.3892/ol.2018.8299

69. Nkrumah-Elie YM, Reuben JS, Hudson AM, *et al*., 2012, The attenuation of early benzo (a) pyrene-induced carcinogenic insults by diallyl disulfide (DADS) in MCF-10A cells. *Nutr Cancer*, 64(7): 1112–1121.

https://doi.org/10.1080/01635581.2012.712738

70. Altonsy MO, Habib TN, Andrews SC, Diallyl disulfide-induced apoptosis in a breast-cancer cell line (MCF-7) may be caused by inhibition of histone deacetylation. *Nutr Cancer*, 64(8): 1251–1260.

https://doi.org/10.1080/01635581.2012.721156

71. Ciocci M, Iorio E, Carotenuto F, *et al*., 2016, H2S-releasing nanoemulsions: A new formulation to inhibit tumor cells proliferation and improve tissue repair. *Oncotarget*, 7(51): 84338–84358.

https://doi.org/10.18632/oncotarget.12609

72. Siddhartha VT, Pindiprolu SKS, Chintamaneni PK,

et al., 2018, RAGE receptor targeted bioconjuguate lipid nanoparticles of diallyl disulfide for improved apoptotic activity in triple negative breast cancer: *In vitro* studies. *Artif Cells Nanomed Biotechnol*, 46(2): 387–397.

https://doi.org/10.1080/21691401.2017.1313267

73. Ji C, Ren F, Ma H, *et al*., 2010, The roles of p38MAPK and caspase-3 in DADS-induced apoptosis in human HepG2 cells. *J Exp Clin Cancer Res*, 29(1): 50.

https://doi.org/10.1186/1756-9966-29-50

74. Hong YS, Ham YA, Choi JH, *et al*., 2000, Effects of allyl sulfur compounds and garlic extract on the expression of Bcl-2, Bax, and p53 in non small cell lung cancer cell lines. *Exp Mol Med*, 32(3): 127–134.

https://doi.org/10.1038/emm.2000.22

75. Das B, Sinha D, 2019, Diallyl disulphide suppresses the cannonical Wnt signaling pathway and reverses the fibronectin-induced epithelial mesenchymal transition of A549 lung cancer cells. *Food Funct*, 10(1): 191–202.

https://doi.org/10.1039/c8fo00246k

76. Thejass P, Kuttan G, 2007, Antiangiogenic activity of diallyl sulfide (DAS). *Int Immunopharmacol*, 7(3): 295–305.

https://doi.org/10.1016/j.intimp.2006.10.011

77. Su B, Su J, Zeng Y, *et al*., 2018, Diallyl disulfide inhibits TGF-β1-induced upregulation of Rac1 and β-catenin in epithelial-mesenchymal transition and tumor growth of gastric cancer. *Oncol Rep*, 39(6): 2797–2806.

https://doi.org/10.3892/or.2018.6345

78. Filomeni G, Aquilano K, Rotilio G, *et al*., 2005, Glutathione-related systems and modulation of extracellular signal–regulated kinases are involved in the resistance of AGS adenocarcinoma gastric cells to diallyl disulfide–induced apoptosis. *Cancer Res*, 65(24): 11735–11742.

https://doi.org/10.1158/0008-5472.CAN-05-3067

79. Das A, Banik NL, Ray SK, 2007, Garlic compounds generate reactive oxygen species leading to activation of stress kinases and cysteine proteases for apoptosis in human glioblastoma T98G and U87MG cells. *Cancer*, 110(5): 1083–1095.

https://doi.org/10.1002/cncr.22888

80. Di C, Sun C, Li H, *et al*., 2015, Diallyl disulfide enhances carbon ion beams–induced apoptotic cell death in cervical cancer cells through regulating Tap73/ΔNp73. *Cell Cycle*, 14(23): 3725–3733.

https://doi.org/10.1080/15384101.2015.1104438

81. Lu HF, Sue CC, Yu CS, *et al*., 2004, Diallyl disulfide (DADS) induced apoptosis undergo caspase-3 activity in human bladder cancer T24 cells. *Food Chem Toxicol*, 42(10): 1543–1552.

https://doi.org/10.1016/j.fct.2003.06.001

82. Yue Z, Guan X, Chao R, *et al*., 2019, Diallyl disulfide induces apoptosis and autophagy in human osteosarcoma MG-63 cells through the PI3K/Akt/mTOR pathway. *Molecules*, 24(14): 2665.

https://doi.org/10.3390/molecules24142665

83. Borkowska A, Sielicka-Dudzin A, Herman-Antosiewicz A, *et al*., 2012, Diallyl trisulfide-induced prostate cancer cell death is associated with Akt/PKB dephosphorylation mediated by P-p66shc. *Eur J Nutr*, 51(7): 817–825.

https://doi.org/10.1007/s00394-011-0260-x

84. Kim SH, Hahm ER, Singh KB, *et al*., 2020, Diallyl trisulfide inhibits leptin-induced oncogenic signaling in human breast cancer cells but fails to prevent chemically-induced luminal-type cancer in rats. *J Cancer Prev*, 25(1): 1–12.

https://doi.org/10.15430/JCP.2020.25.1.1

85. Elsherbiny NM, El-Sherbiny M, Zaitone SA, 2020, Diallyl trisulfide potentiates chemotherapeutic efficacy of doxorubicin in experimentally induced mammary carcinoma: Role of Notch signaling. *Pathol Res Pract*, 216(10): 153139.

https://doi.org/10.1016/j.prp.2020.153139

86. Shin DY, Kim GY, Hwang HJ, *et al*., 2014, Diallyl trisulfide-induced apoptosis of bladder cancer cells is caspase-dependent and regulated by PI3K/Akt and JNK pathways. *Environ Toxicol Pharmacol*, 37(1): 74–83.

https://doi.org/10.1016/j.etap.2013.11.002

87. Geng H, Guo W, Feng L, *et al*., 2021, Diallyl trisulfide inhibited tobacco smoke-mediated bladder EMT and cancer stem cell marker expression via the NF-κB pathway *in vivo*. *J Int Med Res*, 49(3): 0300060521992900.

https://doi.org/10.1177/0300060521992900

88. Wang J, Si L, Wang G, *et al*., 2019, Increased sulfiredoxin expression in gastric cancer cells may be a molecular target of the anticancer component diallyl trisulfide. *Biomed Res Int*, 2019: 4636804.

https://doi.org/10.1155/2019/4636804

89. Jiang XY, Zhu XS, Xu HY, *et al*., 2017, Diallyl trisulfide suppresses tumor growth through the attenuation of Nrf2/Akt and activation of p38/JNK and potentiates cisplatin efficacy in gastric cancer treatment. *Acta Pharmacol Sin*, 38(7): 1048–1058.

https://doi.org/10.1038/aps.2016.176

90. Wang H, Sun N, Li X, *et al*., 2016, Diallyl trisulfide induces osteosarcoma cell apoptosis through reactive oxygen species-mediated downregulation of the PI3K/Akt pathway. *Oncol Rep*, 35(6): 3648–3658.

https://doi.org/10.3892/or.2016.4722

91. Xie WP, Zhang Y, Zhang YK, *et al*., 2018, Treatment of Saos-2 osteosarcoma cells with diallyl trisulfide is associated with an increase in calreticulin expression. *Exp Ther Med*, 15(6): 4737–4742.

https://doi.org/10.3892/etm.2018.6037

92. He P, Wang Z, Sheng B, *et al*., 2020, Diallyl trisulfide regulates cell apoptosis and invasion in human Osteosarcoma U2OS cells through regulating PI3K/AKT/GSK3β signaling pathway. *Histol Histopathol*, 35(12): 1511–1520.

https://doi.org/10.14670/HH-18-299

93. Jiang X, Zhu X, Liu N, *et al*., 2017, Diallyl trisulfide inhibits growth of NCI-H460 *in vitro* and *in vivo*, and ameliorates cisplatin-induced oxidative injury in the treatment of lung carcinoma in xenograft mice. *Int J Biol Sci*, 13(2): 167–178.

https://doi.org/10.7150/ijbs.16828

94. Liu Y, Fu R, Tu S, *et al*., 2021, Extracellular microparticles encapsulated with Diallyl Trisulfide interfere with the inflammatory tumor microenvironment and lung metastasis of invasive melanoma. *Mol Pharmaceutics*, 18(3): 822–835.

https://doi.org/10.1021/acs.molpharmaceut.0c00696

95. Xu S, Pan J, Cheng X, *et al*., 2020, Diallyl trisulfide, a H2S donor, inhibits cell growth of human papillary thyroid carcinoma KTC-1 cells through a positive feedback loop between H2S and cystathionine-gamma-lyase. *Phytother Res*, 34(5): 1154–1165.

https://doi.org/10.1002/ptr.6586

96. Lai KC, Hsu SC, Yang JS, *et al*., 2015, Diallyl trisulfide inhibits migration, invasion and angiogenesis of human colon cancer HT-29 cells and umbilical vein endothelial cells, and suppresses murine xenograft tumour growth. *J Cell Mol Med*, 19(2): 474–484.

https://doi.org/10.1111/jcmm.12486

97. Nakagawa C, Suzuki-Karasaki M, Suzuki-Karasaki M, *et al*., 2020, The mitochondrial Ca2+ overload via voltage-gated Ca2+ entry contributes to an anti-melanoma effect of diallyl trisulfide. *Int J Mol Sci*, 21(2): 491.

https://doi.org/10.3390/ijms21020491

98. Wan HF, Yu LH, Wu JL, *et al*., 2013, Effect of diallyl trisulfide on human ovarian cancer SKOV-3/DDP cell apoptosis. *Asian Pac J Cancer Prev*, 14(12): 7197–7201.

https://doi.org/10.7314/apjcp.2013.14.12.7197

99. Agassi SFT, Yeh TM, Chang CD, *et al*., 2020, Potentiation of differentiation and apoptosis in a human promyelocytic leukemia cell line by garlic essential oil and its organosulfur compounds. *Anticancer Res*, 40(11): 6345–6354.

https://doi.org/10.21873/anticanres.14655

100. Das A, Henderson F Jr, Lowe S, *et al*., 2018, Single agent efficacy of the HDAC inhibitor DATS in preclinical models of glioblastoma. *Cancer Chemother Pharmacol*, 82(6): 945–952.

https://doi.org/10.1007/s00280-018-3684-7

101. Shigemi Z, Furukawa Y, Hosokawa K, *et al*., 2016, Diallyl trisulfide induces apoptosis by suppressing NF-κB signaling through destabilization of TRAF6 in primary effusion lymphoma. *Int J Oncol*, 48(1): 293–304.

https://doi.org/10.3892/ijo.2015.3247

102. Abbaoui B, Riedl KM, Ralston RA, *et al*., 2012, Inhibition of bladder cancer by broccoli isothiocyanates sulforaphane and erucin: Characterization, metabolism, and interconversion. *Mol Nutr Food Res*, 56(11): 1675–1687.

https://doi.org/10.1002/mnfr.201200276

103. Abbaoui B, Telu KH, Lucas CR, *et al*., 2017, The impact of cruciferous vegetable isothiocyanates on histone acetylation and histone phosphorylation in bladder cancer. *J Proteomics*, 156: 94–103.

https://doi.org/10.1016/j.jprot.2017.01.013

104. Shan Y, Zhang L, Bao Y, *et al*., 2013, Epithelial-mesenchymal transition, a novel target of sulforaphane via COX-2/MMP2, 9/Snail, ZEB1 and miR-200c/ZEB1 pathways in human bladder cancer cells. *J Nutr Biochem*, 24(6): 1062–1069.

https://doi.org/10.1016/j.jnutbio.2012.08.004

105. Wang F, Liu P, An H, *et al*., 2020, Sulforaphane suppresses the viability and metastasis, and promotes the apoptosis of bladder cancer cells by inhibiting the expression of FAT1. *Int J Mol Med*, 46(3): 1085–1095.

https://doi.org/10.3892/ijmm.2020.4665

106. Justin S, Rutz J, Maxeiner S, *et al*., 2020, Bladder cancer metastasis induced by chronic Everolimus application can be counteracted by sulforaphane *in vitro*. *Int J Mol Sci*, 21(15): 5582.

https://doi.org/10.3390/ijms21155582

107. Byun S, Shin SH, Park J, *et al*., 2016, Sulforaphene suppresses growth of colon cancer-derived tumors via induction of glutathione depletion and microtubule depolymerization. *Mol Nutr Food Res*, 60(5): 1068–1078.

https://doi.org/10.1002/mnfr.201501011

108. Zhou JW, Wang M, Sun NX, *et al*., 2019, Sulforaphane-induced epigenetic regulation of Nrf2 expression by DNA methyltransferase in human Caco-2 cells. *Oncol Lett*, 18(3): 2639–2647.

https://doi.org/10.3892/ol.2019.10569

109. Yasuda S, Horinaka M, Sakai T, 2019, Sulforaphane enhances apoptosis induced by *Lactobacillus* pentosus strain S-PT84 via the TNFα pathway in human colon cancer cells. *Oncol Lett*, 18(4): 4253–4261.

https://doi.org/10.3892/ol.2019.10739

110. Cheng AC, Shen CJ, Hung CM, *et al.*, 2019, Sulforaphane decrease of SERTAD1 expression triggers G1/S arrest in breast cancer cells. *J Med Food*, 22(5): 444–450.

https://doi.org/10.1089/jmf.2018.4195

111. Castro NP, Rangel MC, Merchant AS, *et al.*, 2019, Sulforaphane suppresses the growth of triple-negative breast cancer stem-like cells *in vitro* and *in vivo*. *Cancer Prev Res (Phila)*, 12(3): 147–158.

https://doi.org/10.1158/1940-6207.CAPR-18-0241

112. Choi YH, 2018, ROS-mediated activation of AMPK plays a critical role in sulforaphane-induced apoptosis and mitotic arrest in AGS human gastric cancer cells. *Gen Physiol Biophys*, 37(2): 129–140.

https://doi.org/10.4149/gpb_2017026

113. Wang Y, Wu H, Dong N, *et al.*, 2021, Sulforaphane induces S-phase arrest and apoptosis via p53-dependent manner in gastric cancer cells. *Sci Rep*, 11(1): 2504.

https://doi.org/10.1038/s41598-021-81815-2

114. Han S, Wang Z, Liu J, *et al.*, 2021, miR-29a-3p-dependent COL3A1 and COL5A1 expression reduction assists sulforaphane to inhibit gastric cancer progression. *Biochem Pharmacol*, 188: 114539.

https://doi.org/10.1016/j.bcp.2021.114539

115. Zhang C, Su ZY, Khor TO, *et al.*, 2013, Sulforaphane enhances Nrf2 expression in prostate cancer TRAMP C1 cells through epigenetic regulation. *Biochem Pharmacol*, 85(9): 1398–1404.

https://doi.org/10.1016/j.bcp.2013.02.010

116. Vyas AR, Moura MB, Hahm ER, *et al.*, 2016, Sulforaphane inhibits c-myc-mediated prostate cancer stem-like traits. *J Cell Biochem*, 117(11): 2482–2495.

https://doi.org/10.1002/jcb.25541

117. Singh KB, Kim SH, Hahm ER, *et al.*, 2018, Prostate cancer chemoprevention by sulforaphane in a preclinical mouse model is associated with inhibition of fatty acid metabolism. *Carcinogenesis*, 39(6): 826–837.

https://doi.org/10.1093/carcin/bgy051

118. Rutz J, Thaler S, Maxeiner S, *et al.*, 2020, Sulforaphane reduces prostate cancer cell growth and proliferation *in vitro* by modulating the cdk-cyclin axis and expression of the CD44 Variants 4, 5, and 7. *Int J Mol Sci*, 21(22): 8724.

https://doi.org/10.3390/ijms21228724

119. Bryant CS, Kumar S, Chamala S, *et al.*, 2010, Sulforaphane induces cell cycle arrest by protecting RB-E2F-1 complex in epithelial ovarian cancer cells. *Molecular Cancer*, 9(1): 1–9.

120. Chang CC, Hung CM, Yang YR, *et al.*, 2013, Sulforaphane induced cell cycle arrest in the G2/M phase via the blockade of cyclin B1/CDC2 in human ovarian cancer cells. *J Ovarian Res*, 6(1): 41.

https://doi.org/10.1186/1757-2215-6-41

121. Gong TT, Liu XD, Zhan ZP, *et al.*, 2020, Sulforaphane enhances the cisplatin sensitivity through regulating DNA repair and accumulation of intracellular cisplatin in ovarian cancer cells. *Exp Cell Res*, 393(2): 112061.

https://doi.org/10.1016/j.yexcr.2020.112061

122. Hsu YC, Chang SJ, Wang MY, *et al.*, 2013, Growth inhibition and apoptosis of neuroblastoma cells through ROS-independent MEK/ERK activation by sulforaphane. *Cell Biochem Biophys*, 66(3): 765–774.

https://doi.org/10.1007/s12013-013-9522-y

123. Yeh CT, Yen GC, 2005, Effect of sulforaphane on metallothionein expression and induction of apoptosis in human hepatoma HepG2 cells. *Carcinogenesis*, 26(12): 2138–2148.

https://doi.org/10.1093/carcin/bgi185

124. Saha K, Fisher ML, Adhikary G, *et al.*, 2017, Sulforaphane suppresses PRMT5/MEP50 function in epidermal squamous cell carcinoma leading to reduced tumor formation. *Carcinogenesis*, 38(8): 827–836.

https://doi.org/10.1093/carcin/bgx044

125. Żuryń A, Krajewski A, Klimaszewska-Wiśniewska A, *et al.*, 2019, Expression of cyclin B1, D1 and K in non-small cell lung cancer H1299 cells following treatment with sulforaphane. *Oncol Rep*, 41(2): 1313–1323.

https://doi.org/10.3892/or.2018.6919

126. Xie C, Zhu J, Jiang Y, *et al.*, 2019, Sulforaphane inhibits the acquisition of tobacco smoke-induced lung cancer stem cell-like properties via the IL-6/ΔNp63α/Notch Axis. *Theranostics*, 9(16): 4827–4840.

https://doi.org/10.7150/thno.33812

127. Chen L, Chan LS, Lung HL, *et al.*, 2019, Crucifera sulforaphane (SFN) inhibits the growth of nasopharyngeal carcinoma through DNA methyltransferase 1 (DNMT1)/Wnt inhibitory factor 1 (WIF1) axis. *Phytomedicine*, 63: 153058.

https://doi.org/10.1016/j.phymed.2019.153058

128. Chu WF, Wu DM, Liu W, *et al.*, 2009, Sulforaphane induces G2–M arrest and apoptosis in high metastasis cell line of salivary gland adenoid cystic carcinoma. *Oral Oncol*, 45(11): 998–1004.

https://doi.org/10.1016/j.oraloncology.2009.05.641

129. Gründemann C, Garcia-Käufer M, Lamy E, *et al.*, 2015, 4-Methylthiobutyl isothiocyanate (Erucin) from rocket plant dichotomously affects the activity of human immunocompetent cells. *Phytomedicine*, 22(3): 369–378.

https://doi.org/10.1016/j.phymed.2014.12.012

130. Melchini A, Traka MH, Catania S, *et al.*, 2013, Antiproliferative activity of the dietary isothiocyanate erucin, a bioactive compound from cruciferous vegetables, on human prostate cancer cells. *Nutr Cancer*, 65(1): 132–138.

https://doi.org/10.1080/01635581.2013.741747

131. Citi V, Piragine E, Pagnotta E, *et al.*, 2019 Anticancer properties of erucin, an H2S-releasing isothiocyanate, on human pancreatic adenocarcinoma cells (AsPC-1). *Phytother Res*, 33(3): 845–855.

https://doi.org/10.1002/ptr.6278

132. Lamy E, Oey D, Eißmann F, *et al.*, 2013, Erucin and benzyl isothiocyanate suppress growth of late stage primary human ovarian carcinoma cells and telomerase activity *in vitro*. *Phytother Res*, 27(7): 1036–1041.

https://doi.org/10.1002/ptr.4798

133. Li G, Zhou J, Budhraja A, *et al.*, 2015, Mitochondrial translocation and interaction of cofilin and Drp1 are required for erucin-induced mitochondrial fission and apoptosis. *Oncotarget*, 6(3): 1834.

https://doi.org/10.18632/oncotarget.2795

134. Tsai SC, Huang WW, Huang WC, *et al.*, 2012, ERK-modulated intrinsic signaling and G2/M phase arrest contribute to the induction of apoptotic death by allyl isothiocyanate in MDA-MB-468 human breast adenocarcinoma cells. *Int J Oncol*, 41(6): 2065–2072.

https://doi.org/10.3892/ijo.2012.1640

135. Sayeed MA, Bracci M, Ciarapica V, *et al.*, 2018, Allyl isothiocyanate exhibits no anticancer activity in MDA-MB-231 breast cancer cells. *Int J Mol Sci*, 19(1): 145.

https://doi.org/10.3390/ijms19010145

136. Qin G, Li P, Xue Z, 2018, Effect of allyl isothiocyanate on the viability and apoptosis of the human cervical cancer HeLa cell line *in vitro*. *Oncol Lett*, 15(6): 8756–8760.

https://doi.org/10.3892/ol.2018.8428

137. Chang PY, Tsai FJ, Bau DT, *et al.*, 2021, Potential effects of allyl isothiocyanate on inhibiting cellular proliferation and inducing apoptotic pathway in human cisplatin-resistant oral cancer cells. *J Formos Med Assoc*, 120(1): 515–523.

https://doi.org/10.1016/j.jfma.2020.06.025

138. Hwang ES, Kim GH, 2009, Allyl isothiocyanate influences cell adhesion, migration and metalloproteinase gene expression in SK-Hep1 cells. *Exp Biol Med (Maywood)*, 234(1): 105–111.

https://doi.org/10.3181/0806-RM-190

139. Lai KC, Lu CC, Tang YJ, *et al.*, 2014, Allyl isothiocyanate inhibits cell metastasis through suppression of the MAPK pathways in epidermal growth factor-stimulated HT29 human colorectal adenocarcinoma cells. *Oncol Rep*, 31(1): 189–196.

https://doi.org/10.3892/or.2013.2865

140. Chiang JH, Tsai FJ, Hsu YM, *et al.*, 2020, Sensitivity of allyl isothiocyanate to induce apoptosis via ER stress and the mitochondrial pathway upon ROS production in colorectal adenocarcinoma cells. *Oncol Rep*, 44(4): 1415–1424.

https://doi.org/10.3892/or.2020.7700

141. Tsai TF, Chen PC, Lin YC, *et al.*, 2020, Benzyl isothiocyanate promotes miR-99a expression through ERK/AP-1-dependent pathway in bladder cancer cells. *Environ Toxicol*, 35(1): 47–54.

https://doi.org/10.1002/tox.22841

142. Lin JF, Tsai TF, Yang SC, *et al.*, 2017, Benzyl isothiocyanate induces reactive oxygen species-initiated autophagy and apoptosis in human prostate cancer cells. Oncotarget, 8(12): 20220–20234.

https://doi.org/10.18632/oncotarget.15643

143. Kim SH, Singh SV, 2019, Role of krüppel-like factor 4-p21CIP1 axis in breast cancer stem-like cell inhibition by benzyl isothiocyanaterole of KLF4 in bCSC suppression by BITC. *Cancer Prev Res (Phila)*, 12(3): 125–134.

https://doi.org/10.1158/1940-6207.CAPR-18-0393

144. Kim SH, Singh SV, 2010, p53-independent apoptosis by benzyl isothiocyanate in human breast cancer cells is mediated by suppression of XIAP expressionxiap suppression in BITC-induced apoptosis. *Cancer Prev Res(Phila)*, 3(6): 718–726.

https://doi.org/10.1158/1940-6207.CAPR-10-0048

145. Huang YP, Jiang YW, Chen HY, *et al.*, 2018, Benzyl isothiocyanate induces apoptotic cell death through mitochondria-dependent pathway in gefitinib-resistant NCI-H460 human lung cancer cells *in vitro*. *Anticancer Res*, 38(9): 5165–5176.

https://doi.org/10.21873/anticanres.12839

146. Ma L, Chen Y, Han R, *et al.*, 2019, Benzyl isothiocyanate inhibits invasion and induces apoptosis via reducing S100A4 expression and increases PUMA expression in oral squamous cell carcinoma cells. *Braz J Med Biol Res*, 52(4): e8409.

https://doi.org/10.1590/1414-431X20198409

147. Wolf MA, Claudio PP, 2014, Benzyl isothiocyanate inhibits HNSCC cell migration and invasion, and sensitizes HNSCC cells to cisplatin. *Nutr Cancer*, 66(2): 285–294.

https://doi.org/10.1080/01635581.2014.868912

148. Yue T, Zuo S, Bu D, *et al.*, 2020, Aminooxyacetic acid (AOAA) sensitizes colon cancer cells to oxaliplatin via exaggerating apoptosis induced by ROS. *J Cancer*, 11(7): 1828–1838.

https://doi.org/10.7150/jca.35375

149. Zhu M, Li W, Dong X, *et al*., 2017, Benzyl-isothiocyanate induces apoptosis and inhibits migration and invasion of hepatocellular carcinoma cells *in vitro*. *J Cancer*, 8(2): 240–248.

https://doi.org/10.7150/jca.16402

150. Ohara M, Kimura S, Tanaka A, *et al*., 2011, Benzyl isothiocyanate sensitizes human pancreatic cancer cells to radiation by inducing apoptosis. *Int J Mol Med*, 28(6): 1043–1047.

https://doi.org/10.3892/ijmm.2011.770

151. Kasiappan R, Jutooru I, Karki K, *et al*., 2016, Benzyl isothiocyanate (BITC) induces reactive oxygen species-dependent repression of STAT3 protein by down-regulation of specificity proteins in pancreatic cancer. *J Biol Chem*, 291(53): 27122–27133.

https://doi.org/10.1074/jbc.M116.746339

152. Han KWW, Po WW, Sohn UD, *et al*., 2019, Benzyl isothiocyanate induces apoptosis via reactive oxygen species-initiated mitochondrial dysfunction and DR4 and DR5 death receptor activation in gastric adenocarcinoma cells. *Biomolecules*, 9(12): 839.

https://doi.org/10.3390/biom9120839

153. Chen PY, Lin KC, Lin JP, *et al*., 2012, Phenethyl isothiocyanate (PEITC) inhibits the growth of human oral squamous carcinoma HSC-3 cells through G0/G1 phase arrest and mitochondria-mediated apoptotic cell death. *Evid Based Complement Alternat Med*, 2012: 718320.

https://doi.org/10.1155/2012/718320

154. Lam-Ubol A, Fitzgerald AL, Ritdej A, *et al*., 2018, Sensory acceptable equivalent doses of β-phenylethyl isothiocyanate (PEITC) induce cell cycle arrest and retard the growth of p53 mutated oral cancer *in vitro* and *in vivo*. *Food Funct*, 9(7): 3640–3656.

https://doi.org/10.1039/c8fo00865e

155. Chou YC, Chang MY, Lee HT, *et al*., 2018, Phenethyl isothiocyanate inhibits *in vivo* growth of xenograft tumors of human glioblastoma cells. *Molecules*, 23(9): 2305.

https://doi.org/10.3390/molecules23092305

156. Wang D, Upadhyaya B, Liu Y, *et al*., 2014, Phenethyl isothiocyanate upregulates death receptors 4 and 5 and inhibits proliferation in human cancer stem-like cells. *BMC Cancer*, 14(1): 591.

https://doi.org/10.1186/1471-2407-14-591

157. Yang MD, Lai KC, Lai TY, *et al*., 2010, Phenethyl isothiocyanate inhibits migration and invasion of human gastric cancer AGS cells through suppressing MAPK and NF-κB signal pathways. *Anticancer Res*, 30(6): 2135–2143.

158. Liu Y, Dey M, 2017, Dietary phenethyl isothiocyanate protects mice from colitis associated colon cancer. *Int J Mol Sci*, 18(9): 1908.

https://doi.org/10.3390/ijms18091908

159. Shao WY, Yang YL, Yan H, *et al*., 2017, Phenethyl isothiocyanate suppresses the metastasis of ovarian cancer associated with the inhibition of CRM1-mediated nuclear export and mTOR-STAT3 pathway. *Cancer Biol Ther*, 18(1): 26–35.

https://doi.org/10.1080/15384047.2016.1264540

160. Hsia TC, Huang YP, Jiang YW, *et al*., 2018, Phenethyl isothiocyanate induces apoptotic cell death through the mitochondria-dependent pathway in gefitinib-resistant NCI-H460 human lung cancer cells *in vitro*. *Anticancer Res*, 38(4): 2137–2147.

https://doi.org/10.21873/anticanres.12454

161. Huang SH, Hsu MH, Hsu SC, *et al*., 2014, Phenethyl isothiocyanate triggers apoptosis in human malignant melanoma A375. S2 cells through reactive oxygen species and the mitochondria-dependent pathways. *Hum Exp Toxicol*, 33(3): 270–283.

https://doi.org/10.1177/0960327113491508

162. Chen Y, Li Y, Wang XQ, *et al*., 2018, Phenethyl isothiocyanate inhibits colorectal cancer stem cells by suppressing Wnt/β-catenin pathway. *Phytother Res*, 32(12): 2447–2455.

https://doi.org/10.1002/ptr.6183

163. Gupta P, Srivastava SK, 2012, Antitumor activity of phenethyl isothiocyanate in HER2-positive breast cancer models. *BMC Med*, 10(1): 80.

https://doi.org/10.1186/1741-7015-10-80

164. Ezeriņa D, Takano Y, Hanaoka K, *et al*., 2018, N-acetyl cysteine functions as a fast-acting antioxidant by triggering intracellular H2S and sulfane sulfur production. *Cell Chem Biol*, 25(4): 447–459.e4.

https://doi.org/10.1016/j.chembiol.2018.01.011

165. Geng YD, Zhang L, Wang GY, *et al*., 2020, Xanthatin mediates G2/M cell cycle arrest, autophagy and apoptosis via ROS/XIAP signaling in human colon cancer cells. *Nat Prod Res*, 34(18): 2616–2620.

https://doi.org/10.1080/14786419.2018.1544976

166. Zuhra K, Tomé CS, Masi L, *et al*., 2019, N-acetylcysteine serves as substrate of 3-mercaptopyruvate sulfurtransferase and stimulates sulfide metabolism in colon cancer cells. *Cells*, 8(8): 828.

https://doi.org/10.3390/cells8080828

167. Jurkowska H, Wróbel M, 2018, Inhibition of human neuroblastoma cell proliferation by N-acetyl-L-cysteine as a result of increased sulfane sulfur level. *Anticancer Res*, 38(9): 5109–5113.

https://doi.org/10.21873/anticanres.12831

168. Li J, Tu HJ, Li J, *et al*., 2007, N-acetyl cysteine inhibits human signet ring cell gastric cancer cell line (SJ-89) cell

growth by inducing apoptosis and DNA synthesis arrest. *Eur J Gastroenterol Hepatol*, 19(9): 769–774.

https://doi.org/10.1097/MEG.0b013e3282202bda

169. Qin W, Li C, Zheng W, *et al*., 2015, Inhibition of autophagy promotes metastasis and glycolysis by inducing ROS in gastric cancer cells. *Oncotarget*, 6(37): 39839–39854.

https://doi.org/10.18632/oncotarget.5674

170. Duan C, Zhang B, Deng C, *et al*., 2016, Piperlongumine induces gastric cancer cell apoptosis and G2/M cell cycle arrest both *in vitro* and *in vivo*. *Tumour Biol*, 37(8): 10793–10804.

https://doi.org/10.1007/s13277-016-4792-9

171. Bondad N, Boostani R, Barri A, *et al*., 2020, Protective effect of N-acetylcysteine on oxaliplatin-induced neurotoxicity in patients with colorectal and gastric cancers: A randomized, double blind, placebo-controlled, clinical trial. *J Oncol Pharm Pract*, 26(7): 1575–1582.

https://doi.org/10.1177/1078155219900788

172. Sayin VI, Ibrahim MX, Larsson E, *et al*., 2014, Antioxidants accelerate lung cancer progression in mice. *Sci Transl Med*, 6(221): 221ra15.

https://doi.org/10.1126/scitranslmed.3007653

173. Li J, Wang XH, Hu J, *et al*., 2020, Combined treatment with N-acetylcysteine and gefitinib overcomes drug resistance to gefitinib in NSCLC cell line. *Cancer Med*, 9(4): 1495–1502.

https://doi.org/10.1002/cam4.2610

174. Gersey ZC, Rodriguez GA, Barbarite E, *et al*., 2017, Curcumin decreases malignant characteristics of glioblastoma stem cells via induction of reactive oxygen species. *BMC Cancer*, 17(1): 99.

https://doi.org/10.1186/s12885-017-3058-2

175. Agarwal A, Muñoz-Nájar U, Klueh U, *et al*., 2004, N-acetyl-cysteine promotes angiostatin production and vascular collapse in an orthotopic model of breast cancer. *Am J Pathol*, 164(5): 1683–1696.

https://doi.org/10.1016/S0002-9440(10)63727-3

176. Monti D, Sotgia F, Whitaker-Menezes D, *et al*. 2017, Pilot study demonstrating metabolic and anti-proliferative effects of *in vivo* anti-oxidant supplementation with N-Acetylcysteine in Breast Cancer. *Semin Oncol*. 44(3):226-232.

https://doi.org/10.1053/j.seminoncol.2017.10.001

177. Panjehpour M, Alaie S, 2010, N-acetylcysteine inhibits cadmium-induced cytotoxicity in human breast cancer cell line (MDA-MB468). *Toxicol Lett*, 196: S308.

https://doi.org/10.1016/j.toxlet.2010.03.972

178. Huang Z, Hu H, 2021, Arginine deiminase induces immunogenic cell death and is enhanced by n-acetylcysteine in murine MC38 colorectal cancer cells and MDA-MB-231 human breast cancer cells *in vitro*. *Molecules*, 26(2): 511.

https://doi.org/10.3390/molecules26020511

179. Supabphol A, Muangman V, Chavasiri W, *et al*., 2009, N-acetylcysteine inhibits proliferation, adhesion, migration and invasion of human bladder cancer cells. *J Med Assoc Thai*, 92(9): 1171–1177.

180. Tang L, Li G, Song L, *et al*., 2006, The principal urinary metabolites of dietary isothiocyanates, N-acetylcysteine conjugates, elicit the same anti-proliferative response as their parent compounds in human bladder cancer cells. *Anticancer Drugs*, 17(3): 297–305.

https://doi.org/10.1097/00001813-200603000-00008

181. Miyajima A, Nakashima J, Tachibana M, *et al*., 1999, N-Acetylcysteine modifies cis-dichlorodiammineplatinum-induced effects in bladder cancer cells. *Jpn J Cancer Res*, 90(5): 565–570.

https://doi.org/10.1111/j.1349-7006.1999.tb00784.x

182. Supabphol MA, 2012, Antimetastatic potential of N-acetylcysteine on human prostate cancer cells. *J Med Assoc Thai*, 95(12): S56–S62.

183. Tozawa K, Okamoto T, Hayashi Y, *et al*., 2002, N-acetyl-L-cysteine enhances chemotherapeutic effect on prostate cancer cells. *Urol Res*, 30(1): 53–58.

https://doi.org/10.1007/s00240-001-0226-1

184. Brum G, Carbone T, Still E, *et al*., 2013, N-acetylcysteine potentiates doxorubicin-induced ATM and p53 activation in ovarian cancer cells. *Int J Oncol*, 42(1): 211–218.

https://doi.org/10.3892/ijo.2012.1680

185. Mantawy EM, Said RS, Kassem DH, *et al*., 2020, Novel molecular mechanisms underlying the ameliorative effect of N-acetyl-L-cysteine against ϒ-radiation-induced premature ovarian failure in rats. *Ecotoxicol Environ Saf*, 206: 111190.

https://doi.org/10.1016/j.ecoenv.2020.111190

186. Mezencev R, Wang L, Xu W, *et al*., 2013, Molecular analysis of the inhibitory effect of N-acetyl-L-cysteine on the proliferation and invasiveness of pancreatic cancer cells. *Anticancer Drugs*, 24(5): 504–518.

https://doi.org/10.1097/CAD.0b013e32836009d7

187. Pillai K, Mekkawy AH, Akhter J, *et al*., 2020, Enhancing the potency of chemotherapeutic agents by combination with bromelain and N-acetylcysteine-an *in vitro* study with pancreatic and hepatic cancer cells. *Am J Transl Res*, 12(11): 7404–7419.

188. Tsuyuki S, Yamauchi A, Nakamura H, *et al*., 1998, Possible availability of N-acetylcysteine as an adjunct to cytokine therapy for hepatocellular carcinoma. *Clin Immunol Immunopathol*, 88(2): 192–198.

https://doi.org/10.1006/clin.1998.4574

189. Dagnino S, Bodinier B, Grigoryan H, *et al*., 2020, Agnostic

cys34-albumin adductomics and DNA methylation: Implication of N-acetylcysteine in lung carcinogenesis years before diagnosis. *Int J Cancer*, 146(12): 3294–3303.

https://doi.org/10.1002/ijc.32680

190. Breau M, Houssaini A, Lipskaia L, *et al*., 2019, The antioxidant N-acetylcysteine protects from lung emphysema but induces lung adenocarcinoma in mice. *JCI Insight*, 4(19): e127647.

https://doi.org/10.1172/jci.insight.127647

191. De Preter G, Deriemaeker C, Danhier P, *et al*., 2016, A fast hydrogen sulfide–releasing donor increases the tumor response to radiotherapyhydrogen sulfide donor potentiates radiotherapy. *Mol Cancer Ther*, 15(1): 154–161.

https://doi.org/10.1158/1535-7163.MCT-15-0691-T

192. Zhen Y, Zhang W, Liu C, *et al*., 2015, Exogenous hydrogen sulfide promotes C6 glioma cell growth through activation of the p38 MAPK/ERK1/2-COX-2 pathways. *Oncol Rep*, 34(5): 2413–2422.

https://doi.org/10.3892/or.2015.4248

193. Zhao L, Wang Y, Yan Q, *et al*., 2015, Exogenous hydrogen sulfide exhibits anti-cancer effects though p38 MAPK signaling pathway in C6 glioma cells. *Biol Chem*, 396(11): 1247–1253.

https://doi.org/10.1515/hsz-2015-0148

194. Cai WJ, Wang MJ, Ju LH, *et al*., 2010, Hydrogen sulfide induces human colon cancer cell proliferation: Role of Akt, ERK and p21. *Cell Biol Int*, 34(6): 565–572.

https://doi.org/10.1042/CBI20090368

195. Faris P, Ferulli F, Vismara M, *et al*., 2020, Hydrogen sulfide-evoked intracellular Ca2+ signals in primary cultures of metastatic colorectal cancer cells. *Cancers (Basel)*, 12(11): 3338.

https://doi.org/10.3390/cancers12113338

196. Ma Z, Bi Q, Wang Y, 2015, Hydrogen sulfide accelerates cell cycle progression in oral squamous cell carcinoma cell lines. *Oral Dis*, 21(2): 156–162.

https://doi.org/10.1111/odi.12223

197. Liu H, Chang J, Zhao Z, *et al*., 2017, Effects of exogenous hydrogen sulfide on the proliferation and invasion of human Bladder cancer cells. *J Cancer Res Ther*, 13(5): 829–832.

https://doi.org/10.4103/jcrt.JCRT_423_17

198. Zhen Y, Wu Q, Ding Y, *et al*., 2018, Exogenous hydrogen sulfide promotes hepatocellular carcinoma cell growth by activating the STAT3-COX-2 signaling pathway. *Oncol Lett*, 15(5): 6562–6570.

https://doi.org/10.3892/ol.2018.8154

199. Ye M, Yu M, Yang D, *et al*., 2020, Exogenous hydrogen sulfide donor NaHS alleviates nickel-induced epithelial-mesenchymal transition and the migration of A549 cells by regulating TGF-β1/Smad2/Smad3 signaling. *Ecotoxicol Environ Saf*, 195: 110464.

https://doi.org/10.1016/j.ecoenv.2020.110464

200. Nagpure BV, Bian JS, 2014, Hydrogen sulfide inhibits A2A adenosine receptor agonist induced β-amyloid production in SH-SY5Y neuroblastoma cells via a cAMP dependent pathway. *PLoS One*, 9(2): e88508.

https://doi.org/10.1371/journal.pone.0088508

201. Qiao P, Zhao F, Liu M, *et al*., 2017, Hydrogen sulfide inhibits mitochondrial fission in neuroblastoma N2a cells through the Drp1/ERK1/2 signaling pathway. *Mol Med Rep*, 16(1): 971–977.

https://doi.org/10.3892/mmr.2017.6627

202. Hassan AY, Maulood IM, Salihi A, 2021, The vasodilatory mechanism of nitric oxide and hydrogen sulfide in the human mesenteric artery in patients with colorectal cancer. *Exp Ther Med*, 21(3): 214.

https://doi.org/10.3892/etm.2021.9646

203. Xiao AY, Maynard MR, Piett CG, *et al*., 2019, Sodium sulfide selectively induces oxidative stress, DNA damage, and mitochondrial dysfunction and radiosensitizes glioblastoma (GBM) cells. *Redox Biol*, 26: 101220.

https://doi.org/10.1016/j.redox.2019.101220

204. Bhattacharyya S, Saha S, Giri K, *et al*., 2013, Cystathionine beta-synthase (CBS) contributes to advanced ovarian cancer progression and drug resistance. *PloS One*, 8(11): e79167.

https://doi.org/10.1371/journal.pone.0079167

205. Forti KM, Figueroa M, Torres B, *et al*., 2016, Calcium sulfide (CaS) nanostructure treatment on non-small cell lung cancer. *FASEB J*, 30: 1099.4–1099.4.

206. Li N, Sun Q, Yu Z, *et al*., 2018, Nuclear-targeted photothermal therapy prevents cancer recurrence with near-infrared triggered copper sulfide nanoparticles. *ACS Nano*, 12(6): 5197–5206.

https://doi.org/10.1021/acsnano.7b06870

207. Li Y, Lu W, Huang Q, *et al*., 2010, Copper sulfide nanoparticles for photothermal ablation of tumor cells. *Nanomedicine (Lond)*, 5(8): 1161–1171.

https://doi.org/10.2217/nnm.10.85

208. Lee ZW, Teo XY, Song ZJ, *et al*., 2017, Intracellular hyper-acidification potentiated by hydrogen sulfide mediates invasive and therapy resistant cancer cell death. *Front Pharmacol*, 8: 763.

https://doi.org/10.3389/fphar.2017.00763

209. Sakuma S, Minamino S, Takase M, *et al*., 2019, Hydrogen sulfide donor GYY4137 suppresses proliferation of human colorectal cancer Caco-2 cells by inducing both cell cycle arrest and cell death. *Heliyon*, 5(8): e02244.

https://doi.org/10.1016/j.heliyon.2019.e02244

210. Szadvari I, Hudecova S, Chovancova B, *et al*., 2019, Sodium/calcium exchanger is involved in apoptosis induced by H2S in tumor cells through decreased levels of intracellular pH. *Nitric Oxide*, 87: 1–9.

https://doi.org/10.1016/j.niox.2019.02.011

211. Lu S, Gao Y, Huang X, *et al*., 2014, GYY4137, a hydrogen sulfide (H2S) donor, shows potent anti-hepatocellular carcinoma activity through blocking the STAT3 pathway. *Int J Oncol*, 44(4): 1259–1267.

https://doi.org/10.3892/ijo.2014.2305

212. Yurinskaya MM, Garbuz DG, Afanasiev VN, *et al*., 2020, Effects of the hydrogen sulfide donor GYY4137 and HSP70 protein on the activation of SH-SY5Y cells by lipopolysaccharide. *Mol Biol (Mosk)*, 54(6): 1018–1028.

https://doi.org/10.31857/S0026898420060142

213. Hasegawa U, Tateishi N, Uyama H, *et al*., 2015, Hydrolysis-sensitive dithiolethione prodrug micelles. *Macromol Biosci*, 15(11): 1512–1522.

https://doi.org/10.1002/mabi.201500156

214. Cai F, Xu H, Cao N, *et al*., 2020, ADT-OH, a hydrogen sulfide-releasing donor, induces apoptosis and inhibits the development of melanoma *in vivo* by upregulating FADD. *Cell Death Dis*, 11(1): 33.

https://doi.org/10.1038/s41419-020-2222-9

215. Dong Q, Yang B, Han JG, *et al*., 2019, A novel hydrogen sulfide-releasing donor, HA-ADT, suppresses the growth of human breast cancer cells through inhibiting the PI3K/AKT/mTOR and Ras/Raf/MEK/ERK signaling pathways. *Cancer Lett*, 455: 60–72.

https://doi.org/10.1016/j.canlet.2019.04.031

216. Ma K, Liu Y, Zhu Q, *et al*., 2011, H2S donor, S-propargyl-cysteine, increases CSE in SGC-7901 and cancer-induced mice: Evidence for a novel anti-cancer effect of endogenous H2S? *PLoS One*, 6(6): e20525.

https://doi.org/10.1371/journal.pone.0020525

217. Wang W, Cheng J, Zhu Y, 2015, The JNK signaling pathway is a novel molecular target for S-propargyl-L-cysteine, a naturally-occurring garlic derivatives: Link to its anticancer activity in pancreatic cancer *in vitro* and *in vivo*. *Curr Cancer Drug Targets*, 15(7): 613–623.

https://doi.org/10.2174/1568009615666150602143943

218. Covarrubias AE, Lecarpentier E, Lo A, *et al*., 2019, AP39, a modulator of mitochondrial bioenergetics, reduces antiangiogenic response and oxidative stress in hypoxia-exposed trophoblasts: Relevance for preeclampsia pathogenesis. *Am J Pathol*, 189(1): 104–114.

https://doi.org/10.1016/j.ajpath.2018.09.007

219. Szczesny B, Módis K, Yanagi K, *et al*., 2014, AP39, a novel mitochondria-targeted hydrogen sulfide donor, stimulates cellular bioenergetics, exerts cytoprotective effects and protects against the loss of mitochondrial DNA integrity in oxidatively stressed endothelial cells *in vitro*. *Nitric Oxide*, 41: 120–130.

https://doi.org/10.1016/j.niox.2014.04.008

220. Xu S, Yang CT, Meng FH, *et al*., 2016, Ammonium tetrathiomolybdate as a water-soluble and slow-release hydrogen sulfide donor. *Bioorg Med Chem Lett*, 26(6): 1585–1588.

https://doi.org/10.1016/j.bmcl.2016.02.005

221. Zhao YN, Chen LH, Yang XL, *et al*., 2020, Inhibition of copper transporter-1 by ammonium tetrathiocarbolybdate in the treatment of pancreatic cancer. *Sichuan Da Xue Xue Bao Yi Xue Ban*, 51(5): 643–649.

https://doi.org/10.12182/20200960101

222. Ryumon S, Okui T, Kunisada Y, *et al*., 2019, Ammonium tetrathiomolybdate enhances the antitumor effect of cisplatin via the suppression of ATPase copper transporting beta in head and neck squamous cell carcinoma. *Oncol Rep*, 42(6): 2611–2621.

https://doi.org/10.3892/or.2019.7367

223. Chisholm CL, Wang H, Wong AHH, *et al*., 2016, Ammonium tetrathiomolybdate treatment targets the copper transporter ATP7A and enhances sensitivity of breast cancer to cisplatin. *Oncotarget*, 7(51): 84439–84452.

https://doi.org/10.18632/oncotarget.12992

224. Chan N, Willis A, Kornhauser N, *et al*., 2017, Influencing the tumor microenvironment: A phase II study of copper-depletion using tetrathiomolybdate (TM) in patients with breast cancer at high risk for recurrence and in preclinical models of lung metastases. *Clin Cancer Res*, 23(3): 666–676.

https://doi.org/10.1158/1078-0432.CCR-16-1326

225. Li X, Li N, Huang L, *et al*., 2020, Is hydrogen sulfide a concern during treatment of lung adenocarcinoma with ammonium tetrathiomolybdate? *Front Oncol*, 10: 234.

https://doi.org/10.3389/fonc.2020.00234

226. Elsheikh W, Blackler RW, Flannigan KL, *et al*., 2014, Enhanced chemopreventive effects of a hydrogen sulfide-releasing anti-inflammatory drug (ATB-346) in experimental colorectal cancer. *Nitric Oxide*, 41: 131–137.

https://doi.org/10.1016/j.niox.2014.04.006

227. De Cicco P, Panza E, Ercolano G, *et al*., 2016, ATB-346, a novel hydrogen sulfide-releasing anti-inflammatory drug, induces apoptosis of human melanoma cells and inhibits melanoma development *in vivo*. *Pharmacol Res*, 114: 67–73.

https://doi.org/10.1016/j.phrs.2016.10.019

228. Kodela R, Chattopadhyay M, Velázquez-Martínez CA, *et al*., 2015, NOSH-aspirin (NBS-1120), a novel nitric

oxide-and hydrogen sulfide-releasing hybrid has enhanced chemo-preventive properties compared to aspirin, is gastrointestinal safe with all the classic therapeutic indications. *Biochem Pharmacol*, 98(4): 564–572.

https://doi.org/10.1016/j.bcp.2015.09.014

229. Chattopadhyay M, Kodela R, Kashfi K, 2013, P09 therapeutic potential of NOSH-aspirin, a dual nitric oxide- and hydrogen sulfide-donating hybrid in colon cancer. *Nitric Oxide*, 31: S37–S38.

https://doi.org/10.1016/j.niox.2013.06.071

230. Kashfi K, Chattopadhyay M, Kodela R, *et al*., 2013 NOSH-aspirin a Dual Nitric Oxide and Hydrogen Sulfide-Releasing Hybrid Reciprocally Regulates NF-κB: S-Nitrosylation vs S-Sulfhydration. Hoboken, New Jersey: Wiley Online Library.

231. Kashfi K, Borgo S, Williams JL, *et al*., 2005, Positional isomerism markedly affects the growth inhibition of colon cancer cells by nitric oxide-donating aspirin *in vitro* and *in vivo*. *J Pharmacol Exp Ther*, 312(3): 978–988.

https://doi.org/10.1124/jpet.104.075994

232. Togashi A, Katagiri T, Ashida S, *et al*., 2005, Hypoxia-inducible protein 2 (HIG2), a novel diagnostic marker for renal cell carcinoma and potential target for molecular therapy. *Cancer Res*, 65(11): 4817–4826.

https://doi.org/10.1158/0008-5472.CAN-05-0120

233. Huang Z, Fu J, Zhang Y, 2017, Nitric oxide donor-based cancer therapy: Advances and prospects. *J Med Chem*, 60(18): 7617–7635.

https://doi.org/10.1021/acs.jmedchem.6b01672

234. Jeong CH, Ryu H, Kim DH, *et al*., 2019, Piperlongumine induces cell cycle arrest via reactive oxygen species accumulation and IKKβ suppression in human breast cancer cells. *Antioxidants (Basel)*, 8(11): 553.

https://doi.org/10.3390/antiox8110553

235. Chattopadhyay M, Kodela R, Santiago G, *et al*., 2020, NOSH-aspirin (NBS-1120) inhibits pancreatic cancer cell growth in a xenograft mouse model: Modulation of FoxM1, p53, NF-κB, iNOS, caspase-3 and ROS. *Biochem Pharmacol*, 176: 113857.

https://doi.org/10.1016/j.bcp.2020.113857

236. Kodela R, Chattopadhyay M, Kashfi K, 2013, Synthesis and biological activity of NOSH-naproxen (AVT-219) and NOSH-sulindac (AVT-18A) as potent anti-inflammatory agents with chemotherapeutic potential. *Medchemcomm*, 4(11): 1472–1481.

https://doi.org/10.1039/C3MD00185G

237. Jia H, Ye J, You J, *et al*., 2017, Role of the cystathionine β-synthase/H2S system in liver cancer cells and the inhibitory effect of quinolone-indolone conjugate QIC2 on the system. *Oncol Rep*, 37(5): 3001–3009.

https://doi.org/10.3892/or.2017.5513

238. Kashfi K, Chattopadhyay M, Kodela R, 2015, NOSH-sulindac (AVT-18A) is a novel nitric oxide-and hydrogen sulfide-releasing hybrid that is gastrointestinal safe and has potent anti-inflammatory, analgesic, antipyretic, anti-platelet, and anti-cancer properties. *Redox Biol*, 6: 287–296.

https://doi.org/10.1016/j.redox.2015.08.012

239. You J, Shi X, Liang H, *et al*., 2017, Cystathionine-γ-lyase promotes process of breast cancer in association with STAT3 signaling pathway. *Oncotarget*, 8(39): 65677–65686.

https://doi.org/10.18632/oncotarget.20057

240. You J, Ma M, Ye J, *et al*., 2017, Down-Regulation of Cystathionine-γ-lyase/H2S System Inhibits Cell Growth in Human Breast Cancer MDA-MB-231 Cells. In: BIO Web of Conferences. EDP Sciences.

241. Chakraborty PK, Xiong X, Mustafi SB, *et al*., 2015, Role of cystathionine beta synthase in lipid metabolism in ovarian cancer. *Oncotarget*, 6(35): 37367–37384.

https://doi.org/10.18632/oncotarget.5424

242. Liu Y, Wang L, Zhang X, *et al*., 2021, A novel cystathionine γ-lyase inhibitor, I194496, inhibits the growth and metastasis of human TNBC via downregulating multiple signaling pathways. *Sci Rep*, 11(1): 1–13.

243. Ye F, Li X, Sun K, *et al*., 2020, Inhibition of endogenous hydrogen sulfide biosynthesis enhances the anti-cancer effect of 3, 3'-diindolylmethane in human gastric cancer cells. *Life Sci*, 261: 118348.

https://doi.org/10.1016/j.lfs.2020.118348

244. Yin P, Zhao C, Li Z, *et al*., 2012, Sp1 is involved in regulation of cystathionine γ-lyase gene expression and biological function by PI3K/Akt pathway in human hepatocellular carcinoma cell lines. *Cell Signal*, 24(6): 1229–1240.

https://doi.org/10.1016/j.cellsig.2012.02.003

245. Pan Y, Ye S, Yuan D, *et al*., 2014, Hydrogen sulfide (H2S)/cystathionine γ-lyase (CSE) pathway contributes to the proliferation of hepatoma cells. *Mutat Res*, 763–764: 10–18.

https://doi.org/10.1016/j.mrfmmm.2014.03.002

246. Pan Y, Zhou C, Yuan D, *et al*., 2016, Radiation exposure promotes hepatocarcinoma cell invasion through epithelial mesenchymal transition mediated by H2S/CSE pathway. *Radiat Res*, 185(1): 96–105.

https://doi.org/10.1667/RR14177.1

247. Yang D, Li T, Li Y, *et al*., 2019, H2S suppresses indoleamine 2, 3-dioxygenase 1 and exhibits immunotherapeutic efficacy in murine hepatocellular carcinoma. *J Exp Clin Cancer Res*, 38(1): 88.

https://doi.org/10.1186/s13046-019-1083-5

248. Fan K, Li N, Qi J, *et al*., 2014, Wnt/β-catenin signaling induces the transcription of cystathionine-γ-lyase, a stimulator of tumor in colon cancer. *Cell Signal*, 26(12):

2801–2808.

https://doi.org/10.1016/j.cellsig.2014.08.023

249. Wang YH, Huang JT, Chen WL, *et al*., 2019, Dysregulation of cystathionine γ-lyase promotes prostate cancer progression and metastasis. *EMBO Rep*, 20(10): e45986.

https://doi.org/10.15252/embr.201845986

250. Kawahara B, Moller T, Hu-Moore K, *et al*., 2017, Attenuation of antioxidant capacity in human breast cancer cells by carbon monoxide through inhibition of cystathionine β-synthase activity: implications in chemotherapeutic drug sensitivity. *J Med Chem*, 60(19): 8000–8010.

https://doi.org/10.1021/acs.jmedchem.7b00476

251. Zhang L, Qi Q, Yang J, *et al*., 2015, An anticancer role of hydrogen sulfide in human gastric cancer cells. *Oxid Med Cell Longev*, 2015: 636410.

https://doi.org/10.1155/2015/636410

252. Wang L, Cai H, Hu Y, *et al*., 2018, A pharmacological probe identifies cystathionine β-synthase as a new negative regulator for ferroptosis. *Cell Death Dis*, 9(10): 1005.

https://doi.org/10.1038/s41419-018-1063-2

253. Sanokawa-Akakura R, Ostrakhovitch EA, Akakura S, *et al*., 2014, A H2S-Nampt dependent energetic circuit is critical to survival and cytoprotection from damage in cancer cells. *PloS One*, 9(9): e108537.

https://doi.org/10.1371/journal.pone.0108537

254. Kim J, Hong SJ, Park JH, *et al*., 2009, Expression of cystathionine β-synthase is downregulated in hepatocellular carcinoma and associated with poor prognosis. *Oncol Rep*, 21(6): 1449–1454.

https://doi.org/10.3892/or_00000373

255. Zhang J, Xie Y, Xu Y, *et al*., 2011, Hydrogen sulfide contributes to hypoxia-induced radioresistance on hepatoma cells. *J Radiat Res*, 52(5): 622–628.

https://doi.org/10.1269/jrr.11004

256. Wang L, Han H, Liu Y, *et al*., 2018, Cystathionine β-synthase induces multidrug resistance and metastasis in hepatocellular carcinoma. *Curr Mol Med*, 18(7): 496–506.

https://doi.org/10.2174/1566524019666181211162754

257. Wang L, Yang Z, Wu Z, *et al*., 2020, Increased expression of cystathionine beta-synthase and chemokine ligand 21 is closely associated with poor prognosis in extrahepatic cholangiocarcinoma. *Medicine (Baltimore)*, 99(38): e22255.

https://doi.org/10.1097/MD.0000000000022255

258. Liu N, Lin X, Huang C, 2020, Activation of the reverse transsulfuration pathway through NRF2/CBS confers erastin-induced ferroptosis resistance. *Br J Cancer*, 122(2): 279–292.

259. Santos I, Ramos C, Mendes C, *et al*., 2019, Targeting glutathione and cystathionine β-synthase in ovarian cancer treatment by selenium–chrysin polyurea dendrimer nanoformulation. *Nutrients*, 11(10): 2523.

https://doi.org/10.3390/nu11102523

260. Chao C, Zatarain JR, Ding Y, *et al*., 2016, Cystathionine-β-synthase inhibition for colon cancer: Enhancement of the efficacy of aminooxyacetic acid via the prodrug approach. *Mol Med*, 22(1): 361–379.

https://doi.org/10.2119/molmed.2016.00102

261. Szabo C, Coletta C, Chao C, *et al*., 2013, Tumor-derived hydrogen sulfide, produced by cystathionine-β-synthase, stimulates bioenergetics, cell proliferation, and angiogenesis in colon cancer. *Proc Natl Acad Sci*, 110(30): 12474–12479.

https://doi.org/10.1073/pnas.1306241110

262. Ascenção K, Dilek N, Augsburger F, *et al*., 2021, Pharmacological induction of mesenchymal-epithelial transition via inhibition of H2S biosynthesis and consequent suppression of ACLY activity in colon cancer cells. *Pharmacol Res*, 165: 105393.

https://doi.org/10.1016/j.phrs.2020.105393

263. Niu W, Chen F, Wang J, *et al*., 2018, Antitumor effect of sikokianin C, a selective cystathionine β-synthase inhibitor, against human colon cancer *in vitro* and *in vivo*. *Medchemcomm*, 9(1): 113–120.

https://doi.org/10.1039/c7md00484b

264. Zhang M, Li J, Huang B, *et al*., 2020, Cystathionine β synthase/hydrogen sulfide signaling in multiple myeloma regulates cell proliferation and apoptosis. *J Environ Pathol Toxicol Oncol*, 39(3): 281–290.

https://doi.org/10.1615/JEnvironPatholToxicolOncol.2020034851

265. Govar AA, Törő G, Szaniszlo P, *et al*., 2020, 3-Mercaptopyruvate sulfurtransferase supports endothelial cell angiogenesis and bioenergetics. *Br J Pharmacol*, 177(4): 866–883.

https://doi.org/10.1111/bph.14574

266. Augsburger F, Randi EB, Jendly M, *et al*., 2020, Role of 3-mercaptopyruvate sulfurtransferase in the regulation of proliferation, migration, and bioenergetics in murine colon cancer cells. *Biomolecules*, 10(3): 447.

https://doi.org/10.3390/biom10030447

267. Bantzi M, Augsburger F, Loup J, *et al*., 2021, Novel aryl-substituted pyrimidones as inhibitors of 3-mercaptopyruvate sulfurtransferase with antiproliferative efficacy in colon cancer. *J Med Chem*, 64(9): 6221–6240.

https://doi.org/10.1021/acs.jmedchem.1c00260

268. Bronowicka-Adamska P, Bentke A, Lasota M, *et al*., 2020, Effect of S-allyl–l-cysteine on MCF-7 cell line 3-mercaptopyruvate sulfurtransferase/sulfane sulfur system, viability and apoptosis. *Int J Mol Sci*, 21(3): 1090.

ACCSCIENCE PUBLISHING

Gene & Protein in Disease

PERSPECTIVE ARTICLE

A hypothesis on the equilibrium between dopamine toxicity and detoxification: The roles of NQO2 and UDP-glucuronosyltransferases

Jean A. Boutin[1,2]*, Gilles Ferry[2], and Karine Reybier[3]

[1]Laboratory of Neuroendocrine Endocrine and Germinal Differentiation and Communication (NorDiC), Univ Rouen Normandie, Inserm, UMR 1239, Rouen, France

[2]Institut de Recherches Servier, 125 chemin de Ronde, Croissy-sur-Seine, France

[3]Pharma-Dev UMR 152, Université de Toulouse, IRD, UPS, Toulouse, France

Abstract

NQO2 and tyrosine hydroxylase are co-expressed in dopaminergic neurons. These neurons produce dopamine, a diol, which, under aerobic conditions, can spontaneously revert to the more stable form, the *o*-quinone. *O*-quinones are preferred substrates of NQO2 over *p*-quinones. In *ad hoc* conditions, NQO2 reduces *o*-quinones into the original diols, leading to a futile cycle, the endpoint of which is a strong local production of reactive oxygen species that is deadly for the cells. This futile cycle can be interrupted by the conjugation of dopamine with UDP-glucuronic acid, leading to a glucuronide that cannot be part of the cycle because the glucuronide is not a substrate of NQO2. In this paper, we confer whether this futile cycle could be one of the causes of the specific death of dopaminergic neuronal population that is the signature of some degenerative diseases.

Keywords: Dopamine; Neurodegenerative diseases; Quinone reductase; Glucuronidation; Reactive oxygen species; Toxicity

***Corresponding author:**
Jean A. Boutin
(ja.boutin.pro@gmail.com)

Citation: Boutin JA, Ferry G, Reybier K., 2023, A hypothesis on the equilibrium between dopamine toxicity and detoxification: The roles of NQO2 and UDP-glucuronosyltransferases. *Gene Protein Dis,* 2(1):277. https://doi.org/10.36922/gpd.227

Received: October 14, 2022
Accepted: January 18, 2023
Published Online: February 1, 2023

1. Drug metabolism and the case of dopamine

Reactive oxygen species (ROS) is a harmful chemical species, and the toxicity of which is well known for decades for its role in a range of pathologies and conditions from cancer[1] to asbestos-induced toxicity[2]. The constant production of ROS and its impact onto subcellular structures (DNA, proteins, and membranes) is associated with the process of aging at the cellular level[3]. More generally, ROS causes harmful lesions in organs in which they are massively generated. To overcome this, a series of antioxidant mechanisms has been developed by evolution[4]. Among other systems, ROS are generated via the redox cycling of quinones, such as menadione[5-7]. We have shown that such a redox cycle occurs in the presence of NQO2, its co-substrate and a series of quinones[8]. We have also shown that the main source of ROS-generating quinone reductase activity in the mouse brain was the activity of the enzyme NQO2[9].

NQO2 is a quinone reductase (E.C. 1.10.5.1) expressed in many tissues of the body[10,11]. Unlike NQO1, NQO2 does not recognize NAD(P)H as a co-substrate, making it a unique example in the literature of quinone reductases[12,13]. Its co-substrates are either

the synthetic *N*-benzyl-dihydronicotinamide (BNAH) or the natural ones: *N*-methyl-dihydronicotinamide (NMH) and *N*-ribosyl-dihydronicotinamide (NRH). The concentration of the latter remains mostly elusive in resting tissues[14-16]. This very fact has led to a key controversy on whether NQO2 is an enzyme with catalytic activity or a pseudo-enzyme without catalytic activity[17], although it remains clear that the same enzyme, NQO2, is present in the genome for several millions of years with the same unique co-substrate recognition as it has been cloned from *Anas platyrhynchos* and *Alligator mississippiensis*[17]. The key questions, which remain unanswered, include: (i) What is its natural co-substrate? Is it NRH? (ii) Where does it come from? Obviously, *in tubo* or *in cellulo*, the enzyme works catalytically and functionally with these co-substrates[11,18,19]. NQO2 reduces *o*- and *p*-quinones when the co-substrate is provided to the pure enzyme[8,13]. NQO2 might have a preferred specificity towards *o*-quinones[20]. This activity also has a "functional" by-product: because the *o*-quinols are particularly unstable, in aerobic conditions, they reversed to their more stable quinone version, while producing ROS[8,20]. Therefore, quinone reductases, by producing diols, indirectly produce ROS species[5,6] in a futile cycle.

Dopamine is an orthoquinol (Figure 1) with a paramount of activities mainly in brain, but also in kidneys and in vasculature[21]. Its dysregulation is involved in degenerative pathologies such as Alzheimer's disease[22] and Parkinson's disease[23], and in general, in neurotoxicity[24]. A link has been suspected for decades between dopamine toxicity and degenerative diseases[25]. Neurons highly expressing this molecule are named dopaminergic neurons, and their death is linked to the progression of these degenerative diseases, at least in some occurrences[26,27]. The definition of dopaminergic neurons corresponds to neurons expressing the tyrosine hydroxylase (TH), an enzyme responsible for the biosynthesis of dopamine from tyrosine[28]. *O*-quinone toxicity has been attributed to the auto-oxidation capacity of its oxidized form[29], although alternative or parallel hypotheses had been explored. The link between dopaminequinone and Parkinson's disease has been reviewed[30-32].

Hydroxylated molecules are eliminated from the body by enzymatic conjugations with polar moieties, such as sulfates or glucuronic acids. These molecules can be endobiotes (bilirubin, steroids, biliary acids, etc.) or xenobiotes (terpenoids, pollutants, and polyaromatic compounds)[33,34]. If not already hydroxylated, they are substrates of the large cytochrome P450 family of enzymes[35]. These enzymes, cytochromes P450 and UDP-glucuronosyltransferases (UGT), are mostly expressed in key organs, that is, liver and kidneys, but also exist in numerous other organs, such as skin and brain[36,37]. UGT, in particular, is clearly active in the brain[38-43]. Incidentally, it has been demonstrated that morphine glucuronide is more active than its aglycone-morphine itself[44,45]. Dopamine glucuronides were identified in mammalian organs and blood[46-51] and found in brain[52-54]. We have also shown that dopamine-treated SH-SY5Y cells expressing UGT1A6 led to the production of dopamine-monoglucuronides, as detected by mass spectrometry[55], demonstrating that dopamine is a substrate of UGT.

We recently showed that NQO2 is co-expressed with tyrosine hydroxylase (TH) in neurons, making this enzyme, by definition, a preferred component of dopaminergic neurons (Boutin and Hirsch, in preparation). We showed

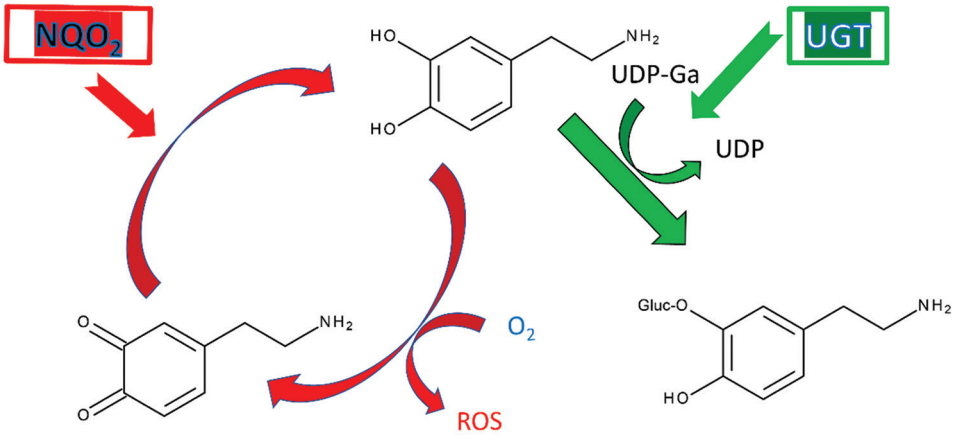

Figure 1. Equilibrium between dopamine toxicity and detoxification. *o*-Quinones can be reduced by NQO2 in the presence of its co-substrate, N-ribosyldihydronicotinamide (NRH), to give an unstable quinol (a diol). This compound, in aerobic conditions, oxidizes back to quinone, generating a burst of toxic ROS. This leads to a futile cycle (quinol/quinone/quinol). *o*-Quinones can be conjugated with glucuronic acid to give glucuronide, thanks to the ubiquitous UDP-glucuronosyltransferase (UGT), in the presence of its co-substrate, UDP-glucuronic acid. Once glucurono-conjugated, the *o*-quinone glucuronide cannot be cycled anymore. The *o*-quinone represented here is dopamine. Red indicates the aspects involved in the toxifying processes, while green the aspects involved in the detoxifying process.

that ROS production in CHO as well as in K562 or SH-SY5Y cells depends on the presence of NQO2. Exploring neurons isolated from NQO2-knockout animals[56], the ROS production was considerably decreased in similar conditions[9]. We concluded that the elevated expression of NQO2 in brain cells in the presence of catechol quinones could lead to ROS-induced cell death via the rapid conversion of superoxide radicals into peroxynitrite by reaction with nitric oxide or into hydrogen peroxide, leading to the highly reactive hydroxyl radicals[9]. Among NQO2 substrates lay oxidized forms of catecholamines such as adrenochrome. Catechols have been shown to co-crystalize with NQO2, which has also been categorized as a catecholamine reductase[57].

In the liver, the activity of oxidoreductase is mainly catalyzed by NQO1, because this enzyme uses NADH as a co-substrate[58,59], which is massively present in liver tissue[60]. NQO2, although expressed in liver, is not capable to reduce compounds due to the low availability of its co-substrate, NRH, as well as the predominant role of NQO1.

Finally, in the last years, the literature reported a possible relationship between NQO2 expression and memory[61-63], before going deeper in a possible relationship between the enzyme regulation and neurogenerative diseases[61,64-67] as well as schizophrenia[68]. These association(s) need further validations, as they were dependent on the patient population tested[69]. Mechanically speaking, an elegant study[70] showed that if the promoter region of *NQO2* gene contains a 29-bp insertion polymorphism, the *NQO2* gene expression is decreased. Mutation in this region would lead to an enhanced expression of NQO2. Such mutation(s) was/were found in post-mortem brain studies of neurodegenerative patients[68]. A physiological hypothesis was also put forward as a possible role for NQO2 in the building of memory[63]. Similarly, we showed that mice devoid of NQO2 were apparently able to learn faster than their wild-type littermates[18,71], linking again memory with NQO2 in a negative correlation way[72]. Reduced NQO2 expression in inhibitory interneurons improves novel object memory. On the contrary, enhanced NQO2 activity would diminish memory after stress episodes[61]. This would form another link between dopaminergic neurons, NQO2 and memory, and following this tentative paradigm, a higher NQO2 expression/activity leads to a lower memory formation[61,73]. On the pharmacological side, potent and specific NQO2 inhibitors, such as S29434 and M11, have neuroprotective properties[18,74].

2. Hypothesis

A speculative but simple idea would be as follows: dopamine is fairly unstable in aerobic conditions, and reacting with oxygen, it is very rapidly transformed in the quinone form. This reaction generates superoxide anions, which decomposes into various ROS (Umek *et al.*[75] and references therein). The kinetic of this reaction is fairly rapid, depending on the pH of the milieu. This reaction occurs concomitantly with the formation of an indole-based quinone for part of the produced oxidized species. The quinone (dopamine quinone or dopaminechrome) is recognized and reduced by NQO2 back into the original quinol in the presence of its co-substrate. Then again, the quinol (dopamine) is oxidized back almost immediately into the quinone. As massive ROS bursts can cause cell death, the colocalization of both dopamine and NQO2 in dopaminergic neurons could be responsible for dopaminergic neuron death, leading to degenerative situations. Thus, the metabolism of dopamine in those neurons is central. Because dopamine glucuronides have been described in brain, and at least one UGT isoform is active in brain, it is clear that if conjugated to glucuronic acid, dopamine cannot enter into this futile cycle of oxidoreduction leading to ROS-mediated toxicity and neuron death.

UGT is a family of conjugated enzymes mainly expressed in liver and kidneys where it detoxifies compounds from the body. UGT is also expressed and active in the brain. NQOs are two enzymes, expressed in many organs. In the liver, the role of NQO1 is clearly to detoxify quinones and to facilitate conjugation, by UGT. Because NQO1 recognizes NADH, which is massively present in the liver, its role is preponderant in this organ, while in the brain, the possible role of NQO2 is speculated in this context. NQO2 does not recognize NAD(P)H as a co-substrate. The origin of NRH remains poorly explored. On the neuron side, the absence of conjugation leads to a futile cycle between quinone and quinol that produces ROS, a toxic entity to the cells.

In summary, as shown in Figure 2, in liver, the predominance of NQO1 and its co-substrate NADH as well as the large amount of UGT and UDPGa, its co-substrate, makes the metabolism of quinone quite safe, from reduction to diol followed by conjugation. In brain, though, the co-expression of NQO2 and tyrosine hydroxylase (TH) might render the installment of this futile cycle very rapid, depending on NQO2 co-substrate availability. The possible role of UGT in this organ is less clear, but the conjugation of diol might stop the quinol/quinone futile cycle. Nevertheless, the presence of dopamine-glucuronides in cerebrospinal fluid[53] indicates the presence of at least one UGT isoform in the brain.

An equilibrium between the conjugation of dopamine and its entrance in the quinone/quinol futile cycle would drive the overall possible toxicity of dopamine, under

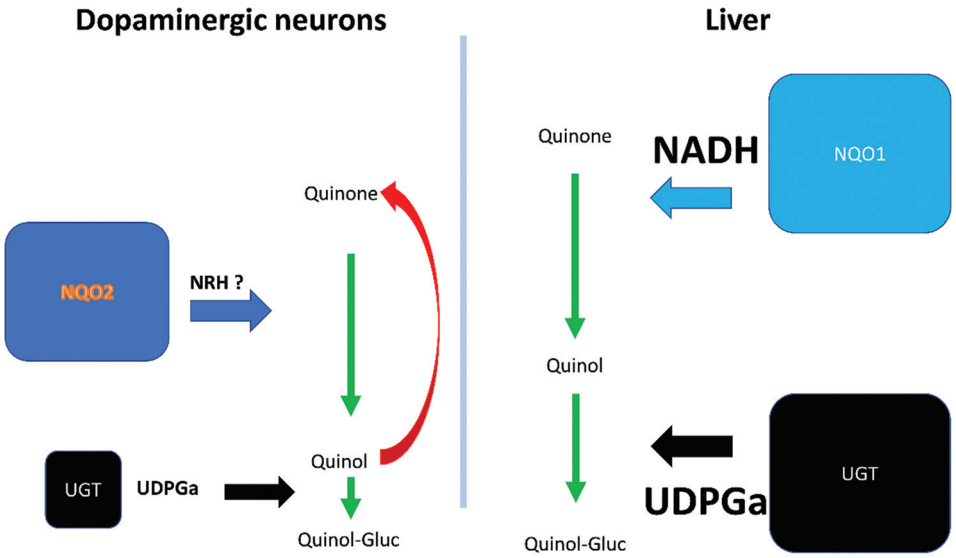

Figure 2. Quantitative comparison in the dopamine toxicity and detoxification equilibrium between liver and brain.

those particular circumstances. Furthermore, a glimpse into the quantitative (very low) and timely (over long period of times) activity of NQO2 would be in line with a low accumulation of ROS in dopaminergic neurons. Therefore, it would translate into the slow injuries and ultimately death of those neurons corresponding to the evolution (worsening) of the degenerative situation over the course of Parkinson's disease[76,77] as well as of Alzheimer's disease[78,79], for example. Among the counteracting mechanisms, UGT could stop or at least limit the cycle, and thus lower the production of ROS. We showed that, in the presence of UGT and UDP-glucuronic acid, the amount of ROS generated during an incubation of cells expressing both UGT and NQO2 in the presence of NRH was strongly diminished[55]. We also showed that in cells, and in the presence of its co-substrate, the main source of ROS production is NQO2, because cells derived from brain of NQO2-knockout mice studied under identical conditions produced marginal amount of ROS[9]. It should be mentioned that the dichotomic role of dopamine in neurodegenerative diseases can be protective and hazardous to them[26,80,81].

Another aspect of the regulation of UGT might be taken into account. It is known for decade that phenobarbital is an inducer of at least some UGT isoforms. These were one of the first pre-cloning proofs of the multi-isoform nature of UGT[82]. The use of differential inductions (phenobarbital and 3-methylcholanthrene) clearly showed the paths towards later characterizations of the UGT isoforms, their purifications and finally, their clonings[33,83]. Furthermore, the use of phenobarbital to try to compensate Crigler-Najjar syndrome or the newborn jaundice has been reported[84,85], showing that the induction of UGT actually works in human. It would be important to verify if such induction of UGT changes (delays) the development of degenerative diseases.

Other conjugative systems present in the brain, such as the sulfotransferases, might also lead to a similar situation[86,87], provided that sulfo-conjugated quinols cannot be substrate of NQO2 (in order to stop the cycle), which probably is the case.

In brief, the amount of available UGT co-substrate, UDP-glucuronic acid, is enough to permit the elimination of dopamine as glucuronide, and most importantly, to identify and quantify the amount of NQO2 co-substrate essential to its activity. Among the possible co-substrates are either NRH, sometimes described as resulting from NADH catabolism, or various nicotinamide catabolites[15,16]. What would make the most sense would be that, under lethal stress, NADH breakdown occurs because cells are in search of adenosine source. When adenosine monophosphate (AMP) molecules are exhausted, NADH would be the next reservoir of nicotinamide derivatives, because its cleavage results in a molecule of AMP and one of nicotinamide.

The respective regulations of NQO2 and UGT expressions are known to depend on environmental factors, such as various pollutants[88-90], that would lead to their differential expressions during life, possibly making the changes in the expression of these enzymes, or the availabilities of either co-substrates, a regulator of the NQO2-dependent neuron toxicity.

As pointed out earlier, the association of some neurodegenerative diseases and enhanced NQO2

Box 1. State of the art and future trends

(A) What is known

(i) Dopaminequinone is spontaneously generated in brain from dopamine.

(ii) Dopaminequinone is a substrate of NQO2 in the brain.

(iii) NQO2 and TH are co-expressed in the dopaminergic neurons.

(iv) NQO2 catalytic activity indirectly leads to the production of ROS.

(v) UGT1A6 produces glucuronide of dopamine.

(vi) UGT is expressed in the brain and glucuronides are found in the LCR.

(vii) UGT can be induced by phenobarbital in human.

(viii) Glucuronidation of dopamine interrupts the futile cycle catalyzed by NQO2, resulting in the cessation of ROS production.

(B) What remains to be demonstrated or reinforced

(i) The presence of UGT in the brain, and its subcellular localization, including at the levels of the neurons as well as its possible co-expression with NQO2.

(ii) The nature of the UGT isoform should be clarified (UGT1A6 or UGT1A10) in the brain.

(iii) The availability of the NQO2 co-substrate (e.g., NRH or NMH).

(iv) The constant but low activity of NQO2 in dopaminergic neurons. (This would correspond to a continuous production of ROS at low levels, and it could correspond to a long process of minimal but repetitive accumulation of injuries in dopaminergic neurons).

(v) The regulations of both NQO2 and UGT expressions – at least the particular isoform in charge of dopamine conjugation. (Particularly regarding their modulations by pollutant factors, in order to document the possible antagonistic effects of UGT dopamine conjugation onto NQO2-dependent toxicity).

(vi) At the cohort levels, could phenobarbital (as inducer of UGT) delays the onset of neurodegenerative diseases?

(vii) Alternative conjugation pathways might play a similar limiting role, such as sulfotransferase(s). (Further studies should complete the picture, in particular, the availability of the co-substrate in the brain, and expression level variation throughout life).

expression is an indication that in some of those pathological situations, NQO2 might have a causal role. Nevertheless, it is highly improbable that every type of neurodegenerative situations is due to both NQO2 and UGT dysregulations. The present commentary is based on our thinking about the enzymes and the situations we encountered over the last 4 decades. To further explore this hypothesis, Box 1 lists the simple questions to be answered in this area. Since they do not seem to be in the mainstreams of neurodegenerative disease research, they may be understudied. Of course, more experiments are warranted to test this hypothesis.

Acknowledgments

None.

Funding

None.

Conflict of interest

The authors declare no conflict of interest.

Author contributions

Conceptualization: Jean A. Boutin, Gilles Ferry, Karine Reybier

Writing – original draft: Jean A. Boutin, Gilles Ferry, Karine Reybier

Writing – review & editing: Jean A. Boutin, Gilles Ferry, Karine Reybier

Ethics approval and consent to participate

Not applicable.

Consent for publication

Not applicable.

Availability of data

Not applicable.

References

1. Stich HF, Anders F, 1989, The involvement of reactive oxygen species in oral cancers of betel quid/tobacco chewers. *Mutat Res*, 214: 47–61.

https://doi.org/10.1016/0027-5107(89)90197-8

2. Kamp DW, Graceffa P, Pryor WA, *et al.*, 1992, The role of free radicals in asbestos-induced diseases. *Free Radic Biol Med*, 12: 293–315.

https://doi.org/10.1016/0891-5849(92)90117-y

3. Hajam YA, Rani R, Ganie SY, *et al.*, 2022, Oxidative stress in human pathology and aging: Molecular mechanisms and perspectives. *Cells*, 11: 552.

https://doi.org/10.3390/cells11030552

4. Lü JM, Lin PH, Yao Q, *et al.*, 2010, Chemical and molecular mechanisms of antioxidants: Experimental approaches and model systems. *J Cell Mol Med*, 14: 840–860.

https://doi.org/10.1111/j.1582-4934.2009.00897.x

5. Nutter LM, Ngo EO, Fisher GR, *et al.*, 1992, DNA strand scission and free radical production in menadione-treated cells. Correlation with cytotoxicity and role of NADPH quinone acceptor oxidoreductase. *J Biol Chem*, 267: 2474–2479.

https://doi.org/10.1016/S0021-9258(18)45903-0

6. Qiu XB, Cadenas E, 1997, The role of NAD(P)H: Quinone oxidoreductase in quinone-mediated p21 induction in

human colon carcinoma cells. *Arch Biochem Biophys*, 346: 241–251.

https://doi.org/10.1006/abbi.1997.0329

7. Criddle DN, Gillies S, Baumgartner-Wilson HK, *et al.*, 2006, Menadione-induced reactive oxygen species generation via redox cycling promotes apoptosis of murine pancreatic acinar cells. *J Biol Chem*, 281: 40485–40492.

https://doi.org/10.1074/jbc.M607704200

8. Reybier K, Perio P, Ferry G, *et al.*, 2011, Insights into the redox cycle of human quinone reductase 2. *Free Radic Res*, 45: 1184–1195.

https://doi.org/10.3109/10715762.2011.605788

9. Cassagnes LE, Chhour M, Pério P, *et al.*, 2018, Oxidative stress and neurodegeneration: The possible contribution of quinone reductase 2. *Free Radic Biol Med*, 120: 56–61.

https://doi.org/10.1016/j.freeradbiomed.2018.03.002

10. Vella F, Ferry G, Delagrange P, *et al.*, 2005, NRH: quinone reductase 2: An enzyme of surprises and mysteries. *Biochem Pharmacol*, 71: 1–12.

https://doi.org/10.1016/j.bcp.2005.09.019

11. Janda E, Nepveu F, Calamini B, *et al.*, 2020, Molecular pharmacology of NRH: Quinone oxidoreductase 2: a detoxifying enzyme acting as an undercover toxifying enzyme. *Mol Pharmacol*, 98: 620–33.

https://doi.org/10.1124/molpharm.120.000105

12. Liao S, Dulaney JT, Williams-Ashman HG, 1962, Purification and properties of a flavoprotein catalyzing the oxidation of reduced ribosyl nicotinamide. *J Biol Chem*, 237: 2981–2987.

13. Zhao Q, Yang XL, Holtzclaw WD, *et al.*, 1997, Unexpected genetic and structural relationships of a long-forgotten flavoenzyme to NAD(P)H: quinone reductase (DT-diaphorase). *Proc Natl Acad Sci U S A*, 94: 1669–1674.

https://doi.org/10.1073/pnas.94.5.1669

14. Formentini L, Moroni F, Chiarugi A, 2009, Detection and pharmacological modulation of nicotinamide mononucleotide (NMN) *in vitro* and *in vivo*. *Biochem Pharmacol*, 77: 1612–1620.

https://doi.org/10.1016/j.bcp.2009.02.017

15. Sonavane M, Hayat F, Makarov M, *et al.*, 2020, Dihydronicotinamide riboside promotes cell-specific cytotoxicity by tipping the balance between metabolic regulation and oxidative stress. *PLoS One*, 15: e0242174.

https://doi.org/10.1371/journal.pone.0242174

16. Makarov MV, Hayat F, Graves B, *et al.*, 2021, Chemical and biochemical reactivity of the reduced forms of Nicotinamide riboside. *ACS Chem Biol*, 16: 604–614.

https://doi.org/10.1021/acschembio.0c00757

17. Islam F, Leung KK, Walker MD, *et al.*, 2022, The unusual cosubstrate specificity of NQO2: Conservation throughout the amniotes and implications for cellular function. *Front Pharmacol*, 13: 838500.

https://doi.org/10.3389/fphar.2022.838500

18. Boutin JA, Bouillaud F, Janda E, *et al.*, 2019, S29434, a quinone reductase 2 inhibitor: Main biochemical and cellular characterization. *Mol Pharmacol*, 95: 269–285.

https://doi.org/10.1124/mol.118.114231

19. Leung KKK, Shilton BH, 2015, Binding of DNA-intercalating agents to oxidized and reduced quinone reductase 2. *Biochemistry*, 54: 7438–7448.

https://doi.org/10.1021/acs.biochem.5b00884

20. Cassagnes LE, Perio P, Ferry G, *et al.*, 2015, In cellulo monitoring of quinone reductase activity and reactive oxygen species production during the redox cycling of 1,2 and 1,4 quinones. *Free Radic Biol Med*, 89: 126–134.

https://doi.org/10.1016/j.freeradbiomed.2015.07.150

21. Crocker AD, 1994, Experimental and clinical pharmacology: Dopamine- mechanisms of action. *Aust Prescr*, 17: 17–21.

https://doi.org/10.18773/austprescr.1994.023

22. Nasrolahi A, Javaherforooshzadeh F, Jafarzadeh-Gharehziaaddin M, *et al.*, 2022, Therapeutic potential of neurotrophic factors in Alzheimer's disease. *Mol Biol Rep*, 49: 2345–2357.

https://doi.org/10.1007/s11033-021-06968-9

23. Grosset D, 2010, Therapy adherence issues in Parkinson's disease. *J Neurol Sci*, 289: 115–118.

https://doi.org/10.1016/j.jns.2009.08.053

24. Miyazaki I, Asanuma M, 2009, Approaches to prevent dopamine quinone-induced neurotoxicity. *Neurochem Res*, 34: 698–706.

https://doi.org/10.1007/s11064-008-9843-1

25. Smythies JR, 1997, Oxidative reactions and schizophrenia: A review-discussion. *Schizophr Res*, 24: 357–364.

https://doi.org/10.1016/s0920-9964(97)00005-4

26. Latif S, Jahangeer M, Maknoon Razia D, *et al.*, 2021, Dopamine in Parkinson's disease. *Clin Chim Acta*, 522: 114–126.

https://doi.org/10.1016/j.cca.2021.08.009

27. Zhu L, Sun C, Ren J, *et al.*, 2019, Stress-induced precocious aging in PD-patient iPSC-derived NSCs may underlie the pathophysiology of Parkinson's disease. *Cell Death Dis*, 10: 105.

https://doi.org/10.1038/s41419-019-1313-y

28. Best JA, Nijhout HF, Reed MC, 2009, Homeostatic mechanisms in dopamine synthesis and release: A mathematical model. *Theor Biol Med Model*, 6: 21.

https://doi.org/10.1186/1742-4682-6-21

29. Asanuma M, Miyazaki I, Diaz-Corrales FJ, *et al.*, 2004, Quinone formation as dopaminergic neuron-specific oxidative stress in the pathogenesis of sporadic Parkinson's disease and neurotoxin-induced parkinsonism. *Acta Med Okayama*, 58: 221–233.

https://doi.org/10.18926/AMO/32105

30. Miyazaki I, Asanuma M, 2008, Dopaminergic neuron-specific oxidative stress caused by dopamine itself. *Acta Med Okayama*, 62: 141–150.

https://doi.org/10.18926/AMO/30942

31. Sulzer D, Zecca L, 2000, Intraneuronal dopamine-quinone synthesis: A review. *Neurotox Res*, 1: 181–195.

https://doi.org/10.1007/BF03033289

32. Hattoria N, Wanga M, Taka H, *et al.*, 2009, Toxic effects of dopamine metabolism in Parkinson's disease. *Parkinsonism Relat Disord*, 15 Suppl 1: S35–S38.

https://doi.org/10.1016/S1353-8020(09)70010-0

33. Boutin JA, 1987, Indirect evidences of UDP-glucuronosyltransferase heterogeneity: how can it help purification? *Drug Metab Rev*, 18: 517–551.

https://doi.org/10.3109/03602538708994131

34. Jackson MR, Fournel-Gigleux S, Harding D, *et al.*, 1988, Examination of the substrate specificity of cloned rat kidney phenol UDP-glucuronyltransferase expressed in COS-7 cells. *Mol Pharmacol*, 34: 638–642.

35. Testa B, Krämer SD, 2007, The biochemistry of drug metabolism an introduction: Part 2. Redox reactions and their enzymes. *Chem Biodivers*, 4: 257–405.

https://doi.org/10.1002/cbdv.200790032

36. Renaud HJ, Cui JY, Khan M, *et al.*, 2011, Tissue distribution and gender-divergent expression of 78 cytochrome P450 mRNAs in mice. *Toxicol Sci*, 124: 261–277.

https://doi.org/10.1093/toxsci/kfr240

37. Tourancheau A, Rouleau M, Guauque-Olarte S, *et al.*, 2018, Quantitative profiling of the UGT transcriptome in human drug-metabolizing tissues. *Pharmacogenomics J*, 18: 251–261.

https://doi.org/10.1038/tpj.2017.5

38. Suleman FG, Ghersi-Egea JF, Leininger-Muller B, *et al.*, 1993, Uridine diphosphate-glucuronosyltransferase activities in rat brain microsomes. *Neurosci Lett*, 161: 219–222.

https://doi.org/10.1016/0304-3940(93)90298-y

39. Leclerc S, Heydel JM, Amossé V, *et al.*, 2002, Glucuronidation of odorant molecules in the rat olfactory system: Activity, expression and age-linked modifications of UDP-glucuronosyltransferase isoforms, UGT1A6 and UGT2A1, and relation to mitral cell activity. *Brain Res Mol Brain Res*, 107: 201–213.

https://doi.org/10.1016/s0169-328x(02)00455-2

40. King CD, Rios GR, Green MD, *et al.*, 2000, UDP-glucuronosyltransferases. *Curr Drug Metab*, 1: 143–161.

https://doi.org/10.2174/1389200003339171

41. Ghosh C, Hossain M, Puvenna V, *et al.*, 2013, Expression and functional relevance of UGT1A4 in a cohort of human drug-resistant epileptic brains. *Epilepsia*, 54: 1562–1570.

https://doi.org/10.1111/epi.12318

42. Ouzzine M, Gulberti S, Ramalanjaona N, *et al.*, 2014, The UDP-glucuronosyltransferases of the blood-brain barrier: Their role in drug metabolism and detoxication. *Front Cell Neurosci*, 8: 349.

https://doi.org/10.3389/fncel.2014.00349

43. Kutsuno Y, Hirashima R, Sakamoto M, *et al.*, 2015, Expression of UDP-glucuronosyltransferase 1 (UGT1) and glucuronidation activity toward endogenous substances in humanized UGT1 mouse brain. *Drug Metab Dispos*, 43: 1071–1076.

https://doi.org/10.1124/dmd.115.063719

44. El-Bachá RS, Leclerc S, Netter P, *et al.*, 2000, Glucuronidation of apomorphine. *Life Sci*, 67: 1735–1745.

https://doi.org/10.1016/s0024-3205(00)00764-5

45. Kilpatrick GJ, Smith TW, 2005, Morphine-6-glucuronide: Actions and mechanisms. *Med Res Rev*, 25: 521–544.

https://doi.org/10.1002/med.20035

46. Landsberg L, Berardino MB, Stoff J, *et al.*, 1978, Further studies on catechol uptake and metabolism in rat small bowel *in vivo*: (1) A quantitatively significant process with distinctive structural specifications; and (2) the formation of a dopamine glucuronide reservoir after chronic l-dopa feeding. *Biochem Pharmacol*, 27: 1365–1371.

https://doi.org/10.1016/0006-2952(78)90121-1

47. Alexander N, Yoneda S, Vlachakis ND, *et al.*, 1984, Role of conjugation and red blood cells for inactivation of circulating catecholamines. *Am J Physiol*, 247: R203–R207.

https://doi.org/10.1152/ajpregu.1984.247.1.R203

48. Gaudin C, Ruget G, Selz F, *et al.*, 1985, Free and conjugated catecholamines in digestive tissues of rats. *Life Sci*, 37: 1469–1474.

https://doi.org/10.1016/0024-3205(85)90177-8

49. Berndt TJ, MacDonald A, Walikonis R, *et al.*, 1993, Excretion of catecholamines and metabolites in response to increased dietary phosphate intake. *J Lab Clin Med*, 122: 80–84.

50. Azoui R, Schneider J, Dong WX, *et al.*, 1997, Red blood cells participate in the metabolic clearance of catecholamines in the rat. *Life Sci*, 60: 357–367.

https://doi.org/10.1016/s0024-3205(96)00659-5

51. Itäaho K, Court MH, Uutela P, *et al.*, 2009, Dopamine is a low-affinity and high-specificity substrate for the human

UDP-glucuronosyltransferase 1A10. *Drug Metab Dispos*, 37: 768–775.

https://doi.org/10.1124/dmd.108.025692

52. Uutela P, Karhu L, Piepponen P, *et al.*, 2009, Discovery of dopamine glucuronide in rat and mouse brain microdialysis samples using liquid chromatography tandem mass spectrometry. *Anal Chem*, 81: 427–434.

https://doi.org/10.1021/ac801846w

53. Suominen T, Uutela P, Ketola RA, *et al.*, 2013, Determination of serotonin and dopamine metabolites in human brain microdialysis and cerebrospinal fluid samples by UPLC-MS/MS: Discovery of intact glucuronide and sulfate conjugates. *PLoS One*, 8: e68007.

https://doi.org/10.1371/journal.pone.0068007

54. Wang PC, Kuchel O, Buu NT, *et al.*, 1983, Catecholamine glucuronidation: An important metabolic pathway for dopamine in the rat. *J Neurochem*, 40: 1435–1440.

https://doi.org/10.1111/j.1471-4159.1983.tb13587.x

55. Chhour M, Perio P, Gayon R, *et al.*, 2021, Association of NQO2 with UDP-glucuronosyltransferases reduces menadione toxicity in neuroblastoma cells. *Front Pharmacol*, 12: 660641.

https://doi.org/10.3389/fphar.2021.660641

56. Mailliet F, Ferry G, Vella F, *et al.*, 2004, Organs from mice deleted for NRH: quinone oxidoreductase 2 are deprived of the melatonin binding site MT3. *FEBS Lett*, 578: 116–120.

https://doi.org/10.1016/j.febslet.2004.10.083

57. Fu Y, Buryanovskyy L, Zhang Z, 2008, Quinone reductase 2 is a catechol quinone reductase. *J Biol Chem*, 283: 23829–23835.

https://doi.org/10.1074/jbc.M801371200

58. Ross D, Kepa JK, Winski SL, *et al.*, 2000, NAD(P)H: quinone oxidoreductase 1 (NQO1): Chemoprotection, bioactivation, gene regulation and genetic polymorphisms. *Chem Biol Interact*, 129: 77–97.

https://doi.org/10.1016/s0009-2797(00)00199-x

59. Ross D, Siegel D, 2004, NAD(P)H: quinone oxidoreductase 1 (NQO1, DT-diaphorase), functions and pharmacogenetics. *Methods Enzymol*, 382: 115–144.

https://doi.org/10.1016/S0076-6879(04)82008-1

60. Goodman RP, Calvo SE, Mootha VK, 2018, Spatiotemporal compartmentalization of hepatic NADH and NADPH metabolism. *J Biol Chem*, 293: 7508–7516.

https://doi.org/10.1074/jbc.TM117.000258

61. Gould NL, Sharma V, Hleihil M, *et al.*, 2020, Dopamine-dependent QR2 pathway activation in CA1 interneurons enhances novel memory formation. *J Neurosci*, 40: 8698–8714.

https://doi.org/10.1523/JNEUROSCI.1243-20.2020

62. Gould NL, Elkobi A, Edry E, *et al.*, 2020, Muscarinic-dependent miR-182 and QR2 expression regulation in the anterior insula enables novel taste learning. *eNeuro*, 7: ENEURO.0067-20.2020.

https://doi.org/10.1523/ENEURO.0067-20.2020

63. Rappaport AN, Jacob E, Sharma V, *et al.*, 2015, Expression of quinone reductase-2 in the cortex is a muscarinic acetylcholine receptor-dependent memory consolidation constraint. *J Neurosci*, 35: 15568–15581.

https://doi.org/10.1523/JNEUROSCI.1170-15.2015

64. Hashimoto T, Nakai M, 2011, Increased hippocampal quinone reductase 2 in Alzheimer's disease. *Neurosci Lett*, 502: 10–12.

https://doi.org/10.1016/j.neulet.2011.07.008

65. Janda E, Lascala A, Carresi C, *et al.*, 2015, Parkinsonian toxin-induced oxidative stress inhibits basal autophagy in astrocytes via NQO2/quinone oxidoreductase 2: Implications for neuroprotection. *Autophagy*, 11: 1063–1080.

https://doi.org/10.1080/15548627.2015.1058683

66. Harada S, Fujii C, Hayashi A, *et al.*, 2001, An association between idiopathic Parkinson's disease and polymorphisms of phase II detoxification enzymes: Glutathione S-transferase M1 and quinone oxidoreductase 1 and 2. *Biochem Biophys Res Commun*, 288: 887–892.

https://doi.org/10.1006/bbrc.2001.5868

67. Wang W, Le WD, Pan T, *et al.*, 2008, Association of NRH: quinone oxidoreductase 2 gene promoter polymorphism with higher gene expression and increased susceptibility to Parkinson's disease. *J Gerontol A Biol Sci Med Sci*, 63: 127–134.

https://doi.org/10.1093/gerona/63.2.127

68. Harada S, Tachikawa H, Kawanishi Y, 2003, A possible association between an insertion/deletion polymorphism of the NQO2 gene and schizophrenia. *Psychiatr Genet*, 13: 205–209.

https://doi.org/10.1097/00041444-200312000-00003

69. Okada S, Farin FM, Stapleton P, *et al.*, 2005, No associations between Parkinson's disease and polymorphisms of the quinone oxidoreductase (NQO1, NQO2) genes. *Neurosci Lett*, 375: 178–180.

https://doi.org/10.1016/j.neulet.2004.11.009

70. Wang W, Jaiswal AK, 2004, Sp3 repression of polymorphic human NRH: quinone oxidoreductase 2 gene promoter. *Free Radic Biol Med*, 37: 1231–1243.

https://doi.org/10.1016/j.freeradbiomed.2004.06.042

71. Benoit CE, Bastianetto S, Brouillette J, *et al.*, 2010, Loss of quinone reductase 2 function selectively facilitates learning behaviors. *J Neurosci*, 30: 12690–12700.

https://doi.org/10.1523/JNEUROSCI.2808-10.2010

72. Brouillette J, Quirion R, 2008, Transthyretin: A key gene involved in the maintenance of memory capacities during aging. *Neurobiol Aging*, 29: 1721–1732.

https://doi.org/10.1016/j.neurobiolaging.2007.04.007

73. Lin R, Liang J, Luo M, 2021, The raphe dopamine system: roles in salience encoding, memory expression, and addiction. *Trends Neurosci*, 44: 366–377.

https://doi.org/10.1016/j.tins.2021.01.002

74. Voronin MV, Kadnikov IA, Zainullina LF, *et al.*, 2021, Neuroprotective properties of quinone reductase 2 inhibitor M-11, a 2-mercaptobenzimidazole derivative. *Int J Mol Sci*, 22: 13061.

https://doi.org/10.3390/ijms222313061

75. Umek N, Geršak B, Vintar N, *et al.*, 2018, Dopamine autoxidation is controlled by acidic pH. *Front Mol Neurosci*, 11: 467.

https://doi.org/10.3389/fnmol.2018.00467

76. Váradi C, 2020, Clinical features of Parkinson's disease: The evolution of critical symptoms. *Biology (Basel)*, 9: 103.

https://doi.org/10.3390/biology9050103

77. Diederich NJ, Uchihara T, Grillner S, *et al.*, 2020, The Evolution-Driven Signature of Parkinson's Disease. *Trends Neurosci*, 43: 475–492.

https://doi.org/10.1016/j.tins.2020.05.001

78. Nobili A, Latagliata EC, Viscomi MT, *et al.*, 2017, Dopamine neuronal loss contributes to memory and reward dysfunction in a model of Alzheimer's disease. *Nat Commun*, 8: 14727.

https://doi.org/10.1038/ncomms14727

79. Kaldun JC, Lone SR, Camps AMH, *et al.*, 2021, Dopamine, sleep, and neuronal excitability modulate amyloid-β-mediated forgetting in Drosophila. *PLoS Biol*, 19: e3001412.

https://doi.org/10.1371/journal.pbio.3001412

80. Segura-Aguilar J, Paris I, Muñoz P, *et al.*, 2014, Protective and toxic roles of dopamine in Parkinson's disease. *J Neurochem*, 129: 898–915.

https://doi.org/10.1111/jnc.12686

81. Wakamatsu K, Nakao K, Tanaka H, *et al.*, 2019, The oxidative pathway to dopamine-protein conjugates and their pro-oxidant activities: Implications for the neurodegeneration of Parkinson's disease. *Int J Mol Sci*, 20: 2575.

https://doi.org/10.3390/ijms20102575

82. Boutin JA, Thomassin J, Siest G, *et al.*, 1985, Heterogeneity of hepatic microsomal UDP-glucuronosyltransferase activities. *Biochem Pharmacol*, 34: 2235–2249.

https://doi.org/10.1016/0006-2952(85)90777-4

83. Mackenzie PI, Bock KW, Burchell B, *et al.*, 2005, Nomenclature update for the mammalian UDP glycosyltransferase (UGT) gene superfamily. *Pharmacogenet Genomics*, 15: 677–685.

https://doi.org/10.1097/01.fpc.0000173483.13689.56

84. Ito T, Katagiri C, Ikeno S, *et al.*, 2001, Phenobarbital following phototherapy for Crigler-Najjar syndrome type II with good fetal outcome: A case report. *J Obstet Gynaecol Res*, 27: 33–35.

https://doi.org/10.1111/j.1447-0756.2001.tb01212.x

85. Passuello V, Puhl AG, Wirth S, *et al.*, 2009, Pregnancy outcome in maternal Crigler-Najjar syndrome type II: A case report and systematic review of the literature. *Fetal Diagn Ther*, 26: 121–126.

https://doi.org/10.1159/000238122

86. Chen B, Tong X, Zhang X, *et al.*, 2022, Sulfation modification of dopamine in brain regulates aggregative behavior of animals. *Natl Sci Rev*, 9: nwab163.

https://doi.org/10.1093/nsr/nwab163

87. Idris M, Mitchell DJ, Gordon R, *et al.*, 2020, Interaction of the brain-selective sulfotransferase SULT4A1 with other cytosolic sulfotransferases: Effects on protein expression and function. *Drug Metab Dispos*, 48: 337–344.

https://doi.org/10.1124/dmd.119.089714

88. Bock KW, Bock-Hennig BS, 2010, UDP-glucuronosyltransferases (UGTs): From purification of Ah-receptor-inducible UGT1A6 to coordinate regulation of subsets of CYPs, UGTs, and ABC transporters by nuclear receptors. *Drug Metab Rev*, 42: 6–13.

https://doi.org/10.3109/03602530903205492

89. Yeager RL, Reisman SA, Aleksunes LM, *et al.*, 2009, Introducing the "TCDD-inducible AhR-Nrf2 gene battery". *Toxicol Sci*, 111: 238–246.

https://doi.org/10.1093/toxsci/kfp115

90. Rashid MH, Babu D, Siraki AG, 2021, Interactions of the antioxidant enzymes NAD(P)H: Quinone oxidoreductase 1 (NQO1) and NRH: Quinone oxidoreductase 2 (NQO2) with pharmacological agents, endogenous biochemicals and environmental contaminants. *Chem Biol Interact*, 345: 109574.

https://doi.org/10.1016/j.cbi.2021.109574

ACCSCIENCE PUBLISHING

Gene & Protein in Disease

ORIGINAL RESEARCH ARTICLE

A novel signature identified by pyroptosis-related lncRNAs clusters predicts prognosis and tumor immune microenvironment for pediatric acute myeloid leukemia

Jie Lu, Xinyu Chang, Guowei Zheng, Xiting Cao, Zhenwei Wang, Hao Zhu, Shuaijie Gao, and Yuanlin Xi*

Department of Epidemiology and Biostatistics, College of Public Health, Zhengzhou University, Zhengzhou 450001, Henan, China

Abstract

Pyroptosis is a recently discovered programmed cell death that is involved in tumor formation, prognosis, and curative effect. Pyroptosis-related long non-coding ribonucleic acids (PR-lncRNAs) play key roles in tumorigenesis and tumor progression. However, the inherent relationship between PR-lncRNAs and the prognosis of pediatric acute myeloid leukemia (AML) remains unclear. For this reason, the association of PR-lncRNAs with the prognosis and tumor microenvironment features was analyzed using the Therapeutically Applicable Research to Generate Effective Treatment (TARGET) database. We classified three clusters based on PR-lncRNAs expressions and identified 841 differentially expressed PR-lncRNAs related to overall survival time. Seven key lncRNAs were then identified by least absolute shrinkage and selection operator (LASSO)-Cox and multivariate Cox. A signature based on these seven lncRNAs was also established, and the patients were separated into two groups according to their risk score. The high-risk group was characterized by poorer prognosis, lower expression of immune checkpoints, lower microsatellite instability or microsatellite stability (MSI-L/MSS), and lower drug sensitivity. The results demonstrated that PR-lncRNAs have a potential effect on the tumor immune microenvironment, clinicopathological features, and prognosis in pediatric AML. The nomogram and decision curve analysis suggested that the risk score is one of the most accurate of any other and provided a basis for the exploration of the immune microenvironment of the cell pyroptosis-associated subtypes in children with AML and the construction of a prognostic model with seven key PR-lncRNAs, which provides an approach to evaluate the prognosis of pediatric AML patients.

Keywords: Pediatric acute myeloid leukemia; Pyroptosis; Long non-coding RNAs; Prognostic signature; Tumor immune microenvironment

***Corresponding author:**
Yuanlin Xi
(xyl@zzu.edu.cn)

Citation: Lu J, Chang X, Zheng G, *et al.*, 2023, A novel signature identified by pyroptosis-related lncRNAs clusters predicts prognosis and tumor immune microenvironment for pediatric acute myeloid leukemia. *Gene Protein Dis*, 2(1):230.
https://doi.org/10.36922/gpd.v2i1.230

Received: October 19, 2022
Accepted: November 22, 2022
Published Online: December 28, 2022

1. Introduction

Acute myeloid leukemia (AML) is a hematologic malignancy with morphological, immunophenotypic, germline, and somatic cytogenetic and genetic abnormalities. Pediatric AML is the second most common form of leukemia in children, with a mortality

rate of 20–40% and a relapse rate of 30%[1]. Although there have been improvements in the prognosis of pediatric AML patients as a result of the latest advances in areas such as molecular pathological diagnostic techniques, risk stratification, and targeted supportive care, the overall survival (OS) in 2021 remains below 70%[1-3]. As known to all, its clinical outcomes and genetic backgrounds are different in each age group[4]. To date, there are only a number of well-designed and systematic studies that focus on the molecular mechanisms of pediatric AML. More efforts are thus needed to identify potential biomarkers that can monitor the prognosis of pediatric AML patients, as well as provide more efficient therapeutic strategies.

Pyroptosis is a gasdermin-mediated programmed cell death (PCD) initiated by inflammasomes that are critical for immunity[5-7]. The previous research has found that pyroptosis causes the release of inflammatory mediators IL-1β and IL-18 and prolongs the exposure of cells to an inflammatory environment, which may add to the risk of tumorigenesis[8]. To date, many studies have reported that pyroptosis is crucial in tumor invasion, proliferation, and metastasis, and it can regulate AML progression[7]. Existing studies have found that dipeptidyl peptidase (DPP)8 and DPP9 (DPP8/9), which are tiny molecules inhibiting serine dipeptidases, are related to pyrolysis through their activation of pro-caspase-1 in human AML cell lines and primary AML samples, which, in turn, trigger cell lysis and death, known as pyroptosis, and inhibit human AML progression. This is thought to be a promising therapeutic strategy for AML[9]. Besides, due to the physical interaction between caspase-associated recruitment domain 8 (CARD8) and caspase-1, the production of caspase-1-dependent interleukin (IL)-1β is negatively regulated in THP-1 (a human-monocyte cell line derived from an AML patient); this is similar to TP92[10,11]. Taking these results together, the role pyroptosis plays in pediatric AML which cannot be overlooked.

Long non-coding RNAs (lncRNAs) are expressed transcripts that do not encode proteins that are more than 200 nt in length. They are involved in the onset and development of AML[12,13]. Besides, it has been found that lncRNAs play crucial roles in humorous cellular processes, including pyroptosis. LncRNAs can regulate the expression of proteins related to the pyroptosis signaling pathway indirectly through miRNAs[14]. This kind of modulation exists in the pathological process of tumorigenesis as well. However, there is little research on pyroptosis-related lncRNAs (PR-lncRNAs) in pediatric AML. In addition, PR-lncRNAs' role in the prognosis of pediatric AML patients and its biological mechanism remain unclear. Furthermore, current evidence has suggested a link between pyroptosis and tumor microenvironment (TME), which is a dynamic network that includes tumor cells, immune cells, and stromal cells[15]. We hypothesize that PR-lncRNAs may affect progression of pediatric AML and the prognosis of these patients by interacting with the immune microenvironment. In this study, based on the Therapeutically Applicable Research to Generate Effective Treatment (TARGET) database, the relationship between PR-lncRNAs and the prognosis of pediatric AML patients was investigated; an evaluation of the predictive ability of the prognostic signature constructed by seven significant PR-lncRNAs was performed; and an exploration of whether PR-lncRNAs have an impact on the molecular microenvironment in pediatric AML was also carried out.

2. Materials and methods

2.1. Data acquisition

The gene expression and clinical data of 1474 pediatric AML samples were retrieved from the TARGET database up to March 1, 2022 (https://ocg.cancer.gov/programs/target). After excluding samples with incomplete clinical data, replications, and normal samples, 1300 pediatric AML samples were included for subsequent analyses.

2.2. Identification of pyroptosis-related lncRNAs and consensus clustering analyses

The lncRNA annotation file from the GENCODE website (GRCh38) (https://www.gencodegenes.org/human/) was used to distinguish lncRNAs and protein-coding genes. Meanwhile, 52 PR-lncRNAs were obtained from a website (http://www.broad.mit.edu/gsea/msigdb/) and relevant studies, as shown in Table S1. Pearson product-moment correlation coefficient was employed to distinguish PR-lncRNAs with $|\text{Pearson R}| > 0.4$ and $P < 0.001$. Univariate Cox regression analysis (Uni-Cox) was implemented to screen prognosis and pyroptosis-related lncRNAs (PPR-lncRNAs), while taking overall survival (OS) as the endpoint. The pediatric AML samples were divided into different clusters according to PPR-lncRNAs expressions by R package "ConsensusClusterPlus."

2.3. Relationship and differences among different clusters

The difference in OS among the clusters was determined using Kaplan–Meier (K-M) curves and a log-rank test. Kyoto Encyclopedia of Genes and Genomes (KEGG) gene sets in Gene Set Enrichment Analysis (GSEA) (version 4.2.3) were applied to three clusters to explore the distinctions of enriched pathways. The Estimation of STromal and Immune cells in MAlignant Tumor tissues using Expression data (ESTIMATE) scoring of the tumor microenvironment and the relative proportions of 22 immune cell infiltrations were calculated using

ESTIMATE and cell type identification by estimating relative subsets of RNA transcription (CIBERSORT) algorithms[16], respectively. Furthermore, the correlations among different subtypes in the expression of five immune checkpoints, including programmed cell death protein 1 (PD-1), programmed cell death-ligand 1 (PD-L1)[17], cytotoxic T-lymphocyte-associated protein 4 (CTLA-4)[18], lymphocyte-activation gene 3 (LAG3)[19], and hepatitis A virus cellular receptor 2 (HAVCR2/TIM-3)[20] pathways, which are implicated in tumor immune evasion and derived from previous studies, were analyzed.

2.4. Differentially expressed lncRNAs recognition and prognosis and pyroptosis-related lncRNAs signature construction

Differently expressed lncRNAs (DE-lncRNAs) within the three clusters were identified by the "limma" package in R according to the following criteria: log2FC ≥ 1 and adjusted $P < 0.001$. Uni-Cox was used to filter for DE-lncRNAs according to prognosis. These lncRNAs were then used to form PPR-lncRNAs signaling to predict the prognosis of pediatric AML patients. First, 1300 pediatric AML samples were randomly sorted into training and testing sets at a ratio of 7:3. LASSO-Cox ten-fold cross-validation and multivariate Cox regression analysis (multi-Cox) were used to establish the PPR-lncRNAs signature in the training set. The formula for calculating the risk score is shown below:

$$\text{riskscore} = \sum_{i=1}^{n} \text{coef}_i * x_i$$

Where coef_i represents the coefficients and x_i represents the count of PPR-lncRNAs expressions. Based on the calculation of the risk score, the pediatric AML samples in the training and testing sets were divided into high- and low-risk groups based on the median risk score of the training set.

2.5. Validation of the signature

K-M curves, ESTIMATE and CIBERSORT scores, and immune checkpoint expression were used to assess the differences between the two groups. Moreover, time-dependent receiver operating characteristic (ROC) curves were used to assess the predictive ability of the prognostic signature for OS.

Subgroup analyses of the selected clinical characteristics (age, gender, race, bone marrow leukemic blast percentage [BM], peripheral blasts [PB], white blood cell at diagnosis [WB], and French-American-British [FAB] category) were performed. Chi-squared (χ^2) test was performed to evaluate the distribution among subtypes, risk scores, and clinical variables. Independent factors in the prognosis of pediatric AML patients were identified through uni-Cox and multi-Cox analyses. Stratification analyses were performed to determine the stability of each clinical factor.

The semi-inhibitory concentration (IC50) values of chemotherapeutic drugs that are generally used to treat AML were estimated by the "prophetic" package in R[21]. Besides, the "PreMSIm" package was used to predict the microsatellite instability (MSI) state in both high- and low-risk groups based on the 15 genes expression.

Furthermore, Gene Ontology (GO) and KEGG enrichment analyses were performed to determine the function of the differentially expressed genes (DEGs) between the two groups. The DEGs were screened with $|\log2FC| \geq 1$ and false discovery rate (FDR) < 0.05.

2.6. Establishments of a nomogram and a decision curve

Combining the signature with clinical factors, a nomogram was constructed, integrating the prognostic signature using the "rms" package in R, to predict the 1-, 3-, and 5-year survival probability of pediatric AML patients. In addition, a decision curve analysis (DCA) was used to calculate the net benefit of each factor on the survival of pediatric AML patients at 1, 3, and 5 years.

2.7. Statistical analysis

In our study, statistical analyses were performed using R software (version 4.1.2). If not specifically stated, all results were regarded as statistically significant when $P < 0.05$.

3. Results

Figure 1. Flow chart of 1300 samples with complete clinical data from the TARGET database. Following Pearson correlation analysis and uni-Cox, 841 prognosis, and pyroptosis-related lncRNAs were obtained. Three clusters were classified by consensus clustering according to pyroptosis-related lncRNAs. Based on these three clusters, prognostic signature construction and immune difference exploration were performed.

Table 1 shows the characteristics of 1300 pediatric AML patients from the TARGET database. All 1300 AML patients with their OS information were used for prognostic model construction. From the expression matrix of 11,535 lncRNAs and 52 pyroptosis-related genes (PRGs), we identified 1792 lncRNAs as significant pyroptosis-associated genes by Pearson (Table S1). Three clusters were classified by unsupervised consensus clustering analysis and uni-Cox based on PR-lncRNAs (Figure 2A-C). The age, gender, and race components did not show any statistical difference ($P > 0.05$). Three-

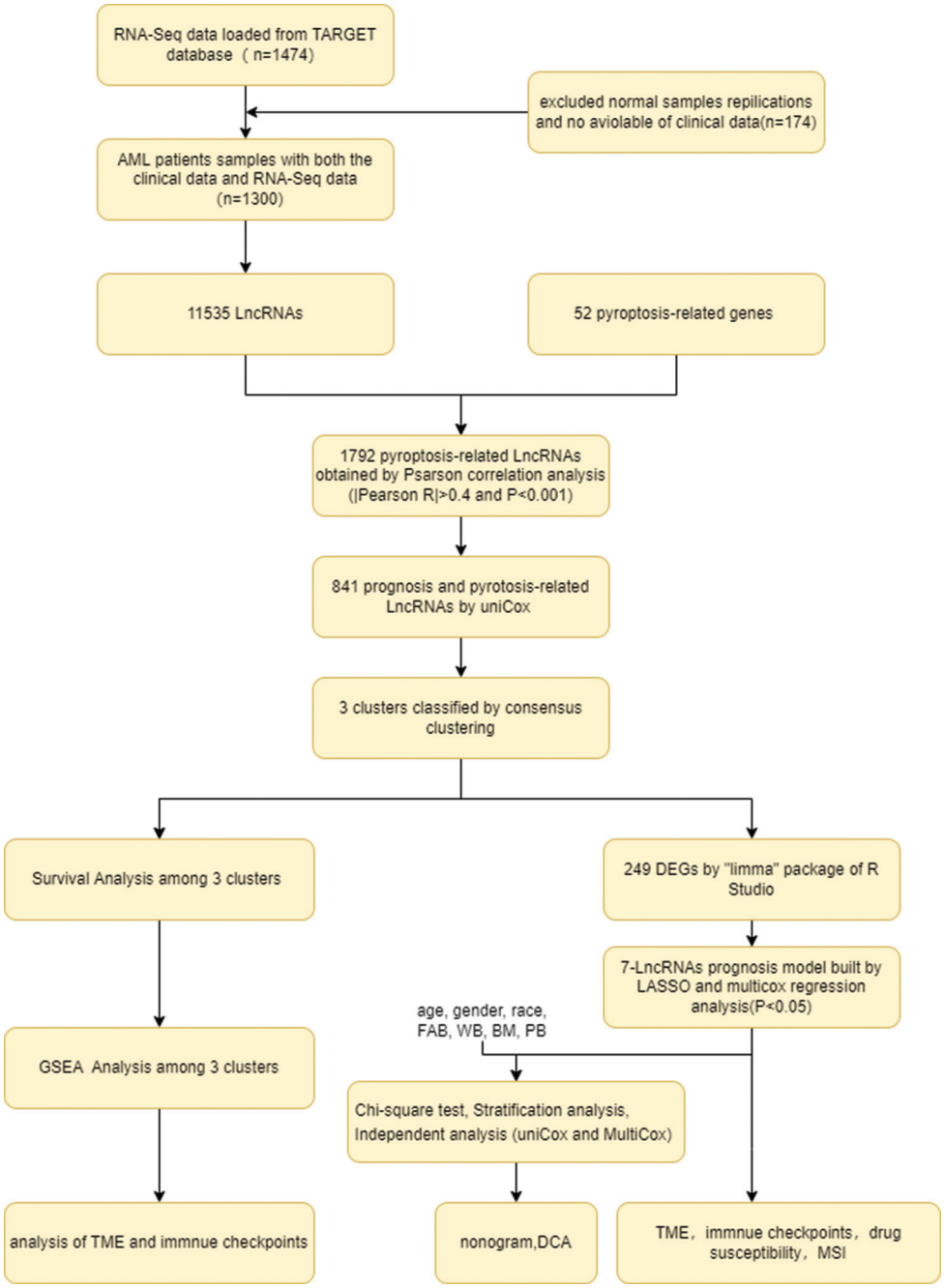

Figure 1. Flow chart of 1300 samples with complete clinical data extracted from the TARGET database.

dimensional (3D) PCA (principal component analysis) showed that the patients can be separated into three clusters by PPR-lncRNAs expressions (Figure 2D).

3.1. Correlations and differences among the three clusters

Table 1 shows that the laboratory indices (WB, BM, and PB) among the three clusters were significantly different. The K–M curve and log-rank test result of clusters 1–3 reflected statistical differences in terms of prognosis (Figure 2E) (P = 0.048), with cluster 3 having a better prognosis than cluster 1 (P = 0.020). Unexpectedly, the curves of clusters 1 and 2, and clusters 2 and 3 did not show significant distinctiveness; hence, the difference in survival from these two comparisons could not be identified. The result of GSEA among the three clusters (Tables S3 and S4) showed that genes in cluster 1 and cluster 2 were enriched in disease and metabolic pathways, and as expected, those

Table 1. Baseline characteristics of 1300 pediatric acute myeloid leukemia patients.

Characteristic	Cluster1 (n = 121)	Cluster2 (n = 137)	Cluster3 (n = 1,042)	Total (n = 1,300)	*P*
Gender					
Male	66 (5.08)	77 (5.92)	538 (41.38)	681 (52.38)	0.531
Female	55 (4.23)	60 (4.62)	504 (38.77)	619 (47.62)	
Age					
<3	21 (1.62)	39 (3.00)	253 (19.46)	462 (35.54)	0.19
3~6	14 (1.08)	12 (0.92)	124 (9.54)	150 (11.54)	
6~14	50 (3.85)	47 (3.62)	322 (24.77)	419 (33.23)	
≥14	36 (2.77)	40 (3.08)	343 (26.38)	419 (33.23)	
Race					
White	84 (6.46)	102 (7.85)	752 (57.85)	938 (72.15)	0.663
Not white	25 (1.92)	28 (2.15)	184 (14.15)	237 (18.23)	
Unknown	12 (0.92)	7 (0.54)	106 (8.15)	125 (9.62)	
WB	81.35±93.70	76.63±86.19	62.77±95.76	65.96±94.76	<0.01
<50	64 (4.92)	71 (5.46)	697 (53.62)	831 (63.92)	
≥31	58 (4.46)	66 (5.08)	344 (26.46)	468 (36.00)	
Unknown	0 (0.00)	0 (0.00)	1 (0.08)	1 (0.08)	
BM	70.15±50.70	71.62±19.54	62.19±25.51	63.97±24.74	<0.01
<70	51 (3.92)	45 (3.46)	491 (37.77)	587 (45.15)	
≥87	66 (5.08)	86 (6.62)	472 (36.31)	624 (48)	
Unknown	4 (0.31)	6 (0.46)	79 (6.08)	89 (6.85)	
PB (%)	59.07±28.14	57.54±27.33	41.46±31.68	44.83±31.63	<0.01
<70	71 (5.46)	83 (6.38)	756 (58.15)	910 (70)	
≥10	49 (3.77)	54 (4.15)	268 (20.62)	371 (28.54)	
Unknown	1 (0.08)	0 (0.00)	18 (1.38)	19 (1.46)	
FAB (%)					
M0	4 (0.31)	4 (0.31)	0 (0.00)	8 (0.62)	<0.01
M1	18 (1.38)	15 (1.15)	0 (0.00)	33 (2.54)	
M2	30 (2.31)	33 (2.54)	0 (0.00)	63 (4.85)	
M3	0 (0.00)	0 (0.00)	0 (0.00)	0 (0.00)	
M4	24 (1.85)	36 (2.77)	0 (0.00)	60 (4.62)	
M5	23 (1.77)	25 (1.92)	2 (0.15)	50 (3.85)	
M6	1 (0.08)	1 (0.08)	1 (0.08)	3 (0.23)	
M7	2 (0.15)	6 (0.46)	2 (0.15)	10 (0.77)	
Unknown	19 (1.46)	17 (1.31)	1,037 (79.77)	1,073 (82.54)	

BM: Bone marrow leukemic blast percentage, FAB: French-American-British category, M1: Acute myeloblastic leukemia with minimal maturation; M2: Acute myeloblastic leukemia with maturation, M3: Acute promyelocytic leukemia, M4: Acute myelomonocytic leukemia, M5: Acute monocytic leukemia, M6: Acute erythroid leukemia, M7: Acute megakaryoblastic leukemia, PB: Peripheral blasts, WB: White blood cell at diagnosis

in cluster 3 were enriched in main immune-associated pathways, such as B-cell and T-cell receptor signaling pathway, Fc epsilon RI, P53, and JAK-STAT signaling pathway, as well as Toll-like and NOD-like receptor signaling and apoptosis (Figure S1).

The interquartile range of age was 9.73 (3.29, 15.08). The minimum age was 0.01, and the maximum age was 29.59.

Seven variables were taken as covariates, and all covariates were taken as categorical variables.

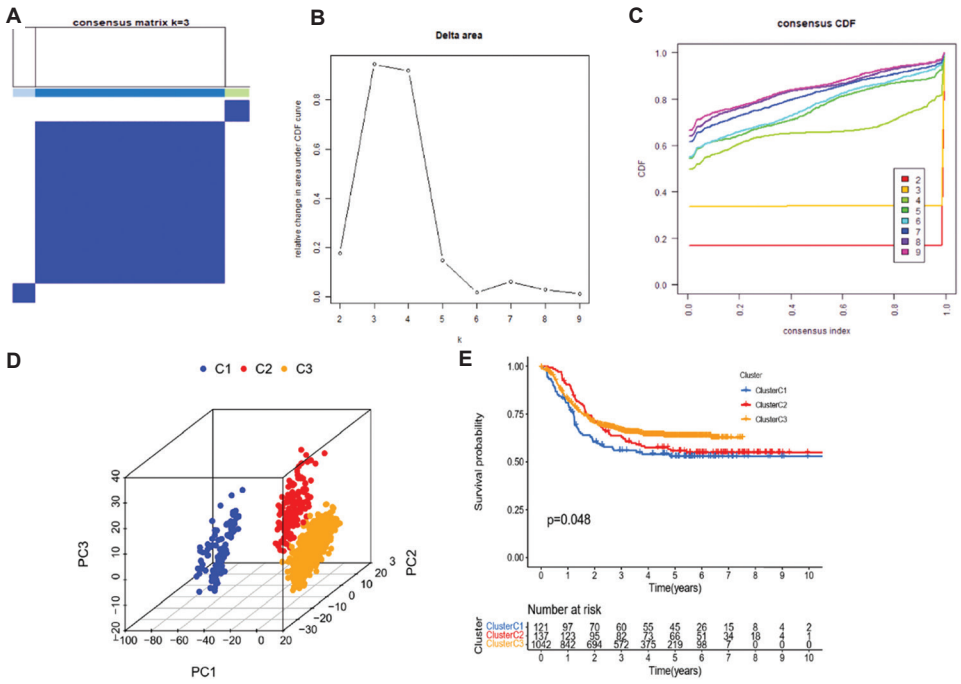

Figure 2. Consensus clustering of 841 prognosis and pyroptosis-related lncRNAs. (A) Consensus clustering matrix for k = 3. (B) Relative change in area under the cumulative distribution function (CDF) curve in pediatric AML. The cluster (k) selection criteria are the CDF changes steadily and its value is not very small. (C) CDF for pediatric AML. Choose the curve with a lower CDF decline slope among the curves with horizontal coordinates ranging from 0.1 to 0.9. (D) Three-dimensional principal component analysis of the three clusters. (E) Kaplan–Meier curves of the overall survival (OS) of pediatric AML patients in clusters 1–3.

The results of ESTIMATE were compared among the three clusters, and the scores were all remarkably lower in cluster 3 but higher in cluster 2 (Figure 3A–C). The tumor purity of three clusters is shown in Figure 3D. Moreover the proportion of each immune cell was compared among the three clusters, as shown in Figure 4A–C. We found that 7, 13, and 9 tumor-infiltrating immunocytes were statistically different between clusters 1 and 2, 2 and 3, as well as 1 and 3, respectively. Resting memory CD4 T-cells, follicular helper T-cells, resting NK cells, activated NK cells, resting (M0) macrophages, activated mast cells, eosinophils, and neutrophils were all significantly higher in cluster 3 (Figure S2). We also compared five important immune checkpoints (Figures 3E–I): PD-1, LAG-3, CTLA-4, PD-L1, and TIM-3. Except for TIM-3, all checkpoints had lower expressions in cluster 3.

3.2. Construction of the prognostic signature

A total of 249 DE-lncRNAs were screened out from the clusters by the "limma" package (shown in Figure 4A) ($log2|FC| > 1, P < 0.001$). Through uni-Cox, 122 prognosis-related DE-lncRNAs were selected with $P < 0.05$ as the threshold (Table S2), and 1300 pediatric AML samples were randomly divided into a training set (n = 912) and a testing set (n = 388) at a ratio of 7:3. Subsequently, LASSO-Cox regression and ten-fold cross-validation were used to reduce the complexity of the candidate lncRNAs, and 21 target lncRNAs were obtained. Seven lncRNAs (Table 2), related to six PRGs (Table S5), were obtained using multi-Cox and included in the final prediction model. Risk score = (-0.103223332 * *TRAF3IP2-AS1* – 0.013058209 * *AL157871.6* – 0.001632721 * *SNHG29* + 0.060510168 * *ASB16-AS1* + 0.083744921 * *AC007216.3* + 0.224003784 * *AP001318.1* + 0.230400789 * *AC127496.5*). The samples were separated into high- and low-risk groups according to the median risk score of the training set. The mortality rates of the samples in the two groups were significantly different based on a visual display of the risk score through ranked dot and scatter plots (Figure 4D–I). The K–M curves showed that the mortality rate of patients in the high-risk group was higher than that in the low-risk group (Figure 5A–C). The ROC curves were used to assess the predictive ability of the risk score for OS. The AUC (area under the ROC curve) was 0.663, 0.659, and 0.645 at 1, 3, and 5 years, respectively, in all groups; the AUC of the training set 1, 3, and 5 years is 0.676, 0.671, and 0.665 at 1, 3, and 5 years, respectively; the AUC of the testing set was 0.620, 0.642, and 0.601 at 1, 3, and 5 years, respectively (Figure 5D–F).

3.3. Validation of the prognosis and pyroptosis-related lncRNAs signature with clinical variables

Based on the clinical variables (gender, age, race, FAB category, WB, BM, and PB), Chi-squared (χ^2) test was

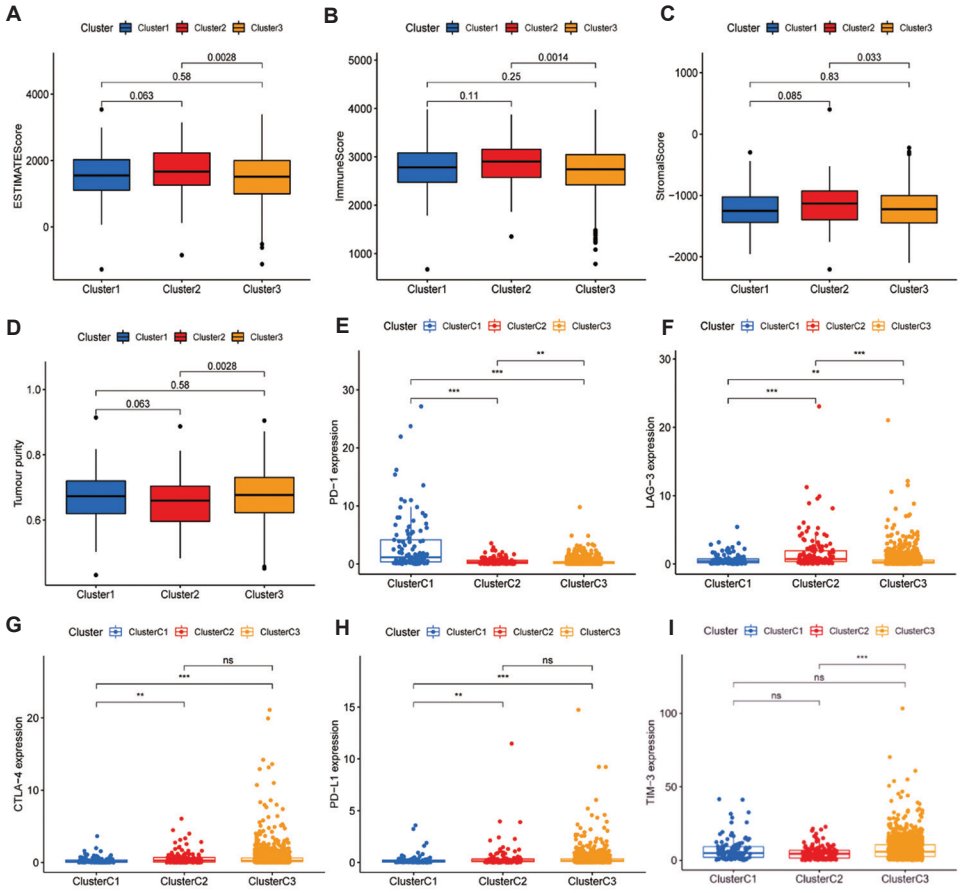

Figure 3. Immunological analysis. (A) Differences in ESTIMATE score among the three clusters. (B) Differences in immune score among the three clusters. (C) Differences in stromal score among the three clusters. (D) Differences in tumor purity among the three clusters. (E–I) Expression of five immune checkpoints in the three clusters: (E) PD-1; (F) LAG-3; (G) CTLA-4; (H) PD-L1; and (I) TIM-3.

performed to determine if there are differences in the baseline data between the two groups. The results showed statistical differences in age, BM, and FAB category. As observed in the heatmap shown in Figure 6, DE-lncRNAs were highly expressed in the high-risk group, especially in cluster 1, and age < 3 was more common with high risk (Figure 7A, C). As Figure 7B shown, the risk score was different in some FAB categories. Uni-Cox and multi-Cox were performed in combination with clinical characteristics and risk scores for prognostic markers to further explore independent prognostic factors (Figure 7D–E). Whether with uni-Cox or multi-Cox, the results showed that the prognostic signature might predict OS in pediatric AML patients independently. In addition, the stratified analyses performed to evaluate whether the prognostic signature retained its predictive ability in different subgroups, including age (< 3; ≥ 3 or < 6; ≥ 6 or < 14; and ≥ 14 years), race (white and others), gender (male and female), WB (< 50 and ≥ 50), PB (< 70 and ≥ 70), BM (70 and ≥ 70), and FAB (M1, M4, and M5), revealed notably lower OS in higher-risk patients compared to lower-risk patients (Figure S3).

3.4. Immune-related analysis

As shown in Figure 8A, the proportions of memory B-cells, plasma cells, naive CD4 T-cells, resting memory CD4 T-cells, resting mast cells, activated mast cells, and eosinophils were significantly lower in high-risk patients. Contrariwise, the proportions of naive B-cells and monocytes were significantly higher in high-risk patients. To identify the differences in tumor-infiltrating immune cells between the two groups, the stromal score, immune score, ESTIMATE score, and tumor purity were compared. As shown in the box chart (Figure 8B), the immune and ESTIMATE scores were significantly lower in the low-risk group; although tumor purity showed a different result, the tumor purity for both the groups was higher than 60. The expression of five important immune checkpoints was compared between the high- and low-risk groups. In the high-risk group, the expression of the checkpoints was higher except for TIM-3 (Figure 8C–G).

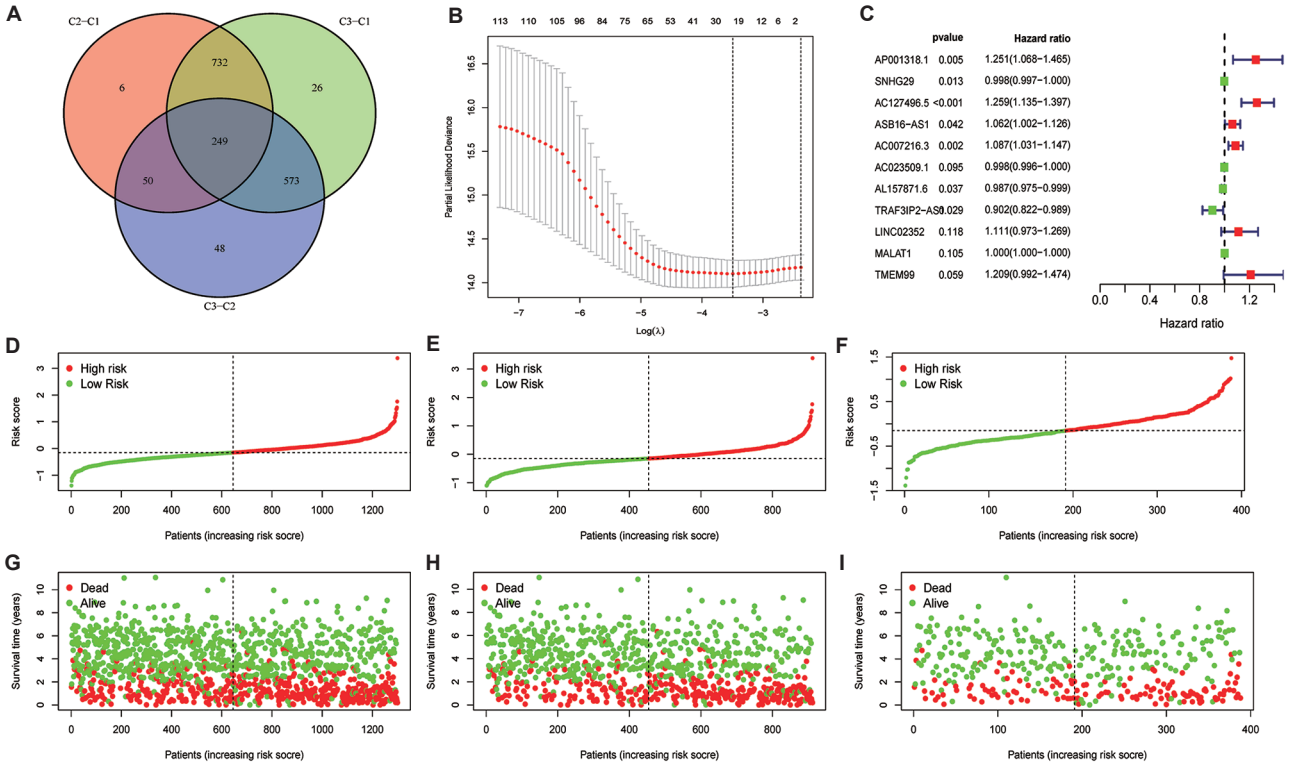

Figure 4. Construction of the prognostic signature of differentially expressed PR-lncRNAs in the training set. (A) Differentially expressed PR-lncRNAs among the three clusters. (B) Result of least absolute shrinkage and selection operator (LASSO) regression. (C) Multivariate Cox regression was performed. (D–I) Ranked dot and scatter plots showing the signature distribution and patient survival status: (D, G) in all sets; (E, H) in the training set; and (F, I) in the testing set.

Table 2. Seven lncRNAs obtained by multi-Cox regression.

LncRNA	Coef	HR	HR.95L	HR.95H	*P*
AP001318.1	0.224	1.251	1.068	1.465	0.0054
SNHG29	−0.002	0.998	0.997	1.000	0.0131
AC127496.5	0.230	1.259	1.135	1.397	0.0000
ASB16-AS1	0.061	1.062	1.002	1.126	0.0417
AC007216.3	0.084	1.087	1.031	1.147	0.0021
AL157871.6	−0.013	0.987	0.975	0.999	0.0373
TRAF3IP2-AS1	−0.103	0.902	0.822	0.989	0.0288

Coef: Coefficient, HR: Hazard ratio, HR.95L: Lower limit of the 95% confidence interval, HR.95H: Higher limit of the 95% confidence interval

3.5. Drug susceptibility analysis

Eight chemotherapy drugs that are commonly used to treat AML were selected to evaluate the sensitivities of the pediatric AML samples in both the groups to these drugs (Figure 9A–H). The results showed that the half maximal inhibitory concentration (IC50) values of the majority of these drugs, including axitinib, bleomycin, lenalidomide, midostaurin, nilotinib, and thapsigargin, were significantly lower in low-risk patients. However, we were unable to demonstrate a similar difference with cytarabine.

3.6. Relationship between risk score and microsatellite instability

MSI is strongly associated with the risk score. As shown in Figure 9I–J, the low-risk group had a high proportion of MSI-H (high microsatellite instability) at 44%, and the average risk score of the patients in the MSI-H group was significantly higher than that in the MSI-L/MSS (low microsatellite instability or microsatellite stability) group ($P < 0.001$).

3.7. Discovery of molecular functions and pathways

To explore the biological functions and signaling pathways of the DEGs between the two groups, GO and KEGG were used. The DEGs between the two groups were identified according to the following criteria: log2| FC| > 1 and FDR < 0.05. The GO analysis that was performed included biological process (BP), molecular function (MF), and cell component (CC). The results of these three parts are presented in Figure 10A, indicating that tumor immunity

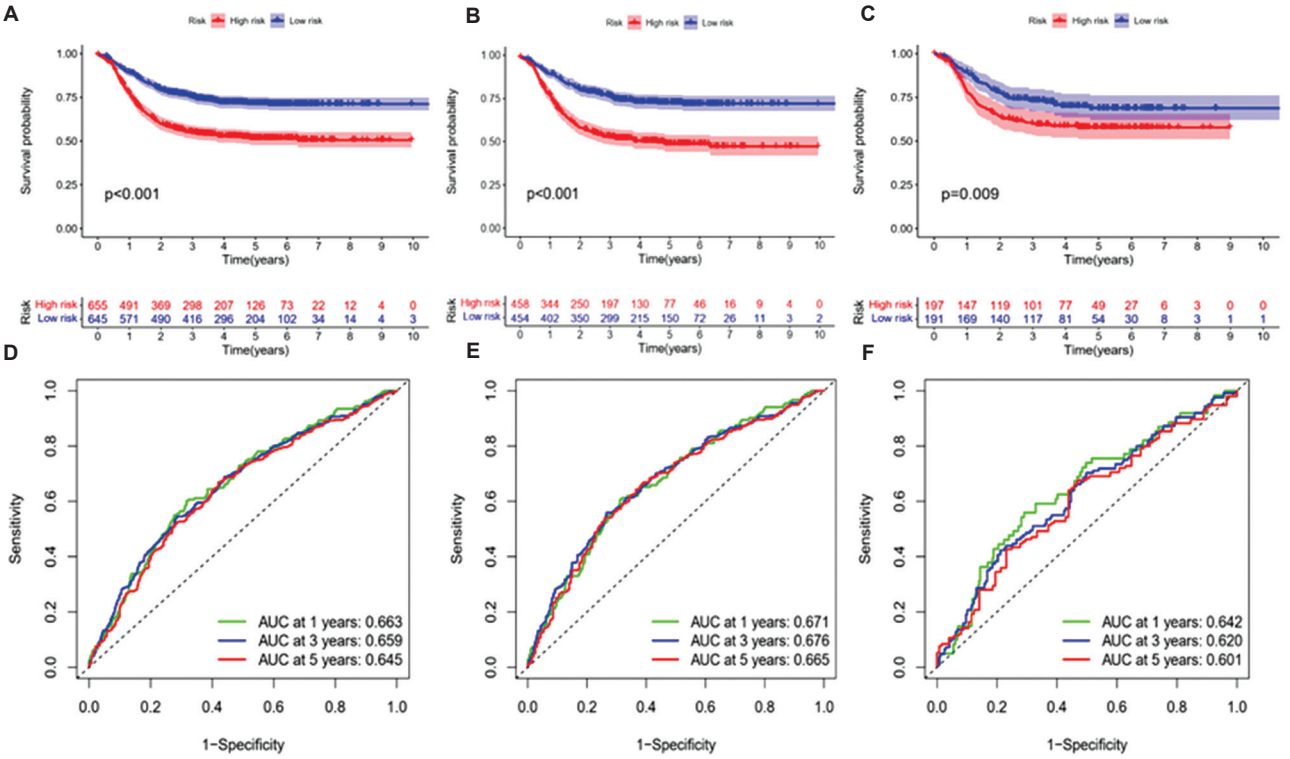

Figure 5. Identification of prognostic signature. (A–C) Kaplan–Meier curves showing that the low-risk group had superior overall survival than the high-risk group: (A) in all sets; (B) in the training set; and (C) in the testing set. (D–F) Area under ROC curves at 1, 3, and 5 years: (D) in all sets; (E) in the training set; and (F) in the testing set.

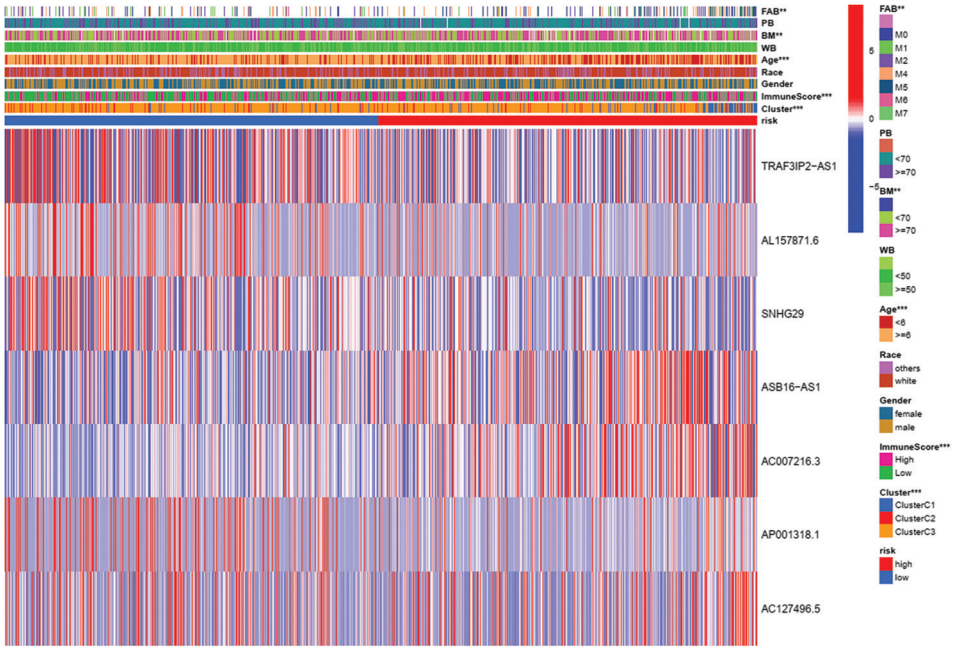

Figure 6. Heatmap. Abbreviations: BM: Bone marrow leukemic blast percentage (%); PB: Peripheral blasts (%); and WB: White blood cell at diagnosis.

and cell metabolism were the DEGs' main functions. KEGG analysis revealed that the enriched pathways were significantly related to the immune and hematopoietic system, including B-cell receptor signaling pathway,

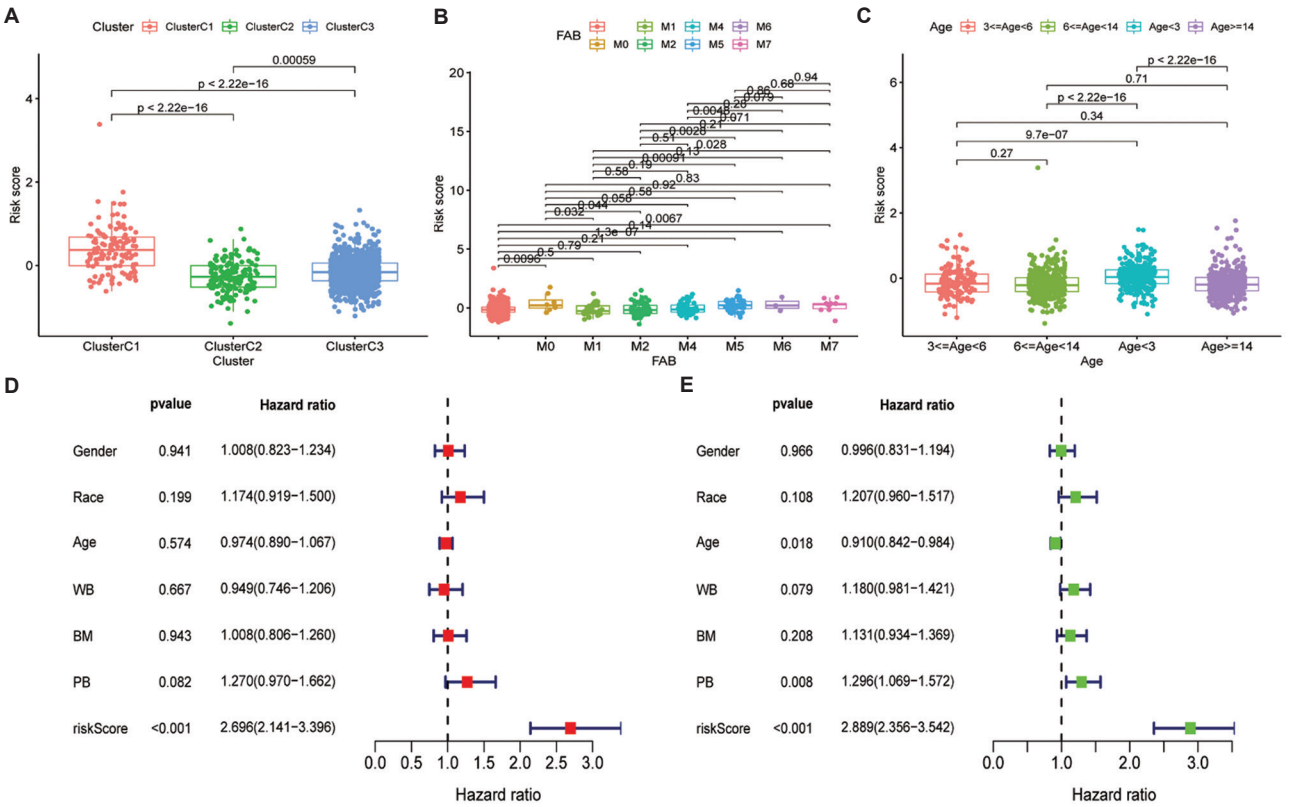

Figure 7. Relationship among the risk score, clinical features, clusters, and immune score in AML. (A–C) Risk score in different characteristics: (A) clusters; (B) FAB category; (C) age. (D) Results of multivariate Cox regression analysis. (E) Results of univariate Cox regression analysis.

human T-cell leukemia virus 1 infection, hematopoietic cell lineage, AML, and chronic myeloid leukemia (Figure 10B).

3.8. Establishments of a nomogram and a decision curve

To further enhance the clinical application value and provide a reliable predictive model for pediatric AML patients, the clinical parameters and risk scores were combined to build a nomogram (Figure 11A). The probability of survival in 1, 3, and 5 years can be calculated by a nomogram incorporating the score of seven PPR-lncRNAs and the clinicopathological parameters; its calibration curve is shown in Figure 11B. In addition, according to the 1-, 3-, and 5-year DCA curves shown in Figure 11C–E, the risk score was the optimal predictor of survival for pediatric AML patients.

4. Discussion

With the rapid advancements in bioinformatics, predicting the prognosis of pediatric AML patients by assessing the risk level of pediatric AML at the molecular level has become a reality. The regulatory mechanisms involved in the lncRNA-mediated regulation of AML suggest that lncRNAs can be used as potential molecular markers to predict the course and survival status of AML patients[22]. Pyroptosis plays a key role in tumorigenesis and tumor progression. At present, studies have found that PR-lncRNAs act as immunotherapy targets or diagnostic and predictive biomarkers for various cancer types, such as uterine corpus endometrial carcinoma, bladder cancer, colorectal cancer, and so on[23-26]. However, there is still a lack of systematic and in-depth studies on the relationship between lncRNAs and the prognosis of AML patients, especially pediatric AML patients.

In our study, we retrieved 1300 transcriptome data and the corresponding clinical data from the TARGET database and identified 841 PR-lncRNAs. We, then, classified three clusters according to the count of PR-lncRNAs expression. WB, BM, and PB were all remarkably lower in cluster 3. Pathways that genes enriched in better prognostic clusters (cluster 3) were mainly important immune-related signaling pathways, including B-cell and T-cell receptor signaling pathways, NOD-like and Toll-like receptor signaling pathways, and Fc epsilon RI signaling pathway, which were derived from GSEA. Comparing the better and the poorer prognostic clusters (cluster 3 and cluster 1), there were significantly different proportions in nine out of 22

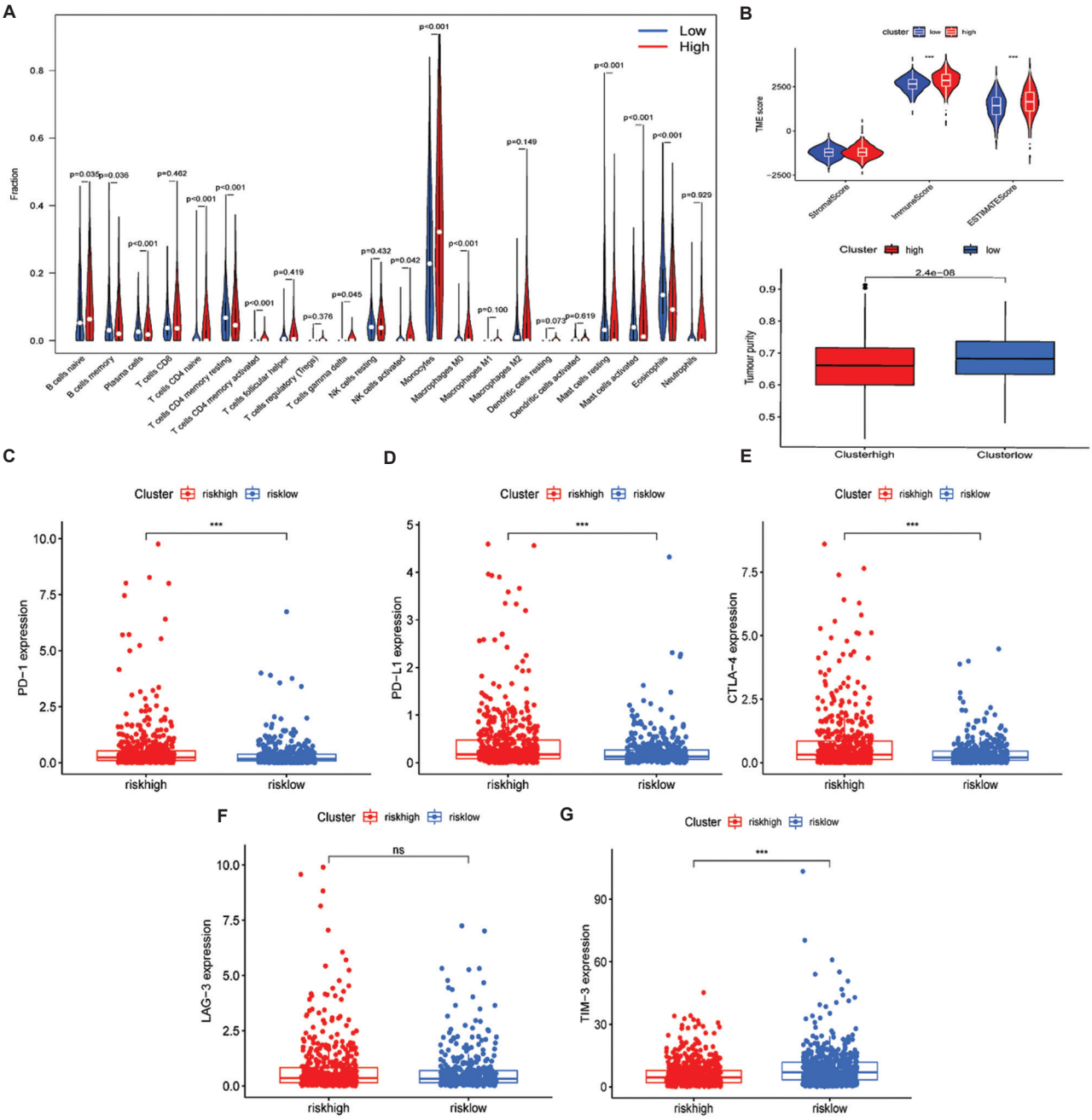

Figure 8. Immunological analysis between high- and low-risk groups. (A) Difference in the proportions of 22 immune cell types between the high- and low-risk groups. (B) Differences in ESTIMATE, stromal, and immune scores, and tumor purity between the two groups. (C–G) Expressions of five immune checkpoints between the two groups: (C) PD-1; (D) PD-L1; (E) CTLA-4; (F) LAG-3; and (G) TIM-3.

immune cell types. Although most of them were at a higher level in better prognosis patients, follicular helper T-cell, eosinophils, and activated NK cells showed the opposite. We classified cluster 3 as an immunoinflammatory subtype characterized by higher immune cell infiltration and better survival level. There were large proportions of monocytes in all populations, which may be related to the molecular types of acute monocytic leukemia (M4) and acute monocytic leukemia (M5). Interestingly, we found that there was no statistical difference between the three clusters based on the result of ESTIMATE. However, tumor purity was >60 for all, which is sufficient to ensure that the number of mutations read does not affect the biological interpretation of genome analysis[27].

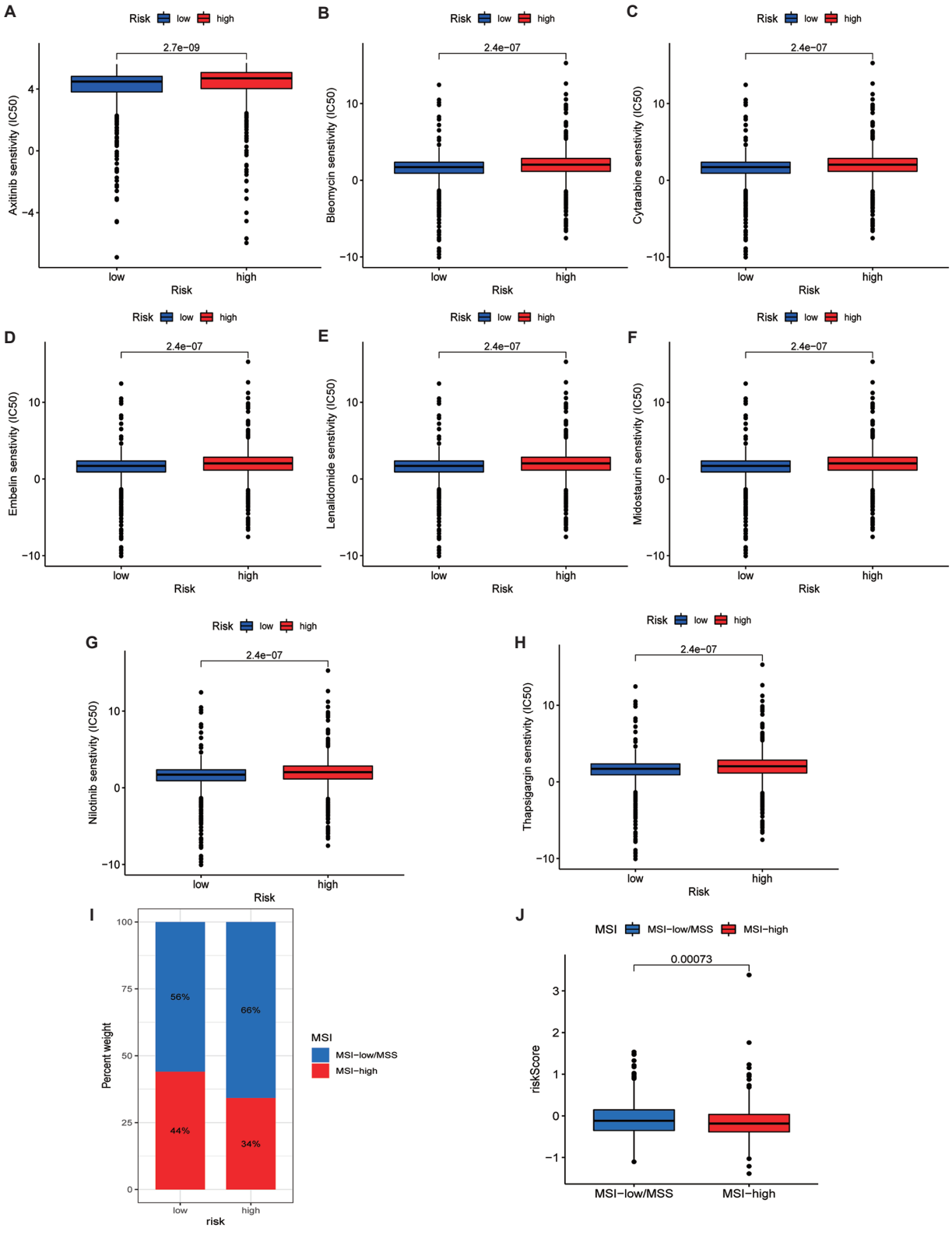

Figure 9. Results of drug sensitivity and microsatellite instability (MSI). (A–H) Relationships between signature and drug sensitivity. (I–J) Relationships between the signature and MSI.

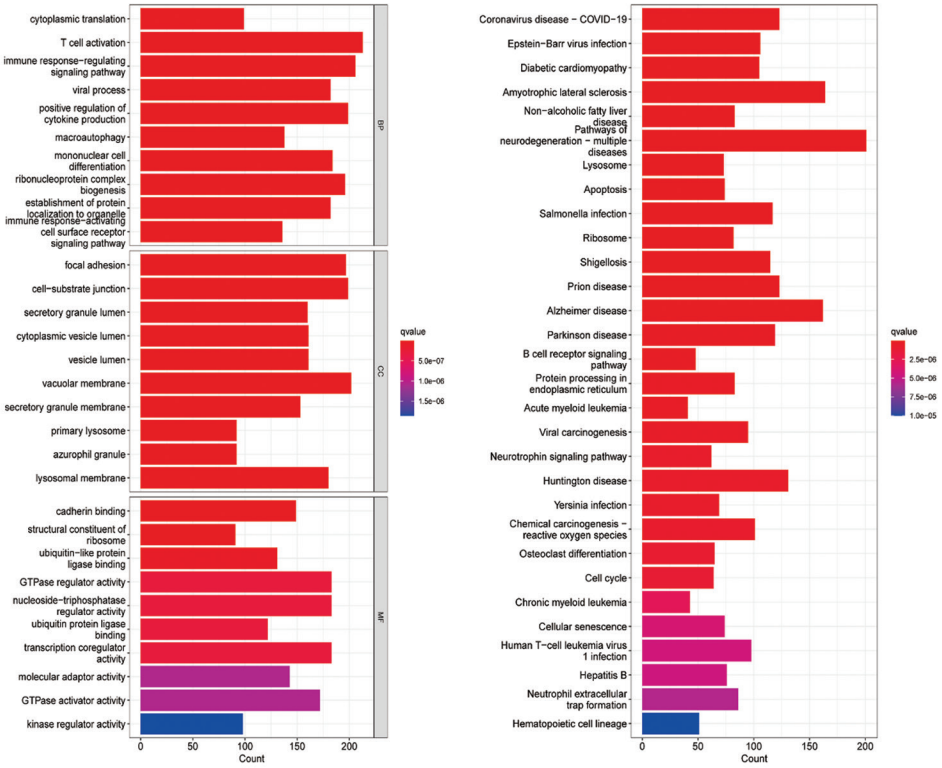

Figure 10. Representative results of Gene Ontology (GO) and Kyoto Encyclopedia of Genes and Genomes (KEGG) analyses. (A) GO and (B) KEGG.

Immune checkpoints are molecules that are expressed on immune cells and can regulate the immune process, thus playing an important role in immune effects[28]. The outcomes showed that there were significant differences in the expression of CTLA-4, PD-1, and PD-L1, which have been proven as essential immune checkpoints in pediatric AML, between clusters 1 and 3, with higher expressions in the poorer prognostic cluster (cluster 1); the results were similar to Jiang's study[29,30]. Interestingly, we also found that LAG3 had the same expression difference in these clusters.

Using LASSO-Cox and multi-Cox, we confirmed that seven out of 841 DE-lncRNAs are deserving of inclusion in the construction of a prognostic signature for predicting OS in pediatric AML, in which the 7 PPR-lncRNAs are *TRAF3IP2-AS1*, *AL157871.6*, *SNHG29*, *ASB16-AS1*, *AC007216.3*, *AP001318.1*, and *AC127496.5*. *TRAF3IP2-AS1*, which was lowly expressed in the high-risk group, has been found to play a key role in the etiopathogenesis of various autoimmune diseases by negatively regulating human IL-17 signaling through the downregulation of activator 1 (Act1) expression[31]. IL-17 is a pro-inflammatory cytokine that is secreted by activated CD4 T-cells, involved in inducing and mediating proinflammatory responses, and increasingly recognized as a risk factor of AML with poorer prognosis[32,33]. In other studies, *TRAF3IP2-AS1* has also been found to be related to N^6-methyladenosine and ferroptosis, affecting the prognosis and treatment of patients[34,35]. *SNHG29*, which was identified as a protective factor in our study, has been found in previous studies that it inhibits the ubiquitination degradation of yes-associated protein (YAP) by binding to it, thus promoting the expression of downstream target gene PD-L1 and subsequently anti-AML immunity[36,37]. Besides, in Han's study, they found that *SNHG29* has a role in carcinogenesis through the miR-223-3p/CTNND1 axis[38]. Besides, Li has found that *SNHG29* can indirectly affect the expression of *BAALC*, a gene upregulated in AML, by sponging miR-380-3p and negatively modulating miR-380-3p expression as a competing endogenous RNA (ceRNA)[39]. The expression of *ASB16-AS1* was positively associated with risk score in our study. In another study, *ASB16-AS1* affected more than ten immune-related signal pathways in multiple cancer types and played a key role in the recruitment and functional regulation of tumor-infiltrating immune cells[40]. In AML therapeutic area, NF-kappa B (NF-κB) pathway has been regarded as a target. In a study conducted by Bosman *et al.*, they discovered that the performance of transforming growth factor-β activated kinase 1 (TAK1) is related to the overexpression

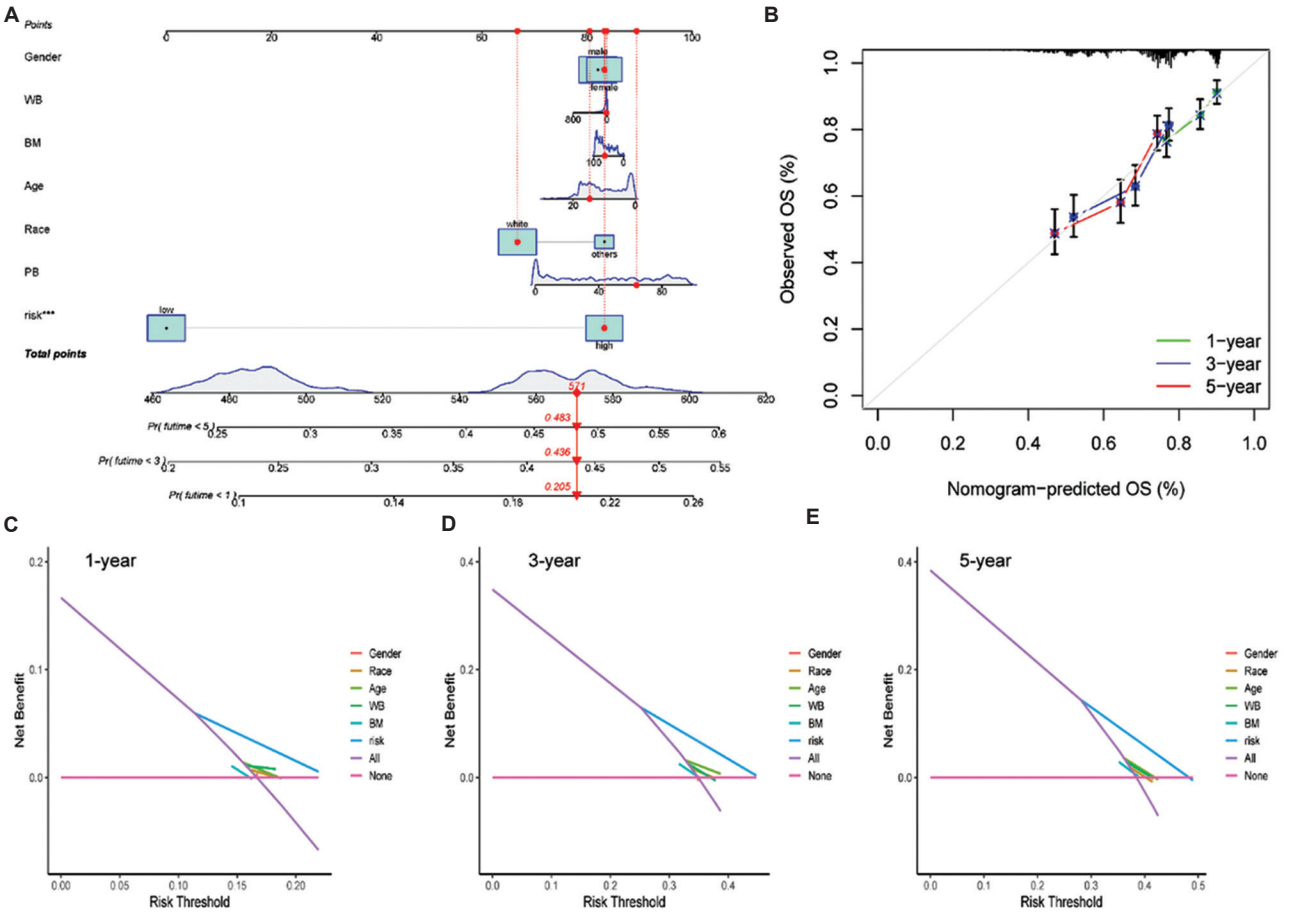

Figure 11. Decision curve and nomogram. (A) A nomogram with gender, race, BM, PB, WBC, age, FAB category, and risk score. (B) 1-, 3-, and 5-year calibration curves. (C–E) Decision curves at 1, 3, and 5 years. BM: Bone marrow leukemic blast percentage (%); PB: Peripheral blasts (%); WB: White blood cell at diagnosis.

and inhibition of NF-κB in AML CD34+cells[41]. In a study on gastric cancer, researchers have found that NF-κB can be stimulated by strengthening the expression of TRIM37 through *ASB16-AS1*[42]. *AC127496.5*, on the other hand, has been found to be one of the predictors of response to anti-PD-1 therapy for patients with cancer other than AML[43]. Unfortunately, we have not found the mechanism of the other three lncRNAs; thus, more research is needed to ascertain their potential roles.

Seven PR-lncRNAs were used to construct the pediatric AML prognostic signature, and the expression levels of those genes were calculated using risk scores. The AUC of the training set was 0.671, 0.676, and 0.665 at 1, 3, and 5 years, respectively. Similar results were obtained for the testing set in validating the model. The prediction model has a considerable effect on the survival prediction of pediatric AML patients, and the prognostic signature has a great predictive ability for these patients.

The low- and high-risk groups were separated according to the median risk score of the training set. Patients in the two groups showed noticeably distinct clinical characteristics, prognosis, TME, immune checkpoint expressions, MSI level, and drug susceptibility. The high-risk group was characterized by poorer prognosis, lower immune checkpoint expressions, MSI-L/MSS, and lower drug susceptibility. Interestingly, we found that one of the immune checkpoints, TIM-3, played a different role from others both in the risk groups and the three clusters. In the previous studies, researchers have found that TIM-3 may be different in AML and other leukemias; also, its representations may not be the same in different FAB categories. Studies have also found that TIM-3 played a different role in acute promyelocytic leukemia (M3) compared with other cases[44,45]. However, we were unable to find any association with M3 in our study. The molecular mechanisms involved in the different outcomes need to be further explored. As expected, the TME differed

in the presence of different PR-lncRNAs expressions. Recent studies have revealed that pyroptosis is a double-edged sword. On the one hand, pyroptosis-induced inflammation facilitates the generation and maintenance of an inflammatory microenvironment surrounding cancer cells, thus facilitating tumor development[46]. On the other hand, the acute activation of pyroptosis leads to the infiltration of various immune cells, thus repressing tumor development. Other studies have shown that many lncRNAs display a strong cell type-specific expression pattern in TME, especially in a variety of immune cell types[47]. Hence, PR-lncRNAs, combining the dual effects of pyroptosis and lncRNAs, may result in a different TME. Regrettably, with our study and previous research evidence, it is still impossible to conclude whether this effect is positive or negative. At the end of this study, we established a decision curve, inclusive of the risk score and clinical parameters. It showed that the risk score was the best predictor among various factors.

In this study, we built a prognostic signature and a nomogram based on seven PR-lncRNAs to predict the prognosis of pediatric AML patients and preliminarily explored the relationship between PR-lncRNAs and immune status, which have not been involved in the previous studies before. Nevertheless, there are still some gaps in our research. First, the data we used in our analysis were obtained from a public database; hence, the accuracy of the data cannot be verified. Second, our study did not include an external testing set; the prognostic signature was constructed and validated through the TARGET cohort. Last but not least, the potential relationship between the risk score and anticancer immunity needs to be further explored. Given the limitations above, the conclusions drawn from our study still require a higher degree of detailed experimental verification.

5. Conclusion

Pyroptosis and lncRNAs play a critical role in the progression of pediatric AML, the prognosis of these patients, and the alteration of TME. Our research validated an original PR-lncRNAs signature that is independently associated with OS. In addition, we identified the relevance of the immune microenvironment in influencing pediatric AML outcomes by analyzing the prognostic signature and immune profiles. The predictive value of the model needs to be examined by accurate clinical data. Moreover, the inherent mechanism by which PR-lncRNAs contribute to antitumor immunity remains to be revealed in future studies.

Acknowledgments

None.

Funding

This work was supported by the Natural Science Foundation of Henan Province, China (Grant No. 212300410402).

Conflict of interest

The authors declare no conflicts of interest.

Author contributions

Conceptualization: Xinyu Chang
Formal analysis: Xinyu Chang, Guowei Zheng, Xiting Cao, Zhenwei Wang, Hao Zhu, Shuaijie Gao
Writing – original draft: Xinyu Chang
Writing – review & editing: Jie Lu, Yuanlin Xi

Ethics approval and consent to participate

Not applicable.

Consent for publication

Not applicable.

Availability of data

The transcriptome data and clinical data of 1474 AML samples were retrieved from the TARGET database up to March 1, 2022 (https://ocg.cancer.gov/programs/target).

References

1. Quessada J, Cuccuini W, Saultier P, *et al*., 2021, Cytogenetics of pediatric acute myeloid leukemia: A review of the current knowledge (in eng). *Genes (Basel)*, 12(6): 924.

   https://doi.org/10.3390/genes12060924

2. Lejman M, Dziatkiewicz I, Jurek M, 2022, Straight to the point-the novel strategies to cure pediatric AML (in eng). *Int J Mol Sci*, 23(4): 1968.

   https://doi.org/10.3390/ijms23041968

3. Egan G, Chopra Y, Mourad S, *et al*., 2021, Treatment of acute myeloid leukemia in children: A practical perspective (in eng). *Pediatr Blood Cancer*, 68(7): e28979.

   https://doi.org/10.1002/pbc.28979

4. Kuwatsuka Y, Tomizawa D, Kihara R, *et al*., 2018, Prognostic value of genetic mutations in adolescent and young adults with acute myeloid leukemia (in eng). *Int J Hematol*, 107(2): 201–210.

   https://doi.org/10.1007/s12185-017-2340-z

5. Hsu SK, Li CY, Lin IL, *et al*., 2021, Inflammation-related pyroptosis, a novel programmed cell death pathway, and its crosstalk with immune therapy in cancer treatment (in eng). *Theranostics*, 11(18): 8813–8835.

   https://doi.org/10.7150/thno.62521

6. Li L, Jiang M, Qi L, *et al.*, 2021, Pyroptosis, a new bridge to tumor immunity (in eng). *Cancer Sci*, 112(10): 3979–3994.

   https://doi.org/10.1111/cas.15059

7. Fang Y, Tian S, Pan Y, *et al.*, 2020, Pyroptosis: A new frontier in cancer (in eng). *Biomed Pharmacother*, 121: 109595.

   https://doi.org/10.1016/j.biopha.2019.109595

8. Xia X, Wang X, Cheng Z, *et al.*, 2019, The role of pyroptosis in cancer: Pro-cancer or pro-"host"? (in eng). *Cell Death Dis*, 10(9): 650.

   https://doi.org/10.1038/s41419-019-1883-8

9. Johnson DC, Taabazuing CY, Okondo MC, *et al.*, 2018, DPP8/DPP9 inhibitor-induced pyroptosis for treatment of acute myeloid leukemia (in eng). *Nat Med*, 24(8): 1151–1156.

   https://doi.org/10.1038/s41591-018-0082-y

10. Razmara M, Srinivasula SM, Wang L, *et al.*, 2002, CARD-8 protein, a new CARD family member that regulates caspase-1 activation and apoptosis (in eng). *J Biol Chem*, 277(16): 13952–13958.

    https://doi.org/10.1074/jbc.M107811200

11. Luo X, Zhang X, Gan L, *et al.*, 2018, The outer membrane protein Tp92 of *Treponema pallidum* induces human mononuclear cell death and IL-8 secretion (in eng). *J Cell Mol Med*, 22(12): 6039–6054.

    https://doi.org/10.1111/jcmm.13879

12. Bhan A, Soleimani M, Mandal SS, 2017, Long noncoding RNA and cancer: A new paradigm (in eng). *Cancer Res*, 77(15): 3965–3981.

    https://doi.org/10.1158/0008-5472.Can-16-2634

13. Bridges MC, Daulagala AC, Kourtidis A, 2021, LNCcation: lncRNA localization and function (in eng). *J Cell Biol*, 220(2): e202009045.

    https://doi.org/10.1083/jcb.202009045

14. He D, Zheng J, Hu J, *et al.*, 2020, Long non-coding RNAs and pyroptosis (in eng). *Clin Chim Acta*, 504: 201–208.

    https://doi.org/10.1016/j.cca.2019.11.035

15. Weber CE, Kuo PC, 2012, The tumor microenvironment (in eng). *Surg Oncol*, 21(3): 172–177.

    https://doi.org/10.1016/j.suronc.2011.09.001

16. Newman AM, Liu CL, Green MR, *et al.*, 2015, Robust enumeration of cell subsets from tissue expression profiles (in eng). *Nat Methods*, 12(5): 453–457.

    https://doi.org/10.1038/nmeth.3337

17. Ohaegbulam KC, Assal A, Lazar-Molnar E, *et al.*, 2015, Human cancer immunotherapy with antibodies to the PD-1 and PD-L1 pathway (in eng). *Trends Mol Med*, 21(1): 24–33.

    https://doi.org/10.1016/j.molmed.2014.10.009

18. Rowshanravan B, Halliday N, Sansom DM, 2018, CTLA-4: A moving target in immunotherapy (in eng). *Blood*, 131(1): 58–67.

    https://doi.org/10.1182/blood-2017-06-741033

19. Maruhashi T, Sugiura D, Okazaki IM, *et al.*, 2020, LAG-3: From molecular functions to clinical applications (in eng). *J Immunother Cancer*, 8(2): e001014.

    https://doi.org/10.1136/jitc-2020-001014

20. Zang K, Hui L, Wang M, *et al.*, 2021, TIM-3 as a prognostic marker and a potential immunotherapy target in human malignant tumors: A meta-analysis and bioinformatics validation (in eng). *Front Oncol*, 11: 579351.

    https://doi.org/10.3389/fonc.2021.579351

21. Li L, Feng Q, Wang X, 2020, PreMSIm: An R package for predicting microsatellite instability from the expression profiling of a gene panel in cancer (in eng). *Comput Struct Biotechnol J*, 18: 668–675.

    https://doi.org/10.1016/j.csbj.2020.03.007

22. Garzon R, Volinia S, Papaioannou D, *et al.*, 2014, Expression and prognostic impact of lncRNAs in acute myeloid leukemia (in eng). *Proc Natl Acad Sci U S A*, 111(52): 18679–18684.

    https://doi.org/10.1073/pnas.1422050112

23. Liu J, Geng R, Ni S, *et al.*, 2022, Pyroptosis-related lncRNAs are potential biomarkers for predicting prognoses and immune responses in patients with UCEC (in eng). *Mol Ther Nucleic Acids*, 27: 1036–1055.

    https://doi.org/10.1016/j.omtn.2022.01.018

24. Ping L, Zhang K, Ou X, *et al.*, 2021, A novel pyroptosis-associated long non-coding RNA signature predicts prognosis and tumor immune microenvironment of patients with breast cancer (in eng). *Front Cell Dev Biol*, 9: 727183.

    https://doi.org/10.3389/fcell.2021.727183

25. Guo M, Xiao ZD, Dai Z, *et al.*, 2020, The landscape of long noncoding RNA-involved and tumor-specific fusions across various cancers (in eng). *Nucleic Acids Res*, 48(22): 12618–12631.

    https://doi.org/10.1093/nar/gkaa1119

26. Lu Z, Tang F, Li Z, *et al.*, 2022, Prognosis risk model based on pyroptosis-related lncRNAs for bladder cancer (in eng). *Dis Markers*, 2022: 7931393.

    https://doi.org/10.1155/2022/7931393

27. Aran D, Sirota M, Butte AJ, 2015, Systematic pan-cancer analysis of tumour purity (in eng). *Nat Commun*, 6: 8971.

    https://doi.org/10.1038/ncomms9971

28. Abril-Rodriguez G, RibasA, 2017, SnapShot: Immune checkpoint inhibitors (in eng). *Cancer Cell*, 31(6): 848–848.e1.

https://doi.org/10.1016/j.ccell.2017.05.010

29. Vago L, Gojo I, 2020, Immune escape and immunotherapy of acute myeloid leukemia (in eng). *J Clin Invest*, 130(4): 1552–1564.

https://doi.org/10.1172/jci129204

30. Jiang F, Wang XY, WangMY, *et al*., 2021, An immune checkpoint-related gene signature for predicting survival of pediatric acute myeloid leukemia (in eng). *J Oncol*, 2021: 5550116.

https://doi.org/10.1155/2021/55501106

31. He R, Wu S, Gao R, *et al*., 2021, Identification of a long noncoding RNA TRAF3IP2-AS1 as key regulator of IL-17 signaling through the SRSF10-IRF1-Act1 axis in autoimmune diseases (in eng). *J Immunol*, 206(10): 2353–2365.

https://doi.org/10.4049/jimmunol.2001223

32. Han Y, Ye A, Bi L, *et al*., 2014, Th17 cells and interleukin-17 increase with poor prognosis in patients with acute myeloid leukemia (in eng). *Cancer Sci*, 105(8): 933–942.

https://doi.org/10.1111/cas.12459

33. Wróbel T, Mazur G, Jazwiec B, *et al*., 2003, Interleukin-17 in acute myeloid leukemia (in eng). *J Cell Mol Med*, 7(4): 472–474.

https://doi.org/10.1111/j.1582-4934.2003.tb00250.x

34. Li J, Zhang J, Tao S, *et al*., 2022, Prognostication of pancreatic cancer using the cancer genome atlas based ferroptosis-related long non-coding RNAs (in eng). *Front Genet*, 13: 838021.

https://doi.org/10.3389/fgene.2022.838021

35. Zhong F, Yao F, Cheng Y, *et al*., 2022, m6A-related lncRNAs predict prognosis and indicate immune microenvironment in acute myeloid leukemia (in eng). *Sci Rep*, 12(1): 1759.

https://doi.org/10.1038/s41598-022-05797-5

36. Ni W, Mo H, Liu Y, *et al*., 2021, Targeting cholesterol biosynthesis promotes anti-tumor immunity by inhibiting long noncoding RNA SNHG29-mediated YAP activation (in eng). *Mol Ther*, 29(10): 2995–3010.

https://doi.org/10.1016/j.ymthe.2021.05.012

37. Chen C, Liang C, Wang S, *et al*., 2020, Expression patterns of immune checkpoints in acute myeloid leukemia (in eng). *J Hematol Oncol*, 13(1): 28.

https://doi.org/10.1186/s13045-020-00853-x

38. Han L, Li Z, Jiang Y, *et al*., 2019, SNHG29 regulates miR-223-3p/CTNND1 axis to promote glioblastoma progression via Wnt/β-catenin signaling pathway (in eng). *Cancer Cell Int*, 19: 345.

https://doi.org/10.1186/s12935-019-1057-x

39. Li S, Wu D, Jia H, *et al*., 2020, Long non-coding RNA LRRC75A-AS1 facilitates triple negative breast cancer cell proliferation and invasion via functioning as a ceRNA to modulate BAALC (in eng). *Cell Death Dis*, 11(8): 643.

https://doi.org/10.1038/s41419-020-02821-2

40. Wu L, Liao W, Wang X, *et al*., 2021, Expression, prognosis value, and immune infiltration of lncRNA ASB16-AS1 identified by pan-cancer analysis (in eng). *Bioengineered*, 12(2): 10302–10318.

https://doi.org/10.1080/21655979.2021.1996054

41. Bosman MC, Schepers H, Jaques J, *et al*., 2014, The TAK1-NF-κB axis as a therapeutic target for AML (in eng). *Blood*, 124(20): 3130–3140.

https://doi.org/10.1182/blood-2014-04-569780

42. Fu T, Ji K, Jin L, *et al*., 2021, ASB16-AS1 up-regulated and phosphorylated TRIM37 to activate NF-κB pathway and promote proliferation, stemness, and cisplatin resistance of gastric cancer (in eng). *Gastric Cancer*, 24(1): 45–59.

https://doi.org/10.1007/s10120-020-01096-y

43. Zhou JG, Liang B, Liu JG, *et al*., 2021, Identification of 15 lncRNAs signature for predicting survival benefit of advanced melanoma patients treated with Anti-PD-1 monotherapy (in eng). *Cells*, 10(5): 977.

https://doi.org/10.3390/cells10050977

44. Rezaei M, Tan J, Zeng C, *et al*., 2021, TIM-3 in leukemia; Immune response and beyond (in eng). *Front Oncol*, 11: 753677.

https://doi.org/10.3389/fonc.2021.753677

45. Kikushige Y, Akashi K, 2012, TIM-3 as a therapeutic target for malignant stem cells in acute myelogenous leukemia (in eng). *Ann N Y Acad Sci*, 1266: 118–123.

https://doi.org/10.1111/j.1749-6632.2012.06550.x

46. Du T, Gao J, Li P, *et al*., 2021, Pyroptosis, metabolism, and tumor immune microenvironment (in eng) *Clin Transl Med*, 11(8): e492.

https://doi.org/10.1002/ctm2.492

47. Park EG, Pyo SJ, Cui Y, *et al*., 2022, Tumor immune microenvironment lncRNAs (in eng). *Brief Bioinform*, 23(1): bbab504.

https://doi.org/10.1093/bib/bbab504

ACCSCIENCE PUBLISHING

Gene & Protein in Disease

ORIGINAL RESEARCH ARTICLE

Alkylation repair homolog 3-regulated esophageal squamous cell carcinoma associated long non-coding RNA 1 is required for maintaining the stemness of esophageal cancer

Yuanbo Cui[1], Yanan Lou[2], Pengju Lv[1], and Wei Cao[1]*

[1]Translational Medicine Center, Zhengzhou Central Hospital Affiliated to Zhengzhou University, Zhengzhou 450007, China

[2]Department of Breast Surgery, Zhengzhou Central Hospital Affiliated to Zhengzhou University, Zhengzhou, 450007, China

Abstract

N[1]-methyladenosine (m[1]A) RNA modification represents one of the essential post-transcriptional modifications in gene expression regulation. Long non-coding RNAs (lncRNAs) are involved in the development of malignant tumors, including esophageal cancer (ESCA). However, whether m[1]A can regulate that lncRNA in cancer cells remains unclear. ESCA cell lines TE1 and KYSE70 were used for functional experiments. The mRNA and protein levels were detected by quantitative reverse transcription polymerase chain reaction and Western blot, respectively. Colony formation and tumor sphere formation assays were used for evaluating ESCA stemness. The m[1]A modification on esophageal squamous cell carcinoma associated long non-coding RNA 1 (ESCCAL-1) transcript was examined by methylated RNA immunoprecipitation. In this study, we report that RNA m[1]A demethylase alkylation repair homolog 3 (ALKBH3)-mediated ESCCAL-1 is implicated in maintaining stem cell-like properties of ESCA. Clinically, ESCCAL-1 was up-regulated in ESCA and positively correlated with tumor stage. In addition, patients with higher ESCCAL-1 expression in tumors had shorter median survival. Functionally, the knockdown of ESCCAL-1 attenuated the stemness of ESCA cells as indicated by decreased sphere formation and colony formation capacities, while overexpression of ESCCAL-1 elicits the opposite biological effects. Moreover, ESCCAL-1 manipulation positively regulated both mRNA and protein levels of KLF4 and CD44, two stemness-related markers. Mechanistically, ALKBH3 upregulated ESCCAL-1 expression in an m[1]A demethylation-dependent manner. Notably, the downregulation of ALKBH3 mimicked the effects of ESCCAL-1 deficiency on ESCA stemness, and this phenomenon is significantly reversed by the enforced expression of ESCCAL-1. Our results revealed the role of m[1]A-mediated ESCCAL-1 in ESCA self-renewal, which expands the understanding of lncRNA post-transcriptional modification in cancer development.

Keywords: ALKBH3; *N*[1]-methyladenosine; ESCCAL-1; Stemness; Esophageal cancer

***Corresponding author:**
Wei Cao
(caowei7@zzu.edu.cn)

Citation: Cui Y, Lou Y, Lv P, *et al.*, 2023, Alkylation repair homolog 3-regulated esophageal squamous cell carcinoma associated long non-coding RNA 1 is required for maintaining the stemness of esophageal cancer. *Gene Protein Dis,* 2(1):305.
https://doi.org/10.36922/gpd.305

Received: December 28, 2022
Accepted: February 21, 2023
Published Online: March 13, 2023

1. Introduction

Esophageal cancer (ESCA), a common digestive system malignancy, is the sixth leading cause of cancer-related death worldwide[1]. Esophageal squamous cell carcinoma (ESCC) is the primary pathological type of ESCA in Asia, while esophageal adenocarcinoma (EAC) is more common in Western countries[2,3]. Although researchers have discovered in recent years that genetic mutations alter susceptibility to ESCA and that epigenetic changes contribute to the development of ESCA[4-6], the detailed mechanisms that drive the tumorigenesis of ESCA are still not well understood. Therefore, uncovering the molecular mechanism of ESCA is expected to contribute to the development of new diagnostic and therapeutic strategies.

Long non-coding RNAs (lncRNAs), non-coding transcripts longer than 200 nucleotides, widely mediate tumor development and influence disease prognosis[7]. We previously used transcriptome sequencing technology to detect differentially expressed lncRNAs in ten pairs of ESCA and adjacent normal tissues and identified esophageal squamous cell carcinoma associated long non-coding RNA 1 (ESCCAL-1) as an upregulated molecule closely related to ESCA[8]. It was further found that ESCCAL-1 can promote the proliferation, metastasis, cycle progression, and apoptosis resistance of ESCA cells[9,10], suggesting that ESCCAL-1 may be a critical oncogenic lncRNA in ESCA occurrence. However, the molecules responsible for the uncontrolled expression of ESCCAL-1 in ESCA and their biological roles still need to be fully understood.

N^1-methyladenosine (m^1A) methylation is one of the eukaryotic cell's most common RNA modifications. Deregulated methylase regulates RNA stability, splicing, translation, and other processes by affecting the m^1A modification of transcripts[11,12]. RNA m^1A modification controls intracellular gene expression profile at the post-transcriptional level and participates in the regulation of tumor initiation and development[13-15]. However, the function of m^1A modification in ESCA and its regulation of lncRNA expression remains unclear.

In this study, we found that high expression of ESCCAL-1 was closely related to the progression and prognosis of ESCA. The absence of ESCCAL-1 inhibits the stem-like properties of ESCA cells, and the forced expression of ESCCAL-1 promotes the self-renewal ability of ESCA. Alkylation repair homolog 3 (ALKBH3), an RNA demethylase, erases the m^1A modification of ESCCAL-1 and causes the upregulation of the latter expression in ESCA. ALKBH3/ESCCAL-1 axis is involved in the stemness maintenance of ESCA, providing a new therapeutic target for this disease.

2. Materials and methods

2.1. Cancer databases

UALCAN is a comprehensive cancer database containing multiple omics data (http://ualcan.path.uab.edu/index.html). We used this database to verify the expression of ESCCAL-1 in ESCA and its relationship with various clinical indicators of patients. Kaplan–Meier Plotter (KMP, http://kmplot.com/analysis/index.php), an online server designed to provide users with clinical data on pan-cancer, was used to analyze the relationship of patient survival between ESCCAL-1 and ESCA. GEPIA (http://gepia.cancer-pku.cn/about.html) is an online interactive website based on RNA-seq data, which is used to analyze the expression of ESCCAL-1 and ALKBH3 as well as their correlation in ESCA.

2.2. Cell culture and transfection

Three ESCA cell lines, including TE1, KYSE70, EC1, and one immortalized esophageal epithelial cell line Het-1A, were cultured in an incubator containing 5% carbon dioxide at 37°C. All cells were maintained in RPMI 1640 medium containing 10% fetal bovine serum and 1% penicillin-streptomycin solution. The lentivirus-based recombinant vectors were purchased from Shanghai GeneChem Company (China) for knockdown (sh-AL1#1, sh-AL1#2) or overexpression (OE-AL1) of ESCCAL-1. The vectors were transfected into ESCA cells with the transfection reagent HitransGA (GeneChem, China). ALKBH3 silencing siRNA was purchased from Shanghai GenePharma Company (China) and transfected into ESCA cells with the transfection agent INTERFERin (Polyplus, France).

2.3. Real-time quantitative reverse transcription polymerase chain reaction

Total RNAs were extracted from the cells using Trizol reagent (Invitrogen, USA). After concentration and purity measurements, 1 μg of RNAs in a 20-μL reaction system were reverse-transcribed into cDNA using a reverse transcription kit (Novoprotein, China). Finally, real-time quantitative reverse transcription polymerase chain reaction (qRT-PCR) was performed using the SYBRGREEN kit (Novoprotein, China) and amplification system (Applied Biosystems, USA). The housekeeping gene *GAPDH* was used as the internal reference, and the relative expression level of the target gene was calculated by method $2^{-\Delta\Delta Ct}$. The primers used are shown in Table S1.

2.4. Tumor sphere formation assay

The transfected cells were uniformly inoculated in low-adhesion six-well plates (CORNING, USA), each

containing 4 mL of sphere-forming medium and 10,000 cells. Dulbecco's modified eagle medium (DMEM)/F12 medium contained 20 ng/mL epidermal growth factor (EGF), 10 ng/mL basic fibroblast growth factor (bFGF), 5 μg/mL insulin, 0.4% bovine serum albumin (BSA), and 1× B27. The plates were placed in an incubator containing 5% carbon dioxide at 37°C for 7 – 12 days. Finally, the spheres were photographed and the number of spheres were analyzed.

2.5. Colony formation assay

The transfected cells were uniformly inoculated in 12-well plates with 1000 cells per well, and placed in an incubator containing 5% carbon dioxide at 37°C for 7 – 10 days. The cell clones were immobilized with paraformaldehyde and stained with crystal violet solution. Finally, cell colonies were photographed and the area of colonies in each well was analyzed.

2.6. Western blot analysis

Total proteins were extracted by RIPA lysis buffer (EpiZyme, China) containing protease inhibitors. After concentration and purity determination, the total proteins were denatured with loading buffer at 100°C for 10 min. Then, 10% polyacrylamide gel was prepared, and an equal amount of protein was added to each lane and electrophoresis was performed. Subsequently, the proteins on the gel were transferred to the polyvinylidene fluoride membrane. After blocking with skimmed milk and incubation with the primary antibody and secondary antibody, the ECL kit and the luminescence imaging analysis system were used to detect the target protein attached to the membrane. Primary antibodies include anti-GAPDH (1:5000, Bioworld, China), anti-CD44 (1:2000, Bioss, China), and anti-KLF4 (1:2000, Bioss, China).

2.7. Methylated RNA immunoprecipitation (MeRIP)

N^1-methyladenosine (m^1A) modification on the ESCCAL-1 transcript was detected by the m^1A MeRIP Kit (GenSeq, China). The experimental procedures were performed according to the user manual. In brief, the Trizol reagent was used to extract total RNAs from cells and the RNA concentration was adjusted to 1 μg/μL with enzyme-free water. The fragment buffer was used to process RNA transcripts. Subsequently, m^1A antibody or control antibody IgG, fragmented RNAs and immunoprecipitation (IP) buffer were added to the prepared immunomagnetic beads and incubated at 4°C for 1 h. Then, m^1A-labeled RNA samples obtained by immunoprecipitation were dissolved in enzyme-free water and detected by polymerase chain reaction (PCR). Specific primers of ESCCAL-1 transcript used for MeRIP-PCR are shown in Table S2.

2.8. Statistical analysis

Statistical analysis and illustration of experimental data were completed by SPSS 19.0 and GraphPad 9.0. Comparison of experimental data between the two groups was conducted by *t*-test, and $P < 0.05$ was considered statistically significant.

3. Results

3.1. ESCCAL-1 is upregulated in ESCA and correlates with patient outcome

We previously identified the dysregulation of lncRNA ESCCAL-1 in ESCA using RNA-seq from ten pairs of tumor samples and adjacent normal samples[8] and verified its elevation in multiple ESCA cohorts[10]. In this study, we analyzed the expression of ESCCAL-1 in 11 normal samples, 80 EAC samples, and 81 ESCC samples by interrogating the cancer database UALCAN. ESCCAL-1 was significantly overexpressed in ESCA (Figure 1A). Moreover, the expression of ESCCAL-1 in ESCC was higher than in EAC (Figure 1A). Then, using this study cohort, we analyzed the relationship between ESCCAL-1 expression and race, sex, and tumor stage in ESCA patients. ESCCAL-1 was found to be more highly expressed in African Americans and Asians than that in Caucasians (Figure 1B). In addition, the expression of ESCCAL-1 in male ESCA was higher than in female ESCA (Figure 1C). To a certain extent, ESCCAL-1 expression increased with the progression of the ESCA tumor stage (Figure 1D). ESCCAL-1 was reported to be closely related to the outcome of ESCA patients in our previous study[8]. Here, we further analyzed the relationship between ESCCAL-1 expression and ESCA prognosis using the survival database KMP. It was found that the median survival time of patients with high ESCCAL-1 expression was significantly shorter than that of patients with low ESCCAL-1 expression in both EAC (16.5 months vs. 46.7 months, Figure 1E) and ESCC (25.4 months vs. 42.1 months, Figure 1F). These findings, in combination with our previous results, suggest that ESCCAL-1 is a bona fide risk factor for ESCA progression and survival.

3.2. ESCCAL-1 is essential for maintaining the stemness of ESCA cells

We have previously shown that knockdown of ESCCAL-1 inhibits ESCA cell growth and metastasis, while overexpression of ESCCAL-1 promotes these malignant phenotypes of ESCA[9,10]. As stem cell-like property is an intrinsic characteristic of tumors and closely related to malignant proliferation and metastasis[16,17], we speculate that ESCCAL-1 might be involved in the stemness maintenance of ESCA. First, we detected the expression of ESCCAL-1 at the ESCA cell level by qRT-PCR and found

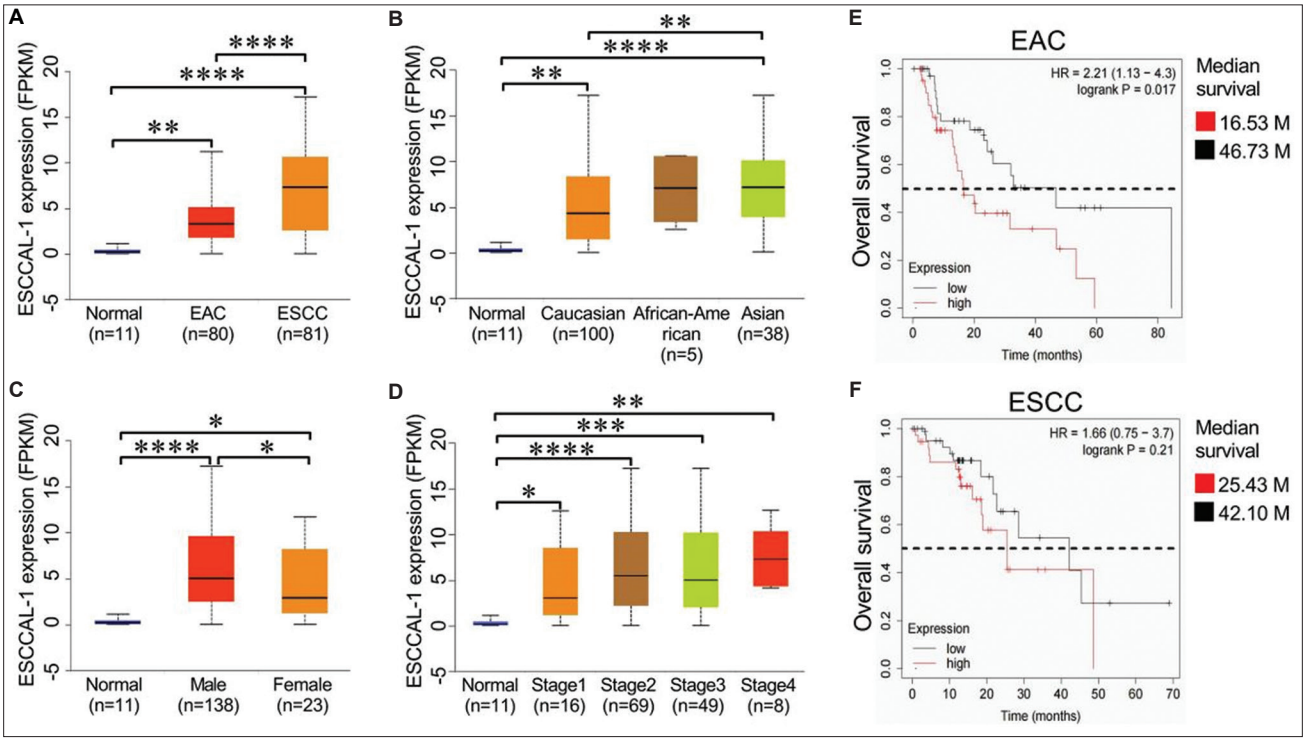

Figure 1. Expression of ESCCAL-1 in ESCA and its relationship with clinical parameters of patients. (A) UALCAN database was used to investigate the transcription levels of ESCCAL-1 in 11 esophageal epithelial samples, 80 EAC samples, and 81 ESCC samples. $^{**}P < 0.01$, $^{****}P < 0.0001$. (B) UALCAN was employed to analyze the relationship between ESCCAL-1 expression and patients' race with ESCA. $^{**}P < 0.01$, $^{****}P < 0.0001$. (C and D) UALCAN was applied to observe the relationship between ESCCAL-1 expression and gender (C) or tumor stage (D) in ESCA. $^{*}P < 0.05$, $^{**}P < 0.01$, $^{***}P < 0.001$, $^{****}P < 0.0001$. (E and F) Kaplan-Meier Plotter database was utilized to analyze the relationship between the expression of ESCCAL-1 and the survival of EAC (E) or ESCC (F) patients.

ESCCAL-1: Esophageal squamous cell carcinoma associated long non-coding RNA 1; ESCA: Esophageal cancer; EAC: Esophageal adenocarcinoma.

that the expression of ESCCAL-1 in the three ESCA cell lines (TE1, KYSE70, EC1) was significantly higher than that of the normal esophageal epithelial cell line Het-1A (Figure 2A). We then used recombinant lentiviral vectors to knockdown (sh-AL1#1, sh-AL1#2; Figure 2B) and overexpress (OE-AL1; Figure 2C) ESCCAL-1 in ESCA cells to perform loss-of-function and gain-of-function experiments. Subsequently, both tumor sphere formation and colony formation assays were used to evaluate the stemness of ESCA cells. Results from tumor sphere formation experiments showed that the knockdown of ESCCAL-1 reduced the sphere-forming ability of TE1 cells by about 60% (Figure 2D and E). In comparison, the overexpression of ESCCAL-1 promoted the sphere-forming capacity of KYSE70 cells by about 40% (Figure 2D and F). Moreover, colony formation experiments confirmed that silencing ESCCAL-1 significantly limited the cloning ability of TE1 cells *in vitro* by more than 60%, while upregulation of ESCCAL-1 enhanced the colony formation of KYSE70 cells by more than two folds (Figure 2G–I). These data indicate that ESCCAL-1 participates in maintaining ESCA stemness.

3.3. ESCCAL-1 regulates stemness-related markers expression

Considering that ESCCAL-1 plays a key role in ESCA stemness, we wondered whether ESCCAL-1 might regulate the expression of stemness-related genes. We used qRT-PCR to detect the changes in mRNA levels of a set of markers associated with stemness[17] (including SOX2, CD44, ALDH1A1, Nanog, ZEB1, KLF4, Myc) in ESCA cells after ESCCAL-1 overexpression or knockdown. We found that overexpression of ESCCAL-1 led to significant upregulation of the transcription levels of these stemness-related genes (Figure 3A), among which CD44 and ALDH1A1 showed the greatest changes. In contrast, the knockdown of ESCCAL-1 resulted in decreased mRNA levels of some stemness markers (Figure 3B). We then cross-compared the results of Figure 3A and B, and found that two stemness markers, CD44 and KLF4, were uniformly positively regulated by ESCCAL-1 (Figure 3C). Subsequent Western blot analysis further confirmed that upregulation of ESCCAL-1 increased the protein levels of CD44 and KLF4 in ESCA cells, while downregulation of ESCCAL-1 decreased the levels of both proteins

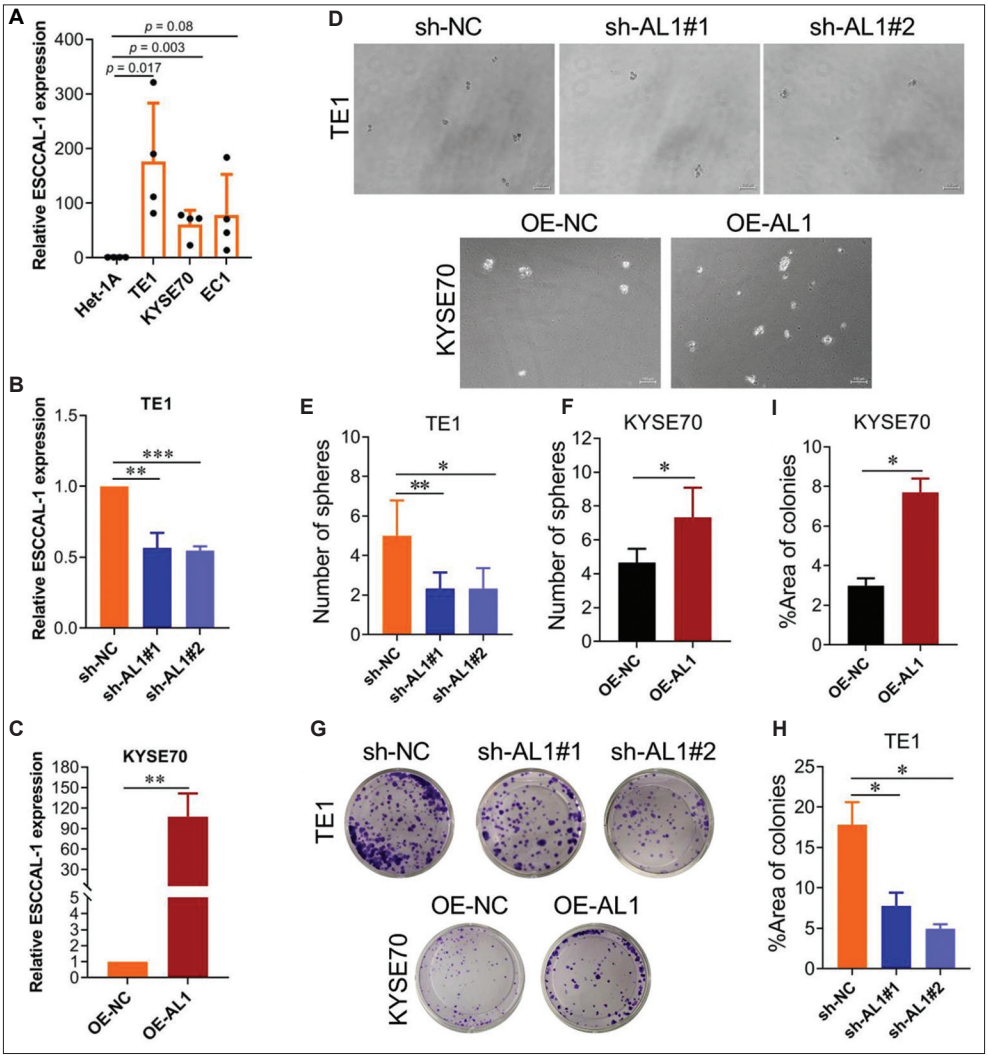

Figure 2. ESCCAL-1 is essential for maintaining ESCA stemness. (A) The transcription levels of ESCCAL-1 in Het-1A, TE1, KYSE70, and EC1 cells were detected by qRT-PCR, n = 4. (B and C) The knockdown (B) and overexpression (C) effects of ESCCAL-1 were tested by qRT-PCR, $n = 3$. $^{**}P < 0.01$, $^{***}P < 0.001$. (D and F) The effects of deletion or overexpression of ESCCAL-1 on the stemness of ESCA cells were evaluated by tumor sphere formation assay, $n = 3$. $^{*}P < 0.05$, $^{**}P < 0.01$. Scale bar = 100 μm. In panel (D), TE1 cells were transfected with sh-AL1, and KYSE70 were transfected with OE-AL1. (G–I) A colony formation assay was used to observe the effects of knockdown ($n = 2$) or upregulation (n = 3) of ESCCAL-1 on ESCA growth. $^{*}P < 0.05$. In panel (G), TE1 cells were transfected with sh-AL1, and KYSE70 were transfected with OE-AL1.
ESCCAL-1: Esophageal squamous cell carcinoma associated long non-coding RNA 1; ESCA: Esophageal cancer; qRT-PCR: quantitative reverse transcription polymerase chain reaction.

(Figure 3D). These results suggest that ESCCAL-1 may be involved in the stemness maintenance of ESCA by regulating the expression of CD44 and KLF4.

3.4. RNA m^{1}A demethylase ALKBH3 mediates ESCCAL-1 expression in ESCA

Given that ESCCAL-1 is upregulated in ESCA, we intended to investigate the upstream mechanism that causes its dysregulation. As a novel RNA modification mode, ALKBH3-mediated m^{1}A modification has been reported recently to play a vital regulatory role in some tumor types, such as liver cancer and cervical cancer[13-15]. To explore whether m^{1}A may regulate ESCCAL-1, we first used the GEPIA database to analyze the expression of m^{1}A demethylase ALKBH3 in ESCA and its correlation with ESCCAL-1. Surprisingly, we found that ALKBH3 and ESCCAL-1 showed increased expression and significant positive correlation in 182 ESCA samples (Figure 4A and B), implying that ALKBH3 may be involved in the regulation of ESCCAL-1 and may play a role in ESCA.

Data from qRT-PCR showed that the expression level of ALKBH3 in three ESCA cell lines (TE1, KYSE70,

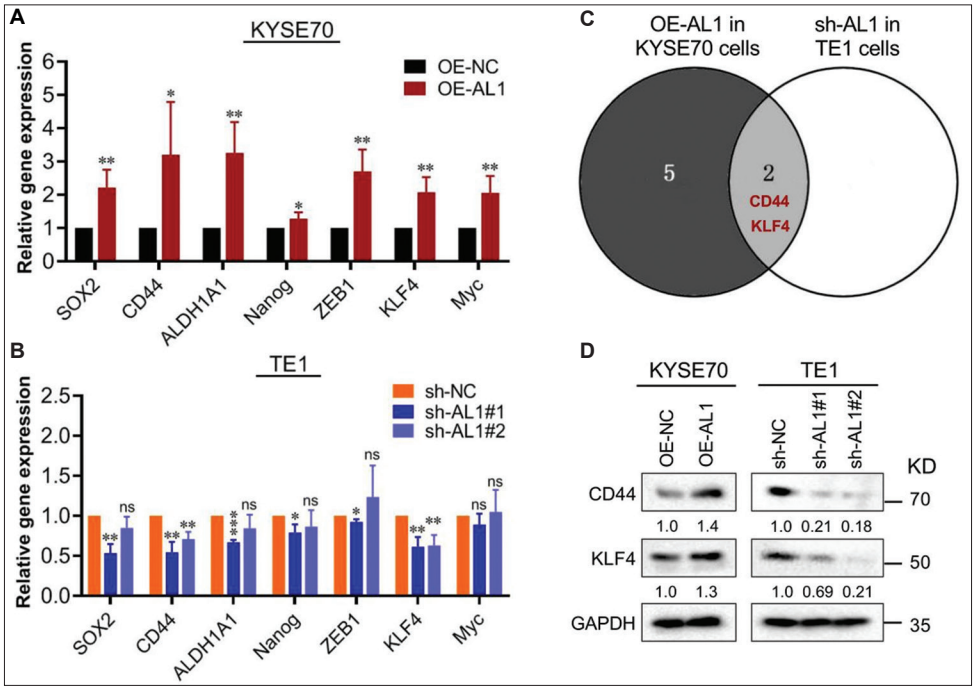

Figure 3. Effects of ESCCAL-1 manipulation on stemness-related gene expression in ESCA cells. (A and B) The effects of ESCCAL-1 overexpression (A, $n = 4$) or knockdown (B, $n = 3$) on mRNA levels of various stemness-associated markers, including SOX2, CD44, ALDH1A1, Nanog, ZEB1, KLF4, and Myc. $^{*}P < 0.05$, $^{**}P < 0.01$, $^{***}P < 0.001$ as compared to OE-NC or sh-NC. (C) The intersection of results from panels (A) and (B) revealed that the expression of CD44 and KLF4 was consistent with that as a result of ESCCAL-1 manipulation. (D) The protein levels of CD44 and KLF4 in ESCA cells after ESCCAL-1 knockdown were detected by Western blot, $n = 3$.
ESCCAL-1: Esophageal squamous cell carcinoma associated long non-coding RNA 1; ESCA: Esophageal cancer.

EC1) was significantly higher than that of normal esophageal epithelial cell line Het-1A (Figure 4C). Moreover, silencing ALKBH3 expression with siRNA can significantly downregulate the level of ESCCAL-1 in ESCA cells (Figure 4D and E). This suggests that ESCCAL-1 is regulated by RNA m^{1}A demethylase ALKBH3. Next, to determine whether ESCCAL-1 harbors m^{1}A modification, we divided the transcript into six regions (R1 to R6), designed six pairs of specific primers (Figure 4F), then conducted an m^{1}A MeRIP assay. We found significant m^{1}A enrichment in the R4 region of ESCCAL-1 transcripts (Figure 4G). Then, ALKBH3 in ESCA cells was knocked down, and the MeRIP experiment was performed. The results showed that downregulating ALKBH3 significantly increased the m^{1}A modification level of ESCCAL-1 transcripts (Figure 4H). These results suggest that ESCCAL-1 is regulated by ALKBH3 in an m^{1}A-dependent manner.

3.5. ALKBH3/ESCCAL-1 axis maintains ESCA stemness

ALKBH3 regulates biological phenotypes of cancer cells by affecting gene expression[13,14]. Since ALKBH3 regulates the expression level of ESCCAL-1 in ESCA, and ESCCAL-1 is vital for the stemness maintenance of ESCA, we speculated that the ALKBH3/ESCCAL-1 axis might participate in ESCA self-renewal. To this end, we performed functional rescue assays. The results showed that silencing ALKBH3 reduced the protein levels of CD44 and KLF4 (Figure 5A) and significantly hindered the clonogenesis and tumor sphere formation ability of ESCA cells (Figure 5B and C), mimicking the biological effects of ESCCAL-1 deletion on ESCA. Notably, overexpression of ESCCAL-1 significantly rescued, at least in part, the effects of ALKBH3 knockdown on the stemness of ESCA cells (Figure 5A–C). These data suggest that the ALKBH3/ESCCAL-1 axis contributes to the stemness maintenance of ESCA (Figure 5D).

4. Discussion

LncRNA is involved in the progression of ESCA and other malignant tumors and can be modified after transcription[18,19]. RNA m^{1}A modification is essential in regulating gene expression in eukaryotic cells[20,21]. However, whether m^{1}A can deregulate lncRNAs in tumor cells remains unclear. Here, we report that RNA m^{1}A demethylase ALKBH3-mediated ESCCAL-1 is required for the stemness maintenance of ESCA.

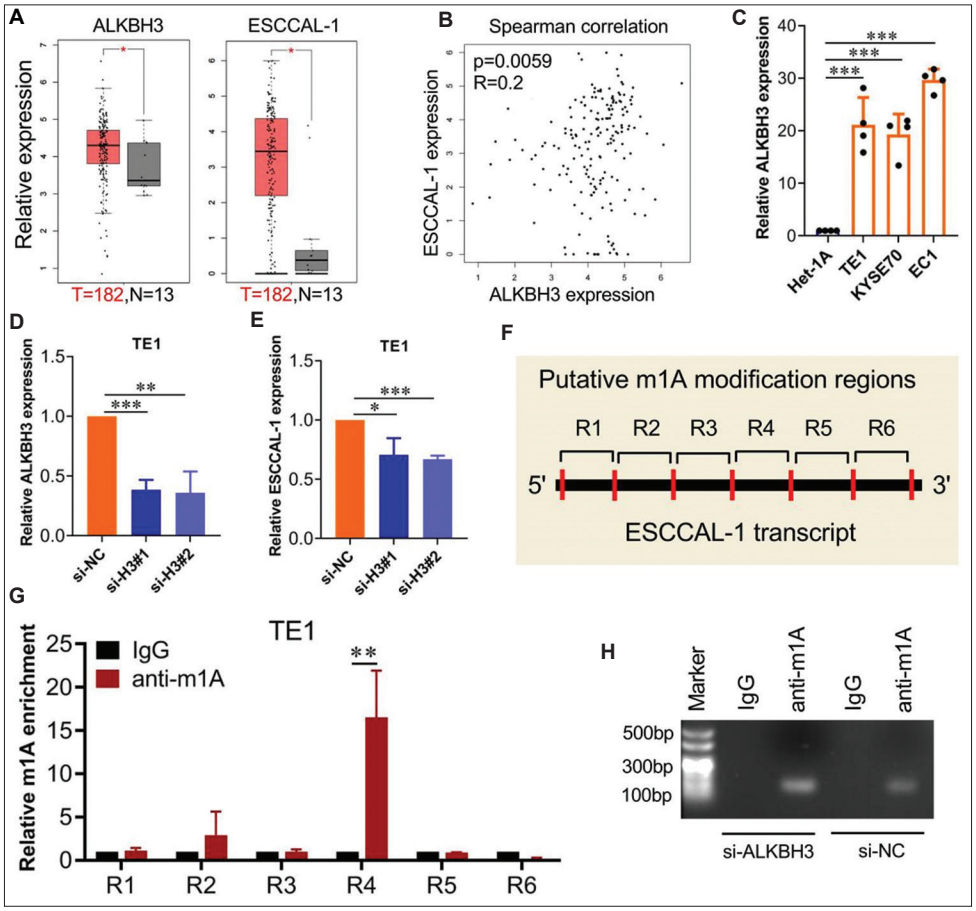

Figure 4. ESCCAL-1 is regulated by ALKBH3 in an m^{1}A-dependent manner. (A) The expression levels of ALKBH3 and ESCCAL-1 in 13 normal tissues and 182 ESCA tissues were analyzed by the GEPIA database. *$P < 0.05$. (B) The GEPIA database was used to investigate the expression correlation between ALKBH3 and ESCCAL-1 in 182 ESCA samples. (C) The mRNA levels of ALKBH3 in Het-1A, TE1, KYSE70, and EC1 cells were tested by qRT-PCR, $n = 4$. ***$P < 0.001$. (D and E) The effect of ALKBH3 silencing on the expression of ALKBH3 and ESCCAL-1 in ESCA cells was evaluated by qRT-PCR, $n = 3$. *$P < 0.05$, **$P < 0.01$, ***$P < 0.001$. (F) The putative presence of m^{1}A-modified regions on ESCCAL-1 transcripts. (G) MeRIP-PCR assay was used to detect m^{1}A modification on ESCCAL-1 transcripts, $n = 3$. **$P < 0.01$. (H) MeRIP-PCR combined with agarose gel electrophoresis was used to evaluate the effect of ALKBH3 knockdown on m^{1}A modification of ESCCAL-1 transcript, $n = 2$.
ESCCAL-1: Esophageal squamous cell carcinoma associated long non-coding RNA 1; ESCA: Esophageal cancer; m^{1}A: N^1-methyladenosine.

Stem cell-like property refers to the self-renewing ability of malignant tumor cells to maintain continuous proliferation and metastasis[22,23]. The stemness nature of tumors allows them to adapt to extreme growth conditions and to combat multiple risk factors[22,23]. Therefore, reducing tumor stemness is critical in eliminating tumor therapeutic resistance[24,25]. In the previous studies, ESCCAL-1 has the carcinogenic effect of promoting ESCA proliferation and metastasis[9,10], two basic intrinsic properties of malignant tumors, and depend on a high degree of self-renewal ability. Therefore, ESCCAL-1 might be associated with the stemness of ESCA. Through a series of functional and molecular expression experiments, we demonstrated that the knockdown of ESCCAL-1 significantly weakened the stemness of ESCA cells and reduced the mRNA and protein levels of two stemness-related genes, *CD44* and *KLF4*. In contrast, overexpression of ESCCAL-1 caused the opposite biological effects. Although we have not clarified the exact mechanisms by which ESCCAL-1 is involved in the maintenance of ESCA stemness, our results preliminarily suggest that ESCCAL-1 may exert its function by regulating the expression of CD44, KLF4, and other stemness markers. This study provides new insights into targeting the ESCCAL-1/stemness axis for ESCA treatment.

In addition to the high expression of ESCCAL-1 in ESCA, we also found that ESCCAL-1 is closely related to tumor stage and patient survival, further supporting the view that ESCCAL-1 is a potential biomarker of ESCA. In addition, we noted that this lncRNA had a special relationship with the gender and race of ESCA patients. Its expression level in male tumor samples was higher than that in female tumor samples, and its expression level in

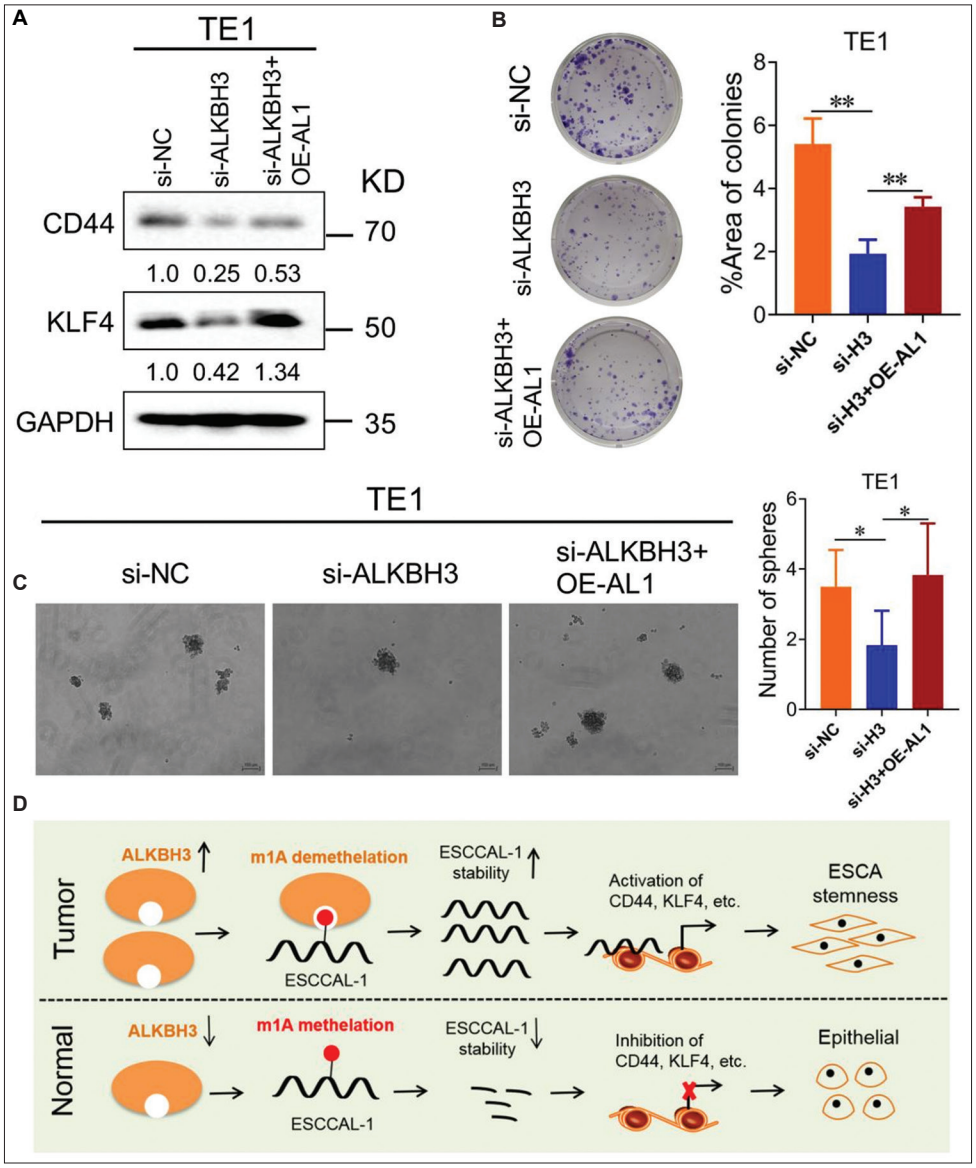

Figure 5. The role of ALKBH3/ESCCAL-1 axis in regulating ESCA stemness. (A) Western blot was applied to examine the protein levels of CD44 and KLF4 in ESCA cells following ALKBH3 silence alone or combined with ESCCAL-1 overexpression, $n = 3$. (B) A colony formation experiment was carried out to observe the role of the ALKBH3/ESCCAL-1 axis in ESCA growth, $n = 3$. $^{**}P < 0.01$. TE1 cells were transfected with si-ALKBH3 or si-ALKBH3 + OE-AL1. (C) Tumor sphere formation assay depicted that overexpression of ESCCAL-1 rescued the effects of ALKBH3 silence on ESCA stemness. $^{*}P < 0.05$. Scale bar = 100 μm. TE1 cells were transfected with si-ALKBH3 or si-ALKBH3 + OE-AL1. (D) A mechanistic model of ALKBH3-mediated ESCCAL-1 in ESCA stemness, $n = 3$.
ESCCAL-1: Esophageal squamous cell carcinoma associated long non-coding RNA 1; ESCA: Esophageal cancer.

Asian tumor samples was significantly higher than that in Caucasian patients. According to Global Cancer Statistics, the incidence of male ESCA patients is two to three folds higher than that of female patients, and the Asian region shows a higher incidence of ESCA compared with Western countries and regions[1]. Therefore, we speculate that ESCCAL-1 might be one of the key factors leading to the male ESCA and Asian ESCA. Androgen receptor signaling is widely considered a risk factor for male genitourinary tumors, such as prostate cancer[26,27]. Moreover, the activation of this signal can be regulated by upstream lncRNAs[26,27]. A recent study has found that the androgen receptor functions as an oncogenic promoter in ESCA[28]. Therefore, ESCCAL-1 might contribute to the difference in ESCA incidence between males and females by regulating the androgen receptor signaling. However, the relationship between ESCCAL-1 and the gender or ethnicity of ESCA patients needs to be further confirmed.

Recent studies have reported that the demethylase ALKBH3 can alter the post-transcriptional level of oncogenic mRNAs and tRNAs by erasing m^1A modification and thus participate in tumor progression[14,15,29,30]. However, whether lncRNAs can also be regulated by m^1A modification is unknown. This study revealed that ALKBH3 caused ESCCAL-1 overexpression in ESCA through m^1A demethylation modification. Significantly, ALKBH3 is involved in the stemness maintenance of ESCA in an ESCCAL-1-dependent manner. This is the first report on the biological role of lncRNA m^1A modification in ESCA, expanding our understanding on the role of lncRNA post-transcriptional modification in the development of ESCA.

5. Conclusions

This study further explored the expression of ESCCAL-1 in ESCA and its relationship with the clinical parameters of patients. High expression of ESCCAL-1 is necessary to maintain the stemness status of ESCA. ALKBH3 promoted the overexpression of ESCCAL-1 in an m^1A-dependent manner. These findings provide a new strategy for clinically targeting the ALKBH3/ESCCAL-1 axis against ESCA.

Acknowledgments

None.

Funding

This study was supported by the Medical Science and Technology Project of Henan Province (LHGJ20200765, SB201903032, SBGJ202003053) and the Key Project of Higher Education in Henan Province (20A310018).

Conflict of interest

The authors declare that there are no competing interests.

Author contributions

Conceptualization: Wei Cao
Formal analysis: Yuanbo Cui
Investigation: Yuanbo Cui, Yanan Lou, Pengju Lv
Writing – original draft: Yuanbo Cui
Writing – review & editing: Wei Cao

Ethics approval and consent to participate

Not applicable.

Consent for publication

Not applicable.

Availability of data

The data are available from the corresponding author upon reasonable request.

References

1. Sung H, Ferlay J, Siegel RL, *et al*., 2021, Global cancer statistics 2020: GLOBOCAN estimates of incidence and mortality worldwide for 36 cancers in 185 countries. *CA Cancer J Clin*, 71(3): 209–249.

   https://doi.org/10.3322/caac.21660

2. Bray F, Ferlay J, Soerjomataram I, *et al*., 2018, Global cancer statistics 2018: GLOBOCAN estimates of incidence and mortality worldwide for 36 cancers in 185 countries. *CA Cancer J Clin*, 68(6): 394–424.

   https://doi.org/10.3322/caac.21492

3. Smyth EC, Lagergren J, Fitzgerald RC, *et al*., 2017, Oesophageal cancer. *Nat Rev Dis Primers*, 3: 17048.

   https://doi.org/10.1038/nrdp.2017.48

4. Song Y, Li L, Ou Y, *et al*., 2014, Identification of genomic alterations in oesophageal squamous cell cancer. *Nature*, 509(7498): 91–95.

   https://doi.org/10.1038/nature13176

5. Cui Y, Chen H, Xi R, *et al*., 2020, Whole-genome sequencing of 508 patients identifies key molecular features associated with poor prognosis in esophageal squamous cell carcinoma. *Cell Res*, 30(10): 902–913.

   https://doi.org/10.1038/s41422-020-0333-6

6. Xi Y, Lin Y, Guo W, *et al*., 2022, Multi-omic characterization of genome-wide abnormal DNA methylation reveals diagnostic and prognostic markers for esophageal squamous-cell carcinoma. *Signal Transduct Target Ther*, 7(1): 53.

   https://doi.org/10.1038/s41392-022-00873-8

7. Slack FJ, Chinnaiyan AM, 2019, The role of non-coding RNAs in oncology. *Cell*, 179(5): 1033–1055.

   https://doi.org/10.1016/j.cell.2019.10.017

8. Cao W, Lee H, Wu W, *et al*., 2020, Multi-faceted epigenetic dysregulation of gene expression promotes esophageal squamous cell carcinoma. *Nat Commun*, 11(1): 3675.

   https://doi.org/10.1038/s41467-020-17227-z

9. Liu J, Mayekar MK, Wu W, *et al*., 2020, Long non-coding RNA ESCCAL-1 promotes esophageal squamous cell carcinoma by down regulating the negative regulator of APOBEC3G. *Cancer Lett*, 493: 217–227.

   https://doi.org/10.1016/j.canlet.2020.09.001

10. Cui Y, Yan M, Wu W, *et al*., 2022, ESCCAL-1 promotes cell-cycle progression by interacting with and stabilizing galectin-1 in esophageal squamous cell carcinoma. *NPJ Precis Oncol*, 6(1): 12.

    https://doi.org/10.1038/s41698-022-00255-x

11. Jin H, Huo C, Zhou T, *et al*., 2022, m^1A RNA modification in gene expression regulation. *Genes (Basel)*, 13(5): 910.

https://doi.org/10.3390/genes13050910

12. Chen Z, Qi M, Shen B, *et al.*, 2019, Transfer RNA demethylase ALKBH3 promotes cancer progression via induction of tRNA-derived small RNAs. *Nucleic Acids Res*, 47(5): 2533–2545.

https://doi.org/10.1093/nar/gky1250

13. Wang Y, Wang J, Li X, *et al.*, 2021, N1-methyladenosine methylation in tRNA drives liver tumourigenesis by regulating cholesterol metabolism. *Nat Commun*, 12(1): 6314.

https://doi.org/10.1038/s41467-021-26718-6

14. Wu Y, Chen Z, Xie G, *et al.*, 2022, RNA m^{1}A methylation regulates glycolysis of cancer cells through modulating ATP5D. *Proc Natl Acad Sci U S A*, 119(28): e2119038119.

https://doi.org/10.1073/pnas.2119038119

15. Lu Q, Wang H, Lei X, *et al.*, 2022, LncRNA ALKBH3-AS1 enhances ALKBH3 mRNA stability to promote hepatocellular carcinoma cell proliferation and invasion. *J Cell Mol Med*, 26(20): 5292–5302.

https://doi.org/10.1111/jcmm.17558

16. Nallasamy P, Nimmakayala RK, Parte S, *et al.*, 2022, Tumor microenvironment enriches the stemness features: The architectural event of therapy resistance and metastasis. *Mol Cancer*, 21(1): 225.

https://doi.org/10.1186/s12943-022-01682-x

17. Chaudhary A, Raza SS, Haque R, 2023, Transcriptional factors targeting in cancer stem cells for tumor modulation. *Semin Cancer Biol*, 88: 123–137.

https://doi.org/10.1016/j.semcancer.2022.12.010

18. Wilkinson E, Cui YH, He YY, 2022, Roles of RNA modifications in diverse cellular functions. *Front Cell Dev Biol*, 10: 828683.

https://doi.org/10.3389/fcell.2022.828683

19. Wang Z, He J, Bach DH, *et al.*, 2022, Induction of m6A methylation in adipocyte exosomal LncRNAs mediates myeloma drug resistance. *J Exp Clin Cancer Res*, 41(1): 4.

https://doi.org/10.1186/s13046-021-02209-w

20. Cui L, Ma R, Cai J, *et al.*, 2022, RNA modifications: Importance in immune cell biology and related diseases. *Signal Transduct Target Ther*, 7(1): 334.

https://doi.org/10.1038/s41392-022-01175-9

21. Li J, Zhang H, Wang H, 2022, N1-methyladenosine modification in cancer biology: Current status and future perspectives. *Comput Struct Biotechnol J*, 20: 6578––6585.

https://doi.org/10.1016/j.csbj.2022.11.045

22. Paul R, Dorsey JF, Fan Y, 2022, Cell plasticity, senescence, and quiescence in cancer stem cells: Biological and therapeutic implications. *Pharmacol Ther*, 231: 107985.

https://doi.org/10.1016/j.pharmthera.2021.107985

23. Du L, Cheng Q, Zheng H, *et al.*, 2022, Targeting stemness of cancer stem cells to fight colorectal cancers. *Semin Cancer Biol*, 82: 150–161.

https://doi.org/10.1016/j.semcancer.2021.02.012

24. Liu C, Zhang Y, Gao J, *et al.*, 2022, A highly potent small-molecule antagonist of exportin-1 selectively eliminates CD44+CD24-enriched breast cancer stem-like cells. *Drug Resist Updat*, 66: 100903.

https://doi.org/10.1016/j.drup.2022.100903

25. Ervin EH, French R, Chang CH, *et al.*, 2022, Inside the stemness engine: Mechanistic links between deregulated transcription factors and stemness in cancer. *Semin Cancer Biol*, 87: 48–83.

https://doi.org/10.1016/j.semcancer.2022.11.001

26. Taheri M, Khoshbakht T, Jamali E, *et al.*, 2021, Interaction between non-coding RNAs and androgen receptor with an especial focus on prostate cancer. *Cells*, 10(11): 3198.

https://doi.org/10.3390/cells10113198

27. Tortora F, Calin GA, Cimmino A, 2021, Effects of long non-coding RNAs on androgen signaling pathways in genitourinary malignancies. *Mol Cell Endocrinol*, 526: 111197.

https://doi.org/10.1016/j.mce.2021.111197

28. Huang F, Chen H, Zhu X, *et al.*, 2021, The oncogenomic function of androgen receptor in esophageal squamous cell carcinoma is directed by GATA3. *Cell Res*, 31(3): 362–365.

https://doi.org/10.1038/s41422-020-00428-y

29. Zhao Y, Zhao Q, Kaboli PJ, *et al.*, 2019, m^{1}A regulated genes modulate PI3K/AKT/mTOR and ErbB pathways in gastrointestinal cancer. *Transl Oncol*, 12(10): 1323–1333.

https://doi.org/10.1016/j.tranon.2019.06.007

30. Woo HH, Chambers SK, 2019, Human ALKBH3-induced m^{1}A demethylation increases the CSF-1 mRNA stability in breast and ovarian cancer cells. *Biochim Biophys Acta Gene Regul Mech*, 1862(1): 35–46.

https://doi.org/10.1016/j.bbagrm.2018.10.008

ACCSCIENCE PUBLISHING

Gene & Protein in Disease

ORIGINAL RESEARCH ARTICLE

A pan-cancer analysis of high mobility group box 1 and its role in human tumorigenesis

Wenqing Long[1], Jiaqi Li[3], Hao Shi[1], Lijun Zhang[1], Liqun Yang[1], Zhuoyan Jiang[1], Lei Xia[1], Lin Wang[1]*, and Hongnu Yu[2]*

[1]Department of Thoracic Surgery, Affiliated Xinhua Hospital of Dalian University, Dalian, Liaoning province, China

[2]Department of Oncology, Affiliated Xinhua Hospital of Dalian University, Dalian, Liaoning province, China

[3]Department of Special Examination, Shaoxing People's Hospital, Shaoxing, Zhejiang province, China

Abstract

Understanding the specific and co-driving mechanisms of carcinogenesis in human tumors is indispensable for cancer research and can guide the development of effective treatment methods for tumors. High mobility group box 1 (HMGB1) participates in a variety of physiological processes of the body and has an inseparable relationship with tumors. In this study, The Cancer Genome Atlas, Gene Expression Omnibus database, Human Protein Atlas, and bioinformatic tools were used to conduct pan-cancer analysis of HMGB1 in various cancers so as to elucidate its role in human tumorigenesis. We analyzed and evaluated the expression of *HMGB1* in tumors, and discovered that overexpression of *HMGB1* usually indicated poor overall survival of adrenocortical carcinoma ($P < 0.01$) and lung adenocarcinoma (LUAD) ($P < 0.05$). High *HMGB1* expression is also associated with unfavorable disease-free survival for patients with adrenocortical carcinoma ($P < 0.001$), cervical squamous cell carcinoma and endocervical adenocarcinoma ($P < 0.01$), head and neck squamous cell carcinoma ($P < 0.05$), LUAD ($P < 0.05$), and sarcoma ($P < 0.05$). The potential mechanism of HMGB1-mediated tumorigenesis is also discussed. In conclusion, our pan-cancer analysis offers a comprehensive description of the carcinogenic roles of HMGB1 in a variety of human cancers.

Keywords: High mobility group box 1; Cancer; Survival; Prognosis

***Corresponding authors:**
Lin Wang
(wanglinbox@sina.com)
Hongnu Yu
(879187182@qq.com)

Citation: Long W, Li J, Shi H, *et al.*, 2023, A pan-cancer analysis of high mobility group box 1 and its role in human tumorigenesis. *Gene Protein Dis*, 2(1):301.
https://doi.org/10.36922/gpd.301

Received: December 15, 2022
Accepted: March 1, 2023
Published Online: March 16, 2023

1. Introduction

In view of the complexity of tumorigenesis, it is vital to conduct a pan-cancer analysis of the significant genes to evaluate their relevance to possible molecular mechanisms and clinical prognosis. Cancer genome repositories and databases, such as The Cancer Genome Atlas (TCGA) and Gene Expression Omnibus (GEO), offer access to many tumor-associated functional genomic datasets that can be used for pan-cancer analysis[1-3].

Situated on chromosome 13q12, the high mobility group box 1 (*HMGB1*) gene encodes and produces the HMGB1 protein[4], which is a highly conserved nuclear protein belonging to the group of nonhistone chromatin-related protein. It was first extracted from the bovine thymus in 1973[5]. HMGB1 consists of two DNA-binding

HMG-box domains (N-terminal A and center B), which constitute the non-specific DNA binding region of HMGB1 and an acidic C-terminal tail[6]. In general, HMGB1 exists in the nucleus and helps maintain the stability of the nucleus as a DNA chaperone. It plays a key role in DNA replication, V(D)J recombination, transcription and chromatin remodeling. However, the expression of HMGB1 has also been found in mitochondria, cytosol, and cell surface membranes, and the protein can be released into the extracellular space[7]. Cytoplasmic HMGB1 participates in immune responses by regulating mitochondrial function, inhibiting apoptosis, and increasing autophagy[8]. On the membrane, HMGB1 can activate platelets, promote neurite growth and axonal sprouting, and induce cell migration. HMGB1 can be secreted into the extracellular environment as a cytokine, and participates in many immune reactions by promoting the maturation and activation of immune cells and the production of cytokine[9]. In addition, extracellular HMGB1 is able to interact with chemokines to advance immune responses[10]. In a word, HMGB1, as a multifunctional protein, plays different biological roles under different circumstances, and more investigations are required to illustrate the potential effects. In pan-cancer analysis, to probe the expression profile of HMGB1 in different tumor types, databases (TGCA and GEO) were used. Except for comparing HMGB1 expression profiles in different tumor types, a number of factors such as survival status, genetic alteration, protein phosphorylation, and related cellular pathways were also taken into account. This comprehensive analysis uncovers potential molecular mechanism of HMGB1 in the pathogenesis and clinical prognosis of a variety of human cancers.

2. Materials and methods

2.1. Gene expression analysis

To observe *HMGB1* expression differences between tumor and adjacent normal tissues, we put HMGB1 into the "Gene_DE" section of tumor immune estimation resource, version2 (TIMER2) web (http://timer.cistrome.org/). With regard to some tumors without corresponding adjacent normal tissues as a control (e.g., TCGA-Mesothelioma [MESO], TCGA-Sarcoma [SARC]), the "Expression analysis-Box plot" plate of the Gene Expression Profiling Interactive Analysis, version 2 (GEPIA2) web server (http://gepia2.cancer-pku.cn/#analysis)[11] was used to obtain box plots of the Genotype-Tissue Expression (GTEx) database, with log2FC (fold change) cutoff = 1, *P*-value cutoff = 0.01, and "Match TCGA normal and GTEx data." HEPIA2 was applied to analyze *HMGB1* expression in different pathological stages of all TCGA cancers. The expression data transformed by log2 (TPM [Transcripts per million] + 1) were used for violin or box plots.

The UALCAN (http://ualcan.path.uab.edu/analysis-prot.html) was used to analyze cancer omics data, allowing us to analyze the protein expression of the Clinical Proteomic Tumor Analysis Consortium (CPTAC) dataset[12]. We investigated the expression level of HMGB1, either total protein or phosphoprotein, between primary tumor or normal tissues.

2.2. Survival analysis

To gain significant map data for overall survival (OS) and disease-free survival (DFS) of *HMGB1* in overall TCGA tumors, GEPIA2 was used in the analysis. Cutoff-low (50%) and cutoff-high (50%) values were used as expression thresholds to separate low and high expression cohorts[11]. The log-rank test was used in the hypothesis testing. Through the "Survival Analysis" plate of GEPIA2, survival plots were obtained.

2.3. Genetic variation analysis

Using the cBioPortal (https://www.cbioportal.org/) web[13-15], we collected the protein structure data, including variation frequency, mutated site information, mutation type, three-dimensional (3D) structure, and copy number alteration (CNA) in overall TCGA tumors. We also obtained survival data, including progression-free survival, OS, disease-specific survival, and DFS differences for the overall TCGA cancer types, regardless of whether there is *HMGB1* genetic variation.

2.4. Immune infiltration analysis

TIMER2 was used to observe the relationship between *HMGB1*expression and immune infiltrates among TCGA tumors. Cancer-associated fibroblast was selected for detailed analysis. The EPIC, MCPCOUNTER, XCELL, and TIDE algorithms were used for estimations. The data was visualized as heatmaps and scatter plots.

2.5. HMGB1 enrichment analysis

STRING (https://string-db.org/) web was used for protein-protein interaction network analysis. We set the following main parameters: minimum required interaction score ("low confidence [0.150]"), meaning of network edges ("evidence"), maximum number of interactors to be displayed ("no more than 50 interactors" in first shell), and active interaction sources ("experiments").

On the basis of the datasets of all TCGA tumors and normal tissues, GEPIA2 was used to obtain the top 100 *HMGB1*-related genes. We performed a pairwise Pearson's correlation analysis between *HMGB1* and selected

genes. The *P*-values and correlation coefficient (R) were calculated and displayed in figures. In addition, TIMER2 was applied to obtain heatmap data of selected genes, including *P*-values and partial correlation (cor) in the purity-adjusted Spearman's rank correlation test.

Jvenn[16] was used for cross-analysis to compare the HMGB1-binding and interacted genes. We integrated these two sets of data for Kyoto Encyclopedia of Genes and Genomes (KEGG) pathway analysis. The "tidyr" and "ggplot2" R packages were applied to show the enrichment pathway. Besides, the "clusterProfiler" R packages were applied to conduct Gene Ontology (GO) enrichment analysis. The R language software (R-4.1.0, 64-bit; https://www.r-project.org/) was applied to this analysis. Two-tailed $P < 0.05$ was considered statistically significant[17]. A simple list of methods and corresponding tools is shown in Table 1.

3. Results

3.1. Gene expression analysis

TIMER2 was used to study *HMGB1* expression among different TCGA tumor types. The results demonstrated that *HMGB1* expression was significantly higher in cholangiocarcinoma (CHOL), colon adenocarcinoma (COAD), esophageal carcinoma (ESCA), head and neck squamous cell carcinoma (HNSC), lung squamous cell carcinoma (LUSC), stomach adenocarcinoma (STAD), liver hepatocellular carcinoma (LIHC), rectum adenocarcinoma (READ) ($P < 0.001$), bladder urothelial carcinoma (BLCA), and glioblastoma multiforme (GBM) ($P < 0.01$) than in the control group. Obviously, there were also some tumor types showing undifferentiated expression (e.g., kidney renal clear cell carcinoma [KIRC], cervical squamous cell carcinoma and endocervical adenocarcinoma [CESC], thyroid carcinoma [THCA], and pheochromocytoma and paraganglioma [PCPG]).

Table 1. Methods and corresponding tools

Methods	Tools
Gene expression analysis	TIMER2, GEPIA2, UALCAN, TCGA, GTEx, CPTAC
Survival analysis	GEPIA2, TCGA, GEO
Genetic variation analysis	cBioPortal, TCGA
Immune infiltration analysis	TIMER2, TCGA
Gene enrichment analysis	STRING, TCGA, GEPIA2, TIMER2, Jvenn, R language

TCGA: The Cancer Genome Atlas; TIMER2: Tumor immune estimation resource, version 2; GTEx: Genotype-tissue expression; CPTAC: Clinical Proteomic Tumor Analysis Consortium; GEPIA2: Gene Expression Profiling Interactive Analysis, version 2; GEO: Gene Expression Omnibus; Jvenn: An interactive Venn diagram viewer.

However, compared with the control group, *HMGB1* expression in kidney chromophobe (KICH), lung adenocarcinoma (LUAD) ($P < 0.001$), and prostate adenocarcinoma (PRAD) ($P < 0.05$) were relatively low (Figure 1A).

We used the GTEx dataset to obtain normal tissue data as a control, and further evaluated the *HMGB1* expression differences between the tumor and normal tissues. The results showed that *HMGB1* was highly expressed in CHOL, COAD, lymphoid neoplasm diffuse large B-cell lymphoma (DLBC), GBM, brain lower grade glioma (LGG), READ, pancreatic adenocarcinoma (PAAD), STAD, and thymoma (THYM) (Figure 1B, $P < 0.05$).

In addition to transcription, CPTAC was used to evaluate HMGB1 at the protein level. As displayed in Figure 1C, we found that the total protein expression of HMGB1 in COAD, GBM, LIHC, ovarian cancer (OV) was significantly higher than that in normal tissues (all $P < 0.001$). However, the HMGB1 protein expression in the breast cancer (BRCA) ($P < 0.01$), uterine corpus endometrial carcinoma (UCEC), LUAD, and PAAD ($P < 0.001$) was decreased.

By using GEPIA2 tool, we probed the relationship between *HMGB1* expression and tumor pathological stage, including adrenocortical carcinoma (ACC), LIHC, skin cutaneous melanoma (SKCM), and THCA (Figure 1D, all $P < 0.05$).

3.2. Survival analysis

On the basis of the expression level of *HMGB1*, cancer cases were divided into low expression group and high expression group. Then, we used TCGA and GEO datasets to explore the correlation between *HMGB1* expression and prognosis of patients with different tumor types. As displayed in Figure 2A, the high expression of *HMGB1* was related to poor OS in ACC ($P < 0.01$) and LUAD ($P < 0.05$) cancers. On the contrary, the low expression of *HMGB1* was related to poor OS in KIRC ($P < 0.05$) and THYM ($P < 0.05$). DFS analysis displayed that the high expression of *HMGB1* was associated with the poor prognosis in ACC ($P < 0.001$), CESC ($P < 0.01$), HNSC ($P < 0.05$), LUAD ($P < 0.05$), and SARC ($P < 0.05$) (Figure 2B).

3.3. Genetic variation analysis

Cancer in humans occurs as a result of an accumulation of genetic changes. We researched the *HMGB1* genetic variations among different tumor samples in the TCGA list. From our analysis, we found that the frequency of *HMGB1* variation (>4%) was the highest in DLBC tumors, mainly including "mutation" and "deep deletion" types. Colorectal cases have the highest frequency in the

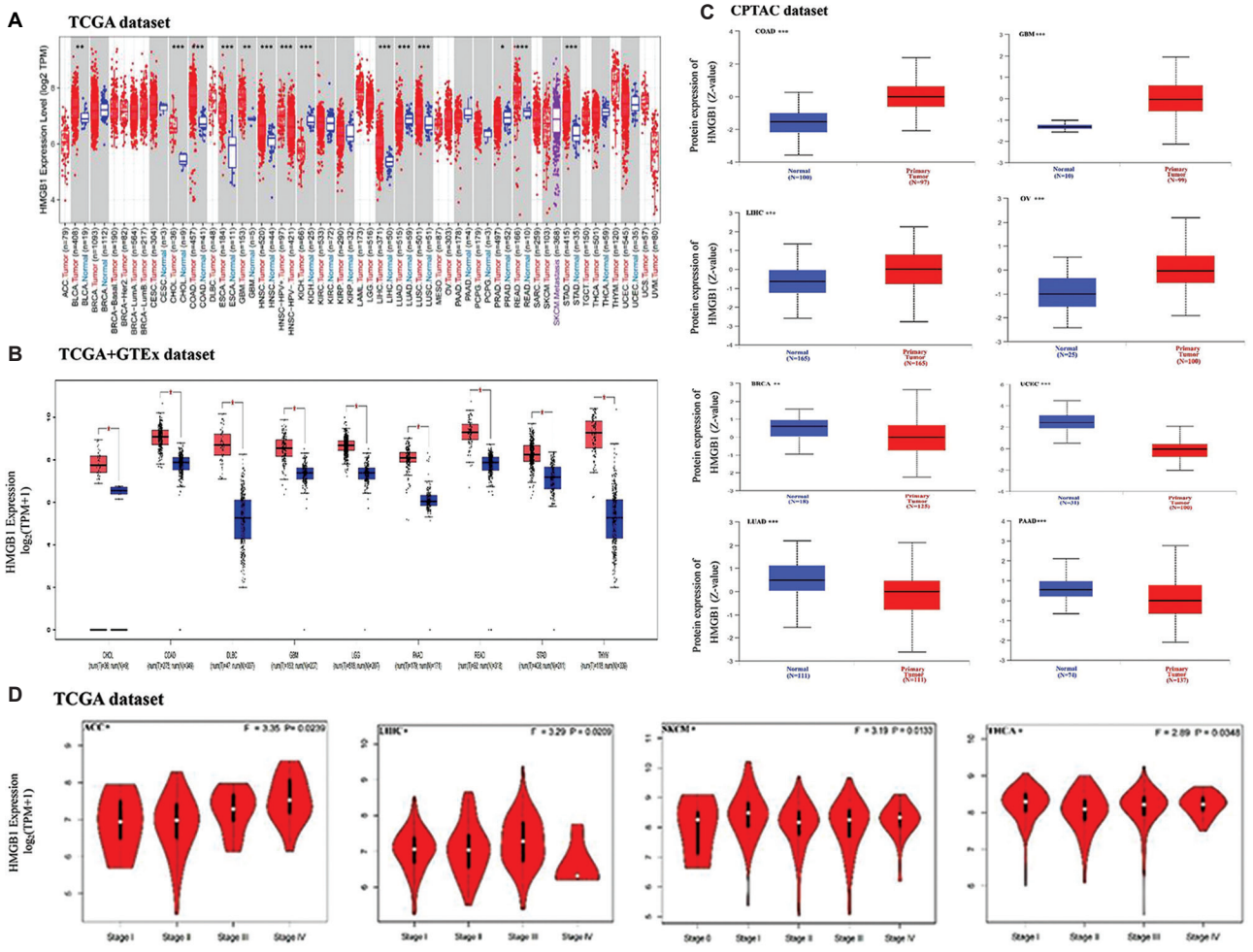

Figure 1. Expression and protein level of HMGB1 in human tumors. (A) Expression level of *HMGB1* in TCGA tumors versus adjacent tissues (if available) as visualized by TIMER2. *$P < 0.05$; **$P < 0.01$; ***$P < 0.001$. (B) Box plot representation of *HMGB1* expression level comparison in CHOL, COAD, DLBC, GBM, LGG, PAAD, READ, STAD, and THYM (TCGA project) relative to the corresponding normal tissues (GTEx database). *$P < 0.05$. (C) Total protein level of HMGB1 in normal tissue and primary COAD, GBM, LIHC, OV, BRCA, UCEC, LUAD, and PAAD. Protein data was extracted and analyzed using CPTAC. **$P < 0.01$; ***$P < 0.001$. (D) Stage-dependent expression level of *HMGB1*. Major pathological stages (stage Ⅰ, stage Ⅱ, stage Ⅲ, and stage Ⅳ) of ACC, LIHC, SKCM, and THCA were assessed and compared using TCGA data. Expression levels are expressed in Log 2 (TPM + 1).
HMGB1: High mobility group box 1; TCGA: The Cancer Genome Atlas; TIMER2: Tumor immune estimation resource, version 2; CHOL: Cholangiocarcinoma; COAD: Colon adenocarcinoma; DLBC: Diffuse large B-cell lymphoma; GBM: Glioblastoma multiforme; LGG: Lower grade glioma; PAAD: Pancreatic adenocarcinoma; READ: Rectum adenocarcinoma; STAD: Stomach adenocarcinoma; THYM: Thymoma; GTEx: Genotype-tissue expression; LIHC: Liver hepatocellular carcinoma; SKCM: Skin cutaneous melanoma; THCA: Thyroid carcinoma; BRCA: Breast cancer; UCEC: Uterine corpus endometrial carcinoma; LUAD: Lung adenocarcinoma; CPTAC: Clinical Proteomic Tumor Analysis Consortium.

"amplification" type of CNA, with a frequency of about ~4% (Figure 3A). It is worthwhile noting that all ACC cases with genetic variation (about ~1% frequency) had *HMGB1* copy number deletion (Figure 3A). Figure 3B shows the types, sites and number of cases of *HMGB1* gene variation. We have not distinguished the main types of genetic changes, and their locations appear to be sporadic, with some belonging to the HMG-box domain. For example, a truncating mutation, R163*/Q alteration, in the HMG-box domain, was only detected in 2 cases of UCEC and 1 case of GBM. The R163*/Q site is in the 3D structure of HMGB1 protein (Figure 3C). Besides, we searched the underlying association between certain genetic variations of *HMGB1* and the clinical survival prognosis of patients with different cancer types. We studied and collected information of various tumor types, and the data in Figure 3D showed that UCEC patients with *HMGB1* variation had better prognosis in terms of progression-free survival (PFS) ($P < 0.05$) than those without *HMGB1* variations. However, no significant differences were observed in OS ($P = 0.0505$), disease-specific survival (DSS) ($P > 0.05$), and DFS ($P > 0.05$).

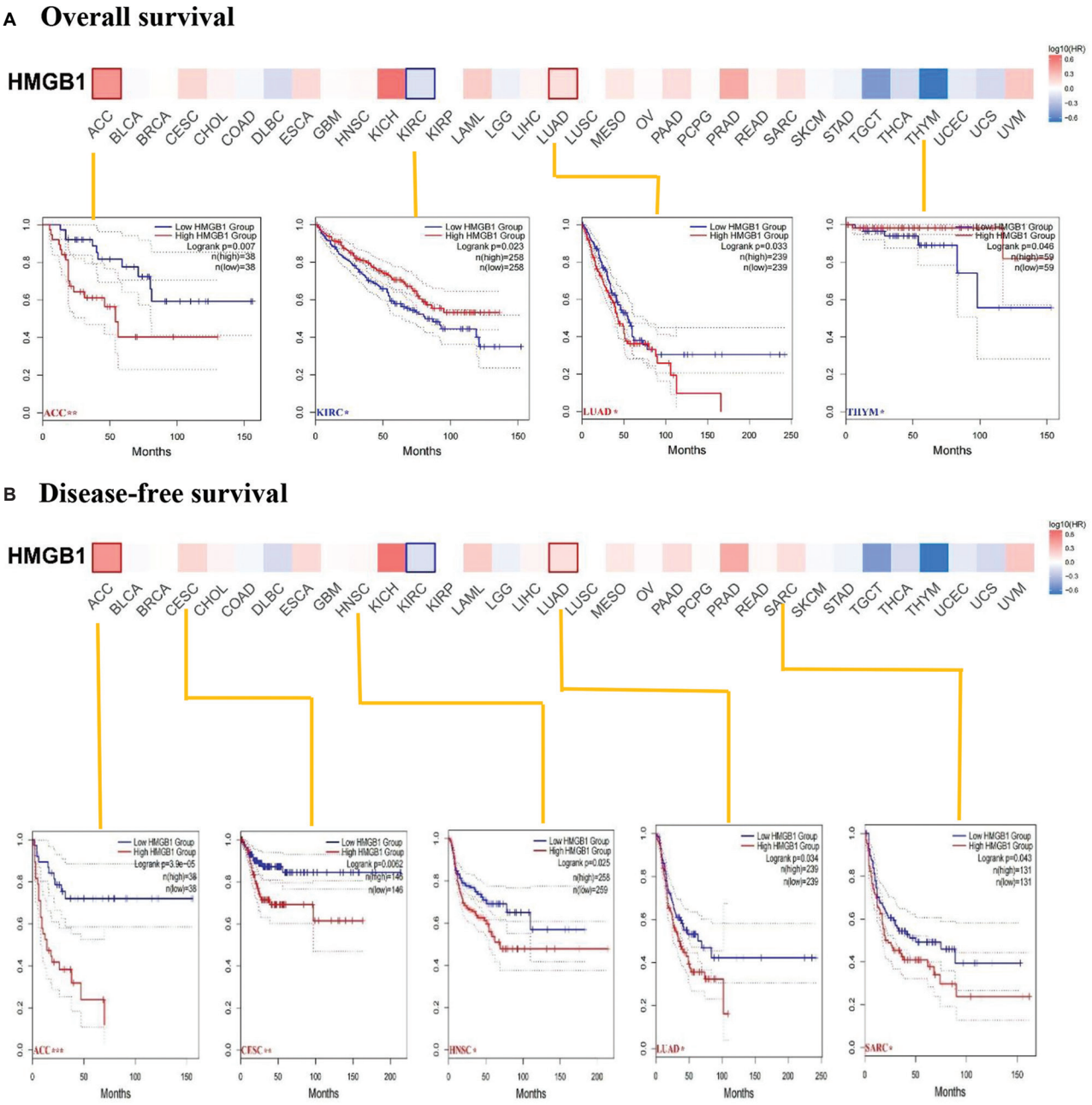

Figure 2. Correlation between the expression level of *HMGB1* and patient survival in TCGA tumors. GEPIA2 was used to evaluate the relationship between *HMGB1* gene expression and overall survival (A) and disease-free survival (B) in all TCGA tumors. Positive results of survival diagram and Kaplan–Meier curves are presented.
HMGB1: High mobility group box 1; TCGA: The Cancer Genome Atlas; GEPIA2: Gene Expression Profiling Interactive Analysis, version 2.

3.4. Protein phosphorylation analysis

Phosphorylation is one of the key processes for protein to exert biological effects, and phosphorylation state (e.g., phosphorylation and dephosphorylation) is known to be critical in the occurrence of tumor. Therefore, the differences of HMGB1 phosphorylation levels between normal tissues and primary tumor tissues were compared. CPTAC dataset was used to analyze three kinds of tumors (BRCA, lung cancer and UCEC) in details. As shown in Figure 4A, we observed that S35 phosphorylation level of HMGB1 in primary tumor tissues of BRCA, lung cancer and UCEC was significantly reduced. At the same time, we found that the S100 phosphorylation level of BRCA and lung cancer was low (Figure 4B–D).

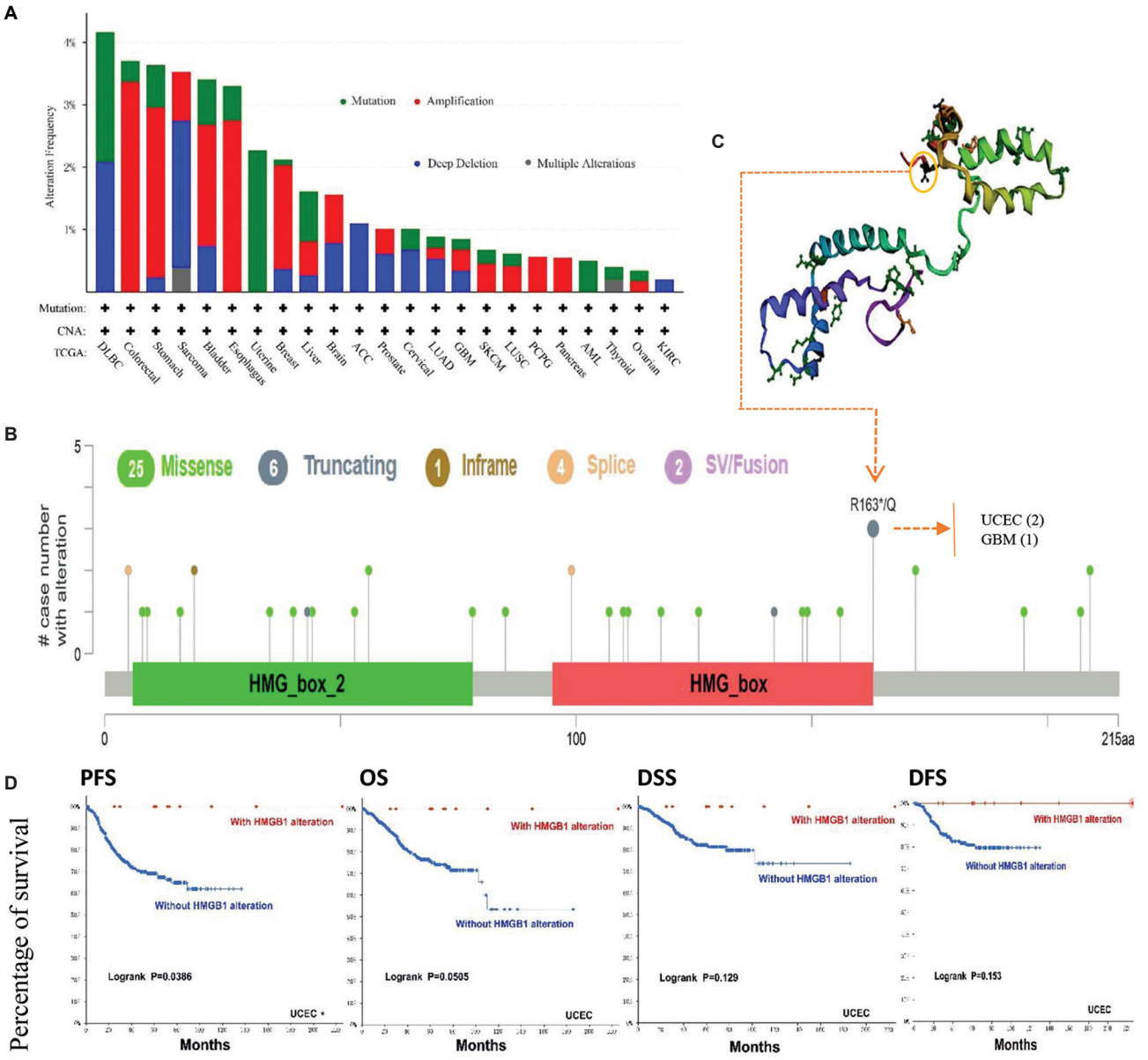

Figure 3. Mutation status of *HMGB1* in TCGA tumors. Mutation status of *HMGB1* in TCGA tumors was analyzed using the cBioPortal tool. The alteration frequency with mutation type (A) and mutation site (B) is displayed. (C) Mutation site (R163*/Q) within the HMG-box domain is shown in the 3D structure of *HMGB1*. (D) Analysis of the correlation between mutation status and PFS, OS, DSS, and DFS of UCEC using the cBioPortal tool.
HMGB1: High mobility group box 1; TCGA: The Cancer Genome Atlas; PFS: Progression-free survival, OS: Overall survival, DSS: Disease-specific survival; DFS: Disease-free survival; UCEC: Uterine corpus endometrial carcinoma.

3.5. Immune infiltration analysis

As a significant part of tumor microenvironment, tumor-infiltrating immune cells are closely related to the development, occurrence and metastasis of tumors[18-20]. Cancer-associated fibroblasts in tumor microenvironment matrix can take part in regulating the function of various tumor infiltrating immune cells[21-23]. In this study, EPIC, MCPCOUNTER, XCELL, and TIDE algorithms were used to seek the potential relationship between different infiltration levels of immune cells and *HMGB1* gene expression across different TCGA tumor types. After analysis, we found that *HMGB1* expression was positively related to the estimated infiltration value of cancer-associated fibroblasts of BRCA-LumA, HNSC-HPV$^-$, MESO, and testicular germ cell tumors (TGCT), but THYM was negatively correlated (Figure 5). The scatterplots of the above-mentioned tumors are shown in Figure 5.

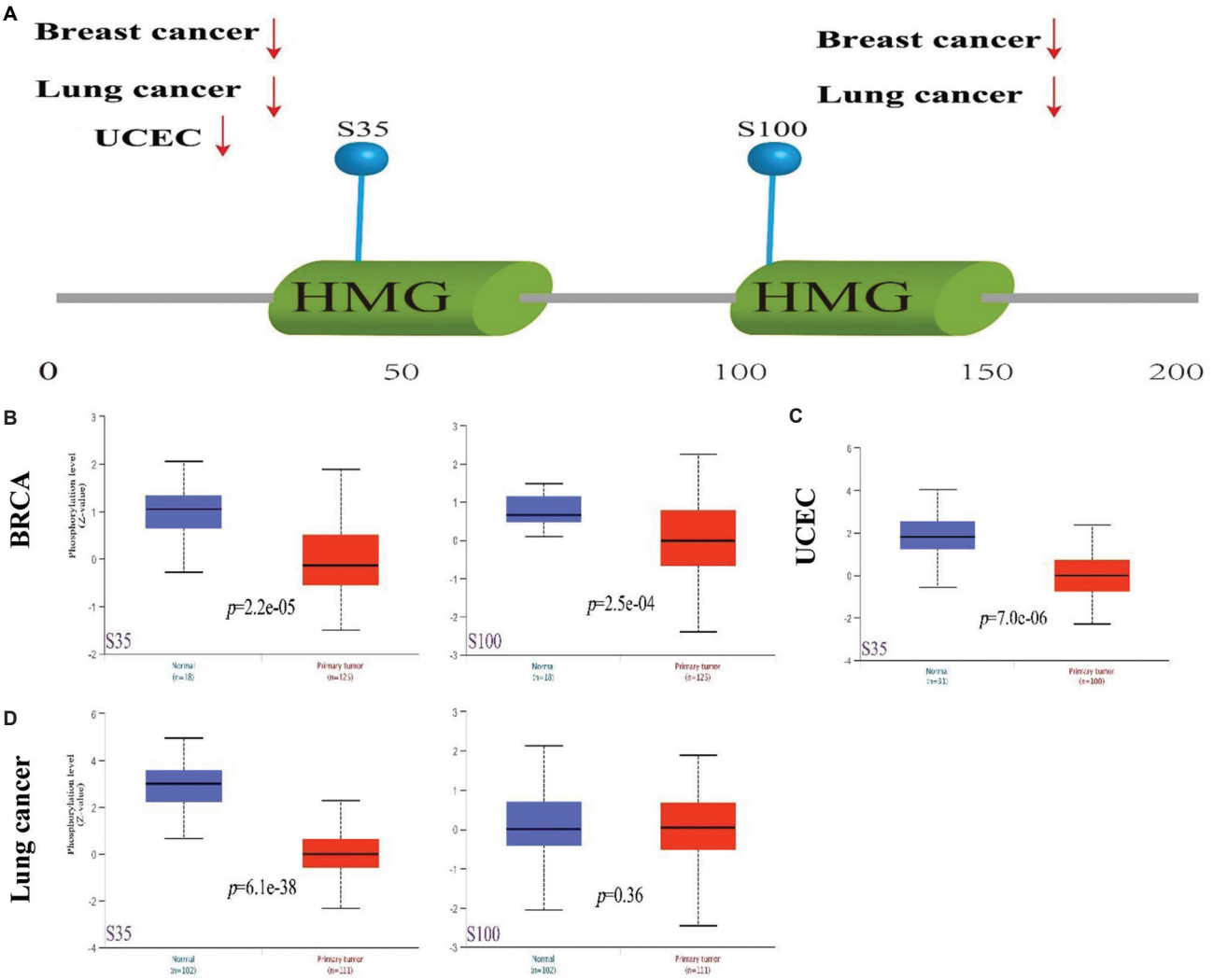

Figure 4. Tumor-associated protein phosphorylation of HMGB1. Comparison of HMGB1 phosphorylated protein levels (S35 and S100 sites) in normal and selected primary tumor tissues. (A) Phosphorylated protein sites detected in HMGB1 based on the CPTAC dataset are shown in the figure. (B–D) Box plots representation of HMGB1 phosphorylated protein levels in BRCA, UCEC and lung cancer.
HMGB1: High mobility group box 1; UCEC: Uterine corpus endometrial carcinoma; CPTAC: Clinical Proteomic Tumor Analysis Consortium; BRCA: Breast cancer.

3.6. HMGB1 enrichment analysis

To further research the molecular mechanism of *HMGB1* gene in the occurrence and development of tumor, the HMGB1-interacting proteins and *HMGB1* expression-related genes were screened by enrichment analyses. STRING was used to get a total of 50 HMGB1 interacting proteins which were verified in the experiments. The relationships of these proteins are displayed in Figure 6A. GEPIA2 was applied to combine all tumor expression data of TCGA to obtain the top 100 genes that are related to *HMGB1* expression. The expression level of *HMGB1* was positively related to that of heterogeneous nuclear ribonucleoproteins A2/B1 (*HNRNPA2B1*) (R = 0.68), heterogeneous nuclear ribonucleoprotein D0 (*HNRNPD*) (R=0.61), heterogeneous nuclear ribonucleoprotein R (*HNRNPR*) (R = 0.63), KH domain-containing, RNA-binding, signal transduction-associated protein 1 (*KHDRBS1*) (R = 0.61), replication factor C subunit 3 (*RFC3*) (R = 0.63), and structure-specific recognition protein 1 (*SSRP1*) (R = 0.55) genes (all $P < 0.001$, Figure 6B). The corresponding heatmap indicated that *HMGB1* was positively correlated with the above six genes in most cancer types (Figure 6C). The interaction analysis of the above groups displayed that there were four common members, namely, SSRP1, SRSF1, SUPT16H, and high mobility group box 2 (HMGB2) (Figure 6D).

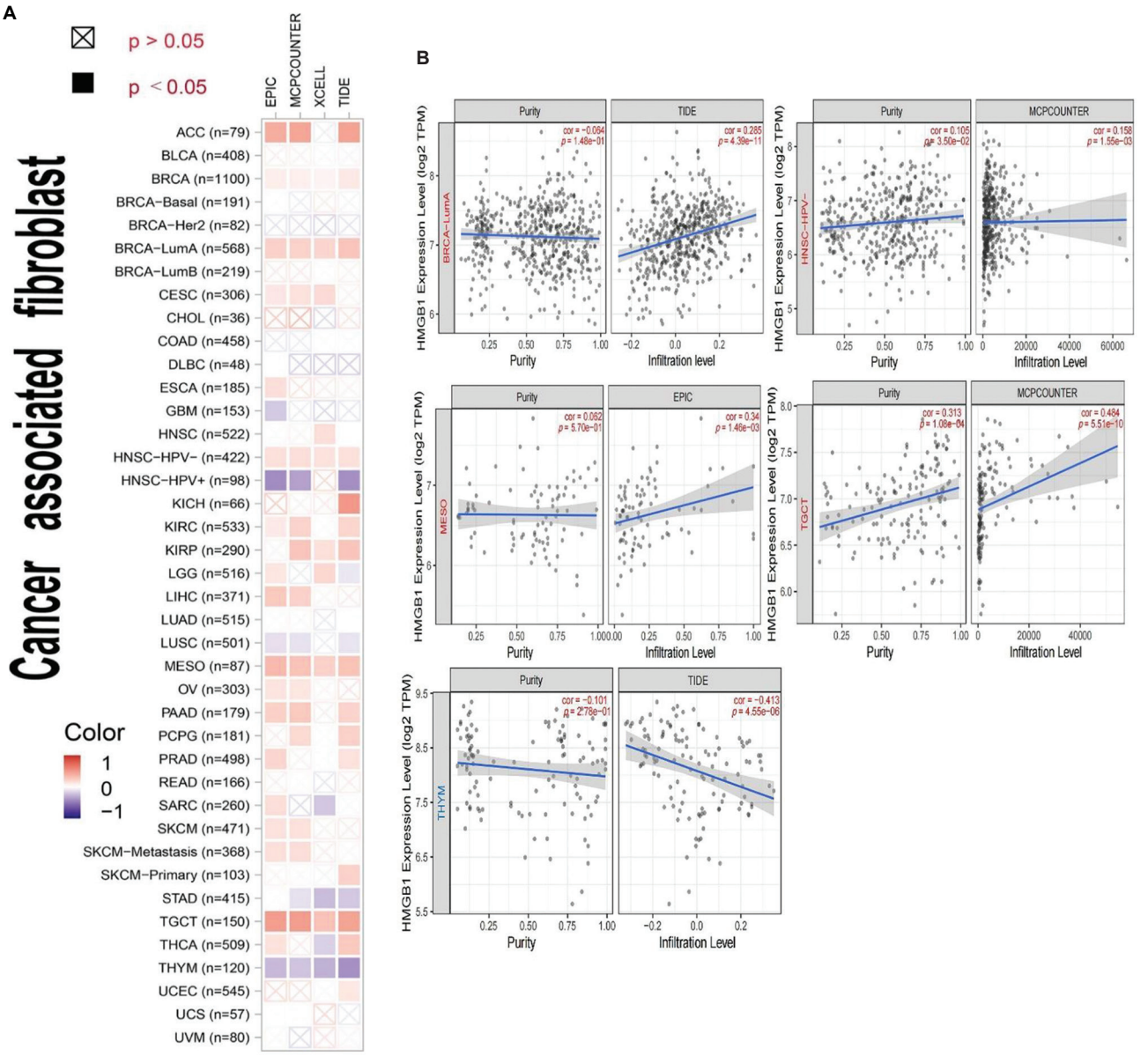

Figure 5. Correlation between *HMGB1* expression level and infiltration of cancer-associated fibroblasts. (A) EPIC, MCPCOUNTER, XCELL, and TIDE algorithms were applied to analyze the correlation between the level of cancer-associated infiltration of fibroblasts and the level of *HMGB1* gene expression in all TCGA tumors. Red color indicates a positive correlation (0–1), and blue color represents a negative correlation (−1–0). $P < 0.05$ is considered statistically significant. Values with no statistically significant correlation are marked with crosses. (B) The associated results of scatter plots of BRCA-LumA, HNSC-HPV-, MESO, TGCT, and THYM are listed.

HMGB1: High mobility group box 1; TCGA: The Cancer Genome Atlas; BRCA: Breast cancer; HNSC: Head and neck squamous cell carcinoma; MESO: Mesothelioma; TGCT: Testicular germ cell tumors; THYM: Thymoma.

KEGG and GO enrichment analyses were used to analyze the above two datasets which we combined. In Figure 6E, KEGG data revealed that "spliceosome" and viral carcinogenesis maybe involved in the influence of HMGB1 on the pathogenesis of tumors. GO enrichment analysis data showed that most of these genes are related to DNA state, such as catalytic activity acting on DNA, chromatin DNA binding, single-stranded DNA binding, telomeric DNA binding, and helicase activity (Figure 6F). A simple list of expression/mutation of HMGB1 among different tumor types and its function is shown in Table 2.

4. Discussion

Many studies have shown that HMGB1 has many biological functions across different cell types and

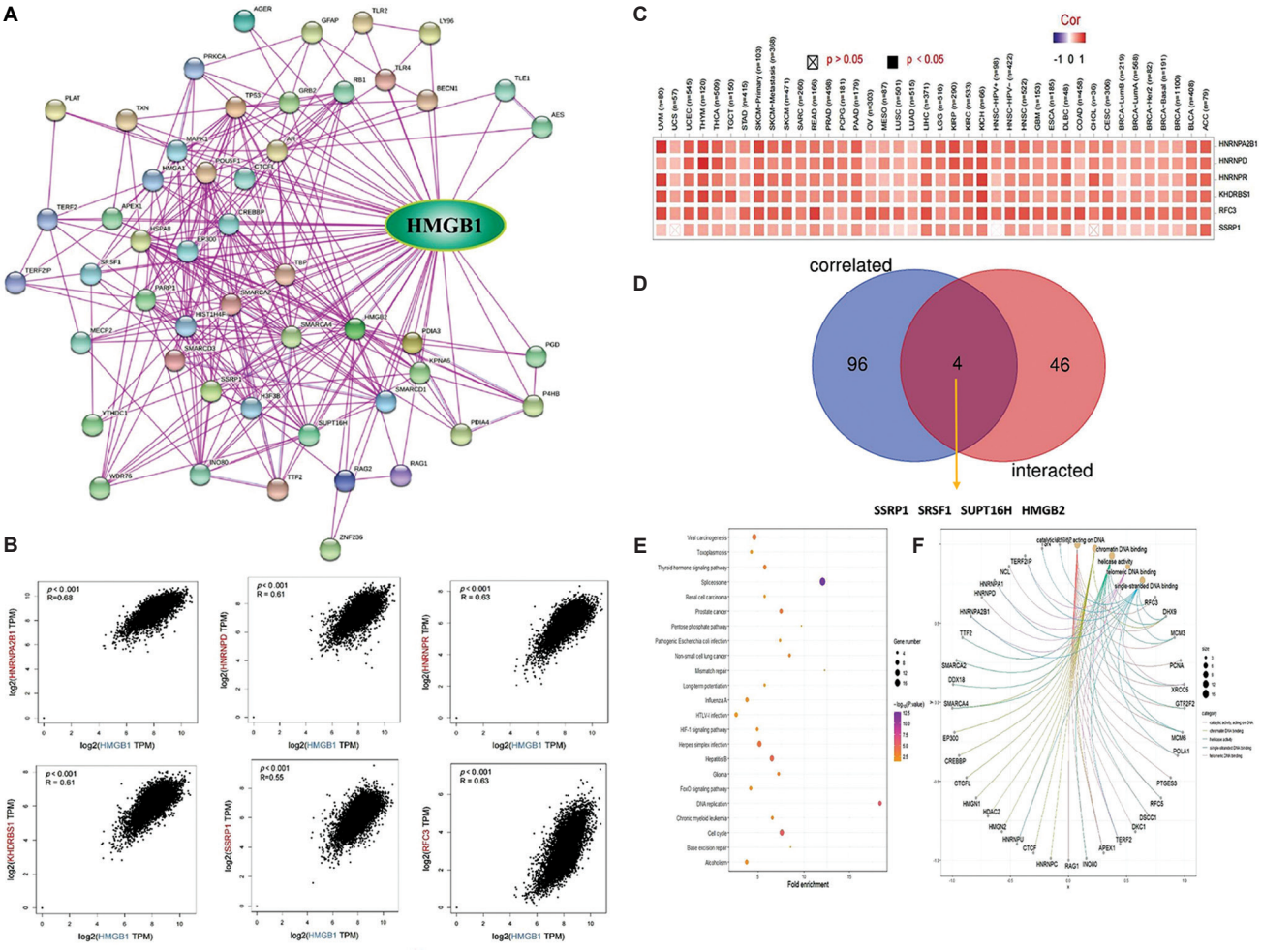

Figure 6. HMGB1 enrichment and pathway analysis. (A) STRING protein network diagram of experimentally determined HMGB1-binding proteins. Colored nodes represent the individual proteins identified. (B) GEPIA2 was used to determine the expression correlation between representative genes (*HNRNPA2B1*, *HNRNPD*, *HNRNPR*, *KHDRBS1*, *RFC3*, and *SSRP1*) of the top *HMGB1*-related genes and *HMGB1* in TCGA tumors. (C) The expression-related data between *HMGB1* and *HNRNPA2B1*, *HNRNPD*, *HNRNPR*, *KHDRBS1*, *RFC3,* and *SSRP1* in TCGA tumors are shown by heatmap. (D) The common members found by the interaction analysis of the HMGB1-binding and correlated genes. (E and F) KEGG and GO analyses based on the HMGB1-binding and interacted genes.

HMGB1: High mobility group box 1; TCGA: The Cancer Genome Atlas; GEPIA2: Gene Expression Profiling Interactive Analysis, version 2; KEGG: Kyoto Encyclopedia of Genes and Genomes; GO: Gene Ontology; *HNRNPA2B1*: Heterogeneous nuclear ribonucleoproteins A2/B1; *HNRNPD***:** Heterogeneous nuclear ribonucleoprotein D0; *HNRNPR*: Heterogeneous nuclear ribonucleoprotein R; *KHDRBS1*: KH domain-containing, RNA-binding, signal transduction-associated protein 1; *RFC3*: Replication factor C subunit 3; *SSRP1*: Structure-specific recognition protein 1.

plays a critical role in many diseases such as cancer and inflammatory diseases[24-27]. Studies have shown that HMGB1 is a highly conservative protein in different species, and its functions in the nucleus are very complex, including stabilizing nucleosome formation, promoting the DNA bending, and increasing DNA transcription, repair, replication, etc[28,29]. Although studies have reported the functions of HMGB1 in many physiological processes, whether HMGB1 is involved in the pathogenesis of different tumor types remains unclear. Therefore, we conducted a pan-cancer analysis of HMGB1. The methods include exploring HMGB1 gene expression in 33 different tumors based on TCGA data, collecting and integrating protein and phosphor-protein data, as well as gene mutations, and other molecular characteristics by making use of GEO and CPTAC databases.

From our results, the expression level of *HMGB1* in CHOL, ESCA, HNSC, LIHC, STAD, LUSC, COAD, READ, BLCA, and GBM tumor tissues is higher than that of control tissues, but low expression was observed in KICH, LUAD, and PRAD. These results are similar to those found in other studies on STAD, COAD, LIHC, and LUAD[30-33]. The differential expression of *HMGB1*

Table 2. Expression/mutation of HMGB1 among different tumor types and its function

Cancer types	Gene expression	Survival	Genetic variation	Protein phosphorylation	Immune infiltration
CHOL	↑				
COAD	↑				
ESCA	↑				
HNSC	↑	↑			↑
LIHC	↑				
LUSC	↑				
READ	↑				
STAD	↑				
BLCA	↑				
GBM	↑				
KIRC	--	↓			
THCA	--				
PCPG	--				
CESC	--	↑			
KICH	↓				
LUAD	↓	↑		↓	
PRAD	↓				
DLBC	↑				
LGG	↑				
PAAD	↑				
THYM	↑	↓			↓
OV	↑				
BRCA	↓			↓	↑
UCEC	↓		↓	↓	
ACC		↑			
SARC		↑			
MESO					↑
TGCT					↑

↑: Tumor-promoting effect; -- : Insignificant correlation; ↓: Tumor-suppressing effect.
CHOL: Cholangiocarcinoma; COAD: Colon adenocarcinoma; ESCA: Esophageal carcinoma; HNSC: Head and neck squamous cell carcinoma; LUSC: Lung squamous cell carcinoma; STAD: Stomach adenocarcinoma; LIHC: Liver hepatocellular carcinoma; READ: Rectum adenocarcinoma; BLCA: Bladder urothelial carcinoma; GBM: Glioblastoma multiforme; KIRC: Kidney renal clear cell carcinoma; CESC: Cervical squamous cell carcinoma and endocervical adenocarcinoma; THCA: Thyroid carcinoma; PCPG: Pheochromocytoma and paraganglioma; KICH: Kidney chromophobe; LUAD: Lung adenocarcinoma PRAD: Prostate adenocarcinoma; DLBC: Diffuse large B-cell lymphoma; LGG: Lower grade glioma PAAD: Pancreatic adenocarcinoma; THYM: Thymoma; OV: Ovarian cancer; BRCA: Breast cancer; ACC: Adrenocortical carcinoma; UCEC: Uterine corpus endometrial carcinoma; MESO: Mesothelioma; SARC: Sarcoma; TGCT: Testicular germ cell tumors

in different tumors may suggest different potential mechanisms and functions. We also found that high *HMGB1* expression may predict the poor OS for patients with ACC and LUAD. These results indicate that *HMGB1* can be used as a biomarker to predict the prognosis of tumor patients.

We discovered that the low expression of *HMGB1* was related to poor OS in some TCGA tumors, such as KIRC and THYM. This is similar to what other studies have found[34]. However, Huang *et al.* revealed that HMGB1 overexpression was significantly correlated with poor prognosis of patients with BLCA[35]. These findings may suggest that HMGB1 expression is not the same across various kinds of tumors. Based on the characteristics of each tumor, high or low expression of HMGB1 may provide a useful reference for the clinical treatment of tumor patients.

As for lung cancer, our research found that high expression of HMGB1 was correlated with poor OS ($P < 0.05$), and poor DFS ($P < 0.05$) in LUAD, but not in LUSC. In fact, many studies have shown that HMGB1 can promote the occurrence, proliferation, and metastasis of lung cancer[36,37], but the molecular mechanism and signaling pathway involving HMGB1 still need to be further clarified.

Compared with the corresponding control tissues, the total protein expression level of HMGB1 in BRCA tumor tissues was relatively lower. Studies have shown that HMGB1 has a close relationship with BRCA. The majority of the BRCA studies have reported that HMGB1 can promote the migration and invasion of BRCA[38,39]. MiR-142-3p can enhance the chemosensitivity of BRCA and inhibit autophagy by targeting *HMGB1*[40]. Our findings are contradictory to the literature reports. We consider that these may be linked to the dual role of HMGB1 in tumors. These results also indicate that HMGB1 may play a crucial role in the treatment of BRCA.

In addition to ACC and LUAD, our survival analysis data also indicated that the high expression of *HMGB1* in CESC, HNSC, and SARC was associated with poor DFS. Li *et al.* and Xu *et al.* suggested that HMGB1 expression was a predictor of shorter OS and DFS in patients with cervical cancer[41,42]. Liu *et al.* also indicated that HMGB1 was upregulated in human HNSC and overexpression of HMGB1 was significantly related to the malignant progression and poor survival rate of HNSC patients, suggesting that HMGB1 might be a potential therapeutic target of HNSC[43].

In this study, our results showed that *HMGB1* expression was positively correlated with the level of cancer-associated fibroblast immune infiltration in certain tumors, including BRCA-LumA, TGCT, HNSC-HPV$^-$, and MESO. Nevertheless, the relationship between *HMGB1* expression and THYM was reversed.

5. Conclusions

Our pan-cancer analysis of *HMGB1* demonstrates that the expression of *HMGB1* is associated with clinical prognosis, protein phosphorylation and immune cell infiltration in various human tumors. These findings are very helpful to decipher the role of HMGB1 in tumorigenesis and to further uncover the functions of HMGB1 in tumors.

Acknowledgments

None.

Funding

None.

Conflict of interest

The authors declare that they have no competing interests.

Author contributions

Conceptualization: Hongnu Yu, Lin Wang
Investigation: Wenqing Long, Jiaqi Li, Hao Shi, Lijun Zhang
Methodology: Wenqing Long, Jiaqi Li, Hao Shi, Lijun Zhang
Formal analysis: Wenqing Long
Writing – original draft: Wenqing Long
Writing – review & editing: Wenqing Long, Liqun Yang, Zhuoyan Jiang, Lei Xia, Lin Wang, Hongnu Yu

Ethics approval and consent to participate

Not applicable.

Consent for publication

Not applicable.

Availability of data

The datasets in this study are available in online repositories, TCGA datasets (https://www.cancer.gov/about-nci/organization/ccg/research/structural-genomics/tcga), GTEx datasets (https://www.genome.go-v/Funded-Programs-Projects/Genotype-Tissue-Expression-Project), and GEO databases (https://www.ncbi.nlm.nih.gov/geo/).

References

1. Blum A, Wang P, Zenklusen JC, 2018, SnapShot: TCGA-Analyzed tumors. *Cell*, 173(2): 530.

   https://doi.org/10.1016/j.cell.2018.03.059

2. Tomczak K, Czerwińska P,Wiznerowicz M, 2015, The cancer genome atlas (TCGA): An immeasurable source of knowledge. *Contemp Oncol* (*Pozn*), 19(1a): A68–A77.

   https://doi.org/10.5114/wo.2014.47136

3. Clough E, Barrett T, 2016, The gene expression omnibus database. *Methods Mol Biol*, 1418: 93–110.

   https://doi.org/10.1007/978-1-4939-3578-9_5

4. Ferrari S, Finelli P, Rocchi M, *et al.*, 1996, The active gene that encodes human high mobility group 1 protein (HMG1) contains introns and maps to chromosome 13. *Genomics*, 35(2): 367–371.

   https://doi.org/10.1006/geno.1996.0369

5. Goodwin GH, Sanders C, Johns EW, 1973, A new group of chromatin-associated proteins with a high content of acidic and basic amino acids. *Eur J Biochem*, 38(1): 14–19.

   https://doi.org/10.1111/j.1432-1033.1973.tb03026.x

6. Li J, Kokkola R, Tabibzadeh S, *et al.*, 2003, Structural basis for the proinflammatory cytokine activity of high mobility

group box 1. *Mol Med*, 9(1–2): 37–45.

7. Kang R, Zhang Q, Zeh HJ 3rd, *et al*., 2013, HMGB1 in cancer: Good, bad, or both? *Clin Cancer Res*, 19(15): 4046–4057.
https://doi.org/10.1158/1078-0432.Ccr-13-0495

8. Huebener P, Gwak GY, Pradere JP, *et al*., 2014, High-mobility group box 1 is dispensable for autophagy, mitochondrial quality control, and organ function *in vivo*. *Cell Metab*, 19(3): 539–547.
https://doi.org/10.1016/j.cmet.2014.01.014

9. Vargas TR, Apetoh L, 2017, Danger signals: Chemotherapy enhancers? *Immunol Rev*, 280(1): 175–193.
https://doi.org/10.1111/imr.12581

10. Gao Q, Wang S, Chen X, *et al*., 2019, Cancer-cell-secreted CXCL11 promoted CD8(+) T cells infiltration through docetaxel-induced-release of HMGB1 in NSCLC. *J Immunother Cancer*, 7(1): 42.
https://doi.org/10.1186/s40425-019-0511-6

11. Tang Z, Kang B, Li C, *et al*., 2019, GEPIA2: An enhanced web server for large-scale expression profiling and interactive analysis. *Nucleic Acids Res*, 47(W1): W556–W560.
https://doi.org/10.1093/nar/gkz430

12. Chen F, Chandrashekar DS, Varambally S, *et al*., 2019, Pan-cancer molecular subtypes revealed by mass-spectrometry-based proteomic characterization of more than 500 human cancers. *Nat Commun*, 10(1): 5679.
https://doi.org/10.1038/s41467-019-13528-0

13. Gao J, Aksoy BA, Dogrusoz U, *et al*., 2013, Integrative analysis of complex cancer genomics and clinical profiles using the cBioPortal. *Sci Signal*, 6(269): pl1.
https://doi.org/10.1126/scisignal.2004088

14. Jiao XD, Qin BD, You P, *et al*., 2018, The prognostic value of TP53 and its correlation with EGFR mutation in advanced non-small cell lung cancer, an analysis based on cBioPortal data base. *Lung Cancer*, 123: 70–75.
https://doi.org/10.1016/j.lungcan.2018.07.003

15. Cerami E, Gao J, Dogrusoz U, *et al*., 2012, The cBio cancer genomics portal: An open platform for exploring multidimensional cancer genomics data. *Cancer Discov*, 2(5): 401–404.
https://doi.org/10.1158/2159-8290.Cd-12-0095

16. Bardou P, Mariette J, Escudié F, *et al*., 2014, jvenn: An interactive Venn diagram viewer. *BMC Bioinformatics*, 15(1): 293.
https://doi.org/10.1186/1471-2105-15-293

17. Cui X, Zhang X, Liu M, *et al*., 2020, A pan-cancer analysis of the oncogenic role of staphylococcal nuclease domain-containing protein 1 (SND1) in human tumors. *Genomics*, 112(6): 3958–3967.
https://doi.org/10.1016/j.ygeno.2020.06.044

18. Fridman WH, Galon J, Dieu-Nosjean MC, *et al*., 2011, Immune infiltration in human cancer: Prognostic significance and disease control. *Curr Top Microbiol Immunol*, 344: 1–24.
https://doi.org/10.1007/82_2010_46

19. Steven A, Seliger B, 2018, The role of immune escape and immune cell infiltration in breast cancer. *Breast Care* (*Basel*), 13(1): 16–21.
https://doi.org/10.1159/000486585

20. Domingues P, González-Tablas M, Otero Á, *et al*., 2016, Tumor infiltrating immune cells in gliomas and meningiomas. *Brain Behav Immun*, 53: 1–15.
https://doi.org/10.1016/j.bbi.2015.07.019

21. Chen X, Song E, 2019, Turning foes to friends: Targeting cancer-associated fibroblasts. *Nat Rev Drug Discov*, 18(2): 99–115.
https://doi.org/10.1038/s41573-018-0004-1

22. Kwa MQ, Herum KM, Brakebusch C, 2019, Cancer-associated fibroblasts: How do they contribute to metastasis? *Clin Exp Metastasis*, 36(2): 71–86.
https://doi.org/10.1007/s10585-019-09959-0

23. Biffi G, Tuveson DA, 2021, Diversity and biology of cancer-associated fibroblasts. *Physiol Rev*, 101(1): 147–176.
https://doi.org/10.1152/physrev.00048.2019

24. Kumari T, Kumar B, 2018, High-mobility group box 1 protein (HMGB1) gene polymorphisms and cancer susceptibility: A comprehensive meta-analysis. *Clin Chim Acta*, 483: 170–182.
https://doi.org/10.1016/j.cca.2018.04.042

25. Tang D, Kang R, Zeh HJ 3rd, *et al*., 2010, High-mobility group box 1 and cancer. *Biochim Biophys Acta*, 1799(1–2): 131–140.
https://doi.org/10.1016/j.bbagrm.2009.11.014

26. Sims GP, Rowe DC, Rietdijk ST, *et al*., 2010, HMGB1 and RAGE in inflammation and cancer. *Annu Rev Immunol*, 28: 367–388.
https://doi.org/10.1146/annurev.immunol.021908.132603

27. Andersson U, Tracey KJ, 2011, HMGB1 is a therapeutic target for sterile inflammation and infection. *Annu Rev Immunol*, 29: 139–162.
https://doi.org/10.1146/annurev-immunol-030409-101323

28. Stros M, 2010, HMGB proteins: Interactions with DNA and chromatin. *Biochim Biophys Acta*, 1799(1–2): 101–113.
https://doi.org/10.1016/j.bbagrm.2009.09.008

29. Lange SS, Vasquez KM, 2009, HMGB1: The jack-of-all-trades protein is a master DNA repair mechanic. *Mol Carcinog*, 48(7): 571–580.
https://doi.org/10.1002/mc.20544

30. Zhang QY, Wu LQ, Zhang T, *et al*., 2015, Autophagy-mediated HMGB1 release promotes gastric cancer cell survival via RAGE activation of extracellular signal-regulated kinases 1/2. *Oncol Rep*, 33(4): 1630–1638.

https://doi.org/10.3892/or.2015.3782

31. Zhang W, An F, Xia M, *et al*., 2019, Increased HMGB1 expression correlates with higher expression of c-IAP2 and pERK in colorectal cancer. *Medicine* (*Baltimore*), 98(3): e14069.

https://doi.org/10.1097/md.0000000000014069

32. Ye L, Zhang Q, Cheng Y, *et al*., 2018, Tumor-derived exosomal HMGB1 fosters hepatocellular carcinoma immune evasion by promoting TIM-1(+) regulatory B cell expansion. *J Immunother Cancer*, 6(1): 145.

https://doi.org/10.1186/s40425-018-0451-6

33. Zuo Z, Che X, Wang Y, *et al*., 2014, High mobility group Box-1 inhibits cancer cell motility and metastasis by suppressing activation of transcription factor CREB and nWASP expression. *Oncotarget*, 5(17): 7458–7470.

https://doi.org/10.18632/oncotarget.2150

34. Hou X, Lin S, Liu Y, *et al*., 2022, Analysis of the tumor microenvironment and mutation burden identifies prognostic features in thymic epithelial tumors. *Am J Cancer Res*, 12(5): 2387–2396.

35. Huang C, Huang Z, Zhao X, *et al*., 2018, Overexpression of high mobility group box 1 contributes to progressive clinicopathological features and poor prognosis of human bladder urothelial carcinoma. *Onco Targets Ther*, 11: 2111–2120.

https://doi.org/10.2147/ott.S155745

36. Wang XH, Zhang SY, Shi M, *et al*., 2020, HMGB1 promotes the proliferation and metastasis of lung cancer by activating the Wnt/β-catenin pathway. *Technol Cancer Res Treat*, 19: 1533033820948054.

https://doi.org/10.1177/1533033820948054

37. Ren Y, Cao L, Wang L, *et al*., 2021, Autophagic secretion of HMGB1 from cancer-associated fibroblasts promotes metastatic potential of non-small cell lung cancer cells via NFκB signaling. *Cell Death Dis*, 12(10): 858.

https://doi.org/10.1038/s41419-021-04150-4

38. Jiao D, Zhang J, Chen P, *et al*., 2021, HN1L promotes migration and invasion of breast cancer by up-regulating the expression of HMGB1. *J Cell Mol Med*, 25(1): 397–410.

https://doi.org/10.1111/jcmm.16090

39. He H, Wang X, Chen J, *et al*., 2019, High-mobility group box 1 (HMGB1) promotes angiogenesis and tumor migration by regulating hypoxia-inducible factor 1 (HIF-1α) expression via the phosphatidylinositol 3-Kinase (PI3K)/AKT signaling pathway in breast cancer cells. *Med Sci Monit*, 25: 2352–2360.

https://doi.org/10.12659/msm.915690

40. Liang L, Fu J, Wang S, *et al*., 2020, MiR-142-3p enhances chemosensitivity of breast cancer cells and inhibits autophagy by targeting HMGB1. *Acta Pharm Sin B*, 10(6): 1036–1046.

https://doi.org/10.1016/j.apsb.2019.11.009

41. Li P, Xu M, Cai H, *et al*., 2019, The effect of HMGB1 on the clinicopathological and prognostic features of cervical cancer. *Biosci Rep*, 39(5): BSR20181016.

https://doi.org/10.1042/bsr20181016

42. Xu Y, Chen Z, Zhang G, *et al*., 2015, HMGB1 overexpression correlates with poor prognosis in early-stage squamous cervical cancer. *Tumour Biol*, 36(11): 9039–9047.

https://doi.org/10.1007/s13277-015-3624-7

43. Liu Y, Xie C, Zhang X, *et al*., 2010, Elevated expression of HMGB1 in squamous-cell carcinoma of the head and neck and its clinical significance. *Eur J Cancer*, 46(16): 3007–3015.

https://doi.org/10.1016/j.ejca.2010.07.016

ACCSCIENCE PUBLISHING

Gene & Protein in Disease

ORIGINAL RESEARCH ARTICLE

Underexpression of SCN7A is associated with poor prognosis in lung adenocarcinoma

Hehui Lv[1,2†], Hongyuan Song[1,2†], Zhouping Qin[1,2†], Rongchun Xing[1,2], and Yulian Chen[1,2*]

[1]First Hospital of Yichang, Hubei, China

[2]People's Hospital of China Three Gorges University, Hubei, China

Abstract

Lung cancer is one of the most common malignancies and the leading cause of cancer-related deaths worldwide. Elucidating the mechanism behind the development of lung cancer at a molecular level could reveal new biomarkers and clinical therapeutic targets. A growing body of evidence has shown an association between ion channel-related genes and the progression of various diseases, including cancer. However, the association is not well-understood. In this study, we identified ion channel-related genes differentially expressed between cancer and normal lung tissue cells. Data were extracted from GSE31552, GSE33532, and GSE103512 lung adenocarcinoma (LUAD) datasets, and the prognostic value of the differentially expressed genes between LUAD and normal lung tissue was evaluated using data in The Cancer Genome Atlas. Only sodium voltage-gated channel alpha subunit 7 (SCN7A) was found to be significantly correlated to prognosis. The expression of SCN7A in LUAD was assessed further by immunological analysis. We also constructed a competing endogenous RNA network of *SCN7A*. Further analyses revealed that the underexpression of SCN7A predicted a poor prognosis in LUAD, with a strong correlation between SCN7A expression and immune cell infiltration as well as immune checkpoint expression. We found that SCN7A is potentially regulated via the OTUD6B-AS1-miR-21-5p-SCN7A axis in LUAD cells and proved that SCN7A inhibits the proliferation and migration of lung cancer cells *in vitro*. Taken together, SCN7A, as an independent prognostic factor, is a promising diagnostic biomarker for LUAD, and the OTUD6B-AS1-miR-21-5p-SCN7A axis is a potential regulatory network of SCN7A expression.

Keywords: Lung adenocarcinoma; Gene Expression Omnibus; The Cancer Genome Atlas; Immune infiltration; Competing endogenous RNA; Prognosis

†These authors have contributed equally to this work.

***Corresponding author:**
Yulian Chen
(chenyulian213586@163.com)

Citation: Lv H, Song H, Qin Z, *et al*., 2023, Underexpression of SCN7A is associated with poor prognosis in lung adenocarcinoma. *Gene Protein Dis*. 2(1):363.
https://doi.org/10.36922/gpd.363

Received: February 8, 2023
Accepted: March 16, 2023
Published Online: March 27, 2023

1. Introduction

Lung cancer is the leading cause of cancer-related mortality worldwide, accounting for nearly 2 million reported cases and 1.76 million deaths in 2020[1]. Non-small cell lung cancer accounts for 80% of all lung malignancies, and the overall 5-year survival rate of lung adenocarcinoma (LUAD) is 5%[2,3]. Despite the numerous treatments available, the prognosis of LUAD remains unsatisfactory. Due to the fact that early-stage lung cancer is usually asymptomatic, the majority of patients with lung cancer are diagnosed at a more

advanced stage[4]. Therefore, we need to understand the molecular mechanism of how lung cancer develops and progresses to identify accurate markers for early diagnosis and novel markers for treating the disease.

Ion channels are involved in many important biological processes (BPs). The association between ion channels and cancer development has been reported in many studies[5,6]. LUAD cells display specific changes in the expression of ion channel-related genes. Since novel diagnostic markers are urgently needed, these genes are promising clinical biomarkers for LUAD diagnosis and prognosis prediction. In addition, the therapeutic potential of ion channel-related genes for solid epithelial tumors and breast cancer have been reported[7-9]. However, we have not identified any ion channel-related gene that could be targeted for LUAD treatment.

In this study, differentially expressed genes (DEGs) related to ion channel between LUAD and normal tissues were identified from LUAD datasets (GSE31552, GSE33532, and GSE103512) in the Gene Expression Omnibus (GEO) database[10-12]. SCN7A was identified to be significantly correlated to prognosis. The expression profile, mutational landscape, immunological role, and prognostic value of SCN7A for LUAD were all analyzed. A competing endogenous RNA (ceRNA) network for SCN7A was also constructed. We found that SCN7A influences the survival of LUAD patients, suggesting that SCN7A may be a protective factor in LUAD and can be utilized to develop new therapeutic approaches.

2. Materials and methods

2.1. Data source and analysis

The GEO database (https://www.ncbi.nlm.nih.gov/geo/) was used to download GSE31552, GSE33532, and GSE103512 datasets for the expression of LUAD genes[13], which were then normalized using the quantiles function. DEGs were identified by "limma" R package based on $P < 0.05$ and $|\log FC| > 1$. The "ggplot2" R package was used to construct a volcano plot and heatmap. The genes related to ion channels were identified from the Kyoto Encyclopedia of Genes and Genomes (KEGG) database (hsa04040), and The Cancer Genome Atlas (TCGA) database (https://tcga-data.nci.nih.gov/tcga/) was used for downloading the TCGA pan-cancer RNA-seq data.

2.2. Gene ontology and Kyoto Encyclopedia of Genes and Genomes enrichment analyses

The Metascape platform integrates gene annotation, enrichment analysis, and interactome analysis by leveraging 40 independent gene expression databases[14]. The BP, cellular component (CC), molecular function (MF), and DEGs-regulated pathways were identified from the Metascape database.

2.3. Expression and prognostic analysis

Wilcox test was performed to analyze the prognostic value of SCN7A for LUAD. Based on the plotted Kaplan-Meier (KM) survival curves, "survival" and "survminer" packages in the R software were used to conduct the survival analysis. The evaluation of the relationship between SCN7A expression and LUAD prognosis was by univariate Cox regression besides utilizing a forest plot to display it graphically.

2.4. Genes related to overall survival in lung adenocarcinoma

The genes significantly related to overall survival (OS) in LUAD were identified by univariate and multivariate analyses. Apart from SCN7A, the other parameters analyzed for inclusion in a predictive nomogram included calcium voltage-gated channel auxiliary subunit alpha2delta 2 (CACNA2D2) and glutamate ionotropic receptor AMPA type subunit 1 (GRIA1), age, gender, and pathological tumor-node-metastasis (pTNM) stage. A forest plot was used to display the effect estimates of the aforementioned parameters on LUAD prognosis.

2.5. Messenger RNA transcription and protein level expression analysis

A Sankey diagram was constructed to visually demonstrate the influence of age, gender, pTNM stage, and *SCN7A* mRNA expression on LUAD prognosis. A map of protein expression in 32 human tissues was taken from the Human Protein Atlas (HPA) database (http://www.proteinatlas.org/)[15]. SCN7A protein expression levels between lung cancer and normal tissues were analyzed in the HPA database. SCN7A expression in lung cancer tissues (167201_B_1_1, 167201_B_1_2, and 167201_B_1_3) and normal tissues (167203_A_1_4, 167203_A_2_4, and 167203_A_3_4) was analyzed.

2.6. Mutations in lung adenocarcinoma tissue cells

cBioPortal (https://www.cbioportal.org/) contains five published datasets and 15 provisional TCGA datasets and provides data for mutational analysis[16,17].

2.7. Immunological analysis

The correlation between immune score and LUAD prognosis was analyzed. TIMER2.0 (http://timer.cistrome.org/) contains data on immune cell infiltration to cancer tissues[18]. The impact of somatic copy number alteration (sCNA) of *SCN7A* on immune infiltration was analyzed using TIMER2.0 data.

2.8. Upstream non-coding RNA analysis

miRGator v3.0 (http://mirgator.kobic.re.kr/miRTargetNExpression.html) was used to predict microRNAs (miRNAs) targeting and binding *SCN7A*[19]. starBase (http://starBase.sysu.edu.cn/), a widely used database for ncRNA-related analysis[20], was used to predict long non-coding RNAs (lncRNAs) binding *SCN7A* and related LUAD prognosis.

2.9. Pathway correlation analysis

The "GSVA" R package was used for pathway correlation assessment, and ssgsea was selected as a parameter in gene set variation analysis (GSVA). Spearman's correlation was performed to evaluate the association between the selected gene expression and LUAD prognosis.

2.10. Quantitative polymerase chain reaction (qPCR)

Total RNA was extracted using Trizol. SynScript® III RT SuperMix for qPCR (Tsingke, TSK314S) was used for reverse transcription. 2×TSINGKE® Master SYBR Green I qPCR Mix-UDG (Tsingke, TSE204) was used for qPCR. The primers used were as follows: GAPDHF, CTGGGCTACACTGAGCACC; GAPDHR, AAGTGGTCGTTGAGGGCAATG; SCN7AF, GCTTCGTAGCAAGTCCTCCA; SCN7AR, GGGTCCACATCTTCCAAGGG.

2.11. Cell counting Kit 8 (CCK8) assay and wound healing assay

After the cell confluency reached 90% in a 6-well plate, it was changed to 2 mL serum-free medium for overnight culture to deplete the residual serum, and scratches were made the following morning. A549 cell was scrapped in a straight line at 0 h, and images at 0 h, and 48 h were acquired for analysis. CCK8 assay was performed using CCK8 (YZ-CK04) at day 1, day 2, day 3, and day 4, measuring the absorbance value at 450 nm.

2.12. Statistical analysis

Rstudio software (R 4.0.3) was used for data analysis. $P < 0.05$ or log-rank $P < 0.05$ was considered statistically significant.

3. Results

3.1. Differentially expressed genes between lung adenocarcinoma and normal tissues

GSE31552, GSE33532, and GSE103512 contained data for 35, 40, and 27 LUAD tissues and 39, 10, and 7 normal tissues, respectively. We identified 267 DEGs between LUAD and normal tissues across the three datasets, of which there were 67 overexpressed and 200 suppressed genes (Figure 1A and B). Relying on Metascape data, GO and KEGG enrichment analyses of the DEGs were performed. In GO enrichment analysis, the main processes were the extracellular matrix, circulatory system process, and response to glucocorticoid (Figure 1C), whereas the main pathways in KEGG enrichment analysis were complement and coagulation cascades and extracellular matrix (ECM)-receptor interaction (Figure 1D).

3.2. Prognostic value of key differentially expressed genes

Ion channel-related DEGs, including *GRIA1*, chloride intracellular channel 5 (*CLIC5*), potassium sodium-activated channel subfamily T member 2 (*KCNT2*), *SCN7A*, and *CACNA2D2*, were identified (Figure 2A). The expression of these five candidate genes in LUAD was validated using the data in TCGA. The findings revealed that *CLIC5* was overexpressed in tumors but underexpressed in adjacent normal tissues, whereas *GRIA1*, *KCNT2*, *SCN7A*, and *CACNA2D2* were underexpressed in tumor tissues but overexpressed in normal tissues (Figure 2B). Further analyses revealed that the overexpression of *GRIA1*, *SCN7A*, and *CACNA2D2* was associated with favorable prognosis (Figure 2C–E), whereas the expression of *CLIC5* and *KCNT2* had no significant effect on LUAD prognosis.

3.3. *SCN7A* as an independent factor for LUAD prognosis

Univariate Cox regression analysis confirmed that *CACNA2D2* (HR = 0.86896, $P = 0.00028$), *GRIA1* (HR = 0.6111, $P = 0.00063$), and *SCN7A* (HR = 0.83379, $P = 0.00409$) had significant associations with the OS of LUAD patients (Figure 3A). Further multivariate regression analysis revealed *SCN7A* (HR = 0.82429, $P = 0.03508$) to be the only independent predictor of LUAD prognosis (Figure 3B). At the same time, we extracted variables with significant differences to construct a nomogram prognostic model to predict the 1-year, 3-year, and 5-year overall survival of LUAD patients (Figure 3C,D). Sankey diagram also showed that the overexpression of *SCN7A* in LUAD was associated with better LUAD prognosis (Figure 4A). These results showed that *SCN7A* is a protective factor for LUAD prognosis.

3.4. Messenger RNA transcription and expression of SCN7A protein in lung adenocarcinoma tissues

TCGA data analysis indicated that *SCN7A* mRNA transcription and the expression of corresponding proteins differed between gender and among different age groups. Interestingly, there was a smaller proportion of patients with high SCN7A expression in stages III and IV than in Stages I and II. Furthermore, compared with the low-expression group, the high-expression group had a lower

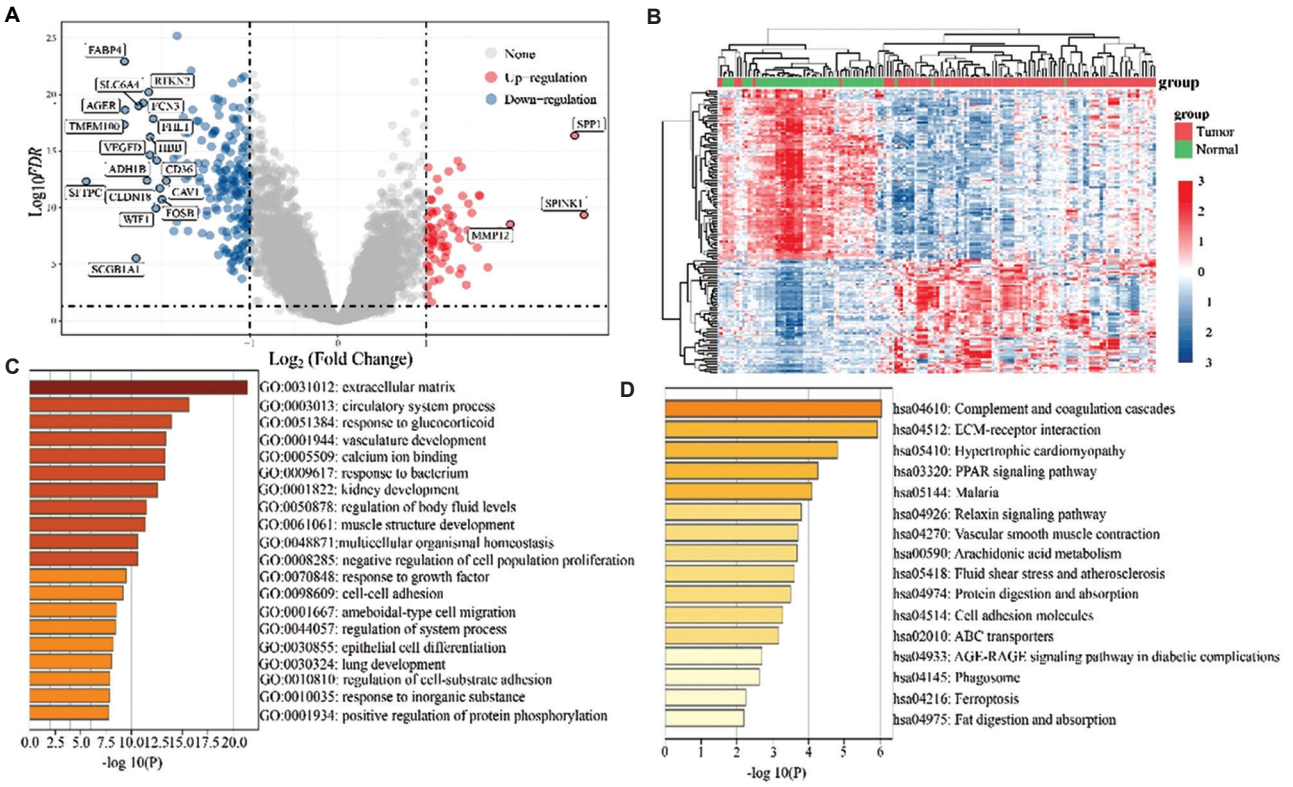

Figure 1. Identification of differentially expressed genes (DEGs) between lung adenocarcinoma and normal tissues from GEO datasets. (A–B) Volcano plot and heatmap of 267 DEGs. (C) Gene ontology enrichment analysis results inclusive of MF, BP, and CC. (D) Kyoto Encyclopedia of Genes and Genomes pathway enrichment analysis results.

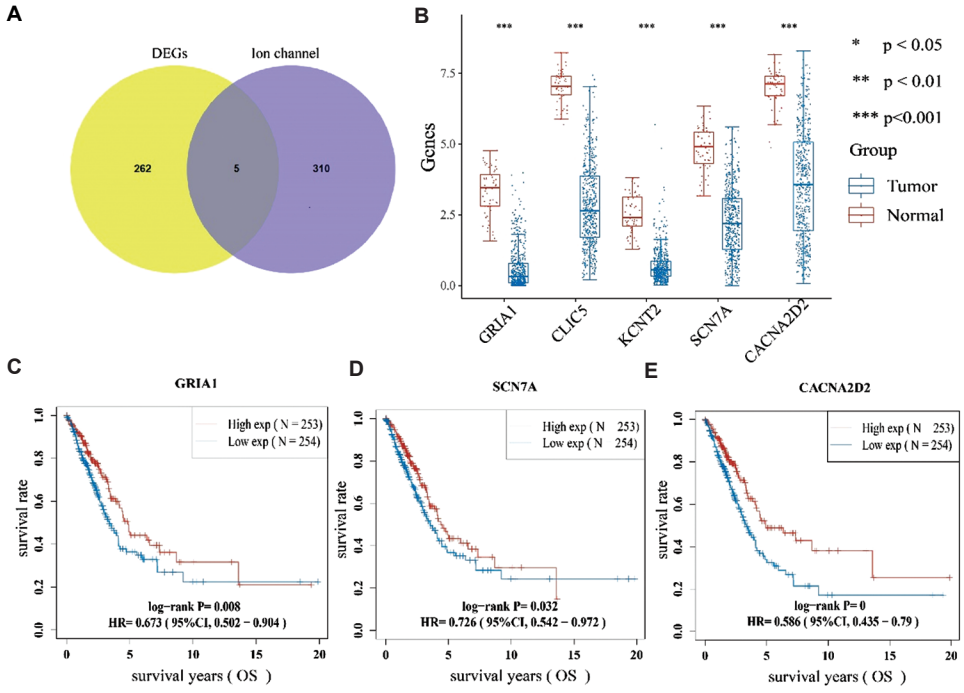

Figure 2. Expression and prognostic analysis of candidate genes. (A) Venn diagram showing five differentially expressed gene (DEGs) overlapping with ion channel-related genes (B) Expression analysis of five candidate genes using the lung adenocarcinoma (LUAD) data in The Cancer Genome Atlas (TCGA): *GRIA1* (*P* = 7.98e-34), *CLIC5* (*P* = 1.88e-35), *KCNT2* (*P* = 1.24e-32), *SCN7A* (*P* = 8.10e-31), and *CACNA2D2* (*P* = 2.03e-29). (C–E) Prognostic value of *GRIA1*, *SCN7A*, and *CACNA2D2* for LUAD using the LUAD data in TCGA.

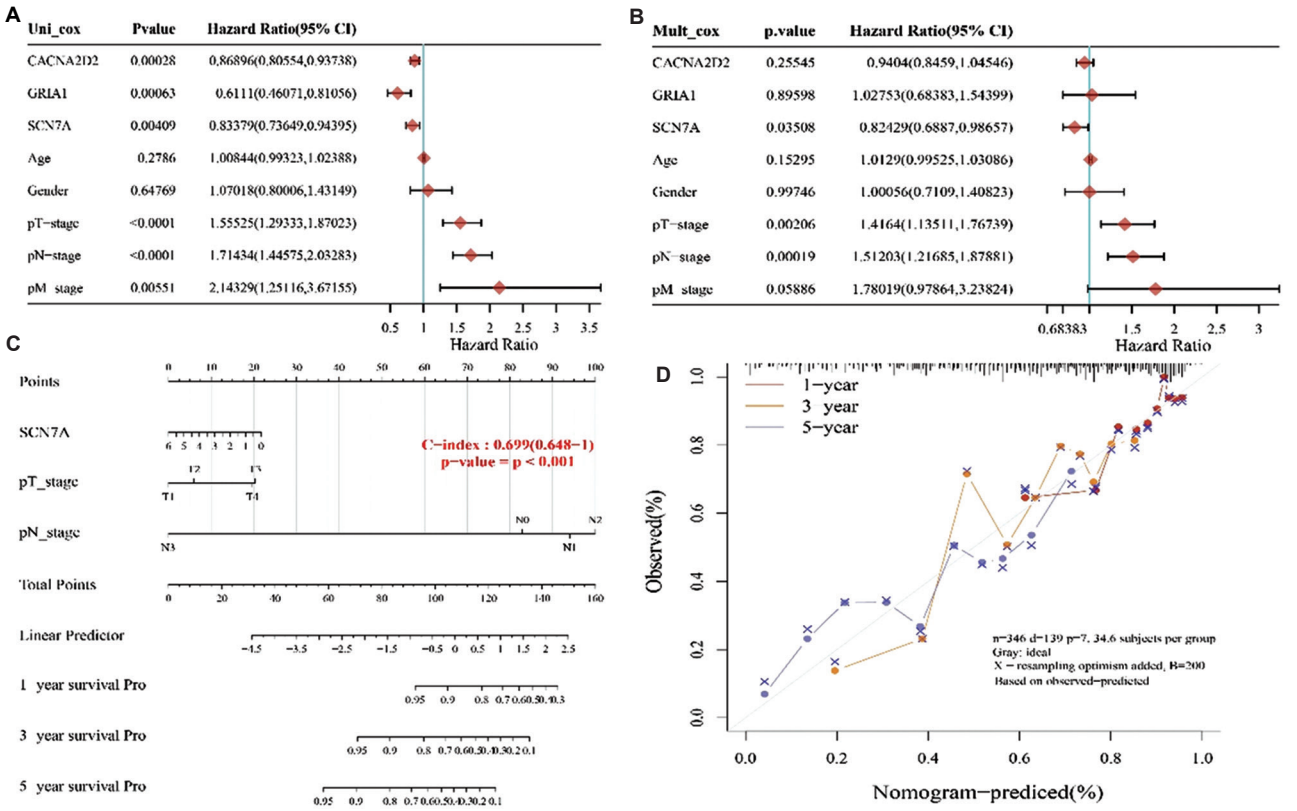

Figure 3. Predictive nomogram showing the prognosis prediction potential of *GRIA1*, *SCN7A*, and *CACNA2D2* for lung adenocarcinoma (LUAD). (A and B) Univariate and multivariate regression analyses of the relationship between *GRIA1*, *SCN7A*, and *CACNA2D2* expression and LUAD prognosis. (C and D) Nomogram of risk score and other clinical characteristics to predict the 1-year, 3-year, and 5-year overall survival (OS) of LUAD patients.

proportion of stage II–IV cancers and a higher proportion of survival (Figure 4A). These results link high SCN7A expression with better survival outcomes.

Immunohistochemistry (IHC) analysis confirmed that SCN7A was moderately expressed in normal tissues but was entirely absent in lung cancer tissues (Figure 4B). These results showed that mRNA and protein levels of SCN7A are lower in LUAD tissues than in normal tissues.

3.5. Mutation studies of SCN7A in lung adenocarcinoma

Since ion channels are involved in many cellular processes, mutations in related genes could cause a variety of diseases[21]. We screened for *SCN7A* mutations in LUAD genes based on the data in cBioPortal database. *SCN7A* mutations were detected in 6% of LUAD tissues, most of which were missense mutations. A total of 28 mutation sites and seven truncation mutations were identified in the genome of LUAD cells (Figure 5).

3.6. Immunological analysis of SCN7A in lung adenocarcinoma

The prognostic value of SCN7A for LUAD was evaluated. We first analyzed how SCN7A expression correlates to immune cell infiltration to the tumor site based on the TIMER score. The results revealed a strong positive association between SCN7A expression and the infiltration of six immune cell subtypes: B cells (r = 0.33, P = 8.1e-15) (Figure 6A), $CD4^+$ T cells (r = 0.34, P = 1.98e-15) (Figure 6B), $CD8^+$ T cells (r = 0.33, P = 2.05e-14) (Figure 6C), neutrophils (r = 0.21, P = 2.04e-06) (Figure 6D), macrophages (r = 0.42, P = 2.36e-23) (Figure 6E), and myeloid dendritic cell (r = 0.35, P = 2.99e-16) (Figure 6F). In addition, the infiltration of the aforementioned immune cells was associated with favorable LUAD prognosis.

We then analyzed the sCNA of *SCN7A* in pan-cancer using data in TIMER2.0 database (Figure 7A). We found that the sCNA of *SCN7A* affects the infiltration of various immune cells, including $CD4^+$ T cells, macrophages, neutrophils, and dendritic cells, in LUAD (Figure 7B).

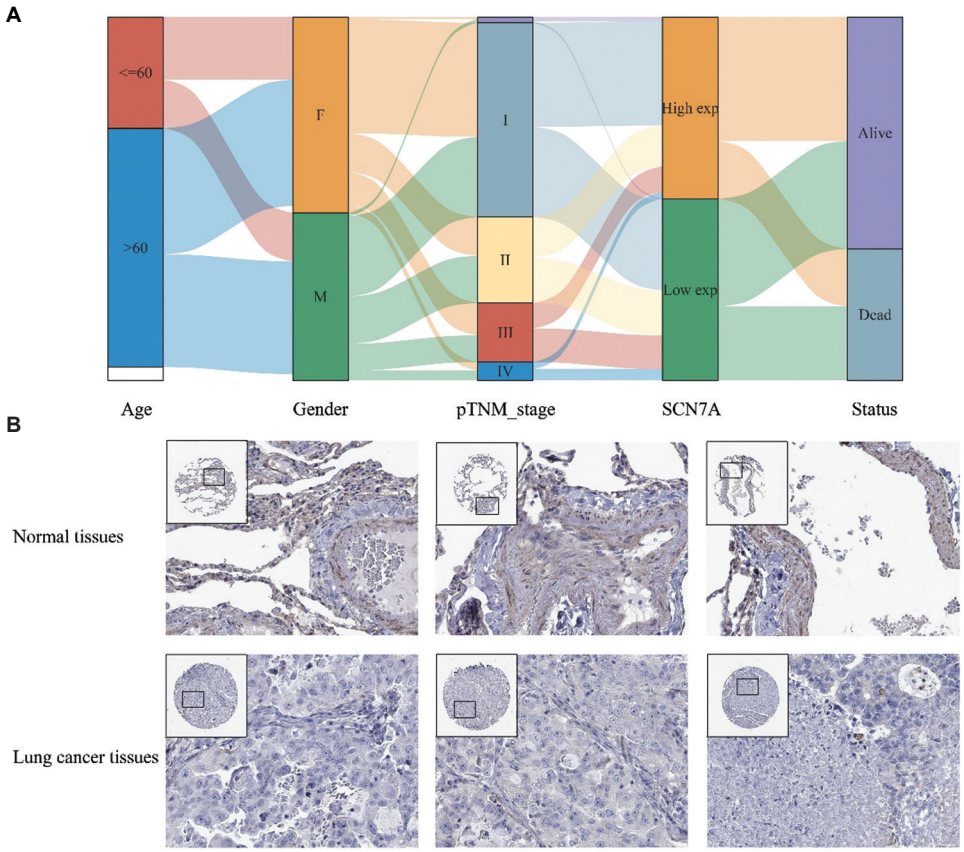

Figure 4. Messenger RNA (mRNA) transcription and expression of SCN7A protein in lung adenocarcinoma (LUAD). (A) Trend in the expression of *SNC7A* mRNA in LUAD among different stages, people of different age, and between gender; and the relationship between SNC7A expression and the overall survival (OS) of LUAD patients. (B) SCN7A protein level in lung cancer tissues and normal tissues from the Human Protein Atlas database.

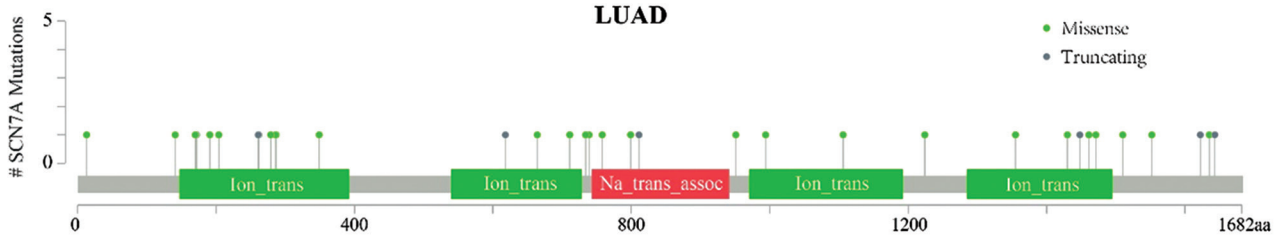

Figure 5. Somatic mutation landscape of *SCN7A* in lung adenocarcinoma (LUAD) cells.

To explore the correlation between SCN7A and immune checkpoint therapy in LUAD, we assessed the correlation between SCN7A expression and immune checkpoints. Cytotoxic T-lymphocyte associated protein 4 (CTLA4), hepatitis A virus cellular receptor 2 (HAVCR2), programmed cell death 1 ligand 2 (PD-L2), and T cell immunoreceptor with Ig and ITIM domains (TIGIT) expressions were positively correlated to SCN7A expression, whereas LAG3 expression showed a negative correlation (Figure 7C).

These results suggest a strong correlation between SCN7A expression and immune cell infiltration to LUAD tissues, consistent with the prognostic results. Thus, SCN7A is a potential biomarker for LUAD prognosis prediction.

3.7. Upstream non-coding RNAs of SCN7A

We searched through miRGator v3.0 database containing data for 25 miRNAs to identify the upstream regulatory mechanism of SCN7A in LUAD. Given how miRNAs regulate gene expression, miRNAs should be negatively correlated with SCN7A. Thus, we selected 15 miRNAs that were negatively correlated with SCN7A for further investigation. The expression of these miRNAs in LUAD

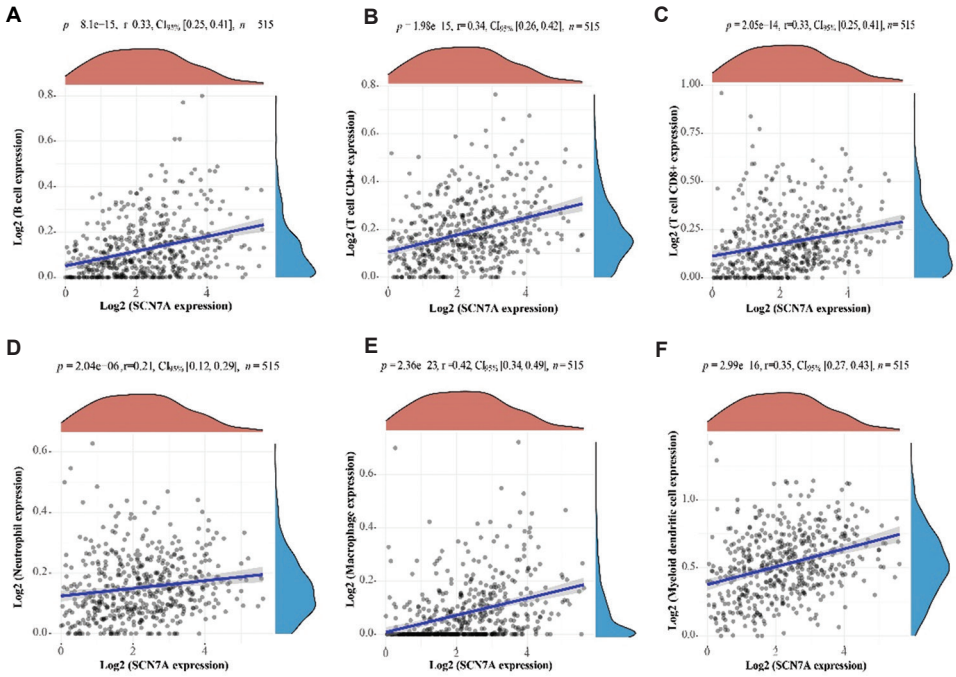

Figure 6. Correlation between SCN7A expression and infiltration of immune cells to the tumor site. (A) B cell. (B) $CD4^+$ T cell. (C) $CD8^+$ T cell. (D) Neutrophil. (E) Macrophage. (F) Myeloid dendritic cell.

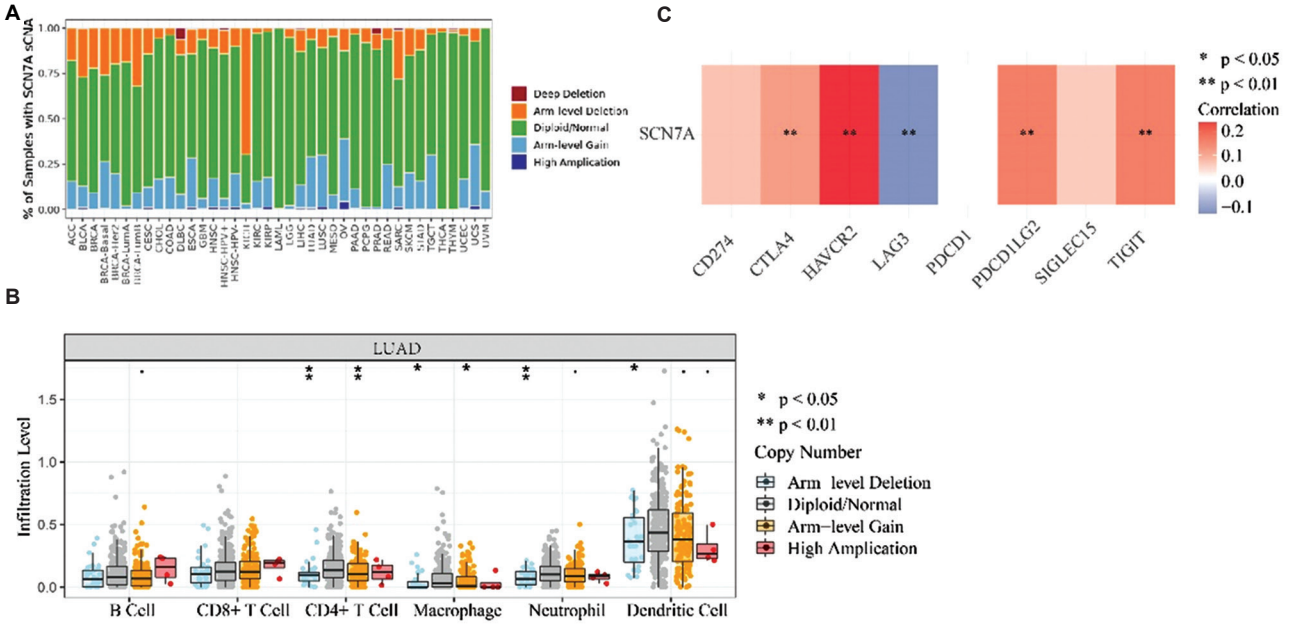

Figure 7. Immunological analysis of SCN7A in cancer. (A) Distribution of the somatic copy number alteration (sCNA) of SCN7A in pan-cancer. (B) Effect of SCN7A sCNA on the infiltration of immune cells to tumor site in lung adenocarcinoma (LUAD). (C) Correlation between the expression of SCN7A and immune checkpoints in LUAD.

was analyzed; 14 miRNAs were found to be overexpressed in LUAD (Figure 8A and Table 1). Further prognostic assessment indicated that high miR-21-5p levels in LUAD were associated with poorer prognosis (Figure 8B) but the other miRNAs had no significant impact on LUAD prognosis.

Through further searches in the starBase database, we identified 14 lncRNAs that bind to miR-21-5p. LncRNAs

Figure 8. Expression and prognostic value analysis of selected microRNAs (miRNAs) in lung adenocarcinoma (LUAD). (A) Expression analysis of 14 selected miRNAs in LUAD. (B) Prognostic value of miR-21-5p for LUAD.

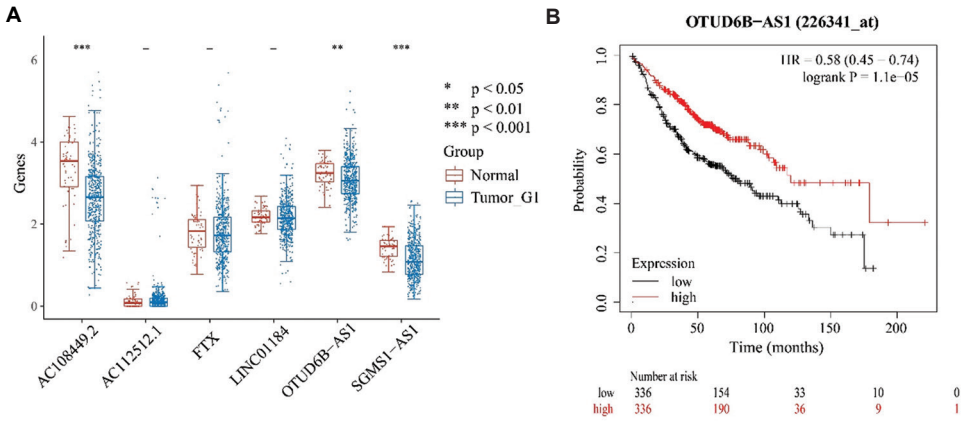

Figure 9. Expression analysis and prognostic potential of selected long non-coding RNAs (lncRNAs) for lung adenocarcinoma (LUAD). (A) Expression analysis of selected lncRNAs in LUAD. (B) Prognostic potential of OTUD6B-AS1 for LUAD.

also compete with miRNAs for binding mRNAs. We found that AC108449.2, AC112512.1, FTX, LINC01184, OTUD6B-AS1, and SGMS1-AS1 regulate the expression of SCN7A by binding to miRNA-21-5p. Further analyses showed that AC108449.2, OTUD6B-AS1, and SGMS1-AS1 were underexpressed in LUAD (Figure 9A). Prognostic analysis revealed an association between OTUD6B-AS1 overexpression and better LUAD prognosis (Figure 9B). Overall, SCN7A expression may be potentially regulated through the OTUD6B-AS1-miR-21-5p-SCN7A axis.

3.8. Pathways regulated by SCN7A in lung adenocarcinoma

We found that SCN7A closely participated in several cellular processes, including hypoxia (r = −0.4, P = 1.06e-21) (Figure 10B), proliferation of tumor cells (r = −0.66, P = 3.56e-66) (Figure 10C), expression of ECM (r = 0.61, P = 1.63e-54) (Figure 10E), angiogenesis (r = 0.29, P = 1.06e-11) (Figure 10F), apoptosis (r = 0.25, P = 1.24e-08) (Figure 10G), DNA repair (r = -0.65, P = 1.41e-62) (Figure 10H), and expression of G2M (r = -0.61, P = 4.25e-54) (Figure 10I). but not in tumor inflammation signature (r=-0.02, p=0.675) (Figure 10A) and EMT markers (r=-0.03, p=0.497) (Figure 10D).

3.9. SCN7A inhibits the proliferation and migration of lung cancer cells *in vitro*

To verify the role of SCN7A in lung cancer cells, SCN7A was overexpressed in A549 cells. We found that the expression of SCN7A increased by nearly 5 times compared with the control group (Figure 11A). We then evaluated the effect of SCN7A on the proliferation ability by CCK8 experiment and found that the overexpression of SCN7A significantly reduced the proliferation ability of A549 cells (Figure 11B). Through wound healing assay, we also found that the overexpression of SCN7A significantly reduced the migration ability of A549 cells (Figure 11C and D). Consistent with our analysis, these results strongly support the potential of SCN7A as a prognostic marker.

3.10. SCN7A expression in other cancer tissues

To investigate the role of SCN7A in other tumors, *SCN7A* gene expression in other cancer tissues was analyzed. Dysregulation of SCN7A was observed in 17 tumor tissues, including bladder cancer (BLCA), breast cancer (BRCA), cervical cancer (CESC), colon cancer (COAD), esophageal cancer (ESCA), head and neck cancer (HNSC), kidney chromophore (KICH), kidney clear cell carcinoma (KIRC), kidney papillary cell carcinoma (KIRP), liver cancer (LIHC), lung squamous cell carcinoma (LUSC), prostate cancer (PRAD), rectal cancer (READ), stomach cancer (STAD), thyroid cancer (THCA), and endometrioid cancer (UCEC) (Figure 12). Further analyses revealed that SCN7A could predict the prognosis of BLCA, LUSC, and ovarian cancer (OV), apart from LUAD (Figure 13). In addition, relying on the TIMER score, SCN7A expression was found to be positively correlated to immune cell infiltration in most cancers, including LUAD (Figure 14). These findings suggest the importance of SCN7A in cancer development and progression.

4. Discussion

At present, lung cancer is one of the most fatal malignancies in the world. Identifying prognostic markers and therapeutic targets for lung cancer are crucial to treating this cancer. Studies have shown that ion channels participate in the development and progression of tumors[22-25], underscoring the need to be aware of the molecular mechanisms behind these events.

The function of *SCN7A* differs from that of other related genes. Precisely, SCN7A does not act as a switch

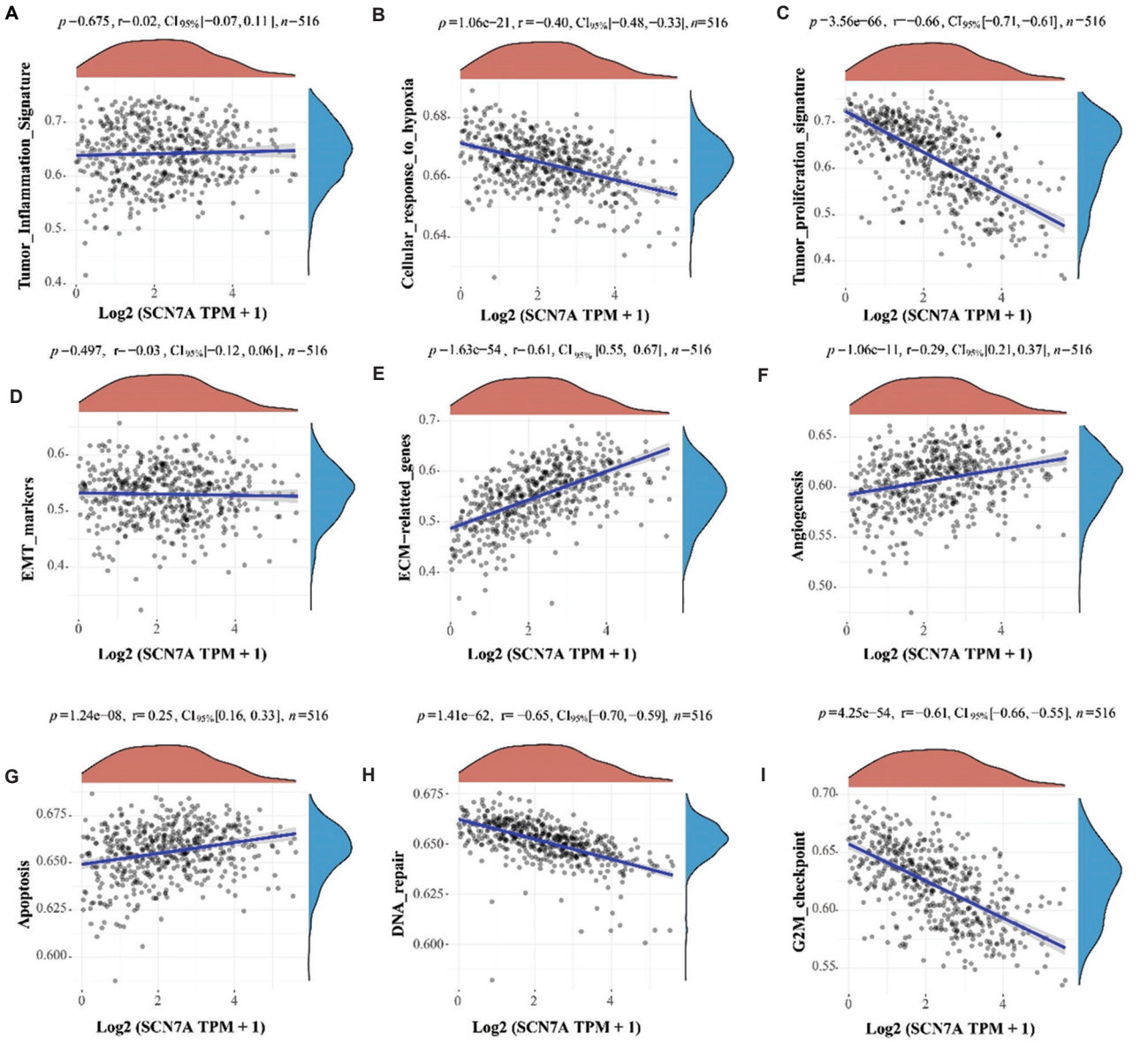

Figure 10. Pathways regulated by SCN7A in lung adenocarcinoma (LUAD) include (A) tumor inflammation, (B) cellular response to hypoxia, (C) tumor proliferation, (D) epithelial-mesenchymal transition (EMT) markers, (E) ECM-related genes, (F) angiogenesis, (G) apoptosis, (H) DNA repair, and (I) expression of G2M checkpoint.

for ion channels but regulates extracellular sodium ion concentration[26]. Current studies on SCN7A in tumors remain scanty. Consistent with the results of a previous study[24], we observed the downregulation of SCN7A protein in LUAD tissues, and this was associated with poor prognosis, implying that SCN7A could participate in LUAD development. Our results also showed that SCN7A has an inhibitory effect on the proliferation and migration of lung cancer cells.

Ion channels participate in inflammatory and immune responses in cancer cells[27,28]. Our results showed that SCN7A was strongly associated with immune cell infiltration. Rabbit models have revealed that SCN7A knockdown reduced the infiltration of macrophages and neutrophils[29,30], consistent with our results. These results indicate that SCN7A may affect the tumor immune microenvironment.

ceRNA mechanism has proven to be involved in regulating gene expression through ncRNAs[31-34]. We identified that SCN7A expression is regulated via the OTUD6B-AS1-miR-21-5p-SCN7A axis. Interestingly, OTUD6B-AS1 has been reported to suppress cancer

Table 1. MicroRNA (miRNA) expression between lung adenocarcinoma and normal tissues

miRNA	Fold change	*P*-value	False discovery rate
hsa-miR-21-5p	9.2	6.10e-101	1.60e-97
hsa-miR-93-5p	2.73	2.00e-11	3.60e-10
hsa-miR-570-3p	3.84	3.30e-06	3.10e-05
hsa-miR-590-3p	3.08	1.10e-23	6.10e-22
hsa-miR-182-3p	15.57	7.00e-05	0.00054
hsa-miR-17-3p	2	2.30e-09	3.30e-08
hsa-miR-576-5p	2.14	8.80e-07	9.00e-06
hsa-miR-577	124.3	1.30e-20	5.70e-19
hsa-miR-20a-5p	4.76	1.20e-26	7.20e-25
hsa-miR-155-5p	2.07	0.00048	0.0031
hsa-miR-556-5p	13.6	5.10e-06	4.60e-05
hsa-miR-331-5p	1.34	1.20e-06	1.20e-05
hsa-miR-106b-5p	1.38	1.20e-13	2.60e-12
hsa-miR-96-3p	15.09	0.00044	0.0029

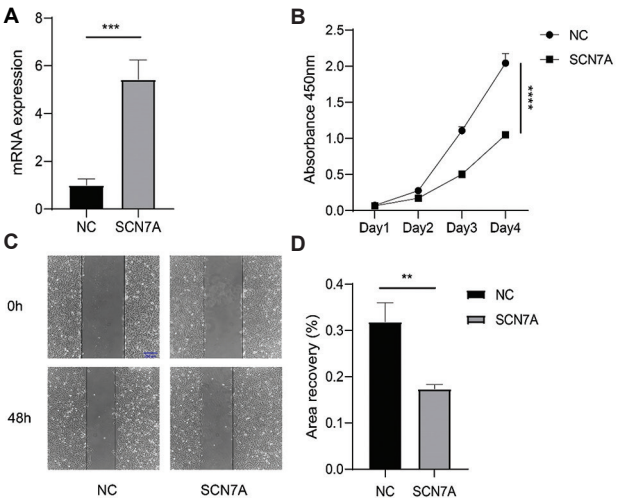

Figure 11. SCN7A as a protective factor in lung cancer cells. (A) *SCN7A* mRNA expression between the control group and SCN7A overexpression group. (B) Proliferation ability between the control group and SCN7A overexpression group. (C and D) Migration ability between the control group and SCN7A overexpression group (scale bar: 200μm). $^{**}P < 0.01$, $^{***}P < 0.001$, $^{****}P < 0.0001$.

progression in colorectal and thyroid cancers[35-37]. miR-21-5p contributes to lung cancer progression by inhibiting SMAD family member 7 (SMAD7) expression[38], while miR-21-5p inhibitors can effectively suppress lung cancer progression[39]. These studies suggest that the OTUD6B-AS1-hsa-mir-21-5p-SCN7A axis may have an important role in LUAD.

We also identified mutations and the role of SCN7A in pan-cancer prognosis. We found that SCN7A could

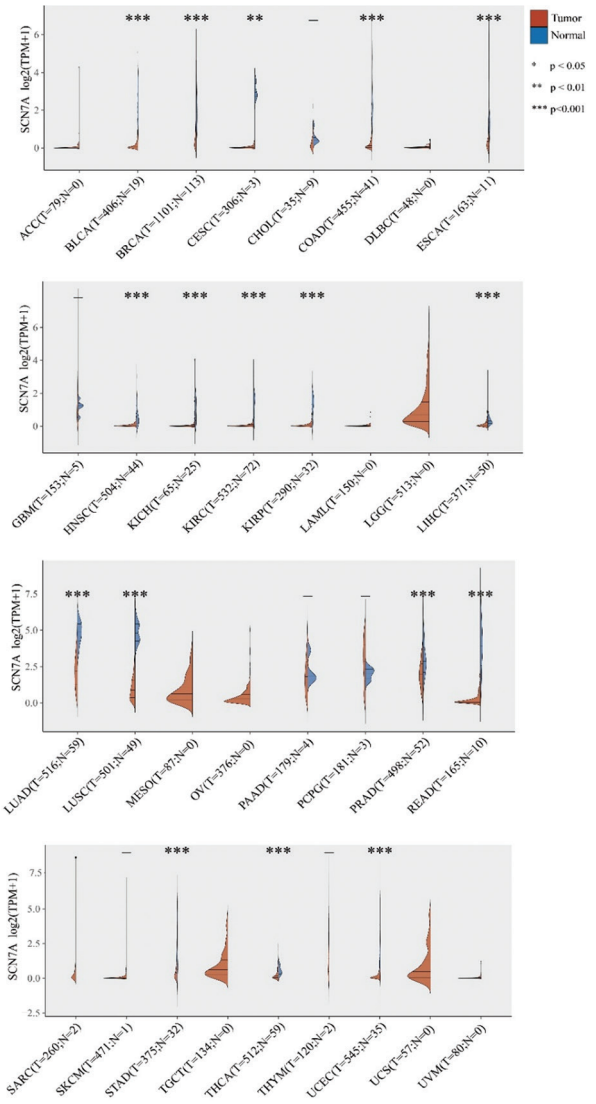

Figure 12. Expression of SCN7A in pan-cancer tissues.

predict the prognoses of LUSC and OV besides LUAD. Notably, SCN7A has been reported to be associated with poor prognosis in LUSC[40]. Our correlation analysis revealed a positive association between SCN7A expression and immune cell infiltration to most tumor tissues. These results suggest that SCN7A has significant research value in pan-cancer.

In conclusion, our work demonstrated that the underexpression of SCN7A predicts a poor prognosis in LUAD, thus indicating that SCN7A is a potential target in the treatment of LUAD. Notably, OTUD6B-AS1 and miR-21-5p are the ncRNAs that regulate SCN7A expression. The role of SCN7A in LUAD prognosis needs to be validated by *in vivo* studies.

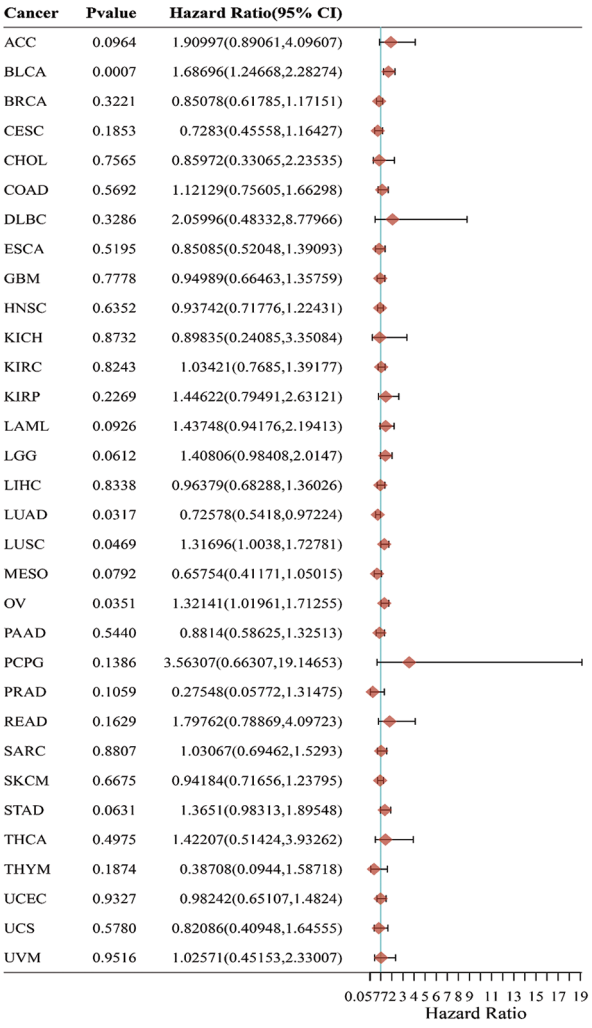

Figure 13. Prognostic value of SCN7A for pan-cancer.

Acknowledgments

None.

Funding

None.

Conflict of interest

The authors declare that they have no competing interests.

Author contributions

Conceptualization: Hehui Lv, Hongyuan Song, Zhouping Qin, Yulian Chen
Formal analysis: Hehui Lv, Hongyuan Song, Zhouping Qin
Methodology: Hehui Lv, Hongyuan Song, Zhouping Qin
Writing – original draft: Rongchun Xing
Writing – review & editing: Rongchun Xing, Yulian Chen

All authors have read and agreed to the published version of the manuscript.

Ethics approval and consent to participate

Not applicable.

Consent for publication

Not applicable.

Availability of data

The datasets in this study are available in online repositories, TCGA datasets (https://www.cancer.gov/about-nci/organization/ccg/research/structural-genomics/tcga), and GEO databases (https://www.ncbi.nlm.nih.gov/geo/).

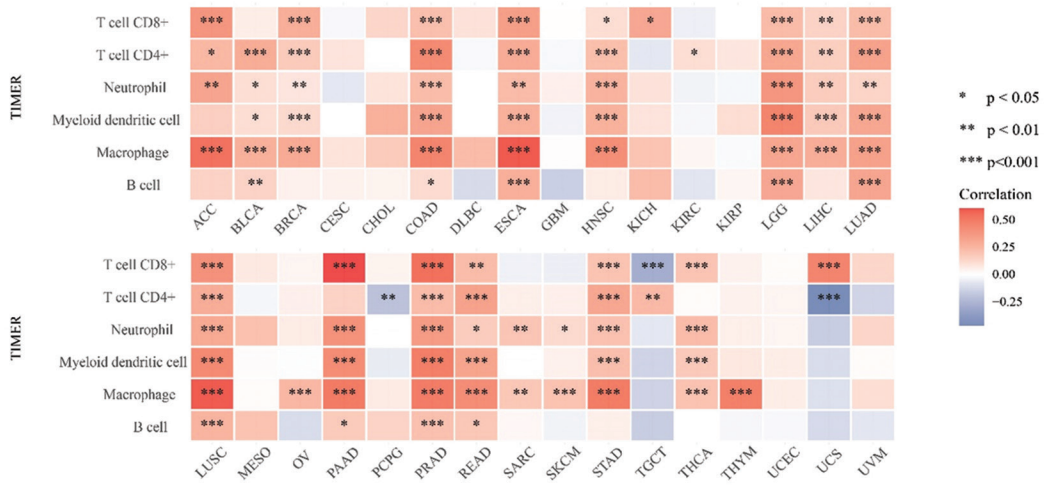

Figure 14. Relationship between SCN7A and immune cell infiltration to pan-cancer tissues.

References

1. Thai AA, Solomon BJ, Sequist LV, *et al*., 2021, Lung cancer. *Lancet*, 398(10299): 535–554.

   https://doi.org/10.1016/S0140-6736(21)00312-3

2. Siegel RL, Miller KD, Jemal A, 2019, Cancer statistics, 2019. *CA Cancer J Clin*, 69(1): 7–34.

   https://doi.org/10.3322/caac.21551

3. Knight SB, Crosbie PA, Balata H, *et al*., 2017, Progress and prospects of early detection in lung cancer. *Open Biol*, 7(9): 170070.

   https://doi.org/10.1098/rsob.170070

4. Nooreldeen R, Bach H, 2021, Current and future development in lung cancer diagnosis. *Int J Mol Sci*, 22(16): 8661.

   https://doi.org/10.3390/ijms22168661

5. Bulk E, Todesca LM, Schwab A, 2021, Ion channels in lung cancer. *Rev Physiol Biochem Pharmacol*, 181: 57–79.

   https://doi.org/10.1007/112_2020_29

6. Farfariello V, Prevarskaya N, Gkika D, 2021, Ion channel profiling in prostate cancer: Toward cell population-specific screening. *Rev Physiol Biochem Pharmacol*, 181: 39–56.

   https://doi.org/10.1007/112_2020_22

7. Fu S, Hirte H, Welch S, *et al*., 2017, First-in-human phase I study of SOR-C13, a TRPV6 calcium channel inhibitor, in patients with advanced solid tumors. *Invest New Drugs*, 35(3): 324–333.

   https://doi.org/10.1007/s10637-017-0438-z

8. Fairhurst C, Watt I, Martin F, *et al*., 2015, Sodium channel-inhibiting drugs and survival of breast, colon and prostate cancer: A population-based study. *Sci Rep*, 5: 16758.

   https://doi.org/10.1038/srep16758

9. Martin F, Ufodiama C, Watt I, *et al*., 2015, Therapeutic value of voltage-gated sodium channel inhibitors in breast, colorectal, and prostate cancer: A systematic review. *Front Pharmacol*, 6: 273.

   https://doi.org/10.3389/fphar.2015.00273

10. Lin J, Marquardt G, Mullapudi N, *et al*., 2014, Lung cancer transcriptomes refined with laser capture microdissection. *Am J Pathol*, 184(11): 2868–2884.

    https://doi.org/10.1016/j.ajpath.2014.06.028

11. Meister M, Belousov A, Xu EC, *et al*., 2014, Intra-tumor heterogeneity of gene expression profiles in early stage non-small cell lung cancer. *J Bioinform Res Stud*, 1(1): 21.

12. Brouwer-Visser J, Cheng WY, Bauer-Mehren A, *et al*., 2018, Regulatory T-cell genes drive altered immune microenvironment in adult solid cancers and allow for immune contextual patient subtyping. *Cancer Epidemiol Biomarkers Prev*, 27(1): 103–112.

    https://doi.org/10.1158/1055-9965.EPI-17-0461

13. Barrett T, Wilhite SE, Ledoux P, *et al*., 2013, NCBI GEO: Archive for functional genomics data sets--update. *Nucleic Acids Res*, 41(Database issue): D991–D995.

    https://doi.org/10.1093/nar/gks1193

14. Zhou Y, Zhou B, Pache L, *et al*., 2019, Metascape provides a biologist-oriented resource for the analysis of systems-level datasets. *Nat Commun*, 10(1): 1523.

    https://doi.org/10.1038/s41467-019-09234-6

15. Uhlen M, Fagerberg L, Hallström BM, *et al*., 2015, Proteomics. Tissue-based map of the human proteome. *Science*, 347(6220): 1260419.

    https://doi.org/10.1126/science.1260419

16. Gao J, Aksoy BA, Dogrusoz U, *et al*., 2013, Integrative analysis of complex cancer genomics and clinical profiles using the cBioPortal. *Sci Signal*, 6(269): pl1.

    https://doi.org/10.1126/scisignal.2004088

17. Cerami E, Gao J, Dogrusoz U, *et al*., 2012, The cBio cancer genomics portal: An open platform for exploring multidimensional cancer genomics data. *Cancer Discov*, 2(5): 401–404.

    https://doi.org/10.1158/2159-8290.CD-12-0095

18. Li T, Fu J, Zeng Z, *et al*., 2020, TIMER2.0 for analysis of tumor-infiltrating immune cells. *Nucleic Acids Res*, 48(W1): W509–W514.

    https://doi.org/10.1093/nar/gkaa407

19. Cho S, Jang I, Jun Y, *et al*., 2013, MiRGator v3.0: A microRNA portal for deep sequencing, expression profiling and mRNA targeting. *Nucleic Acids Res*, 41(Database issue): D252–D257.

    https://doi.org/10.1093/nar/gks1168

20. Li JH, Liu S, Zhou H, *et al*., 2014, starBase v2.0: Decoding miRNA-ceRNA, miRNA-ncRNA and protein-RNA interaction networks from large-scale CLIP-Seq data. *Nucleic Acids Res*, 42(Database issue): D92–D97.

    https://doi.org/10.1093/nar/gkt1248

21. Camerino DC, Tricarico D, Desaphy JF, 2007, Ion channel pharmacology. *Neurotherapeutics*, 4(2): 15.

    https://doi.org/10.1016/j.nurt.2007.01.013

22. Petho Z, Najder K, Bulk E, *et al*., 2019, Mechanosensitive ion channels push cancer progression. *Cell Calcium*, 80: 79–90.

    https://doi.org/10.1016/j.ceca.2019.03.007

23. Anderson KJ, Cormier RT, Scott PM, 2019, Role of ion channels in gastrointestinal cancer. *World J Gastroenterol*, 25(38): 5732–5772.

    https://doi.org/10.3748/wjg.v25.i38.5732

24. Li W, Zhou K, Li M, *et al*., 2022, Identification of SCN7A as the key gene associated with tumor mutation burden in gastric cancer. *BMC Gastroenterol*, 22(1): 45.

https://doi.org/10.1186/s12876-022-02112-4

25. Yan Y, He W, Chen Y, *et al*., 2021, Comprehensive analysis to identify the encoded gens of sodium channels as a prognostic biomarker in hepatocellular carcinoma. *Front Genet*, 12: 802067.

https://doi.org/10.3389/fgene.2021.802067

26. Dolivo D, Rodrigues A, Sun L, *et al*., 2021, The Na(x) (SCN7A) channel: An atypical regulator of tissue homeostasis and disease. *Cell Mol Life Sci*, 78(14): 5469–5488.

https://doi.org/10.1007/s00018-021-03854-2

27. Feske S, Wulff H, Skolnik EY, 2015, Ion channels in innate and adaptive immunity. *Annu Rev Immunol*, 33: 291–353.

https://doi.org/10.1146/annurev-immunol-032414-112212

28. Bujak JK, Kosmala D, Szopa IM, *et al*., 2019, Inflammation, cancer and immunity-implication of TRPV1 channel. *Front Oncol*, 9: 1087.

https://doi.org/10.3389/fonc.2019.01087

29. Zhao J, Xie P, Galiano RD, *et al*., 2019, Imiquimod-induced skin inflammation is relieved by knockdown of sodium channel Na_x. *Exp Dermatol*, 28(5): 576–584.

https://doi.org/10.1111/exd.13917

30. Zhao J, Jia S, Xie P, *et al*., 2020, Knockdown of sodium channel Na(x) reduces dermatitis symptoms in rabbit skin. *Lab Invest*, 100(5): 751–761.

https://doi.org/10.1038/s41374-020-0371-1

31. Ghafouri-Fard S, Shoorei H, Anamag FT, *et al*., 2020, The role of non-coding rnas in controlling cell cycle related proteins in cancer cells. *Front Oncol*, 10: 608975.

https://doi.org/10.3389/fonc.2020.608975

32. Razavi ZS, Tajiknia V, Majidi S, *et al*., 2021, Gynecologic cancers and non-coding RNAs: Epigenetic regulators with emerging roles. *Crit Rev Oncol Hematol*, 157: 103192.

https://doi.org/10.1016/j.critrevonc.2020.103192

33. Fabrizio FP, Sparaneo A, Muscarella LA, 2020, NRF2 regulation by noncoding RNAs in cancers: The present knowledge and the way forward. *Cancers (Basel)*, 12(12): 3621.

https://doi.org/10.3390/cancers12123621

34. Gao S, Ding B, Lou W, 2020, microRNA-dependent modulation of genes contributes to ESR1's effect on ERalpha positive breast cancer. *Front Oncol*, 10: 753.

https://doi.org/10.3389/fonc.2020.00753

35. Cai Y, Li Y, Shi C, *et al*., 2021, LncRNA OTUD6B-AS1 inhibits many cellular processes in colorectal cancer by sponging miR-21-5p and regulating PNRC2. *Hum Exp Toxicol*, 40(9): 1463–1473.

https://doi.org/10.1177/0960327121997976

36. Wang W, Cheng X, Zhu J, 2021, Long non-coding RNA OTUD6B-AS1 overexpression inhibits the proliferation, invasion and migration of colorectal cancer cells via downregulation of microRNA-3171. *Oncol Lett*, 21(3): 193.

https://doi.org/10.3892/ol.2021.12454

37. Wang Z, Xia F, Feng T, *et al*., 2020, OTUD6B-AS1 inhibits viability, migration, and invasion of thyroid carcinoma by targeting miR-183-5p and miR-21. *Front Endocrinol (Lausanne)*, 11: 136.

https://doi.org/10.3389/fendo.2020.00136

38. Tang J, Li X, Cheng T, *et al*., 2021, miR-21-5p/SMAD7 axis promotes the progress of lung cancer. *Thorac Cancer*, 12(17): 2307–2313.

https://doi.org/10.1111/1759-7714.14060

39. Zhou X, Liu H, Pang Y, *et al*., 2022, UTMD-mediated delivery of miR-21-5p inhibitor suppresses the development of lung cancer. *Tissue Cell*, 74: 101719.

https://doi.org/10.1016/j.tice.2021.101719

40. Bao L, Zhang Y, Wang J, *et al*., 2016, Variations of chromosome 2 gene expressions among patients with lung cancer or non-cancer. *Cell Biol Toxicol*, 32(5): 419–435.

https://doi.org/10.1007/s10565-016-9343-z

ACCSCIENCE PUBLISHING

Gene & Protein in Disease

CASE REPORT

Autoimmune thyroid disease in narcolepsy: A case report

Chaofan Geng[1], Zhenzhen Yang[2], and Hongju Zhang[1,3]*

[1]Henan University People's Hospital, Henan Provincial People's Hospital, Zhengzhou 450003, China

[2]Fuwai Central China Cardiovascular Hospital, Henan Provincial People's Hospital, Zhengzhou 450003, China

[3]Zhengzhou University People's Hospital, Henan Provincial People's Hospital, Zhengzhou 450003, China

Abstract

While the previous studies have discussed the association of narcolepsy with autoimmune diseases, autoimmune thyroid disease (IATD) has rarely been described in patients with narcolepsy. The association of narcolepsy with thyroid disease is intriguing for speculating the causal or coexisting autoimmune disorder. We report a case of narcolepsy Type 1 with IATD, presenting with excessive daytime sleepiness (EDS), cataplexy attacks, and unexplainable weight gain. Oral modafinil and sodium oxybate were used for treatment and prevention. During the 1-year follow-up, the patient's EDS and cataplexy attacks improved. However, the patient developed hypothyroidism and was subsequently prescribed with thyroid replacement therapy.

Keywords: Autoimmune thyroid disease; Narcolepsy; Mechanism; Autoimmunity; Case report

***Corresponding author:**
Hongju Zhang
(hongjuz@sina.com)

Citation: Geng C, Yang Z, Zhang H, 2023, Autoimmune thyroid disease in narcolepsy: A case report. *Gene Protein Dis,* 2(1):235. https://doi.org/10.36922/gpd.v2i1.235

Received: October 25, 2022
Accepted: December 19, 2022
Published Online: January 11, 2023

1. Background

Narcolepsy is a chronic sleep disorder, primarily associated with excessive daytime sleepiness (EDS), cataplexy attacks, sleep paralysis, and hypnagogic hallucinations[1,2], which affects one in every 2,000 individuals[3]. Autoimmune-mediated destruction of hypocretin neurons is thought to be the main pathophysiological mechanism of narcolepsy[4,5]. More than 98% of narcolepsy patients with cataplexy are *HLA-DQB1*06:02* positive[6,7]. Although the previous studies have reported the association of narcolepsy with autoimmune diseases[8], no reports of autoimmune thyroid disease (AITD) have ever been described in patients with narcolepsy. Furthermore, the pathogenesis of narcolepsy-associated autoimmune disorders has yet to be established. In this report, we present a case of narcolepsy with AITD as comorbidity.

2. Case presentation

A 14-year-old female patient presented to the hospital with a 5-year history of EDS, inexplicable weight gain, and cataplexy attacks. The patient reported that she often falls asleep during class, while doing her homework, or using her cellphone without any obvious cause, and then wakes up after 3 – 5 min; she also reported that whenever she was emotionally agitated, she would experience a transient weakness in both lower

limbs, causing her to fall down, but would be relieved after a few seconds; she also experienced sleep fragmentation at night with excessive dreams. At the same time, she was surprised to find that her body weight had increased by approximately 25 kg within a year. A standard neurological examination and a neuropsychological assessment of the patient were performed by a neurologist. She scored 18 points on the epworth sleepiness scale, which was used to assess the degree of subjective sleepiness[9], and 12 points on the Pittsburgh Sleep Quality Index, suggesting average sleep quality. The magnetic resonance imaging and magnetic resonance angiography of her brain were normal. She was otherwise well with no significant comorbidity or family history of neurological illness. Given these clues, polysomnography (PSG) and multiple sleep latency test (MSLT) were performed on the patient to further clarify the diagnosis. PSG study showed a total sleep time of 579.5 min, sleep efficiency of 76.5%, and apnea-hypopnea index of 1.7/h, which can exclude obstructive sleep apnea (Table 1). Her MSLT showed a mean sleep latency of 0.7 min and four sleep-onset rapid eye movement periods (SOREMPs) in five naps without notable sleep paralysis. Her cerebrospinal fluid hypocretin-1, measured by enzyme-linked immunosorbent assay, was 71.54 pg/mL. In addition, she was found to be *HLA-DQB*06:02* positive. According to the International Classification of Sleep Disorders, 3rd edition (ICSD-3), we diagnosed the case as narcolepsy Type 1 (NT1).

Laboratory tests for the patient, including complete blood count, renal function, electrolytes, cardiac enzymes, liver enzymes, sex hormones, fasting growth hormone, autoimmune encephalitis antibody, immunoglobulin, and complement tests, were all normal. However, her serum 25-hydroxyvitamin D (25(OH)D) level was 12.45 ng/mL (normal range >20 ng/mL), and her thyroid function test showed abnormally high levels of thyroglobulin antibody (TgAb) and thyroid peroxidase antibody (TPOAb) (Table 2). Her thyroid gland was normal in texture and size. Following-up with the patient's past medical history, the patient had not consumed any antithyroid drugs. There was also no antecedent history of thyroidectomy, neck radiotherapy, and radioactive iodine (^{131}I) therapy for hyperthyroidism. Based on her medical history and laboratory tests, she was diagnosed with AITD. Given the patient's normal thyroid function, no treatment was administered. Only modafinil was prescribed to improve the patient's sleep symptoms. After a year of follow-up, the patient's sleep symptoms and thyroid function were re-evaluated. We found a significant improvement in the patient's EDS; however, she developed hypothyroidism. Otherwise, there was also significant improvement in her cataplexy attacks. Following a discussion with the patient and her family members, the patient was started on thyroid replacement therapy so as to achieve a euthyroid state, while still receiving modafinil.

The research protocol of this study was approved by the Research Ethics Committee of Henan Provincial People's Hospital, and the participant signed the written informed consent forms.

3. Discussion

The previous studies have found that the prevalence rate of immunopathological diseases is higher in patients with narcolepsy[8,10,11]. Cataplexy, in particular, is often associated with comorbid immunopathological diseases associated with narcolepsy[8]. However, to the best of our knowledge, this is the first case of narcolepsy with AITD. According to the ICSD-3 diagnostic criteria for narcolepsy, this case was not difficult to diagnose. In addition, the previous studies have also demonstrated that weight gain, in particular, is often related to narcolepsy with cataplexy[12-14]. Impaired feeding behavior, including binge eating, nocturnal eating, and increased food cravings, may contribute to this phenomenon[15]. In addition, abnormal energy metabolism and reduced spontaneous activity are also important factors that contribute to the altered body mass index[16].

AITD is characterized by the dysfunction of thyroid tissue by antibody-mediated immune inflammation[17]. TPOAb and TgAb are the main thyroid autoantibodies that cause thyroid destruction and suppression of function. They are sensitive indicators for the diagnosis and prognosis of autoimmune thyroid disease[18]. Elevated levels of TPOAb and TgAb are early manifestations in patients with Hashimoto's thyroiditis (HT) and may have initiated certain pathophysiological changes in the thyroid gland, albeit the normal thyroid function occasionally.

Table 1. Result of PSG

	TST (min)	AWN/h	WASO (%)	SE (%)	N1 (%)	N2 (%)	N3 (%)	REM (%)	AI (event/h)	PLMI (event/h)	AHI (event/h)
Value	579.5	4.0	13.4	76.5	29.2	43.4	11.9	15.5	6.1	0.4	1.7

PSG: Polysomnography; AHI: Apnea-hypopnea index; AI: Arousal index; AWN/h: Awakenings per hour; N1, N2, N3: Standard non-rapid eye movement sleep stages; PLMI: Periodic limb movement index; REM: Rapid eye movement sleep; REML: Rapid eye movement sleep latency; SE: Sleep efficiency; TST: Total sleep time; WASO: Wakefulness after sleep onset

Table 2. Laboratory studies

Variables	Baseline value	Normal range
T_3	1.36 ng/mL	0.91–2.18 ng/mL
T_4	7.02 μg/dL	5.91–13.2 μg/dL
FT_3	6.11 pmol/L	3.93–7.7 pmol/L
FT_4	14.24 pmol/L	12.6–21 pmol/L
TSH	2.38 uIU/mL	0.51–4.3 uIU/mL
TgAb	12.1 IU/mL	0–4 IU/mL
TPOAb	243.53 IU/mL	0–9 IU/mL

T_3: Triiodothyronine; T_4: Thyroxine; FT_3: Free triiodothyronine; FT_4: Free thyroxine; TGAb: Thyroglobulin antibody; TPOAb: Thyroid peroxidase antibody; TSH: Thyroid stimulating hormone

In this case, the patient's thyroid function was normal on admission but she tested positive for thyroid antibodies. The previous studies have suggested that abnormal thyroid function may be preceded by prolonged thyroid autoimmune abnormalities and that most thyroid function abnormalities are predominantly hypothyroid[19]. In this case, despite the short follow-up period, abnormal thyroid function was observed after a year, thus suggesting that annual screening of thyroid function is necessary for narcolepsy patients with positive thyroid antibodies.

It is noteworthy that although the exact mechanisms leading to neuronal destruction in narcolepsy remain unclear[20], environmental trigger, genetic factors, viral infections, and autoimmunity have been found to be associated with the pathogenesis of narcolepsy[21,22]. Epidemiological studies have reported a significant six to nine times increase in incidence of narcolepsy in 2010[23], and analyses have suggested that the cause of the increased incidence in 2010 may be closely related to H1N1 influenza infection in the winter of 2009 and the AS03-adjuvanted influenza A vaccine[23-25]. Studies have also found an association between upper respiratory tract *Streptococcus pyogenes* infection and narcolepsy[26]. In addition, the association of narcolepsy with human leukocyte antigen (HLA) has been extensively investigated, in which the frequency of *HLA-DQB1*06:02* and *HLA-DQA1*01:02* motifs has been found to be associated with the onset of the disease[27]. However, there is a growing body of evidence supporting the hypothesis that narcoleopsy is a T cell-mediated autoimmune disease that attacks hypocretin neurons[21,28].

There are different mechanisms to explain the causal relationship between narcolepsy and autoimmune diseases. One explanation for the observed association between narcolepsy and AITD is the common immunological pathogenetic pathway. The previous studies have shown that patients with one autoimmune disease are usually at an increased risk of developing another autoimmune disease[8]. *HLA-DRB1*0803* and *DQB1*0601* haplotypes have been found to be strongly linked with AITD[29]. We suspect that HLA-related homologous genes could make it easier for specific autoantigens to be presented to self-reactive T cells, leading to defects in peripheral autoimmune responses and resulting in autoimmune diseases. All in all, narcolepsy and AITD may share common susceptibility genes, thus supporting the hypothesis that common genetic variants lead to immune dysregulation and autoimmune susceptibility. However, the specific susceptibility loci and genes shared by narcolepsy and AITD remain unknown, thereby requiring further research in this area.

Vitamin D has been shown to be an immunomodulatory hormone[30]. Although the patient was measured for Vitamin D deficiency in our case, we were unable to infer with certainty the cause of the deficiency. At present, the relationship between Vitamin D and narcolepsy is understudied, and the findings are inconsistent[31,32]. Interestingly, the previous studies have found that Vitamin D deficiency contributes to the development of AITD[33]. T cells have immunomodulatory properties[34].

Maintaining the T helper 17 cell/regulatory T cell (Th17/Treg) balance that occurs during chronic inflammation is an important key point in the treatment of autoimmune diseases[35]. A growing body of evidence has demonstrated that Vitamin D is associated with the inhibition of Th17 cell differentiation and the upregulation of Tregs[36].

In addition, the previous studies have demonstrated that pro-inflammatory cytokines interleukin 6 (IL-6) is upregulated in narcolepsy patients[37]. This finding supports the hypothesis that inflammation is associated with the pathophysiology of narcolepsy[38]. Cytokines are involved in the pathogenesis of thyroid disease; they play a role in the immune system and directly target thyroid follicular cells[39]. Cytokines also have certain roles in promoting and suppressing the development of autoimmune diseases[40]. We hypothesize that appetitive-regulating cell-associated antigens may be expressed in thyroid tissue; thus, when Th17/Treg ratio imbalance and immune balance disruption occur, the corresponding antibodies produced against hypocretin neuron-associated antigens will act on the thyroid tissue and promote the development of AITD.

4. Conclusion

Given that both narcolepsy and AITD have a basic defect in immune regulation as a shared, similar disease mechanism, thyroid autoantibodies and thyroid function should be checked regularly to facilitate early detection and treatment of abnormal thyroid function and to prevent complications. Nevertheless, we lack

sufficient data to demonstrate whether AITD is more likely to occur in narcolepsy patients. Therefore, the future studies should focus on autoimmune disorders in larger sample sizes of narcolepsy patients to explore the pathophysiological mechanisms of narcolepsy with immunopathological diseases. This would allow us to better understand the significance of immune-related processes in the pathophysiology of these disorders.

Acknowledgments

None.

Funding

No funding was received in drafting this manuscript.

Conflict of interest

The authors have no conflict of interest to declare.

Author contributions

Data curation: Chaofan Geng
Writing – original draft: Chaofan Geng, Zhenzhen Yang
Writing – review & editing: Hongju Zhang

Ethics approval and consent to participate

The research protocol of this study was approved by the Research Ethics Committee of Henan Provincial People's Hospital. The patient/participant provided a written informed consent to participate in this study.

Consent for publication

A written informed consent was obtained from the patient for the publication of any potentially identifiable images or data included in this article.

Availability of data

The data presented in the study can be obtained from the corresponding author on reasonable request.

References

1. Bassetti CL, Adamantidis A, Burdakov D, *et al*., 2019, Narcolepsy-clinical spectrum, aetiopathophysiology, diagnosis and treatment. *Nat Rev Neurol*, 15(9): 519–539.

   https://doi.org/10.1038/s41582-019-0226-9

2. Postiglione E, Antelmi E, Pizza F, *et al*., 2018, The clinical spectrum of childhood narcolepsy. *Sleep Med Rev*, 38: 70–85.

   https://doi.org/10.1016/j.smrv.2017.04.003

3. Luo G, Yogeshwar S, Lin L, *et al*., 2021, T cell reactivity to regulatory factor X4 in Type 1 narcolepsy. *Sci Rep*, 11(1): 7841.

   https://doi.org/10.1038/s41598-021-87481-8

4. Andlauer O, Moore HT 4th, Hong SC, *et al*., 2012, Predictors of hypocretin (orexin) deficiency in narcolepsy without cataplexy. *Sleep*, 35(9): 1247–1255F.

   https://doi.org/10.5665/sleep.2080

5. Liblau RS, Vassalli A, Seifinejad A, *et al*., 2015, Hypocretin (orexin) biology and the pathophysiology of narcolepsy with cataplexy. *Lancet Neurol*, 14(3): 318–328.

   https://doi.org/10.1016/s1474-4422(14)70218-2

6. Kachooei-Mohaghegh-Yaghoobi L, Rezaei-Rad F, Sadeghniiat-Haghighi K, *et al*., 2020, The impact of the HLA DQB1 gene and amino acids on the development of narcolepsy. *Int J Neurosci*, 132(7): 706–713.

   https://doi.org/10.1080/00207454.2020.1835903

7. Bourgin P, Zeitzer JM, Mignot E, 2008, CSF hypocretin-1 assessment in sleep and neurological disorders. *Lancet Neurol*, 7(7): 649–662.

   https://doi.org/10.1016/s1474-4422(08)70140-6

8. Martinez-Orozco FJ, Vicario JL, Villalibre-Valderrey I, *et al*., 2014, Narcolepsy with cataplexy and comorbid immunopathological diseases. *J Sleep Res*, 23(4): 414–419.

   https://doi.org/10.1111/jsr.12143

9. Johns MW, 1991, A new method for measuring daytime sleepiness: The epworth sleepiness scale. *Sleep*, 14(6): 540–545.

   https://doi.org/10.1093/sleep/14.6.540

10. Peraita-Adrados R, Lammers GJ, De Andres C, *et al*., 2013, A patient with narcolepsy with cataplexy and multiple sclerosis: Two different diseases that may share pathophysiologic mechanisms? *Sleep Med*, 14(7): 695–696.

    https://doi.org/10.1016/j.sleep.2013.03.015

11. Ekbom K, 1966, Familial multiple sclerosis associated with narcolepsy. *Arch Neurol*, 15(4): 337–344.

    https://doi.org/10.1001/archneur.1966.00470160003001

12. Schuld A, Hebebrand J, Geller F, *et al*., 2000, Increased body-mass index in patients with narcolepsy. *Lancet*, 355(9211): 1274–1275.

    https://doi.org/10.1016/s0140-6736(05)74704-8

13. Cohen A, Mandrekar J, St Louis EK, *et al*., 2018, Comorbidities in a community sample of narcolepsy. *Sleep Med*, 43: 14–18.

    https://doi.org/10.1016/j.sleep.2017.11.1125

14. Poli F, Pizza F, Mignot E, *et al*., 2013, High prevalence of precocious puberty and obesity in childhood narcolepsy with cataplexy. *Sleep*, 36(2): 175–181.

    https://doi.org/10.5665/sleep.2366

15. Chabas D, Foulon C, Gonzalez J, *et al*., 2007, Eating disorder and metabolism in narcoleptic patients. *Sleep*, 30(10): 1267–1273.

https://doi.org/10.1093/sleep/30.10.1267

16. Zhang M, Thieux M, Inocente CO, *et al*., 2022, Characterization of rapid weight gain phenotype in children with narcolepsy. *CNS Neurosci Ther*, 28(6): 829–841.

https://doi.org/10.1111/cns.13811

17. Huang KH, Tai MC, Lee LC, *et al*., 2018, Positron emission tomography/computed tomography scan of Vogt-Koyanagi-Harada syndrome with associated autoimmune thyroid disease: A case report and literature review. *Medicine* (*Baltimore*), 97(9): e0047.

https://doi.org/10.1097/md.0000000000010047

18. Radetti G, Gottardi E, Bona G, *et al*., 2006, The natural history of euthyroid Hashimoto's thyroiditis in children. *J Pediatr*, 149(6): 827–832.

https://doi.org/10.1016/j.jpeds.2006.08.045

19. Umpierrez GE, Latif KA, Murphy MB, *et al*., 2003, Thyroid dysfunction in patients with Type 1 diabetes: A longitudinal study. *Diabetes Care*, 26(4): 1181–1185.

https://doi.org/10.2337/diacare.26.4.1181

20. Wiendl H, Gross CC, Bauer J, *et al*., 2021, Fundamental mechanistic insights from rare but paradigmatic neuroimmunological diseases. *Nat Rev Neurol*, 17(7): 433–447.

https://doi.org/10.1038/s41582-021-00496-7

21. Pedersen NW, Holm A, Kristensen NP, *et al*., 2019, CD8+ T cells from patients with narcolepsy and healthy controls recognize hypocretin neuron-specific antigens. *Nat Commun*, 10(1): 837.

https://doi.org/10.1038/s41467-019-08774-1

22. Mahlios J, De la Herran-Arita AK, Mignot E, 2013, The autoimmune basis of narcolepsy. *Curr Opin Neurobiol*, 23(5): 767–773.

https://doi.org/10.1016/j.conb.2013.04.013

23. Wijnans L, Lecomte C, de Vries C, *et al*., 2013, The incidence of narcolepsy in Europe: Before, during, and after the influenza A(H1N1)pdm09 pandemic and vaccination campaigns. *Vaccine*, 31(8): 1246–1254.

https://doi.org/10.1016/j.vaccine.2012.12.015

24. Han F, Lin L, Warby SC, *et al*., 2011, Narcolepsy onset is seasonal and increased following the 2009 H1N1 pandemic in China. *Ann Neurol*, 70(3): 410–417.

https://doi.org/10.1002/ana.22587

25. Partinen M, Kornum BR, Plazzi G, *et al*., 2014, Narcolepsy as an autoimmune disease: The role of H1N1 infection and vaccination. *Lancet Neurol*, 13(6): 600–613.

https://doi.org/10.1016/S1474-4422(14)70075-4

26. Aran A, Lin L, Nevsimalova S, *et al*., 2009, Elevated anti-streptococcal antibodies in patients with recent narcolepsy onset. *Sleep*, 32(8): 979–983.

https://doi.org/10.1093/sleep/32.8.979

27. Mignot E, Lin L, Rogers W, *et al*., 2001, Complex HLA-DR and-DQ interactions confer risk of narcolepsy-cataplexy in three ethnic groups. *Am J Hum Genet*, 68(3): 686–699.

https://doi.org/10.1086/318799

28. Mahoney CE, Cogswell A, Koralnik IJ, *et al*., 2019, The neurobiological basis of narcolepsy. *Nat Rev Neurosci*, 20(2): 83–93.

https://doi.org/10.1038/s41583-018-0097-x

29. Li L, Liu S, Yu J, 2020, Autoimmune thyroid disease and Type 1 diabetes mellitus: Same pathogenesis; new perspective? *Ther Adv Endocrinol Metab*, 11: 2042018820958329.

https://doi.org/10.1177/2042018820958329

30. Bellan M, Andreoli L, Mele C, *et al*., 2020, Pathophysiological role and therapeutic implications of Vitamin D in autoimmunity: Focus on chronic autoimmune diseases. *Nutrients*, 12(3): 789.

https://doi.org/10.3390/nu12030789

31. Dauvilliers Y, Evangelista E, Lopez R, *et al*., 2017, Vitamin D deficiency in Type 1 narcolepsy: A reappraisal. *Sleep Med*, 29: 1–6.

https://doi.org/10.1016/j.sleep.2016.05.008

32. Carlander B, Puech-Cathala AM, Jaussent I, *et al*., 2011, Low Vitamin D in narcolepsy with cataplexy. *PLoS One*, 6(5): e20433.

https://doi.org/10.1371/journal.pone.0020433

33. Wang J, Lv S, Chen G, *et al*., 2015, Meta-analysis of the association between Vitamin D and autoimmune thyroid disease. *Nutrients*, 7(4): 2485–2498.

https://doi.org/10.3390/nu7042485

34. Alamo A, Condorelli RA, La Vignera S, *et al*., 2019, Autoimmune thyroid disease following treatment with alemtuzumab for multiple sclerosis. *Int J Immunopathol Pharmacol*, 33: 2058738419843690.

https://doi.org/10.1177/2058738419843690

35. Zhao R, Zhang W, Ma C, *et al*., 2021, Immunomodulatory function of Vitamin D and its role in autoimmune thyroid disease. *Front Immunol*, 12: 574967.

https://doi.org/10.3389/fimmu.2021.574967

36. Bishop EL, Ismailova A, Dimeloe S, *et al*., 2021, Vitamin D and immune regulation: Antibacterial, antiviral, anti-inflammatory. *JBMR Plus*, 5(1): e10405.

https://doi.org/10.1002/jbm4.10405

37. Mohammadi S, Mayeli M, Saghazadeh A, *et al*., 2020, Cytokines in narcolepsy: A systematic review and meta-analysis. *Cytokine*, 131: 155103.

https://doi.org/10.1016/j.cyto.2020.155103

38. Dauvilliers Y, Jaussent I, Lecendreux M, *et al*., 2014, Cerebrospinal fluid and serum cytokine profiles in narcolepsy with cataplexy: A case-control study. *Brain Behav Immun*, 37: 260–266.

https://doi.org/10.1016/j.bbi.2013.12.019

39. Mikos H, Mikos M, Obara-Moszynska M, *et al*., 2014, The role of the immune system and cytokines involved in the pathogenesis of autoimmune thyroid disease (AITD). *Endokrynol Pol*, 65(2): 150–155.

https://doi.org/10.5603/ep.2014.0021

40. Ganesh BB, Bhattacharya P, Gopisetty A, *et al*., 2011, Role of cytokines in the pathogenesis and suppression of thyroid autoimmunity. *J Interferon Cytokine Res*, 31(10): 721–731.

https://doi.org/10.1089/jir.2011.0049

Our Journals

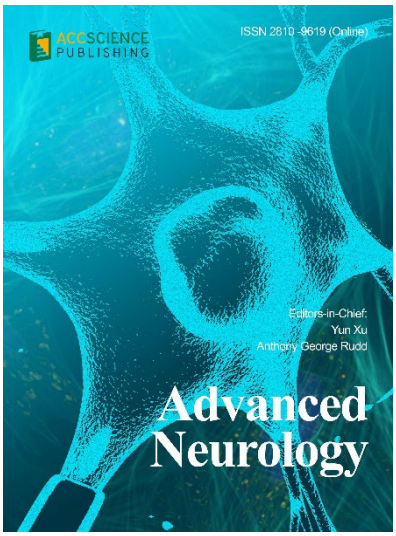

Advanced Neurology is a peer-reviewed and open-access journal that aims to publish and disseminate novel research in the breadth of neurology and neuroscience. The journal aims to advance our understanding in the nervous system and provide a platform to neuroscientists and physicians to showcase their findings in original fundamental and clinical research as well as to present new ideas that highlight the changes in the neurological clinical practice.

Advanced Neurology covers subject areas, including but not limited to the following:

- Neurological disorders
- Neurodegenerative disease
- Cerebrovascular disease
- Epilepsy and movement disorders
- Neuroimmune disease
- Neurological infections
- Muscle disease
- Molecular and cellular neuroscience
- Systems neuroscience
- Cognitive neuroscience
- Computational modeling of nervous system

Global Translational Medicine is a quarterly journal that focuses on medicine, biological sciences, and biomaterials engineering. The goal of *Global Translational Medicine* is to provide a platform to researchers for showcasing their latest research works in translational medicine so as to advance the field towards the betterment of human health. Despite the advancement of omics and new technologies, the process of transforming these technologies and scientific research results into effective therapies and putting them into clinical use still has a long way to go. *Global Translational Medicine* provides a platform to fill the gaps in preclinical and inter-disciplinary research, to promote clinical translation of scientific research results, and to contribute to the conception of new and improved preventive measures as well as diagnostic and therapeutic techniques of diseases.

Global Translational Medicine covers the following themes: cardiovascular disease, metabolism/diabetes/obesity, neuroscience/neurology, cancer, biomaterials and their applications in medicine, proteomics/metabolomics, pharmacogenomics, biomarkers, bioinformatics and data mining, animal and clinical research, and medical methods arising from interdisciplinary crossover.

Start a new journal

Write to us via email if you are interested to start a new journal with AccScience Publishing. Please attach your CV, professional profile page and a brief pitch proposal in your email. We shall inform you of our decision whether we are interested to collaborate in starting a new journal.

Contact: info@accscience.com

https://accscience.com/journal/GPD

Contact
www.accscience.com
8 Burn Road, #15-03 Trivex, Singapore 369977
Email: editorial@accscience.com
Phone: +65 8182 1586